The role of SATB1 in medial ganglionic eminence-derived cortical interneuron differentiation

Melania Kalaitzidou

January 2014

MRC – National Institute for Medical Research
Division of Molecular Neurobiology

University College London
Division of Biosciences
Research Department of Cell and Developmental Biology

A thesis submitted to University College London for the degree of Doctor of Philosophy

Declaration of authenticity

I, Melania Kalaitzidou confirm that the work presented in this thesis is my own. Where information has been derived from other sources I confirm that this has been indicated in the thesis.

Abstract

Brain function depends on the activity of cortical γ-aminobutyric acid-producing (GABAergic) interneurons, which participate in the formation of inhibitory circuits and control the activity of excitatory glutamatergic pyramidal neurons. Cortical GABAergic interneurons are extremely diverse in morphology, electrophysiology and molecular marker expression. A plethora of transcription factors that control aspects of this diversity has now been identified. Among them, the LIM-homeodomain transcription factor LHX6 is required for the differentiation of parvalbumin$^+$ (PV$^+$) and somatostatin$^+$ (SST$^+$) cortical interneurons. However, little is known about the molecular cascades operating downstream of LHX6 to control the maturation of these two major interneuron subtypes. With a focus on identifying region- and stage-specific factors regulating interneuron maturation, a genome-wide gene expression analysis was conducted in our laboratory and identified the gene encoding the chromatin organiser protein SATB1 as an LHX6 target in the E15.5 mouse cortex.

In this thesis, we investigate the *in vivo* role of SATB1 in cortical interneuron terminal differentiation. Using a constitutive *Satb1*-null mouse established in our laboratory we demonstrate that *Satb1* regulates multiple aspects of SST$^+$ interneuron maturation. In contrast, by generating mice with a specific deletion of *Satb1* in PV$^+$ interneurons (*PV-Cre;Satb1-flox*) we show that *Satb1* is not required for the maturation of this group of inhibitory neurons. Moreover, interneuron-specific deletion of *Satb1* with the *Nkx2.1-Cre* line reveals a disruption of the excitation/inhibition balance in the brain and a significant loss of both SST$^+$ and PV$^+$ interneurons. Finally, we show that SATB1 and the general neuronal maturation marker KCC2 are coexpressed in mature cortical interneurons. By performing overexpression experiments in brain slices we observed regulation of *Kcc2* expression by SATB1, but failed to detect any reciprocal

regulation of *Satb1* by KCC2. Overall, our findings provide a basis for understanding the terminal differentiation of interneurons in the mammalian cortex.

Table of contents

List of figures

List of tables

List of abbreviations

4-OHT	4-Hydroxytamoxifen
5HT3aR	Ionotropic serotonin receptor 5HT3a
Aa	Amino acid
Ach	Acetylcholine
AEP	Anterior entopeduncular area
ALP	Alkaline phosphatase
ANR	Anterior neural ridge
AP	Anteroposterior
AVE	Anterior visceral endoderm
BDNF	Brain-derived neurotrophic factor
ß-gal	Beta-galactosidase
BMP	Bone morphogenetic protein
Br	Bregma
BSA	Bovine serum albumin
BUR	Base unpairing region
CB	Calbindin-D28K
CBP	Calcium binding protein
CCK	Cholecystokinin
cDNA	Complementary deoxyribonucleic acid
CFuPN	Corticofugal projection neuron
CGE	Caudal Ganglionic Eminence
ChAT	Choline acetyltransferase
ChIP	Chromatin immunoprecipitation
cKO	Conditional knockout
CMS	Caudal migratory stream
CMV	Cytomegalovirus
CNS	Central Nervous System
CP	Cortical plate
CPN	Callosal projection neuron
CR	Calretinin
CRH	Corticotropin releasing hormone
CThPN	Corticothalamic projection neuron

DIG	Digoxygenin
DIV	Days *in vitro*
DV	Dorsoventral
EEG	Electroencephalogram
ES cell	Embryonic stem cell
EUCOMM	European conditional mouse mutagenesis program
FACS	Fluorescence-activated cell sorting
FGF	Fibroblast growth factor
GABA	γ - aminobutyric acid
GDNF	Glial cell line derived neurotrophic factor
GFP	Green fluorescent protein
HD	Homeodomain
HGF/SF	Hepatocyte growth factor/scatter factor
hPLAP	Human placental alkaline phosphatase
IEG	Immediate early gene
IPC	Intermediate progenitor cell
IPSC	Inhibitory postsynaptic current
IRES	Internal ribosome entry site
ISH	*in situ* hybridisation
IZ	Intermediate zone
KO	Knockout
LGE	Lateral Ganglionic Eminence
M1	Primary motor cortex
MAR	Matrix Attachment Region
MCS	Multi-cloning site
MGE	Medial Ganglionic Eminence
mRNA	Messenger ribonucleic acid
MSN	Medium-sized spiny projection neuron
MZ	Marginal Zone
nNOS	Neuronal nitric oxide synthase
NPY	Neuropeptide Y
NRG1	Neuregulin-1
NRP1	Neuropilin 1
NT4	Neurotrophin 4

PBS	Phosphate Buffered Saline
PCR	Polymerase chain reaction
PFA	Paraformaldehyde
PKC	Protein kinase C
PLAP	Placental Alkaline Phosphatase
POA	Preoptic Area
polyA	Polyadenylation sequence
PP	Preplate
PV	Parvalbumin
RA	Retinoic acid
RGC	Radial glial cell
RLN	Reelin
RMS	Rostral migratory stream
S1BF	Somatosensory cortex barrel field
SA	Splice acceptor
SAR	Scaffold attachment region
SCPN	Subcerebral projection neuron
SEM	Standard error of the mean
Shh	Sonic hedgehog
shRNA	short hairpin RNA
siRNA	small interfering RNA
SP	Subplate
SST	Somatostatin
STDEV	Standard deviation of the mean
SVZ	Subventricular Zone
TUNEL	Terminal deoxynucleotidyl transferase dUTP - nick end labeling
ULD	Ubiquitin-like domain
V1	Primary visual cortex
VIP	Vasoactive intestinal peptide
VP	Vaginal plug
VSCC	Voltage-sensitive calcium channel
VZ	Ventricular Zone
wt	wild type
YFP	Yellow fluorescent protein

Acknowledgements

First, I would like to thank Vassilis Pachnis for giving me the opportunity to work on this project, his supervision and advice. I am particularly grateful to Myrto Denaxa for our collaboration, her guidance and support. She initiated the SATB1 project and I thank her for taking me onboard and sharing with me her expertise on the subject. I would also like to thank Guilherme Neves for introducing me to the adult mouse brain in my early days in the lab and for his continuous feedback and advice on my work. Both Myrto and Guilherme have been very generous, thoughtful and extremely kind and I feel very lucky to have worked with them. I also need to thank Reena Lasrado and Anna Garefalaki who collaborated for the generation of the *Satb1*$^{-}$ line.

I give my thanks to Vale, Reena and Catia for their warm welcome when I first joined the lab and to Myrto, Chryssa, Angeliki and Dafni for making late evenings in the lab fun. Thanks also to the rest of the people in the Pachnis lab and in the Molecular Neurobiology Division and to Eileen for being so friendly and helpful. I am also grateful to the various NIMR facilities with which I have collaborated over the years and especially the people at Laidlaw Green for taking care of my many mouse lines.

This journey wouldn't be the same without the support of friends and family. To Angeliki Tsagaratou, thank you for being a true friend, even when 6,000 miles away. To Christos, thank you for everything really. For your unconditional love and support, for the adventures we've shared and for making London our home. I feel incredibly lucky to have you in my life. Finally, I am grateful to my family for their encouragement and support and most importantly for trusting me and allowing me to make my own decisions in life. I dedicate this work to my mother Eva and my late father Theodoros.

Chapter 1

Introduction

1.1 The forebrain

1.1.1 Anatomy and function of the adult forebrain

The telencephalon is undoubtedly the most complex region of the mammalian brain, not only in terms of architecture, but also with regards to neuronal cell type heterogeneity and function. Coordination between its pallial (cortex) and subpallial (basal ganglia, most of the septum and some amygdala nuclei) components (Figure 1.1) is absolutely critical for normal brain function (Watson *et al*., 2012).

The basal ganglia comprise a group of four principal nuclei located at the ventral forebrain, namely the striatum, the globus pallidus, the subthalamic nucleus and the substantia nigra, which communicate between them via both excitatory and inhibitory connections but are also linked to the cortex and the thalamus. The basal ganglia are mainly implicated in motor planning and execution, as well as in habit learning and addiction (reviewed in Strausfeld and Hirth, 2013).

The cerebral cortex is the outer-most layer of the brain and can be divided into three regions, according to their phylogenetic origin: the archicortex, which is the evolutionarily oldest cortical subdivision and corresponds to the hippocampus, the paleocortex, which includes the periamygdala, perirhinal, entorhinal and piriform cortices and the neocortex, which includes the somatosensory, motor and visual cortices. The archicortex and paleocortex participate in memory formation, navigation and olfaction, and the neocortex is associated with higher cognitive functions (Squire *et al*., 2008; Purves *et al*., 2012). The focus of this study will be the neocortex, the evolutionarily most recent part of the cortex and one that has shown extensive growth in terms of size and complexity, particularly in humans.

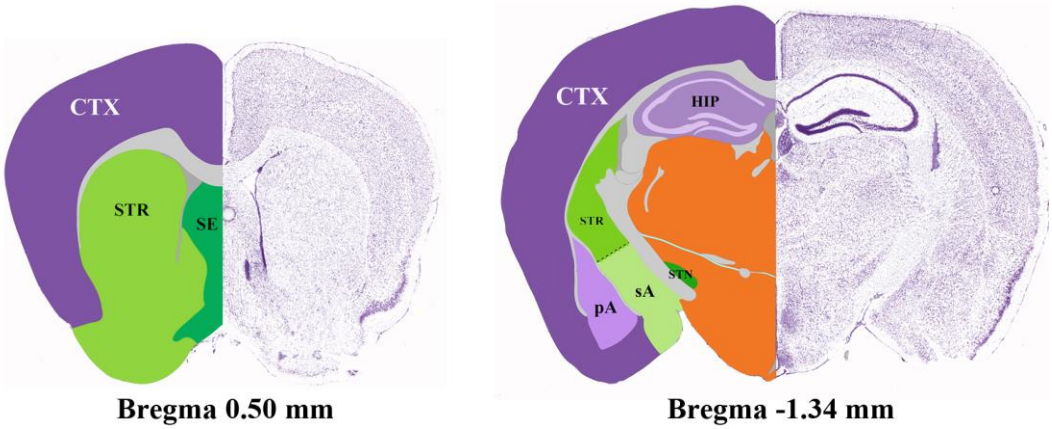

Figure 1.1 The adult mouse forebrain. Coronal sections of the adult mouse forebrain, at rostral (Bregma 0.50 mm) and caudal levels (Bregma -1.34 mm), stained with Nissl (right hemisphere) and pseudocoloured (left hemisphere) to highlight the various areas. Regions of pallial origin (CTX, HIP, pA) are highlighted in shades of purple, whereas regions of subpallial origin (STR, SE, STN, sA) are highlighted in shades of green. Note that some parts of the amygdala are of pallial origin, whereas other parts are of subpallial origin. Areas not mentioned herein are coloured in orange. CTX= cortex, STR= striatum, SE= septum, HIP= hippocampus, STN= subthalamic nucleus, pA= amygdala nuclei of pallial origin, sA= amygdala nuclei of subpallial origin. Modified from the Allen Brain Atlas.

1.1.2 Lamination and connectivity of the neocortex

The neocortex is a laminated structure consisting of six horizontal layers (I-VI), occupied by two neuronal cell types with opposing actions: the excitatory projection neurons and the inhibitory interneurons, which together constitute the major components of cortical circuits (reviewed in Gao *et al*., 2013).

Cortical layers are formed as projection neurons born in the ventricular (VZ) and subventricular (SVZ) zones of the developing pallium migrate along the fibres of radial glial cells (RGCs). The first projection neurons will form the preplate (PP), which is subsequently split into the superficial marginal zone (MZ) and the underlying subplate (SP), by neurons forming the cortical plate (CP). The CP will develop into layers II-VI of the cortex, whereas the MZ will form layer I. Importantly, these layers are generated

in an "inside-out manner", with the earliest-born neurons colonising the deep cortical layers (VI – V), whereas later-born neurons occupy successively upper layers (IV – II) (Figure 1.2; reviewed in Kwan *et al.*, 2012). During this process of "inside-out" migration of newly-generated projection neurons, the MZ plays a fundamental role in regulating the laminar position acquired by these cells (reviewed in Kwan *et al.*, 2012). In particular, the MZ contains a unique population of neurons, the Cajal-Retzius cells, which secrete the extracellular matrix protein Reelin (RLN), a well-studied regulator of cortical lamination (reviewed in Tissir and Goffinet, 2003). Lack of *Reelin* activity in *Reeler* mouse mutants, or perturbation of the RLN signalling pathway, result in severe disorganisation of cortical laminae (reviewed in D'Arcangelo, 2005). Examination of *Reeler* mice revealed that late-born projection neurons fail to migrate past their early-born counterparts and as a result, splitting of the PP by CP neurons is arrested and cortical lamination is somewhat inverted (reviewed in D'Arcangelo, 2005).

It has long been appreciated that the cellular content of each layer of the mature neocortex is unique and that neurons within the same layer have common connectivity patterns. Layer I lacks projection neurons but contains their dendritic tufts and axonal terminations, as well as Cajal-Retzius cells. Layers II-III comprise callosal projection neurons (CPNs), which mediate communication between the two telencephalic hemispheres by sending their axons across the corpus callosum. In primary sensory areas, layer IV is where spiny stellate cells, which receive thalamic input, are found, and finally, layers V-VI contain corticofugal projection neurons (CFuPNs) that project their axon collaterals to the thalamus, spinal cord or other subcortical areas. Layers V-VI also contain a small population of CPNs (reviewed in Gao *et al*., 2013). Moreover, there is synaptic connectivity between the various cortical layers. This is best described in the model of the "canonical cortical microcircuit", which is based on initial work in the cat visual cortex as well as numerous subsequent studies. According to this model, thalamic

information reaches the cortex via layer IV, where it is amplified, and is subsequently relayed to layers II-III and from there to layers V-VI. Direct projections from layer IV to layers V-VI are also possible (reviewed in Douglas and Martin, 2007).

1.1.3 Neuronal subtypes of the neocortex

As mentioned above, cortical circuits consist of excitatory projection neurons and inhibitory interneurons. These two neuronal populations are responsible for mediating the complex functions of the cortex and their coordinated activity maintains the fine balance between excitation and inhibition in the brain.

Projection neurons, also known as pyramidal neurons because of their characteristic pyramid-shaped soma, represent the majority of cortical neurons (70-80%) and use the excitatory neurotransmitter glutamate. Their dendrites are characterised by the presence of numerous spines and as their name implies, projection neurons extend axons and transmit information to distant cortical and subcortical regions (reviewed in Molyneaux *et al.*, 2007). They are born in the VZ and SVZ of the pallium during embryogenesis and migrate along the fibres of RGCs to form the six horizontal layers of the cortex (section 1.1.2 and Figure 1.2).

Cortical projection neurons are a heterogeneous population, in terms of neurochemical content, physiological properties and connectivity. Classification of projection neurons according to their axonal pathways (hodology) has proved to be one of the most widely used and reliable ways to group these cells. According to hodology, projection neurons are classified into associative, which project within the same hemisphere, commissural, which send axons to the opposite cortical hemisphere and corticofugal, which are further subdivided into corticothalamic (CThPN) and subcerebral (SCPN) neurons, projecting to the thalamus or brainstem and spinal cord

respectively. SCPNs are further subdivided into corticotectal, corticopontine and corticospinal neurons (reviewed in Molyneaux *et al*., 2007).

In addition, great progress has been made over the past decade in unravelling the genetic programs that drive projection neuron subtype specification and diversity. It is now established that competition between key transcription factors orchestrates the acquisition of CPN, CThPN or SCPN identity (reviewed in Molyneaux *et al.*, 2007 and Greig *et al*., 2013). Specification of SCPNs requires the zinc-finger transcription factor FEZF2 and its downstream effector CTIP2. FEZF2 represses TBR1, a transcription factor required for CThPN development, and conversely, TBR1 opposes the action of FEZF2 and CTIP2 to instruct acquisition of CThPN identity. The same is also true for SOX5, which represses FEZF2 and CTIP2 until CThPN development is complete, thus ensuring that CThPNs and SCPNs are generated in the correct order. Finally, SATB2 regulates CPN specification by repressing CThPN and SCPN identities (reviewed in Molyneaux *et al.*, 2007 and Greig *et al*., 2013).

Interneurons on the other hand, represent approximately 20-30% of all cortical neurons in the mouse and, with the exception of spiny stellate cells and certain excitatory peptidergic interneurons, they use the inhibitory neurotransmitter γ-aminobutyric acid (GABA) (reviewed in Markram *et al*., 2004). Cortical interneurons contain aspiny dendrites and based on their morphology they were described by Ramón y Cajal in 1899 as "short axon cells". Indeed, their axons project locally within the cortex, the only exception being the long-range projection GABAergic neurons, forming connections between different cortical areas or between the cortex and subcortical areas (reviewed in Tamamaki and Tomioka, 2010). In contrast to pyramidal cells, cortical interneurons are born in the ganglionic eminences (GEs) of the subpallium (section 1.3.1) and migrate tangentially in order to reach the cortex (section 1.3.3). The majority of cortical interneurons (derived from the medial ganglionic

eminence) follow the same "inside-out" mode of generation as the projection neurons (Valcanis and Tan 2003; Miyoshi *et al.*, 2007), whereas others (derived from the caudal ganglionic eminence) seem to preferentially occupy upper cortical layers, irrespective of their time of birth (Rubin *et al*., 2010; Miyoshi *et al.*, 2010; Miyoshi and Fishell, 2011). Cortical interneurons are going to be our focus throughout this thesis and their heterogeneity, development and function will be extensively discussed in the following sections.

1.1.4 Embryonic development of the forebrain

The forebrain (prosencephalon), the anterior-most part of the neural tube, is one of the three primary brain vesicles that form during early development, along with the midbrain (mesencephalon) and the hindbrain (rhombencephalon). It is further subdivided into an anterior and a posterior part, the telencephalon and diencephalon respectively (reviewed in Rallu *et al*., 2002).

Following the formation of the neural plate at around embryonic day 6.0 (E6.0), diffusible cues from the Node and the anterior visceral endoderm (AVE) act to induce and maintain anterior neural tissues at E7.0. Subsequently, signals from the anterior neural ridge (ANR) antagonise posteriorising cues and thus promote telencephalic development. At E8.0, the two sides of the telencephalic primordium fuse and by E9.0 the two telencephalic vesicles have formed. Already at this stage, distinct markers are discernible along the dorsoventral (DV) axis of the telencephalic vesicles. Finally, further subdivisions within the telencephalon will lead to the formation of the dorsal, lateral and ventral proliferative zones by E11.0 (reviewed in Rallu *et al*., 2002).

Specifically, the dorsal telencephalon is divided into an anterior/lateral domain that will form the neocortex and a posterior/medial region that will give rise to the choroid plexus, the cortical hem and the hippocampus. The ventral telencephalon is also

partitioned into distinct domains, a medial one known as the medial ganglionic eminence (MGE) that will give rise to the globus pallidus, a more lateral domain, the lateral ganglionic eminence (LGE) that will later form the striatum and a posterior region named caudal ganglionic eminence (CGE), the primordium of the amygdala (reviewed in Hébert and Fishell, 2008).

Patterning of the developing forebrain, which generates the above-mentioned subdivisions, relies on the following general principle: cells which are under the influence of diffusible molecules produced by transient signaling centres have the ability to translate these signals into spatial information by inducing various combinations of transcription factors, and hence acquire unique identities (reviewed in Edlund and Jessell, 1999).

Ventral telencephalic identity is specified by the secreted glycoprotein Sonic hedgehog (SHH; Chiang *et al.*, 1996), which is expressed in the ventral midline, first in mesodermal tissue of the head process and by E9.5 within the MGE of the ventral telencephalon itself (reviewed in Rallu *et al*., 2002). In fact, SHH promotes patterning of the ventral telencephalon not directly, but rather by antagonising the zinc-finger transcription factor GLI3 (reviewed in Rallu *et al*., 2002), which plays a role in dorsal telencephalon patterning (Theil *et al*., 1999; Tole *et al*., 2000). Notably, although ventral repression of GLI3 by SHH is required for normal DV patterning of the developing telencephalon, reciprocal dorsal repression of SHH by GLI3 does not seem to be necessary (Rash and Grove, 2007).

SHH and GLI3 signalling aside, other extrinsic cues and transcription factors also contribute to telencephalic patterning. Ventral identity is assigned by the forkhead transcription factor FOXG1, which is expressed in the telencephalic anlage and directly induces expression of FGF8, a member of the Fibroblast Growth Factor family (reviewed in Hébert and Fishell, 2008). Conversely, FGF8 expression is negatively

regulated by GLI3. In particular, GLI3 is required to inhibit FGF expression, thereby preventing excess FGF signalling in the dorsal telencephalon that would otherwise lead to its ventralisation (Kuschel *et al*., 2003; Rash and Grove, 2007).

Furthermore, the secreted signalling molecules of the Bone Morphogenetic Protein (BMP) and Wingless/Int (WNT) families participate in patterning of the dorsal telencephalon. BMPs and WNTs are expressed along the dorsal telencephalic midline and play a critical role for the development of the hippocampus. BMP signalling is also required for the generation of the choroid plexus and cortical hem (reviewed in Hébert and Fishell, 2008).

Finally, based mostly on avian studies (Marklund *et al.*, 2004), patterning of the intermediate telencephalon, i.e. the lateral and ventral pallium and the LGE, is thought to be orchestrated by retinoic acid (RA) signalling (reviewed in Lupo *et al*., 2006).

1.1.5 The ganglionic eminences (GEs)

1.1.5.1 Generation and morphology of the GEs

The ganglionic eminences were first identified as anatomical landmarks of the subpallium and were described as swellings of proliferating cells, emanating from the walls of the ventral telencephalon into the ventricles. The first GE to become anatomically evident in the murine subpallium is the MGE, which appears at around E11.0. One day later, at E12.0, the LGE emerges dorso-laterally to the MGE (Smart, 1976). The MGE and LGE are prominent at more anterior telencephalic areas, separated by the interganglionic sulcus, whereas at more caudal levels they are said to fuse into one structure, thus forming the CGE (Smart, 1985; reviewed in Brazel *et al*., 2003).

1.1.5.2 Molecular specification of the GEs

The initial anatomical description of the GEs was followed by extensive analysis of their molecular profile. Based on the expression of a plethora of genes, the ventral telencephalon is subdivided into the following five regions: the MGE, the LGE, the CGE, the preoptic area/anterior entopeduncular area (POA/AEP) and the septum (Flames *et al.*, 2007), the molecular profiles of which are described below and summarised in Table 1.1.

Specification of the **MGE** initiates with the expression of the homeobox gene *Nkx2.1* in the ventral-most telencephalon at E8.5 (Shimamura *et al.*, 1995), via the action of SHH from the underlying axial mesendoderm (Shimamura and Rubenstein, 1997; Sussel *et al.*, 1999). By E9.5, *Nkx2.1* is detected in the MGE overlapping with *Shh* and in a pattern complementary to *Pax6* (Corbin *et al.*, 2003). In fact, NKX2.1 is required for the expression of *Shh* in this region (Sussel *et al.*, 1999) and in turn, SHH acts to maintain expression of *Nkx2.1* within the MGE (Xu *et al.*, 2005; Gulacsi and Anderson, 2006). By E12.5, *Nkx2.1* is detected in both the proliferative (VZ/SVZ) and the post-mitotic (mantle) zones of the MGE, while it is excluded from the LGE (Sussel *et al.*, 1999). Importantly, loss of function studies have established that *Nkx2.1* is critical for the specification of MGE identity, as the MGE of *Nkx2.1*$^{-/-}$ mutants fails to acquire its mature morphological and molecular characteristics and is respecified into an LGE-like structure (Sussel *et al.*, 1999).

The basic helix-loop-helix transcription factor MASH1 also plays an important role in formation of the MGE, by regulating the generation of neuronal precursors in the SVZ and neurons in the post-mitotic mantle zone. *Mash1*$^{-/-}$ mutants are characterised by a reduced size of the MGE at caudal levels and a complete absence of this region rostrally. However, this is not due to a defect in the specification of MGE progenitors, as *Nkx2.1* expression is maintained at caudal MGE levels. Rather, loss of *Mash1*

activity results in a dramatic reduction in the proliferation of VZ progenitors and a subsequent deficit in the generation of SVZ precursors (Casarosa *et al.*, 1999).

Emergence of the **LGE,** at the molecular level, is marked at E10.0 by the expression of *Gsx2* in a small domain, which will eventually expand, between the *Nkx2.1*$^{+}$ ventral telencephalon and the *Pax6*$^{+}$ dorsal region (Corbin *et al.*, 2003). Importantly, cross-repression between GSX2 and PAX6 defines the border between the LGE and the cortex respectively (Toresson *et al.*, 2000) whereas the expression of *Nkx2.1* delineates the border between the LGE and the MGE (Sussel *et al.*, 1999).

Both *Gsx2* and its homologue *Gsx1* are expressed within the VZ of the LGE, with *Gsx2* more strongly expressed dorsally and conversely, *Gsx1* showing a stronger expression ventrally (Yun *et al.*, 2001). Analysis of *Gsx2*$^{-/-}$ mouse mutants has highlighted a requirement for *Gsx2* in the specification of LGE fate. In these mutants the size of the LGE is reduced, and its character is dorsalised: expression of subpallial markers such as *Dlx1/2* and *Mash1* is lost in the LGE, while the dorsal markers *Pax6* and *Ngn2* expand ventrally (Corbin *et al.*, 2000; Toresson *et al.*, 2000; Yun *et al.*, 2001). Examination of *Gsx1*$^{-/-}$;*Gsx2*$^{-/-}$ compound mutants revealed a similar but more severe phenotype (Toresson and Campbell, 2001). This finding, along with the fact that *Gsx1* expression expands to cover the whole LGE in *Gsx2*$^{-/-}$ mutants, indicates a compensatory role for GSX1 in LGE development (Toresson and Campbell, 2001). Interestingly, recent studies have demonstrated that despite the compensatory function of GSX1 and GSX2 in the specification of the LGE, these two transcription factors play opposing roles in the regulation of proliferation and differentiation of neuronal progenitors in the VZ of the LGE (Pei *et al.*, 2011). Specifically, a series of misexpression and neurosphere assay experiments showed that GSX2 maintains progenitors in a dividing state, while GSX1 enhances neurogenesis, partly by downregulating GSX2 (Pei *et al.*, 2011).

Based on both anatomical criteria and gene expression data, the **CGE** could be described as a caudal extension of the LGE and MGE. Indeed, the CGE shares many molecular markers in common with the MGE and LGE, such as *Nkx2.1*, *Lhx6*, *Gsx2*, *Dlx1/2*, *Mash1* and others (Nery *et al.*, 2002; Flames *et al.*, 2007).

Yet, several lines of evidence suggest that the CGE is genetically distinct from the MGE and LGE. The first evidence comes from loss of function studies: in *Nkx2.1*-null mutants, expression of the striatal marker *Ebf1* expands ventrally within the MGE, whereas it remains unaffected in the CGE (Nery *et al.*, 2002). Similarly, in *Gsx2*$^{-/-}$ mutant mice *Dlx2* expression is reduced in the LGE and *Ngn2* expands ventrally, yet similar changes are not observed in the CGE (Nery *et al.*, 2002). Therefore, neither *Nkx2.1* nor *Gsx2* are required for CGE fate specification, highlighting the distinct character of the CGE. Moreover, two different transcriptome analyses of the CGE, LGE and MGE have identified the chicken ovalbumin upstream promoter-transcriptional factor II (COUP-TFII) as being preferentially enriched within the CGE (Kanatani *et al.*, 2008; Willi-Monnerat *et al*., 2008), providing new insight into the molecular identity of this region.

Table 1.1 Molecular identity of the ganglionic eminences

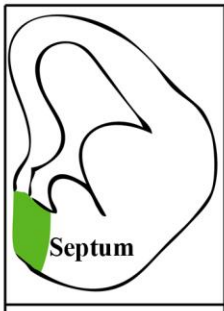				
Nkx2.1^{ventral}	Nkx2.1		Nkx2.1	Nkx2.1^{ventral}
	Lhx6			Lhx6^{ventral}
	Lhx7			
	Mash1	Mash1		Mash1
Gsx2	Gsx2	Gsx2		Gsx2
Gsx1	Gsx1	Gsx1^{ventral}	Gsx1	Gsx1
	Coup-tfII^{dorsal}	Coup-tfII^{ventral}		Coup-tfII
			Nkx5.1^{dorsal}	
Nkx6.2^{ventral}	Nkx6.2^{dorsal}	Nkx6.2^{ventral}	Nkx6.2^{ventral}	Nkx6.2^{ventral}
			Dbx1^{ventral}	
Zic4				
Lhx5				
Vax1	Vax1	Vax1	Vax1	Vax1

Index. Top panels are schematic representations of coronal hemisections of the E13.5 telencephalon, shown in a rostral to caudal direction. Each GE is represented by a unique colour and each column indicates the expression profile of a particular GE. Genes that are exclusively expressed or highly enriched in a given GE are highlighted with the colour corresponding to that GE. For example, *Coup-tfII* is enriched in the CGE but lower expression is also detected in the MGE/LGE border. Similarly, *Lhx6* expression is considered to be MGE-specific, however a small expression domain also exists at posterior levels, to what is described as the ventral CGE. Expression of *Zic4* and *Lhx5* is unique to the septum and *Nkx5.1* and *Dbx1* are uniquely expressed in dorsal and ventral domains of the POA respectively. Words in superscript specify the subregion within the GE where a gene is expressed. Blank cells indicate no expression.

Anatomically, the **POA** lies directly below the anterior commissure and above the optic chiasm, at the border between the telencephalon and the diencephalon (Puelles, 2000). At a coronal plane of section, the POA/AEP is situated immediately ventral to the MGE and in fact, these two regions share expression of *Nkx2.1* (Sussel *et al.*, 1999; Flames *et al.*, 2007; Gelman *et al.*, 2009).

However, progenitors of the POA are molecularly distinct from their MGE counterparts, as they express *Shh* and *Nkx6.2*, which are not found in the proliferative zone of the adjacent ventral MGE and lack expression of the MGE markers *Lhx6*, *Gsx2* and *Olig2* (Flames *et al.*, 2007; Gelman *et al.*, 2009). Further characterisation of the molecular profile of the POA revealed that the homeobox gene *Nkx5.1* is exclusively expressed in postmitotic cells at the most dorsal part of this region, which was termed pPOA1. Right adjacent to pPOA1, lies the ventral progenitor zone pPOA2, which is characterised by the largely non-overlapping expression of *Dbx1* and *Nkx6.2* (Gelman *et al.*, 2009 and 2011).

The **septum** is positioned between the telencephalic lateral ventricles, directly above the anterior commissure and under the corpus callosum, and it consists of both pallial and subpallial areas, the latter defined by *Dlx2* expression (Puelles, 2000). Some progenitor domains of the septum share expression of various genes with its neighbouring MGE, LGE, and POA, such as *Nkx2.1*, *Gsx2* and *Shh* (Flames *et al.*, 2007) as well as *Vax1*, a mediator of FGF and SHH signalling (Taglialatela *et al.*, 2004). *Vax1*-deficient mice are characterised by a complete absence of the septum (Bertuzzi *et al.*, 1999; Hallonet *et al.*, 1999; Taglialatela *et al.*, 2004), while MGE and LGE identities remain unchanged (Hallonet *et al.*, 1999; Taglialatela *et al.*, 2004). The septum also expresses genes that are excluded from the other subpallial GEs, such as *Lhx5* (Flames *et al.*, 2007) and *Zic4* (Gaston-Massuet *et al.*, 2005; Rubin *et al.*, 2010),

which may play an important, yet undiscovered, role in bestowing the septum with its identity.

1.1.6 Proliferative zones of the embryonic forebrain: the VZ and SVZ

The VZ and SVZ correspond to the proliferative areas of the developing telencephalon, which harbour the progenitors that generate its neuronal and glial lineages. They constitute two adjacent layers, present both ventrally within the GEs of the subpallium and dorsally into the neocortex, lining the ventricles. As development proceeds, the proliferative capacity and the size of the VZ decline, whereas the proliferative index of the expanding SVZ increases (reviewed in Brazel *et al*., 2003).

The role of the VZ and SVZ in neuronal production has been well studied in the cortex and deserves mention. Before the onset of neurogenesis, neural progenitors of the VZ divide symmetrically to increase their numbers and subsequently acquire radial glial morphology. RGCs in the VZ will then divide asymmetrically to either generate neurons and more RGCs or intermediate progenitor cells (IPCs) and RGCs. IPCs will settle in the SVZ, where they will undergo symmetric divisions to produce neurons (Figure 1.2; reviewed in Kwan *et al*., 2012). Similarly, recent studies demonstrated that subpallial progenitors, at least in the MGE and POA, are in fact RGCs that participate in either direct neurogenesis by asymmetric division at the VZ, or indirect neurogenesis by generating IPCs, which will divide symmetrically at the SVZ (Brown *et al*., 2011).

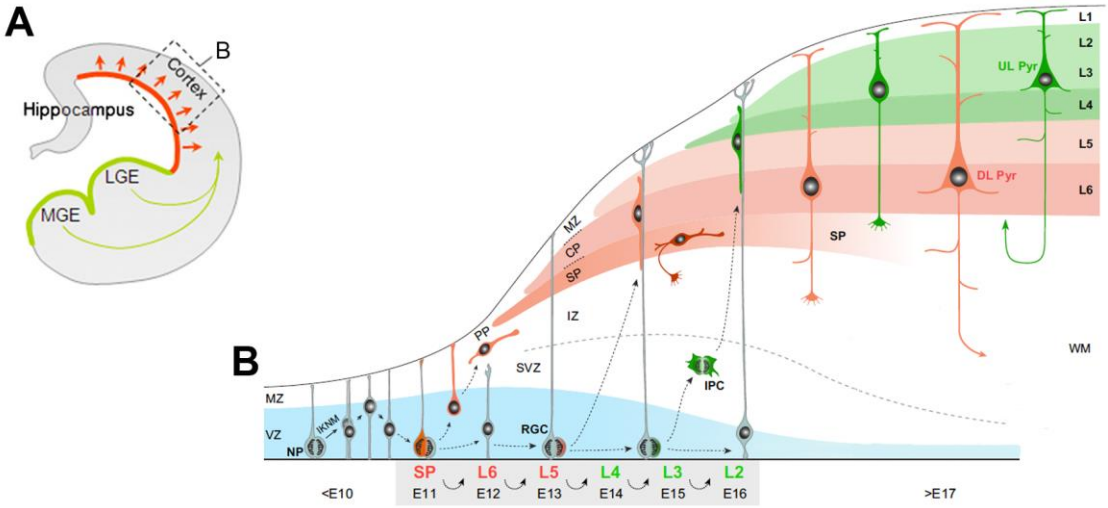

Figure 1.2 "Inside-out" generation of cortical projection neurons. (A) Schematic of a coronal hemisection of the E13.5 mouse telencephalon depicting the generation of projection neurons from the VZ of the cortex (red) and the generation of cortical interneurons in the ventral GEs, as well as their migration towards the cortex (light green). **(B)** Schema of the boxed area in A showing the birth of projection neurons at the E11-E17 cortex. The first projection neurons (orange), generated from asymmetric divisions of RGCs, will settle in the PP, which is later split into the MZ and SP by neurons forming the CP. The CP will develop into L2-6 of the cortex whereas the MZ will form L1. Early-born neurons (orange) migrate along radial glia fibers and settle in the SP and deep cortical layers, whereas later-born neurons (green), which come largely from symmetric divisions of IPCs in the SVZ, will occupy upper layers. L1-L6= cortical layers 1-6, WM= white matter, NP= neural progenitor, RGC= radial glial cell, IPC= intermediate progenitor cell, UL Pyr= upper layer pyramidal cell, DL Pyr= deep layer pyramidal cell, IKNM= interkinetic nuclear migration. (A) is taken from Merot *et al*., 2009, with permission. (B) was adapted with permission from Kwan *et al*., 2012.

1.2 Forebrain interneuron diversity

1.2.1 Cortical interneurons

Perhaps one of the most striking features of cortical inhibitory interneurons is their extreme diversity: they are categorised into multiple subtypes according to their morphological, molecular, physiological and connectivity properties (reviewed in

Markram *et al.*, 2004; Ascoli *et al.*, 2008; Fishell and Rudy, 2011). Evidence suggests that this diversity is critical for endowing the cortical inhibitory system with its great sensitivity and complexity in order to balance out the excitation provided by pyramidal cells (reviewed in Markram *et al.*, 2004; Huang *et al.*, 2007). Cortical interneuron function and classification are discussed in greater detail in the following paragraphs.

1.2.1.1 Physiology of cortical interneurons and their role in disease

GABAergic interneurons are the major components of the brain to control hyperexcitability, through the formation of local inhibitory networks that regulate and synchronise the output of pyramidal neurons. Not only they ensure the overall activity equilibrium within neural circuits but they also generate network oscillations to gate information and support higher brain function (reviewed in Rossignol, 2011; Marín, 2012). Moreover, during the first days of postnatal rodent development, cortical and hippocampal interneurons generate early activity patterns, which are thought to regulate maturation and connectivity of both interneurons and pyramidal cells (reviewed in Rossignol, 2011).

Importantly, even subtle disruptions in the excitation/inhibition balance in cortical or hippocampal circuits can have severe consequences in circuit stability and homeostasis, which are manifested as a wide spectrum of neurological disorders. These include epilepsy, autism and schizophrenia (reviewed in Rossignol, 2011; Marín, 2012) as well as anxiety disorders (reviewed in Möhler, 2012). Increasing evidence from human patients and experimental rodent models indicate a causal relationship between the loss of GABAergic interneurons or the impaired development and/or function of these cells and the development of neurological disorders (reviewed in Marín, 2012). Elucidating cortical interneuron diversity and function is therefore critical for the development of new therapies against neuropsychiatric conditions.

1.2.1.2 Classification of cortical interneurons

Research over the past years has contributed in unravelling the vast diversity of cortical interneuron properties. However there still is no definite number of how many interneuron subtypes exist, or consensus for their categorization in groups. Efforts to classify cortical interneurons are based on defining the morphological, molecular and physiological features of these cells. In fact, the Petilla Interneuron Nomenclature Group introduced a comprehensive terminology to describe these features (Ascoli *et al.*, 2008) and has recently developed a web-based tool for the automatic classification of cortical interneurons based on morphology and axonal arborisation patterns (DeFelipe *et al*., 2013). Here I will present the interneuron classification scheme by Markram *et al*. (Markram *et al*., 2004), followed by a summary of the major cortical interneuron subtypes as proposed by Fishell and Rudy (Fishell and Rudy, 2011) in table 1.2.

Based on somatic and dendritic **morphology**, axonal arborisation and target specificity Markram *et al*. categorised cortical interneurons into the following classes: **Basket cells (BCs)** target the somata and proximal dendrites of pyramidal cells as well as interneurons. According to their axonal and dendritic morphology they are categorised into large basket cells (LBCs), small basket cells (SBCs) and nest basket cells (NBCs), which altogether represent nearly half of the total interneuronal population. **Chandelier cells (ChCs)** can be either multipolar or bitufted, with their somata localized in layers II-VI. They innervate the axon initial segment of pyramidal cells and got their name from their characteristic axon terminals that form vertical rows of high-density synaptic boutons, resembling a chandelier. **Martinotti cells (MCs)** have bitufted morphology and very elaborate dendritic trees. They are found in layers II-VI but extend their axons to layer I where they spread horizontal collaterals in neighbouring columns. MCs target proximal and distal dendrites of pyramidal cells as well as perisomatic dendrites and somata. **Bipolar cells (BPCs)** are small, oval or

spindle-shaped cells with dendrites extending vertically into layers I and VI, were they make contact with only a few target cells on their basal dendrites. **Double bouquet cells (DBCs)** are bitufted, vertically oriented, dendritic-targeting cells preferentially located in supragranular layers. **Bitufted cells (BTCs)** resemble BPCs and DBCs in morphology and target specificity but differ in the fact that their axons have wider horizontal arborisation. **Neurogliaform cells (NGCs)** are small, round-shaped cells whose dendrites form a characteristic spherical field. Their axons are highly branched with fine boutons targeting the dendrites of pyramidal cells.

Initial classification of the **electrical properties** of cortical interneurons was based on their firing responses, when excited by a depolarising current. According to this, interneurons can be **fast spiking (FS)**, **low-threshold spiking (LTS)** otherwise known as **burst spiking non-pyramidal (BSNP)**, **regular spiking non-pyramidal (RSNP)**, **late spiking (LS)** and **irregular spiking (IS)** (reviewed in Markram *et al.*, 2004). A different classification approach, commonly used in conjunction with the first, takes into account the steady-state response of interneurons following a current injection and divides them into **non-accommodating (NAC)**, **accommodating (AC)**, **stuttering (STUT)**, **irregular spiking (IS)** and **bursting (BS)** (Gupta *et al.*, 2000; reviewed in Markram *et al.*, 2004). Importantly though, these firing responses do not correspond to a unique morphological or molecular type of interneuron: one type of interneuron may present several discharge patterns and similarly, a firing pattern can appear in various types of interneurons. Notably, electrical behaviour of a neuron depends on the types and numbers of ion channels it expresses, as well as their distribution on the cell membrane (reviewed in Markram *et al.*, 2004). Whole-cell recordings combined with single-cell mRNA expression profiling, have associated the ion channel and calcium-binding protein composition of an interneuron with its electrical properties (Toledo-Rodriguez *et al.*, 2004). For example, expression of the

voltage-gated potassium channels Kv3.1 and Kv3.2 typically correlates with fast spiking responses in PV^+ cells (Erisir *et al.*, 1999; Toledo-Rodriguez *et al.*, 2004).

The hallmark of inhibitory interneuron **molecular identity** is the expression of the neurotransmitter **GABA** and its synthesising enzyme **glutamic acid decarboxylase (GAD)**. GAD catalyses the rate limiting step in GABA synthesis from glutamate and comes in two isoforms, a big 66.6 kDa (GAD67) and a smaller 65.4 kDa (GAD65) isoform, produced by two different genes, *Gad1* and *Gad2* respectively (Erlander *et al.*, 1991). Both GAD67 and GAD65 are widely distributed in the cortex (Tamamaki *et al.*, 2003; López-Bendito *et al.*, 2004). Apart from the universal expression of GABA, cortical interneurons are characterised by the expression of neuropeptides, calcium-binding proteins or a combination of both.

The **calcium-binding proteins (CBPs)** expressed in cortical interneurons are Parvalbumin (PV), Calretinin (CR) and Calbindin (CB). They belong to the EF-hand family of CBPs and function as "buffers", decreasing the cytoplasmic concentration of Ca^{2+} and thereby modulating the amplitude of Ca^{2+} transients in the cell (reviewed in Schwaller *et al*., 2002).

PV is found in approximately 40% of the total GABAergic population of the mouse cortex (reviewed in Rudy *et al*., 2011). The first sparse and weakly stained PV^+ cells appear at P10 in layer V of the murine cortex and by P16 they become widespread in all cortical areas with their numbers increasing dramatically in layers II-VI (del Rio *et al.*, 1994). PV-expressing interneurons do not co-label with CR or any neuropeptides, although some overlap between PV and CB has been reported (Gonchar *et al.*, 2008). Morphologically, the majority of PV^+ interneurons are either BCs or ChCs and strongly associate with fast spiking properties (reviewed in Fishell and Rudy, 2011).

CR immunoreactivity in the mouse cortex is present in about 24% of $GABA^+$ interneurons in layers I-VI, with a preferred localisation in supragranular layers I-III

(Gonchar *et al.*, 2008). The coexpression of CR with various neuropeptides is discussed in the following paragraphs.

CB$^+$ interneurons are present in all cortical layers with the exception of layer I and similar to CR$^+$ cells they are more prevalent in supragranular layers. However, CB is also expressed in pyramidal neurons, making it a less specific marker for cortical interneurons (Kawaguchi and Kubota, 1997; Gonchar *et al.*, 2008).

Neuropeptides are widely distributed in central nervous system (CNS) neurons along with conventional neurotransmitters, influencing emotional and cognitive processes (reviewed in van den Pol, 2012). Neuropeptides expressed in cortical interneurons include Somatostatin (SST), Neuropeptide Y (NPY), Vasoactive intestinal peptide (VIP), Cholecystokinin (CCK) and Corticotropin-releasing hormone (CRH).

SST protein is first observed in deep layers of the mouse cortex just after birth and its expression becomes more widespread across layers I-VI during the first postnatal week (Gonchar *et al.*, 2008). SST$^+$ interneurons are the second largest group of GABAergic interneurons in the cortex (reviewed in Rudy *et al.*, 2011) and colocalise quite extensively with CR in layers II/III (Xu *et al.*, 2006 and 2010a; Gonchar *et al.*, 2008), and also with NPY (Gonchar *et al.*, 2008; Xu *et al.*, 2010a) but never with PV (Xu *et al.*, 2006 and 2010a; Gonchar *et al.*, 2008). Both SST$^+$;CR$^-$ and SST$^+$;CR$^+$ interneurons are classified as MCs, although differences between the connectivity, dendritic arborisation and origin of these two groups of SST$^+$ interneurons have been reported (reviewed in Fishell and Rudy, 2011).

NPY$^+$ interneurons are more abundant in layers II/III and VI, where they colocalise with CR and SST (Gonchar *et al.*, 2008; Xu *et al.*, 2010a). Recent studies combining whole-cell recordings with real-time PCR have identified three types of NPY$^+$ inhibitory cells: NG-like cells that also express nNOS, MC-like SST$^+$ neurons and PV$^+$ fast spiking BCs (Karagiannis *et al.*, 2009).

VIP does not colocalise with the major populations of PV^+ or SST^+ interneurons (reviewed in Rudy *et al.*, 2011; Xu *et al.*, 2010a). It is most commonly expressed along with CR in BPCs and BTCs, in layers II/III (reviewed in Fishell and Rudy, 2011).

CCK-expressing cells represent only 5% of GABAergic interneurons in layers I-VI of the mouse cortex. They mostly colocalise with CR or NPY and less frequently with SST and VIP (Gonchar *et al.*, 2008). Studies in the rat frontal cortex reveal that CCK^+ interneurons have the morphology of BCs and belong to the non-fast spiking group (Kawaguchi and Kondo, 2002).

CRH (also known as corticotropin releasing factor-CRF) expression has been reported in GABAergic interneurons in layers II-VI of the rat cortex (Karube *et al.*, 2004; Kubota *et al.*, 2011). CRH^+ cells in upper layers (II/III) were also positive for VIP and CRH^+ cells in deeper layers (V/VI) coexpressed SST. On the contrary, there was no colocalization of CRH with either PV or NPY. CRH^+ interneurons have morphologies of either SBCs or DBCs (Kubota *et al.*, 2011).

Although **nNOS** does not belong to either the CBP or neuropeptide families it is worth describing its expression in the cortex, where it is found mostly in long-range projection GABAergic neurons (Tomioka *et al.*, 2005). These are typically categorised into type I and type II cells. Type I neurons express high levels of nNOS, have large somata located in deeper cortical layers and nearly all of them express SST and NPY. On the contrary, type II cells are preferentially located in upper layers, show weaker nNOS expression, have smaller somata and coexpress a wide range of markers (Magno *et al.*, 2012; Jaglin *et al.*, 2012; Perrenoud *et al.*, 2012).

Expression of the **RLN** glycoprotein has been reported in cortical interneurons from P21 onwards, either alone or in combination with SST, CR or NPY (Miyoshi *et al*., 2010; Gelman *et al*., 2011). RLN^{+only} interneurons have been identified as late-spiking NGCs, residing in cortical layers I-III (Miyoshi *et al*., 2010; Lee *et al*., 2010).

Table 1.2 Classes of GABAergic interneurons in the mouse cortex. Modified from Fishell and Rudy, 2011. Schematics taken with permission from Markram *et al*., 2004.

Class	Morphology	Molecular marker	Firing pattern
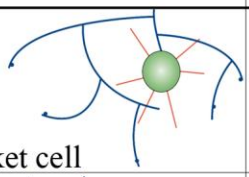 FS basket cell	Multipolar dendrites, dense local axon	PV	Fast-spiking (FS)
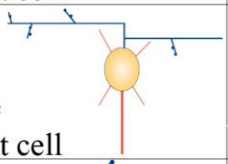 Large basket cell	Multipolar dendrites, axonal arborisations to upper and lower cortical layers	CCK	Burst-spiking or regular-spiking
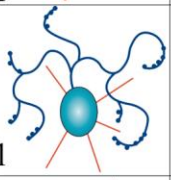 Small basket cell	Multipolar, bipolar, or bitufted dendrites, dense and highly-branching axons	CCK/VIP	Burst-spiking or regular-spiking
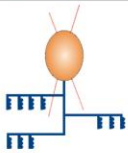 Chandelier cell	Multipolar or bitufted dendrites, highly branched axons with vertical rows of boutons	PV	Fast-spiking (FS)
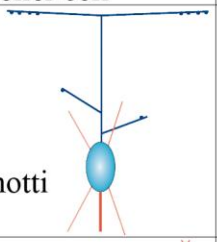 Martinotti cell	Axon ascends to layer I and forms dense arborisations	SST SST/CR	Low-threshold spiking (LTS)
 Bipolar cell	Small soma, dendrites extending up to layer I and down to VI	VIP	Fast-adapting or bursting
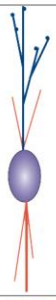 Bitufted cell	Bitufted dendrites arising from opposite ends of the soma, axons extending more widely compared to bipolar cells	VIP/CR	Irregular-spiking
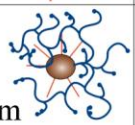 Neurogliaform cell	Multipolar, highly branched dendrites and axons	5HT3aR/ Reelin	Late-spiking

1.2.2 Hippocampal interneurons

The hippocampus comprises the evolutionarily oldest part of the cerebral cortex and anatomically it lies underneath the six-layered neocortex. Therefore, it is not surprising that similarly to their neocortical counterparts hippocampal interneurons are generated in the GEs of the subpallium and have to migrate long distances to reach their final position in the hippocampus (Pleasure *et al.*, 2000; Fogarty *et al.*, 2007; Gelman *et al.*, 2009; Tricoire *et al.*, 2011). Typically, classification of hippocampal interneurons is based on the same criteria used for cortical interneurons; that is, neurochemical content, morphology, synaptic targets and firing patterns, with at least 21 classes of hippocampal interneurons described in the CA1 subfield (reviewed in Klausberger and Somogyi, 2008).

Interestingly, there are both interneuron subtypes unique to the hippocampus and interneurons that share many properties (functional and lineal) in common with their cortical counterparts. Similarities between hippocampal and neocortical interneurons include the presence of PV^+ and CCK^+ BCs, and also the oriens-lacunosum moleculare (O-LM) cells. The expression of SST in O-LM cells, combined with the extension of long axons targeting distal apical dendrites and their physiological properties all point to an analogy with Martinotti cells of the neocortex (Tricoire *et al.*, 2011; reviewed in Fishell and Rudy, 2011). However, homology between neocortical and hippocampal interneurons is in some cases ambiguous. For example, although neurogliaform cells of the neocortex and the hippocampus share common morphological features and functions, the hippocampal cells express nNOS and are in their majority derived from the MGE, as opposed to the CGE origin of neocortical neurogliaform cells (Tricoire *et al.*, 2010; reviewed in Fishell and Rudy, 2011).

1.2.3 Striatal interneurons

The majority of neurons in the striatum consist of medium-sized spiny projection neurons (MSNs), whereas interneurons comprise a mere 2-3% of the striatal neuronal population in rodents (Rymar *et al.*, 2004). Striatal interneurons are further subdivided into cholinergic and GABAergic cells (reviewed in Kawaguchi *et al.*, 1995) and both of these neuronal types are derived from the MGE, similarly to most cortical interneurons. Specifically, they are derived from *Nkx2.1*$^{+}$ MGE progenitors (Marín *et al.*, 2000; Nóbrega-Pereira *et al.*, 2008), which upon exit from the cell cycle will express the LIM-HD transcription factors LHX6 and LHX7. Precursors that maintain LHX6 differentiate into GABAergic striatal interneurons, and conversely, precursors that express LHX7 and ISLET-1 will downregulate LHX6 and become cholinergic striatal interneurons (Fragkouli *et al.*, 2009; Lopes *et al*., 2012; section 1.4.2 herein).

GABAergic interneurons comprise about 2% of the total striatal population (Rymar *et al.*, 2004) and based on their neurochemical content they are organised into PV^{+} cells, CR^{+} cells, or cells expressing SST, NPY and nNOS (reviewed in Kawaguchi *et al.*, 1995 and Tepper and Bolam, 2004). Each of these molecularly and morphologically distinct groups of striatal interneurons present different firing properties and play unique roles in the function of the striatum, their main task being to modulate the firing pattern of MSNs (reviewed in Tepper and Bolam, 2004).

Cholinergic interneurons, despite representing only 0.3% of striatal interneurons, are easily identified by their large cell bodies. They are characterised by expression of choline acetyltransferase (ChAT), the enzyme that catalyses the rate limiting step in acetylcholine (Ach) synthesis. They receive input from the thalamus and cortex but also from the substantia nigra of the midbrain, and primarily innervate MSNs but also GABAergic interneurons (reviewed in Tepper and Bolam, 2004).

1.3 Development of cortical interneurons

Development of cortical interneurons is a complex and protracted process starting at early embryogenesis with proliferation of progenitors in the GEs of the ventral telencephalon, followed by tangential migration of specified, post-mitotic precursors, acquisition of the appropriate laminar position, terminal differentiation and integration into circuits within the postnatal cortex (Batista-Brito and Fishell, 2009). Each of these developmental steps is crucial for the formation of functional cortical networks and will be discussed in detail in the following paragraphs.

1.3.1 Ventral telencephalic origin of cortical interneurons

In contrast to pyramidal neurons, which are born in the VZ of the pallium and migrate radially, cortical interneurons are generated in the GEs of the subpallium and reach the cortex via tangential migration. The very first evidence for the existence of non-radially oriented cells in the cortex was based on morphology and came from Golgi stainings and electron microscopy studies (reviewed in Marín and Rubenstein, 2001). The presence of tangentially positioned cells in the cortex was subsequently confirmed by retroviral labeling experiments, cell dispersion studies in X-inactivated mosaics, DiI labelling in brain slice cultures and BrdU birthdating experiments (reviewed in Marín and Rubenstein, 2001).

Insight into the origin of these neurons that were positioned perpendicularly to the cortical radial glia came first from the work of de Carlos and colleagues, which showed that focal injection of lipophilic tracers into the LGE of live rat embryos resulted into tracing of labelled cells within the cortex (de Carlos *et al.*, 1996). Employing the same experimental approach in embryos *in vivo* and embryonic brains *in vitro* (Tamamaki *et al.*, 1997) or brain slices maintained in culture (Anderson *et al.*, 1997a) produced similar results. Importantly, Anderson *et al.* not only established that

GABAergic interneurons are born in the ventral telencephalon and migrate tangentially towards the cortex but also provided genetic evidence for the requirement of *Dlx1/2* in this process: examination of brain slices from *Dlx1*$^{-/-}$;*Dlx2*$^{-/-}$ mutants revealed no detectable movement of cells from the LGE to the cortex at embryonic stages and a greatly reduced number of GABA^{+} neurons in the neonatal cortex (Anderson *et al.*, 1997a). Further genetic loss of function analyses of transcription factors expressed in the early MGE and/or LGE came in support of the Anderson findings. The total GABAergic population of *Nkx2.1*$^{-/-}$ cortices was almost halved in size by E18.5 (Sussel *et al.*, 1999) and loss of *Mash1* function also resulted in a 50% reduction of the GABA^{+} cortical population (Casarosa *et al.*, 1999).

Finally, further studies revealed that radially and tangentially migrating cells in the cortex actually belong to separate lineages and additionally demonstrated that radially positioned neurons express glutamate, whereas tangentially migrating cells are GABAergic (Mione *et al.*, 1997; Tan *et al.*, 1998). Again, work by Anderson and colleagues unequivocally established *in vivo* that cortical projection neurons and interneurons arise from the cortex and the subcortical telencephalon, respectively. In detail, focal injections of [^{3}H] thymidine into the VZ of the neocortex of P1 ferrets resulted almost exclusively in the labelling of glutamatergic projection neurons, whereas injections into the striatal VZ labelled GABAergic interneurons and not vice versa (Anderson *et al.*, 2002).

The genetic and experimental evidence mentioned above provided solid proof for the ventral telencephalic origin of cortical interneurons and in the same time paved the way for the discovery that GABAergic neurons are in fact generated in multiple subpallial regions. Subsequently, a plethora of transplantation studies and genetic fate-mapping experiments established the exact spatial and temporal origins of every interneuron subtype, as well as the percentages of interneurons generated from each

region. It is now widely accepted that the vast majority of cortical interneurons originate in three subpallial progenitor areas, namely the MGE, CGE and POA (Figure 1.3; reviewed in Gelman and Marín, 2010).

1.3.1.1 The MGE is the main source of cortical interneurons

The MGE contributes to the generation of the majority, nearly 60%, of interneurons in the mouse cortex and in particular it gives rise to the PV^+ and SST^+ subsets (Figure 1.3; Butt *et al.*, 2005; Fogarty *et al*., 2007; Miyoshi *et al*., 2010).

Initial evidence for a population of MGE-derived GABAergic interneurons came from lipophilic tracer studies (Lavdas *et al.*, 1999; Anderson *et al.*, 2001; Jimenez *et al.*, 2002), while subsequent work shed more light on the molecular identity of these neurons. The transplantation experiments of Anderson *et al*. using BrdU labelled MGE neuroepithelium revealed coexpression with CB in tangentially migrating cells (Anderson *et al.*, 2001) and *in vivo* grafting of MGE cells labelled with human placental alkaline phosphatase (hPLAP) showed coexpression with PV, SST or CR in the neocortex of adult animals (Wichterle *et al.*, 2001). *In vitro* transplantation of dissociated, E12.5-E16.5, MGE-derived cells onto P0 cortical feeders resulted in the generation of PV^+ and SST^+ interneurons after 28 days in culture (Xu *et al.*, 2004) and similar results were obtained from the ultrasound-guided transplantation studies of Butt and colleagues: E13.5 MGE transplants were homotopically grafted into host embryos *in vivo* and their fate was examined at P21, revealing differentiation mainly into PV^+ and SST^+ neurons. These cells were preferentially located in deep cortical layers and their firing properties and morphology were in accordance to their biochemical profile (Butt *et al.*, 2005). In support of these findings, heterotopic and heterochronic transplantation of dissociated E12.5-E13.5 MGE donor cells into the cortex of P3-P4 pups also demonstrated differentiation of the grafted cells into PV^+ and SST^+ neurons

one or two months later (Alvarez-Dolado *et al.*, 2006). Interestingly, transplantation experiments using only dorsal or ventral parts of the MGE indicate a preferential generation of SST^+ and PV^+ cells respectively (Figure 1.3; Flames *et al*., 2007; Wonders *et al.*, 2008) and suggest that the MGE could possibly be further subdivided into distinct progenitor domains. In summary, the above findings argue that some aspects of cortical interneuron identity are already specified at the progenitor level, before these cells reach the cortex.

Genetic fate mapping based on the Cre-Lox technology came in support of the MGE transplantation results. Two different *Nkx2.1-Cre* transgenic lines were used in two independent studies, both of which concluded that the MGE produces primarily PV^+ and SST^+ interneurons, whereas its contribution to CR^+ and NPY^+ cells is significantly smaller (Fogarty *et al*., 2007; Xu *et al*., 2008). By using the *Nkx6.2-Cre* line, which labels the dorsal MGE, Fogarty *et al*. showed that this subdivision of the MGE generates larger numbers of CR^+ and NPY^+ interneurons compared to the most ventral $Nkx2.1^+$ domain (Fogarty *et al*., 2007). In addition, fate mapping of the *Lhx6-Cre* lineage revealed a 100% contribution to the PV-, SST- and CB-expressing populations and a smaller contribution to CR- and NPY-expressing cells (Fogarty *et al*., 2007). Similarly, by targeting the $Olig2^+$ domain of the MGE, Miyoshi *et al*. established that 50% of the generated interneurons at both early and late time points belong to the PV^+ fast spiking subset and 30% of the fate mapped cells are $SST^+;CR^-$ Martinotti interneurons, born only at early time points (E9.5-E12.5). On the contrary, $SST^+;CR^+$ cells were generated mostly at later stages, around E15.5 (Miyoshi *et al*., 2007). In particular, $SST^+;CR^+$ interneurons are mainly generated from the $Nkx6.2^+$ dorsal MGE domain (Fogarty *et al*., 2007; Sousa *et al*., 2009).

Finally, genetic loss of function studies confirmed that MGE-expressed transcription factors are critical for the specification of PV^+ and SST^+ character.

Primary cultures or MGE transplants from *Nkx2.1*$^{-/-}$ mutants failed to generate any cells expressing PV, SST, or NPY after several weeks *in vitro* (Xu *et al.*, 2004) and conditional deletion of *Nkx2.1* in *Olig2*-expressing MGE precursors resulted in a fate switch of PV- and SST-expressing interneurons into VIP$^+$ and CR$^+$ cells (Butt *et al*., 2008), which are of CGE origin (section 1.3.1.2). Downstream of NKX2.1, *Lhx6* is also critical for the specification of MGE-derived interneurons, as *Lhx6*-deficient mice show dramatic reductions in the number of PV$^+$ and SST$^+$ interneurons (Liodis *et al*., 2007; Zhao *et al*., 2008; section 1.4.3). Moreover, *Sox6* functions genetically downstream of LHX6 to control primarily the differentiation of PV$^+$ interneurons (Batista-Brito *et al*., 2009) and similarly, *Dlx5/6* activity is also required for the differentiation of these cells (Wang *et al*., 2010).

1.3.1.2 The CGE as a source of cortical interneurons

The CGE is the second largest source of GABAergic interneurons, contributing to the generation of about 30% of the total interneuronal population of the cortex, mainly generating RLN$^+$, CR$^+$ and VIP$^+$ interneurons (Figure 1.3; Miyoshi *et al*., 2010; Rubin *et al*., 2010).

The pioneering work of Nery *et al*. was the first to provide evidence that the CGE constitutes a progenitor region molecularly distinct from the MGE and LGE, producing interneurons with unique characteristics. After homotopic/isochronic transplantation of CGE cells, large cohorts of cells were seen migrating out of the CGE following posterior routes towards the cortex and hippocampus and importantly, transplanted cells within the cortex were identified as interneurons by the expression of GABA, SST and CB (Nery *et al*., 2002). Further transplantation studies, either *in vitro* from E14.5 CGE donors (Xu *et al*., 2004) or *in utero* from E13.5 and E15.5 CGE tissue (Butt *et al.*, 2005) established that the main interneurons generated from this region are

CR^+ cells. Notably, generation of cortical interneurons from the CGE is temporally regulated: at E13.5 the CGE contributes almost equally to CR^+, VIP^+ and NPY^+ RSNP interneurons with bipolar, bitufted, or double bouquet morphology, whereas at E15.5 the main contribution is towards CR-expressing bipolar RSNP cells (Butt *et al.*, 2005).

Inducible (Miyoshi *et al*., 2010) and subtractive (Rubin *et al*., 2010) genetic fate mapping of the CGE revealed that generation of cortical interneurons starts and peaks with a delay of 3 days compared to the MGE. Moreover, the same studies proved that, in contrast to their MGE counterparts, CGE-derived cells preferentially occupy upper cortical layers (Butt *et al*., 2005; Miyoshi *et al*., 2010; Rubin *et al*., 2010) irrespective of their birthdate (Miyoshi *et al*., 2010; Miyoshi and Fishell, 2011). The majority of interneurons generated in both studies correspond to VIP^+ and $RLN^+;SST^-$ cells.

Interestingly, the transcription factors directing the specification of CGE-derived interneurons are beginning to be elucidated. Genetic loss of function data for CGE-expressed genes indicate a role for *Dlx1/2* in the specification of CGE interneurons, as *Dlx1*$^{-/-}$*;Dlx2*$^{-/-}$ cortical cultures are almost completely devoid of CR^+ bipolar cells (Xu *et al*., 2004). Moreover, examination of mutants deficient for the SHH signalling effector Smoothened, revealed an upregulation of GSX2 in MGE progenitors and a concomitant production of CR^+ bipolar interneurons by these cells, indicating that GSX2 can instruct the specification of CR^+ cells characteristic of the CGE (Xu *et al*., 2010b). This was further proved by examination of *Gsx2* conditional mutants, which demonstrated a dramatic reduction in the number of $CR^+;SST^-$ interneurons (Xu *et al*., 2010b). Surprisingly, although COUP-TFII is enriched in the CGE (section 1.1.5.2), analysis of the first COUP-TFII mutant mice did not reveal any significant differentiation defects of CR^+ or VIP^+ CGE-derived cortical interneurons (Tang *et al*., 2012). Similarly, although the expression of the transcription factor SP8 marks a subpopulation of CGE-derived RLN^+, VIP^+ and bipolar CR^+ interneurons, examination of *Dlx5/6-Cre;Sp8-flox*

and *Nestin-Cre;Sp8-flox* conditional mutants showed no overall change in the number or distribution of these cells (Ma *et al*., 2012).

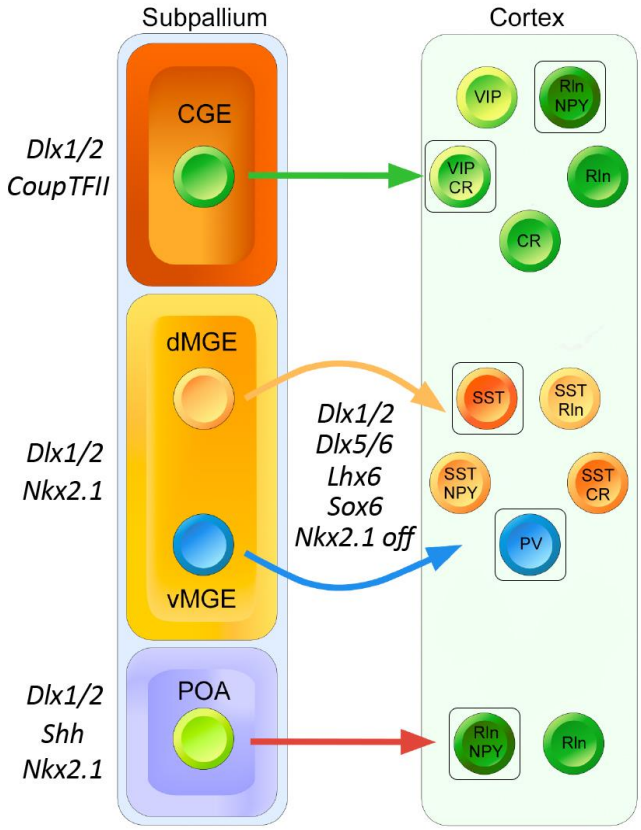

Figure 1.3 Contribution of ventral forebrain progenitor regions to the various interneuron subsets in the cortex. The MGE is the major source of cortical interneurons, with its dorsal and ventral regions preferentially generating SST^+ and PV^+ cells respectively. One of the main subsets arising from the CGE is that of bitufted or bipolar $VIP^+;CR^+$ interneurons. The CGE also contributes to the $RLN^+;NPY^+$ population of multipolar interneurons, along with the POA. These four major cortical interneuron subsets are depicted within black boxes. Each progenitor region is characterised by the expression of a unique set of transcription factors and can be further subdivided into smaller progenitor groups, not illustrated here for simplicity reasons. Modified with permission from Gelman *et al*., 2012.

1.3.1.3 The POA generates several subsets of cortical interneurons

Recent studies provided evidence that the POA represents the third major region of cortical interneuron generation, producing the remaining 10% of the GABAergic neurons in the mouse cortex (Figure 1.3; Gelman *et al.*, 2009; Gelman *et al.*, 2011).

Fate-mapping of a small population of dorsal POA cells (pPOA1), using the *Nkx5.1-Cre* mouse line showed that this region generates up to 4% of the total cortical interneuron population. It gives rise to NPY^+ and/or RLN^+ cells with multipolar morphology and rapidly adapting firing properties (Gelman *et al.*, 2009), resembling CGE derived interneurons (Miyoshi *et al.*, 2010). Another progenitor domain of the POA (pPOA2), mapped by using the *Dbx1-Cre* line, generates a wide diversity of GABAergic interneurons: 50% and 25% of the labelled cells are PV^+ and SST^+ respectively, which are however molecularly distinct from MGE-derived interneurons since most of the $Dbx1^+$ POA-derived cells do not express LHX6. Moreover, 15% of the $Dbx1^+$ progeny in the POA express RLN and a few cells were found to coexpress CR, nNOS or VIP (Gelman *et al.*, 2011). Taken together, these findings highlight a novel and significant contribution of the POA in the generation of cortical interneuron diversity. The mechanisms that specify POA interneuron identity remain elusive.

1.3.1.4 The LGE as a source of cortical interneurons

Although multiple studies have established the LGE as a source for olfactory bulb interneurons (Wichterle *et al*., 2001; Toresson and Campbell, 2001; Stenman *et al.*, 2003; Kohwi *et al.*, 2007), its contribution to the tangentially migrating population of cortical interneurons remains controversial, albeit not totally ruled out.

The detection of labelled cells within the LGE in the pioneering studies on cortical interneuron migration (de Carlos *et al.*, 1996; Tamamaki *et al.*, 1997; Anderson *et al.*, 1997a; section 1.3.1 herein) led to the assumption that the LGE is the main source

of cortical interneurons. Later on, although the MGE was established as the major site contributing to cortical interneurons (Wichterle *et al.*, 1999 and 2001; Anderson *et al.*, 2001), several studies suggested that the LGE still contributes to this population of cells. A few examples deserve mention: DiI tracing on rat brain slices with excised MGEs still shows robust migration to the pallium (Jimenez *et al.*, 2002) and BrdU labeling in mice indicates that during later stages of neurogenesis the LGE produces a small number of cells that migrate to the cortex via the SVZ and express GABA (Anderson *et al.*, 2001). Moreover, *Nkx2.1*$^{-/-}$ mutants, although lacking normal MGE tissue, exhibit a recovery of tangential migration by E16.5, in further support of the hypothesis that the LGE contributes to cortical interneurons at late embryonic stages (Anderson *et al.*, 2001). However, the above findings have been challenged by the fact that many of the observed cells are actually MGE-derived interneurons that migrate through the LGE on their way to the cortex (Lavdas *et al.*, 1999; Wichterle *et al.*, 1999 and 2001; Jimenez *et al.*, 2002).

The idea that the LGE contributes to cortical interneurons remains disputable due to the lack of molecular markers or genetic approaches to specifically target it and fate-map its derivatives. Although subtractive fate-mapping experiments have successfully targeted the LGE and CGE (Rubin *et al.*, 2010), future studies that will exclusively labell the LGE will certainly prove informational. Recently, the combinatorial expression of SP8 and COUP-TFII was used to mark a group of dLGE cells, which migrate towards the cortex (Cai *et al.*, 2013). The same study, provided further evidence for the contribution of the dLGE to cortical interneurons by showing that brain slice cultures that contained the LGE but not the CGE generate SP8^{+};COUP-TFII^{+} cells in the cortex. Importantly, their findings argue against the possibility that these cells migrate from the MGE or that they are misrouted OB interneurons (Cai *et al.*, 2013).

1.3.1.5 Other sources of cortical interneurons

The possibility that the septum is a potential source of cortical interneurons was raised by reports of GABAergic neurons migrating from the septal/retrobulbar area rostrally towards the olfactory bulb and then dorsally into the neocortex both in rats (Meyer *et al*., 1998) and mice (Anderson *et al*., 1999). Time-lapse imaging (Ang *et al*., 2003) as well as analysis of *Vax1*-deficient mice, which show severely reduced migration from the septum and significant lack of cortical interneurons (Taglialatela *et al*., 2004) provided further support to this hypothesis. However, these findings could be attributed to the widespread *Vax1* expression in the GEs of the ventral telencephalon and to the fact that *Vax1*$^{-/-}$ mutants have reduced expression of *Dlx*, which is required for cortical interneuron migration (section 1.3.3.1), in the MGE (Taglialatela *et al*., 2004). Indeed, more recent lines of evidence, based on genetic fate mapping using the septum-specific *Zic4-Cre* line, suggest that the septal region does not contribute to any of the cortical interneuron subsets (Rubin *et al*., 2010).

The cortex itself was put forward as a likely site of cortical interneuron origin based on observations in humans (Letinic *et al*., 2002; Fertuzinhos *et al*., 2009) and higher non-human primates (Petanjek *et al*., 2009). However, the latest studies in the field argue against this idea and highlight the developing human and monkey GEs as the main sources of cortical GABAergic interneurons (Ma *et al*., 2013; Hansen *et al*., 2013). Neuronal precursors in the human and monkey GEs share expression of common transcription factors with their mouse counterparts, such as NKX2.1, COUP-TFII and SP8, and streams of migrating interneurons emerging from the MGE and travelling towards the cortex have been observed (Ma *et al*., 2013; Hansen *et al*., 2013), again in similarity to mice. Importantly, cell fate analyses proved that most cortical interneurons in the primate cortex express the same transcription factors that were identified in the GEs, providing further evidence for their ventral origin (Ma *et al*., 2013; Hansen *et al*.,

2013). In rodents, cortical progenitor cultures have been shown to generate $GABA^+$ cells (Götz *et al*., 1995; Xu *et al*., 2004), however these results should be interpreted bearing in mind that some of these cultures contained FGF, which is a ventralising factor (Gabay *et al*., 2003; Pollard *et al*., 2008). In contrast, more recent fate-mapping studies of cortical progenitors and their descendants, using the *Emx1-Cre* line (Gorski *et al*., 2002), have failed to demonstrate generation of cortical GABAergic interneurons from the pallial proliferative zones (Gorski *et al*., 2002; Kohwi *et al*., 2007). Overall, no definitive conclusions have been drawn on the contribution of pallial progenitors in cortical interneuron generation in either humans or rodents.

1.3.2 Specification of cortical interneurons

The mechanisms by which interneuron diversity is established have been in the centre of cortical development studies for years and recent findings have provided critical insight into this process. Several lines of evidence suggest that cortical interneuron identity is specified at the progenitor level within the GEs and importantly, it is assigned by both the spatial and temporal origin of the cell.

In analogy to the spinal cord (Jessell, 2000), multiple progenitor pools defined by the combinatorial expression of transcription factors exist in the ventral forebrain in the form of GEs and every GE can be further divided into subdomains expressing different sets of transcription factors. Each of these domains generates specific interneuron subtypes (reviewed in Gelman and Marín, 2010) and the transplantation and genetic studies described in sections 1.3.1.1 - 1.3.1.3 come in support of this concept. Another similarity with neuronal specification in the spinal cord is that the GEs are responsive to SHH. In fact, the levels of SHH signalling directly influence the identity of an interneuron, with high levels of SHH directing the generation of SST^+ rather than PV^+ cells (Xu *et al*., 2010b). Moreover, *Nkx2.1* has been shown to promote MGE fate

and simultaneously repress LGE and CGE fates (Butt *et al*., 2008), similar to how homologous homeobox genes specify cell fates in the spinal cord. Additional findings suggest that interneuron diversity can also arise from changes in temporal competence of progenitors within the same region. Studies from the Fishell group have elucidated this process by establishing that, both in the MGE (Miyoshi *et al*., 2007) and CGE (Butt *et al*., 2005), molecularly and electrophysiologically distinct interneurons arise at early versus late embryonic time points (sections 1.3.1.1 and 1.3.1.2).

Finally, a breakthrough clonal analysis study of the MGE and POA progenitor zones has provided novel insight into the intrinsic mechanisms underpinning cortical interneuron identity. Retroviral labelling of the *Nkx2.1*$^{+}$ neuroepithelium of the ventral forebrain demonstrated that cortical interneurons are clonally related. Clonally labelled cells were grouped together in vertical or horizontal clusters in the adult brain. In some of these clusters all interneurons expressed the same neurochemical marker, yet in other clusters different markers (PV and SST) were detected in different cells (Brown *et al*., 2011). Hence, confirmation now exists that cortical interneuron subtypes derived from a common progenitor are clonally related.

1.3.2.1 Modulation of the genetic program of interneuron specification by the cortical environment

The hypothesis that the cortical microenvironment can have an impact on certain aspects of the development of GABAergic interneurons was formulated by the Fishell group, not long ago. According to this hypothesis, although several aspects of cortical interneuron identity, such as neurochemical content, are specified at the progenitor level by genetic programs within the GEs, other aspects, such as synaptic connectivity for example, are specified by the influence of the postmitotic environment exerted upon the developmental program initiated in progenitors (Batista-Brito and Fishell, 2009).

Recent lines of evidence from the same group come in support of this idea by demonstrating that neuronal activity influences the development of specific interneuron subtypes, namely the RLN^+ and CR^+ CGE-derived cortical interneurons (De Marco García *et al*., 2011). By temporally regulating the expression of the inward rectifying potassium channel Kir2.1, which lowers the resting membrane potential of a cell (Yu *et al*., 2004), neuronal activity was attenuated selectively in cortical interneurons of the CGE, highlighting two critical functions during CGE interneuron development: between P0-P3 activity regulates laminar positioning of RLN^+ and CR^+ cells within the cortex, whereas from P3 onwards activity, through glutamate receptors, controls the morphological development of these cells by influencing the extent of axonal arborisation and dendritic tree complexity (De Marco García *et al*., 2011).

1.3.3 Migration of cortical interneurons

Migration of cortical interneurons unfolds in three sequential steps. First, GABAergic interneurons migrate tangentially from the GEs towards the cortex following defined migratory streams. Second, they disperse within the cortex via established routes in different compartments, mainly in the MZ as well as in the lower intermediate zone (IZ) and SVZ. Finally, they switch to a radial mode of migration and enter the cortical plate (reviewed in Métin *et al*., 2006).

Following the initial studies that identified the MGE as a source of cortical interneurons (Lavdas *et al.*, 1999; Wichterle *et al.*, 1999 and 2001; Anderson *et al.*, 2001), time-lapse microscopy imaging of intact embryos or brains and telencephalic slice cultures has revealed a major stream of interneurons, emanating from the MGE and migrating laterally and dorsally towards the cortex (Ang *et al*., 2003; Yozu *et al*., 2005). A second group of interneurons arises from the CGE and migrates caudally to reach the cortex and hippocampus (Nery *et al*., 2002; Yozu *et al*., 2005), forming what

is known as the caudal migratory stream (CMS). Finally, a third cohort of migrating interneurons arises from the LGE and moves rostrally to populate the olfactory bulb (Wichterle *et al.*, 1999 and 2001).

Based on studies of the lateral-medial migratory stream from the MGE it is now known that the first interneurons enter the cortex just after E12 at the level of the PP (Lavdas *et al*., 1999; Tanaka *et al*., 2003; Ang *et al*., 2003; Yozu *et al*., 2005). Shortly after, at around E13.5 when the PP is split into the MZ and the SP by the forming CP, two cohorts of tangentially migrating interneurons are observed: the group of cells that entered the cortex first is still visible in the MZ, although the major contribution now comes from interneurons entering the cortex from the lower IZ/SVZ (Lavdas *et al*., 1999; Anderson *et al*., 2001; Tanaka *et al*., 2003; López-Bendito *et al*., 2004).

Within the MZ, interneurons move in multiple directions (Ang *et al*., 2003; Tanaka *et al*., 2003, 2006 and 2009) in an unpredictable manner termed "random walk" (Tanaka *et al*., 2009). It is suggested that this phase of multidirectional migration allows interneurons to disperse in the cortex and possibly sense the environment for cues that will direct them to their appropriate position within the CP (Tanaka *et al*., 2003, 2006 and 2009). After this waiting period in the MZ, these cells will extend their leading process towards the CP and descend into it (Polleux *et al*., 2002; Ang *et al*., 2003). Similarly, interneurons travelling in the lower IZ/SVZ will also enter the CP, either directly (Polleux *et al*., 2002; Nadarajah *et al*., 2002) or after migrating into the VZ first (Nadarajah *et al*., 2002). This final "cortical integration stage" involves a switch to a radial mode of migration (Polleux *et al*., 2002; Ang *et al*., 2003; Tanaka *et al*., 2003).

1.3.3.1 Regulation of tangential migration into the cortex

Given the remarkable distance that GABAergic interneurons have to travel in order to reach their final destination in the pallium, their migration must be tightly

regulated to ensure correct organisation and thus function of the cortex. This critical task is undertaken by transcription factors expressed in migrating interneurons, motogenic factors, and guidance molecules that pilot cells through the appropriate paths (Figure 1.4).

Transcription factors controlling tangential migration of cortical interneurons include NKX2.1, DLX1/2, LHX6 and ARX. Control of telencephalic interneuronal migration by NKX2.1 provides an elegant example whereby a transcription factor directly regulates the expression of a guidance molecule. Specifically, NKX2.1 binds to regulatory elements of the *Neuropilin-2* (*Nrp2*) locus and represses its expression in striatal interneurons, thus allowing them to enter the *Semaphorin*-expressing striatum, as NRP2 is the receptor for the repulsive molecule Semaphorin 3F. Conversely, postmitotic cortical interneurons downregulate *Nkx2.1*, therefore express *Nrp2*, respond to the chemorepellent action of the striatum and deflect towards the cortex (Nóbrega-Pereira *et al*., 2008). An analogous role has been described for DLX1 and DLX2 in directly repressing *Nrp2* expression (Le *et al*., 2007). In fact, evidence suggests that the reduced tangential migration to the cortex of *Dlx1/2* double mutants (Anderson *et al*., 1997a) is due to aberrant expression of *Nrp2* in the mutant cells (Le *et al*., 2007). *In vivo* and *in vitro* work from several groups has highlighted an important role for the homeodomain transcription factor ARX in GABAergic interneuron migration (Kitamura *et al*., 2002; Colombo *et al*., 2007; Friocourt *et al*., 2008). Notably, it was demonstrated that *Arx* is a direct target of DLX2 and hence functions as a mediator of the *Dlx*-dependent interneuron migration program (Colasante *et al*., 2008). Finally, several studies have implicated the LIM-homeodomain transcription factor LHX6 in cortical interneuron migration (Alifragis *et al*., 2004; Liodis *et al*., 2007; Zhao *et al*., 2008), as will be described in section 1.4.3.

Motogenic factors expressed in the developing cortex include the hepatocyte

growth factor/scatter factor (HGF/SF) and the neurotrophins BDNF, NT4 and GDNF. In support of the idea that motogenic factors guide migrating cells towards the cortex, the receptors for these molecules, namely c-Met for HGF, TrkB for BDNF and NT4, GFRa1 for GDNF, are expressed in cortical interneurons (Powell *et al*., 2001; Polleux *et al*., 2002 and references therein; Pozas and Ibáñez, 2005). Slice culture and explant assays have established that HGF (Powell *et al*., 2001) and GDNF (Pozas and Ibáñez, 2005), both of which are expressed in the cortex and the proliferative zones of the GEs, can indeed increase the motility of tangentially migrating interneurons *in vitro*. Conversely, administration of exogenous HGF in culture (Powell *et al*., 2001) or loss of GDNF or GFRa1 activity *in vivo* (Pozas and Ibáñez, 2005) result in disrupted migration and reduced numbers of GABAergic cells in the cortex, respectively. Moreover, tangential migration is triggered by addition of BDNF or NT4 in MGE-cortex co-cultures, and impeded by the Trk receptor inhibitor K252a (Polleux *et al*., 2002). Finally, *TrkB*$^{-/-}$ mice exhibit reduced numbers of CB^{+} cells migrating to the cortex (Polleux *et al*., 2002). However, the reduced numbers of GABAergic cells observed in the above studies could in fact be due to impaired neuronal differentiation rather than decreased migration, as both GDNF (Pozas and Ibáñez, 2005) and BDNF (Fiumelli *et al*., 2000) have been shown to promote a GABAergic phenotype.

Guidance molecules play a fundamental role in cortical interneuron migration, by exerting both chemorepulsive and chemoattractant effects, guiding cells away from the ventral telencephalon and towards the cortex respectively (Figure 1.4).

One of the first challenges that migrating GABAergic interneurons face is to successfully pave their way to the pallium by avoiding the striatum. It is now established that the chemorepulsive guidance molecules Semaphorin 3A (Sema3A) and 3F (Sema3F) as well as their receptors NRP1 and NRP2 regulate this process (Marín *et al*., 2001). Sema3A/3F are expressed in the striatum, whereas migrating cortical

interneurons express NRP1/2 and are thus repelled to the cortex (Marín *et al*., 2001).

Another group of secreted chemorepulsive factors expressed in the basal telencephalon are the SLIT (SLIT1 and 2) glycoproteins (Yuan *et al*., 1999; Bagri *et al*., 2002). Their receptors, the ROBOs (ROBO 1, 2 and 3), are found within the cortex (Bagri *et al*., 2002; Andrews *et al*., 2008; Barber *et al*., 2009). Based on their expression pattern it was originally suggested that SLIT1/2 could be responsible for the chemorepulsive function of the POA (Marín *et al*., 2003). However, migration towards the cortex was not disrupted in *Slit1*$^{-/-}$;*Slit2*$^{-/-}$ compound mutants (Marín *et al*., 2003). Similarly, no cortical interneuron migration defects were observed in *Robo1*$^{-/-}$, *Robo2*$^{-/-}$ (Andrews *et al*., 2008) or *Robo3*$^{-/-}$ (Barber *et al*., 2009) single mutants. Compound loss of *Robo1*, *Robo2* and *Robo3* activity however resulted in a significant reduction in the number of interneurons within the cortex (Barber *et al*., 2009), pointing to compensatory actions of the three ROBO receptors in regulating cortical interneuron migration. These results should be interpreted with some caution though, since ROBOs also influence cell proliferation in the developing forebrain (Andrews *et al*., 2008; Barber *et al*., 2009) and the relationship between these factors and their ligands in controlling this process remains largely unknown.

Chemoattraction towards the cortex is mediated by Neuregulin-1 (NRG1) and one of its receptors, ErbB4, which is expressed in tangentially migrating interneurons (Flames *et al*., 2004). NRG1 comes in two isoforms, a membrane bound one (NRG1-CRD) found in a corridor of the LGE next to the *Semaphorin*-expressing striatum and a secreted one (NRG1-Ig) in the cortex (Flames *et al*., 2004). Specifically, NRG1-CRD-expressing cells form a permissive substrate for tangentially migrating interneurons allowing them to proceed towards the cortex, which in turn attracts them by expressing NRG1-Ig. Disrupting ErbB4 function *in vitro* renders migrating cells unresponsive to the attractant activity of the cortex and loss of ErbB4/NRG1 signalling *in vivo* results in

reduced GABAergic interneuron numbers in the pallium (Flames *et al*., 2004).

Recent evidence suggests that guidance of migrating interneurons in the IZ/SVZ and MZ paths of the cortex is mediated by chemokine signalling. CXCL12 (also known as stromal-derived factor 1, SDF-1) is a chemoattractant for interneurons, expressed in the meninges and the IZ/SVZ of the developing cortex (Stumm *et al*., 2003; Tiveron *et al*., 2006; López-Bendito *et al*., 2008). Its receptor CXCR4 is expressed in migrating interneurons in the same areas (Stumm *et al*., 2003; Tiveron *et al*., 2006; López-Bendito *et al*., 2008). Analysis of mutant mice that specifically lack CXCL12 in the IZ/SVZ but not in the MZ revealed an absence of migrating interneurons in the former route and a concomitant accumulation in the later (Tiveron *et al*., 2006). Moreover, interneurons in *Cxcr4*$^{-/-}$ mutants migrate preferentially *via* the CP rather than the established routes (Tiveron *et al*., 2006).

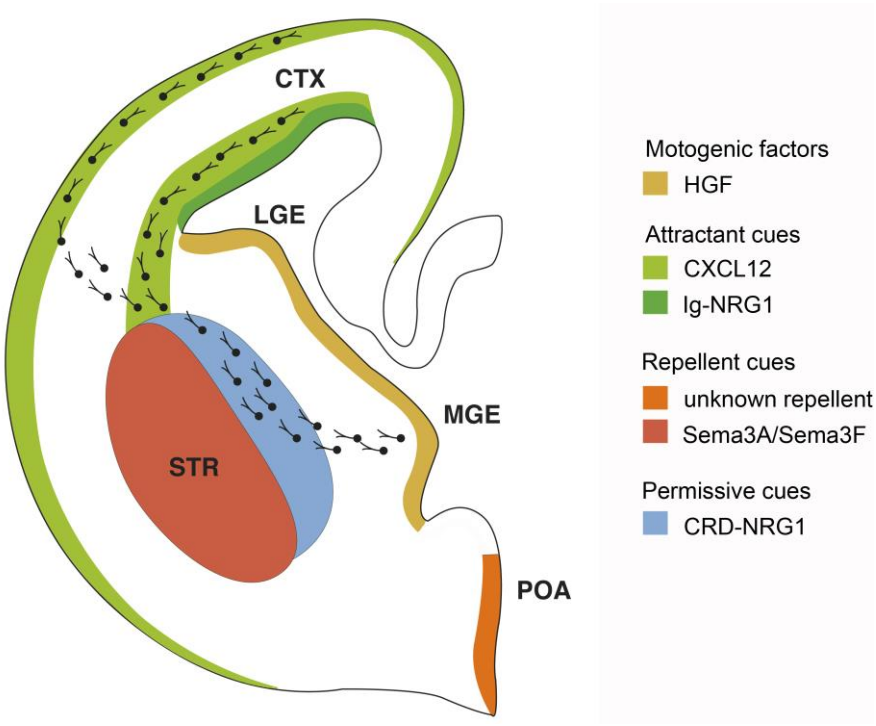

Figure 1.4 Guidance cues regulating tangential migration of cortical interneurons. Schematic representation of a coronal hemisection of the mouse forebrain depicting the tangential migration of cortical interneurons from the MGE to the cortex. MGE-derived interneurons are guided towards the cortex by motogenic factors in the MGE and chemoattractant cues in the cortex. A still unidentified repellent cue from the POA prevents these cells from migrating ventrally. Whilst in the subpallium, cortical interneurons are repelled from the striatum and use a permissive corridor of LGE cells instead, in order to advance to the cortex. Upon reaching the cortex, chemokines ensure that these cells will be restricted to the MZ and SVZ and motogenic factors aid their migration. CTX= cortex, STR= striatum, MGE= medial ganglionic eminence, LGE= lateral ganglionic eminence, POA= preoptic area. Schematic generated by Hayley Wood, NIMR photographics.

1.3.3.2 Transition from tangential to radial migration

Following entry into the cortex via the MZ and IZ/SVZ, tangentially positioned interneurons switch their orientation in oblique or perpendicular angles and invade the CP (Polleux *et al*., 2002; Ang *et al*., 2003; Tanaka *et al*., 2003 and 2009). The mechanisms underlying this critical step are just beginning to be elucidated.

CXCL12-CXCR4 signalling seems to be regulating this process, as analysis of *Cxcr4*$^{-/-}$ mutants demonstrated premature entry of interneurons into the CP and subsequent altered laminar positioning (López-Bendito *et al*., 2008). CXCR7, the second receptor for CXCL12, is also expressed in tangentially migrating interneurons in the cortical MZ and SVZ, along with CXCR4 (Tiveron *et al*., 2010; Sánchez-Alcañiz *et al*., 2011; Wang *et al*., 2011). Notably, CXCR7 expression is highly associated with interneurons entering the CP, suggesting that it could be acting to alter the responsiveness of cortical interneurons to CXCL12, and hence assist their exit from the MZ and SVZ (Tiveron *et al*., 2010). In fact, studies from the Marin group have demonstrated that loss of *Cxcr7* function in migrating interneurons renders them unresponsive to CXCL12, as CXCR7 is required to sustain the protein levels of CXCR4 (Sánchez-Alcañiz *et al*., 2011). Specifically, CXCR7 acts as a scavenger, to reduce excess CXCL12 in the cortex and prevent degradation of CXCR4 (Sánchez-Alcañiz *et al*., 2011). It is therefore, not surprising that *Cxcr7*-deficient mice show a similar phenotype to *Cxcr4*$^{-/-}$ mutants, with early entry of interneurons into the CP and altered layer distribution (Sánchez-Alcañiz *et al*., 2011; Wang *et al*., 2011). Interestingly though, CXCR4 and CXCR7 receptors regulate cortical interneuron migration via distinct functions: they activate different signalling pathways and have opposing actions in regulating cell motility and leading process morphology (Wang *et al*., 2011).

A potential role for the gap junction subunit Connexin 43 (CX43) has also been suggested in the switch between tangential and radial migration. Using a short hairpin RNA (shRNA) approach in rat brain slice cultures it was demonstrated that knocking down CX43 levels reduced the number of radially oriented cells in the cortex and resulted in an accumulation of cells close to the pial surface. Interestingly, the same study provided evidence for the existence of gap junctions between cortical radial glia and radially migrating interneurons (Elias *et al*., 2010).

1.3.3.3 Termination of cortical interneuron migration

Live imaging of brain slices from mice whose cortical interneurons are genetically labelled with GFP, documented that the speed of movement, and motility in general, decreased from late embryonic stages onwards and pausing frequency increased concomitantly. Migration ceased by P6-P7 for the majority of cells (Bortone and Polleux, 2009). In addition, it was demonstrated that the control of migration rate is intrinsically determined. Firstly, heterochronically plated immature interneurons onto mature cortical feeders *in vitro* did not show reduced rate of migration compared to isochronic controls and secondly, some interneurons responded to the addition of GABA by pausing, whereas others in the same culture remained unaffected (Bortone and Polleux, 2009). Interestingly, the potassium-chloride (K^+-Cl^-) cotransporter KCC2 was identified as the intrinsic factor that regulates termination of cortical interneuron migration in response to GABA (Bortone and Polleux, 2009).

KCC2 is a neuron-specific K^+- Cl^- exporter participating in the regulation of the Cl^- equilibrium potential, which in turn controls the response, depolarising or hyperpolarising, elicited by activation of ionotropic GABA receptors upon release of GABA (reviewed in Ben-Ari *et al*., 2007). During embryonic development and early postnatal life the intracellular Cl^- concentration is increased in immature interneurons due to high expression levels of the Na^+-K^+-$2Cl^-$ cotransporter NKCC1, which imports Cl^- into the cell, and thus generates a positive Cl^- equilibrium potential. Therefore, binding of GABA to ionotropic $GABA_A$ receptors results in discharge of Cl^- from the cell and membrane depolarisation. Conversely, mature neurons upregulate KCC2, which exports Cl^- from the cell, thus reverses the Cl^- equilibrium potential and renders GABA hyperpolarising (reviewed in Ben-Ari *et al*., 2007). In other words, KCC2 mediates the switch from excitatory GABA in immature neurons during development to inhibitory GABA in mature neurons (Rivera *et al*., 1999).

The above observations were incorporated by Bortone and colleagues in the following model for the termination of cortical interneuron migration: during embryonic stages when cells express low levels of KCC2, ambient GABA and glutamate act in concert, through $GABA_A$ and AMPA/NMDA receptors respectively, to induce interneuron depolarisation and Ca^{2+} influx via voltage-sensitive calcium channels (VSCCs) to promote cell motility. However, the upregulation of KCC2 later during development switches the action of GABA to hyperpolarising, resulting in less Ca^{2+} entering the cell and reduced interneuron motility. Finally, the influx of Ca^{2+} is further reduced due to a decrease of ambient glutamate, which also results in reduced AMPA/NMDA receptor activation, eventually driving migrating interneurons to a complete halt (Bortone and Polleux, 2009).

1.4 The LIM homeodomain transcription factor LHX6

LHX6 belongs to the LHX6/LHX7 group of LIM homeodomain (LIM-HD, otherwise known as LHX) transcription factors, which represent a subfamily of LIM domain proteins.

1.4.1 LIM domain proteins

The LIM domain was originally discovered in three homeodomain transcription factors, namely: **L**in-l1 of *C. elegans* (Freyd *et al*., 1990), **I**sl-1 of the rat (Karlsson *et al*., 1990) and **M**ec-3 of *C. elegans* (Way and Chalfie, 1988), hence the name **LIM**. This highly conserved cysteine- and histidine-rich domain consists of two tandem zinc-fingers (Figure 1.5, B; Michelsen *et al*., 1994; Pérez-Alvarado *et al*., 1994 and 1996; Konrat *et al*., 1997) and is involved in protein-protein interactions (Feuerstein *et al*., 1994; Schmeichel and Beckerle, 1994; Arber and Caroni, 1996).

LIM proteins are classified according to the N- or C-terminal position of their

LIM domains, the presence of other motifs such as homeodomains or PDZ domains and their subcellular localisation, which can be either nuclear or cytoplasmic (reviewed in Kadrmas and Beckerle, 2004). Nuclear LIM proteins control gene expression, while their cytoplasmic counterparts are involved in cytoskeletal organisation. Notably, some LIM proteins can shuttle between nucleus and cytoplasm upon stimulation from a signalling cascade (reviewed in Zheng and Zhao, 2007).

LIM-HD, otherwise known as LHX, proteins contain two N-terminally located tandem LIM domains followed by a C-terminal homeodomain (Figure 1.5, A), which confers DNA binding specificity (reviewed in Dawid *et al*., 1998). They are found exclusively in the cell nucleus, where they act as transcription factors: through their ability to interact with other proteins, either directly or via cofactors, they play fundamental roles in tissue-specific gene regulation and cell fate decisions. LHX proteins can be subdivided into six groups based on sequence conservation within their homeodomain. They exert their developmental functions in a multitude of systems, and irrespective of which group they belong to, they are all expressed in the nervous system, pointing to an evolutionarily conserved role in neural development, from nematodes to vertebrates (reviewed in Hobert and Westphal, 2000).

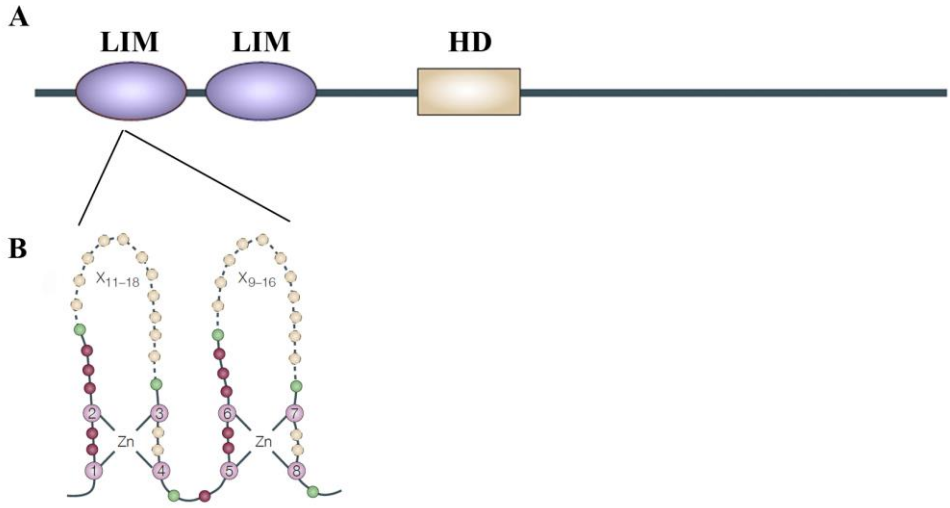

Figure 1.5 Domains of the LHX proteins. (A) Schematic representation of the domain structure of LHX proteins, which characteristically contain two N-terminal LIM domains, followed by a C-terminal homeodomain. **(B)** Schematic representation of the two tandem zinc-finger motifs of a LIM domain. Each LIM domain coordinates two Zn ions, with amino acid residues 1-4 binding the first Zn ion and residues 5-8 binding the second Zn ion. LIM= LIM domain, HD= homeodomain, Zn= zinc. Modified with permission from Kadrmas and Beckerle, 2004.

1.4.2 The LHX6/LHX7 group of LIM-HD proteins

Lhx6 and *Lhx7* (also known as *Lhx8*), the two vertebrate homologues of the LHX6/LHX7 group, were first identified by screening mRNA from mouse embryo enteric neuroblasts and a mouse head cDNA library. The overall amino acid sequence similarity of LHX6 and LHX7 is 75% and both proteins contain two LIM domains followed by a homeodomain. Initial RNA *in situ* hybridisation studies in the mouse embryo revealed that their expression patterns during development are highly overlapping, both in the first branchial arch and in the basal forebrain, suggesting a critical role in head development (Grigoriou *et al*., 1998).

Both Lhx6 and Lhx7 mRNAs are detected in the oral mesenchyme of the maxillary and mandibular process within the first branchial arch at E9.5-10.5 but are

excluded from the oral epithelium. During the course of odontogenesis their expression becomes progressively restricted to the mesenchyme of individual teeth and is finally downregulated by P2 (Grigoriou *et al*., 1998; Denaxa *et al*., 2009). Genetic loss of function studies using embryos deficient for both *Lhx6* and *Lhx7* highlighted a requirement for both of these genes for molar tooth development (Denaxa *et al*., 2009) as well as for normal cranial skeleton and palatal formation (Zhao *et al*., 1999; Mori *et al*., 2004; Denaxa *et al*., 2009).

Expression of *Lhx6* and *Lhx7* within the MGE starts at around E10.5 in the SVZ and mantle zone and is excluded from the adjacent LGE (Grigoriou *et al*., 1998). However, these two genes subsequently develop distinct expression patterns. *Lhx6* expression persists in GABAergic interneurons migrating out of the MGE and through the LGE towards the cortex as well as in mature cortical interneurons (section 1.4.3), whereas expression of *Lhx7* is restricted to the ventral telencephalon, in striatal cholinergic interneurons and cholinergic projection neurons of the basal forebrain (Asbreuk *et al*., 2002; Zhao *et al*., 2003; Fragkouli *et al*., 2005). Analysis of several different *Lhx7*-deficient mouse models demonstrated a requirement for LHX7 for the differentiation of these two types of cells (Zhao *et al*., 2003; Mori *et al*., 2004; Fragkouli *et al*., 2005). Moreover, recent studies established that loss of *Lhx7* function results in a respecification of cholinergic striatal interneurons into GABAergic cells, revealing a role of LHX7 in maintaining cholinergic identity in striatal interneurons (Fragkouli *et al*., 2009; Lopes *et al*., 2012).

Finally, *Lhx6* and *Lhx7* are also expressed in certain areas of the hypothalamus (Grigoriou *et al*., 1998) and *Lhx6* is implicated in the processing of reproductive odour signals in a pathway connecting the posterio-dorsal medial amygdalar nucleus with the reproductive hypothalamic nuclei (Choi *et al*., 2005).

Taken together, the above studies suggest fundamental roles of *Lhx6* and *Lhx7*

during multiple aspects of embryonic head development, from cranial skeleton and tooth development, to generation of specific CNS neuronal populations and the control of behavioural decisions.

1.4.3 The role of LHX6 in cortical interneuron development

As *Nkx2.1*$^{+}$ progenitors of the MGE exit the cell cycle, expression of *Lhx6* is induced by direct binding of NKX2.1 to the *Lhx6* promoter (Du *et al.*, 2008). From this point onwards, *Lhx6* expression is maintained in tangentially migrating interneurons of the IZ, SP and MZ (Lavdas *et al.*, 1999; Liodis *et al.*, 2007) as well as in differentiated interneurons of the postnatal cortex. Specifically, *Lhx6* is preferentially expressed in nearly 100% of MGE-derived interneurons of the PV^{+} and SST^{+} subtypes (Liodis *et al.*, 2007; Fogarty *et al.*, 2007), suggesting that it may have a key role in the development of MGE-derived sublineages of cortical interneurons.

The role of *Lhx6* in the specification, migration and differentiation of cortical interneurons has been analyzed by several groups, using a variety of *in vivo* and cell culture approaches. The first loss of function data for *Lhx6* came from small interfering RNA (siRNA) studies. Focal electroporation of an Lhx6 siRNA in the MGE of E13.5 mouse embryonic brain slices inhibited the tangential migration of GABAergic interneurons into the cortex. However, the same siRNA approach did not impede the production of GABA or its synthesizing enzymes GAD65/67 in dissociated MGE cultures (Alifragis *et al.*, 2004).

Subsequently, the generation of the first *Lhx6* mutant animals revealed a crucial role of LHX6 in the tangential and radial migration of GABAergic interneurons into the cortex and their differentiation into PV^{+} and SST^{+} cells. Although *Lhx6*$^{-/-}$ animals present a delay in the front of migration of GABAergic interneurons at embryonic stages, examination of their cortices at P15 revealed that the number of Gad1^{+} cells is

similar to wild types. However, their distribution into the various cortical layers is affected. Furthermore, *Lhx6*-null mutants display a severe reduction in both SST^+ and PV^+ interneuron numbers (93% and 89% respectively) and a less pronounced reduction (38%) in CR-expressing cells (Liodis *et al.*, 2007). The above findings suggest that *Lhx6* does not participate in the specification of the GABA phenotype of MGE progenitors, an observation that agrees with the findings of Alifragis and colleagues (Alifragis *et al.*, 2004), but rather it is essential for the migration and differentiation of interneurons into specific subtypes.

Independent work, using an *Lhx6* loss of function allele that expresses placental alkaline phosphatase (PLAP) has confirmed the observations of Liodis *et al*. $Lhx6^{PLAP/PLAP}$ mutants show defects in tangential migration and laminar positioning of cortical interneurons, as well as severe reductions in the PV^+ and SST^+ populations. This study also proves that LHX6 mediates these effects by controlling expression of factors implicated in interneuron migration and differentiation such as *Cxcr4* and *Arx* (Zhao *et al.*, 2008).

Although the above studies established the requirement of LHX6 for the differentiation of MGE-derived interneurons, they did not address the question of whether LHX6 is intrinsically required for this process or whether the differentiation defect is secondary to altered positioning of interneurons within the $Lhx6^{-/-}$ cortex. A recent study, using an $Lhx6^{LacZ}$ hypomorphic allele, proved that while a single copy of $Lhx6^{LacZ}$ is enough to rescue the cortical interneuron migration defect, it is not sufficient to restore the normal differentiation of SST^+ interneurons. On the contrary, the number and migration of PV^+ interneurons are unaffected in *Lhx6* hypomorphic mutants, meaning that low levels of *Lhx6* activity are sufficient to regulate PV^+ interneuron development but do not allow normal development of their SST^+ counterparts (Neves *et al.*, 2012). The same study also proposes that the SST^+ interneuron differentiation

defects lead to altered function of inhibitory dendritic synapses at the CA1 hippocampal field and subsequent development of epileptic seizures (Neves *et al.*, 2012).

On the whole, LHX6 is required intrinsically and in a dose dependent manner, for both the migration and differentiation of MGE-derived interneurons as well as the formation of functional inhibitory circuits.

1.4.3.1 Downstream effectors of LHX6 in cortical interneuron development

With the role of LHX6 in cortical interneuron differentiation well-established, recent studies have set out to identify effector genes that act downstream of LHX6 in this process.

The first gene described to function genetically downstream of LHX6 was *Sox6*, which regulates the laminar positioning and differentiation of cortical interneurons, predominantly of the PV^+ subtype (Batista-Brito *et al.*, 2009). *Sox6* is expressed in MGE-derived interneurons (Batista-Brito *et al.*, 2009; Azim *et al.*, 2009) with an expression pattern closely resembling that of *Lhx6* and similarly to *Lhx6*$^{-/-}$ animals, *Sox6*-deficient mice exhibit defects in the differentiation of PV^+ and SST^+ interneurons (Batista-Brito *et al.*, 2009; Azim *et al.*, 2009). Notably, the PV^+ subset was more severely affected than the SST^+ one, indicating that SOX6 is required predominantly for PV-expressing interneuron differentiation (Batista-Brito *et al.*, 2009).

Interestingly, a recent genome-wide gene expression profiling study, conducted in our laboratory, on dorsal forebrain tissue from E15.5 *Lhx6*$^{-/-}$ mutants and control littermates identified several genes downstream of LHX6 (Denaxa *et al.*, 2012). Among these genes, *Satb1* (special AT-rich sequence binding protein 1) presents great interest.

1.5 The genome organiser protein SATB1

Satb1 was first cloned from a human testis cDNA library and was found to be predominantly expressed in thymocytes, although low levels of Satb1 transcripts were also detected in the testis and the brain (Dickinson *et al.*, 1992). Its mouse homolog was isolated from a thymus cDNA library shortly after (Nakagomi *et al.*, 1994). *Satb1*, along with its close homolog *Satb2*, which was identified in the mouse much later (Dobreva *et al.*, 2003; Britanova *et al.*, 2005), are the only members of the SATB subfamily of Cut class homeobox genes and consist of two Cut domains followed by a homeodomain (Dickinson *et al.*, 1997; Dobreva *et al.*, 2003; Britanova *et al.*, 2005). Both SATB1 and SATB2 play important roles in chromatin organisation and regulation of gene expression (Yasui *et al.*, 2002; Dobreva *et al.*, 2003; Gyorgy *et al.*, 2008) and interestingly, their functions are cell-type specific. SATB1 plays a fundamental role in T-cell development and breast cancer progression (section 1.5.2), whereas SATB2 regulates osteoblast differentiation (Dobreva *et al.*, 2006) and specification of upper layer cortical projection neurons (Alcamo *et al.*, 2008; Britanova *et al.*, 2008). Our focus here will be on SATB1.

SATB1 is a nuclear matrix protein (Dickinson *et al.*, 1992; de Belle *et al.*, 1998; Seo *et al.*, 2005), one of its most prominent characteristics being its specificity for binding to AT-rich DNA sequences, called matrix or scaffold attachment regions (MARs or SARs; Dickinson *et al.*, 1992; de Belle *et al.*, 1998). As the name suggests, MARs have a high affinity for the nuclear matrix, a three-dimensional, non-chromatin structure of the cell nucleus, which comprises an external nuclear lamina and an internal ribonucleic protein network (Nickerson, 2001). MARs consist of DNA sequences that contain only adenine (A), thymine (T), and cytosine (C) residues on one strand and A, T, and guanine (G) residues on the other strand. When subjected to negative superhelical strain, these "ATC sequences" have the tendency to unwind, hence the

name base unpairing regions (BURs; Kohwi-Shigematsu and Kohwi, 1997). Double stranded BURs are typified by a distinctive sugar-phosphate backbone, which is recognised by SATB1 thus enabling the protein to bind to the minor groove of double stranded DNA (Dickinson *et al.*, 1992). Binding of SATB1 to MARs results in the formation of characteristic loops and higher order chromatin organisation (de Belle *et al*., 1998; Cai *et al*., 2003 and 2006; Kumar *et al*., 2007), with important functional implications (section 1.5.2).

1.5.1 Functional domains of the SATB1 protein

Given the high selectivity of SATB1 for MARs, the first studies on SATB1 focused on identifying its MAR binding domain. This domain was mapped at amino acid (aa) residues 346-495 and fine mapping of the identified polypeptide demonstrated that its N- and C-terminal ends are both necessary and sufficient for the recognition of the ATC sequence context and DNA binding (Nakagomi *et al*., 1994).

Subsequent studies identified two Cut-like repeats in SATB1, one located at the centre of the MAR binding domain (aa 370-445) and the other positioned at residues 493-568 (Dickinson *et al*., 1997). Focusing on the Cut repeat residing within the MAR binding domain of SATB1 Yamaguchi and colleagues solved its solution structure and demonstrated that it binds to the major groove of DNA (Yamaguchi *et al*., 2006).

Homology searches between SATB1 and known HD proteins identified an HD at the C-terminus of SATB1, spanning residues 641-702. This domain functions in a unique manner to increase the binding affinity of SATB1 to its target sequence: it promotes the tethering of the MAR binding domain of SATB1 to the core-unwinding element of a BUR (Dickinson *et al*., 1997). Moreover, identification of the palindromic consensus binding sequence of SATB1, which contains two repeats of the conserved HD binding element “TAATA”, led to the proposal that high affinity binding of SATB1

is mediated by its HD (Purbey *et al*., 2008).

The N-terminal end of SATB1 contains a dimerisation domain (aa 90-204) that participates in the formation of SATB1 homodimers, or heterodimers between SATB1 and other proteins (Galande *et al*., 2001). This region features sequence homology to known PDZ domains involved in protein-protein interactions and is necessary for the DNA binding activity of SATB1. Following studies, confirmed the requirement for dimerisation in order for SATB1 to achieve high affinity binding to DNA (Purbey *et al*., 2008). Purbey *et al*. formulated a model according to which, high affinity binding of SATB1 to the minor groove of DNA is established by its HD, whereas the Cut repeat within the MAR binding domain contacts the major groove with low affinity. Dimerisation of SATB1 via its PDZ domain is essential to increase affinity to its consensus target sequence (Purbey *et al*., 2008).

However, the crystal structure of the N-terminal domain (amino acids 71-172) of SATB1 was recently solved, demonstrating a resemblance to a typical ubiquitin domain rather than a PDZ domain as was previously believed (Galande *et al*., 2001), hence the name ubiquitin-like domain (ULD; Wang *et al*., 2012). Interestingly, the isolated crystal structure corresponded to four ULD regions and mutational analysis confirmed that SATB1 forms a tetramer under normal conditions *in vitro*. This oligomerisation is required for DNA binding and in fact it is proposed that the SATB1 tetramer can bind to two DNA sequences at the same time, thus providing a possible model for the higher order organisation of chromatin at SATB1-bound genomic loci (Figure 1.6; Wang *et al*., 2012).

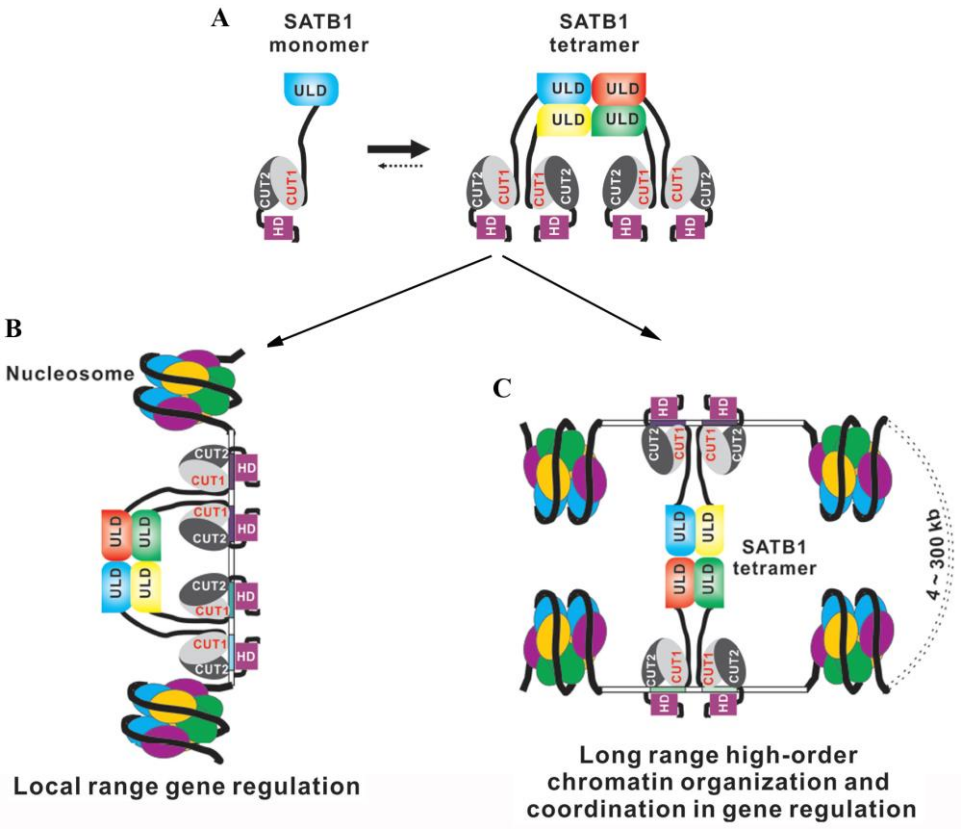

Figure 1.6 Proposed model for the function of SATB1 tetramers in transcriptional regulation. (A) SATB1 monomers assemble into tetramers via interaction through their N-terminal ULD domain. This is essential for recognition of target sequences and DNA binding. **(B)** Binding of a SATB1 tetramer to gene regulatory regions via its HDs mediates local transcriptional regulation. **(C)** SATB1 tetramers can regulate chromatin architecture through binding to promoter regions, which can be as far as 300 kb away, thus bridging together distant genes for coordinated transcriptional regulation. ULD= ubiquitin-like domain, HD= homeodomain, CUT= cut-like domains. Modified with permission from Wang *et al*., 2012.

1.5.2 Genome organising function of SATB1 and associated co-factors

The biological significance of the nuclear matrix and MARs in the regulation of transcription has long been appreciated. MARs are often found near enhancers (reviewed in Boulikas, 1995) and the nuclear matrix harbors the transcriptional machinery (Nickerson, 2001). Therefore, the finding that SATB1 tethers MARs to the

nuclear matrix (reviewed in Galande *et al*., 2007) prompted the investigation of a possible role of SATB1 in regulating gene transcription. Indeed, initial studies on SATB1 function demonstrated that it acts as a transcriptional repressor in a cell line system *in vitro* (Kohwi-Shigematsu *et al*., 1997) and that it is involved in negative regulation of the mouse mammary tumour virus (MMTV) locus (Liu *et al*., 1997) and positive regulation of the CD8 locus (Banan *et al*., 1997).

Interestingly, analysis of the first *Satb1*$^{-/-}$ mutants provided evidence that SATB1 can control the expression of multiple genes (Alvarez *et al*., 2000). At least ten genes, including cytokine receptor and apoptosis-related genes, were found to be dysregulated in *Satb1*$^{-/-}$ thymocytes leading to arrested T-cell development at the double positive stage (Alvarez *et al*., 2000). Similarly, SATB1 was found to regulate expression of over 1,000 genes to promote breast cancer growth and metastasis (Han *et al*., 2008).

Subsequent studies revealed that an important aspect of SATB1 function is the long-range, coordinated regulation of chromatin architecture and gene expression (Yasui *et al*., 2002; Cai *et al*., 2003). Immunofluorescence in thymocytes revealed the so-called "cage-like" network of SATB1-bound chromatin loops surrounding heterochromatin regions (Figure 1.7, A) and histone modification analysis showed that genomic regions bound to this network are acetylated, with acetylation marks extending up to 10 kb away from the SATB1 binding site (Cai *et al*., 2003). Consistent with the presence of histone marks at SATB1-bound genomic loci, SATB1 was shown to interact with the histone-modifying enzyme HDAC1 at the IL-2Ra locus to promote an inactive chromatin state (Yasui *et al*., 2002). It also recruits the ACF1 and ISWI chromatin-remodelling factors at the same locus, to organise nucleosome positioning, up to 7 kb away from its position (Yasui *et al*., 2002).

Moreover, SATB1 compacts chromatin at the T-helper 2 (T_H2) cytokine locus and promotes the coordinated transcription of interleukins 4, 5 and 13 (Cai *et al*., 2006).

Upon activation of T_H2 cells, SATB1 binds to its target sequences within the T_H2 cytokine locus and folds chromatin into loops. Notably, urea-chromatin immunoprecipitation experiments demonstrated that RNA polymerase II, the chromatin-remodeling factor Brg1, and the transcription factors GATA3, STAT6 and c-Maf are all associated with the cytokine locus after activation, co-localising with SATB1 (Cai *et al*., 2006).

Along the same lines, SATB1 participates in chromatin looping and transcriptional regulation of the major histocompatibility complex (MHC) class I locus, by recruiting the promyelocytic leukemia (PML) protein (Figure 1.7, B). Notably, SATB1 and PML bind not only to MARs but also to upstream regulatory regions of certain genes within the locus, suggesting that SATB1 acts as a genuine transcription factor for these genes, aside from being an architectural component of the MHC I locus (Kumar *et al*., 2007). SATB1 also binds to other upstream regulatory elements, including the IL-2 and IL-2Ra promoters in T-cells (Kumar *et al*., 2005) and the $gp91^{phox}$ promoter in myeloid cells (Hawkins *et al*., 2001).

In summary, SATB1 is a classical transcription factor, but also functions to integrate higher order chromatin looping with histone modifications, chromatin remodelling and the recruitment of transcription factors, all of which collectively contribute towards the positive or negative regulation of gene expression: hence the title "genome organiser".

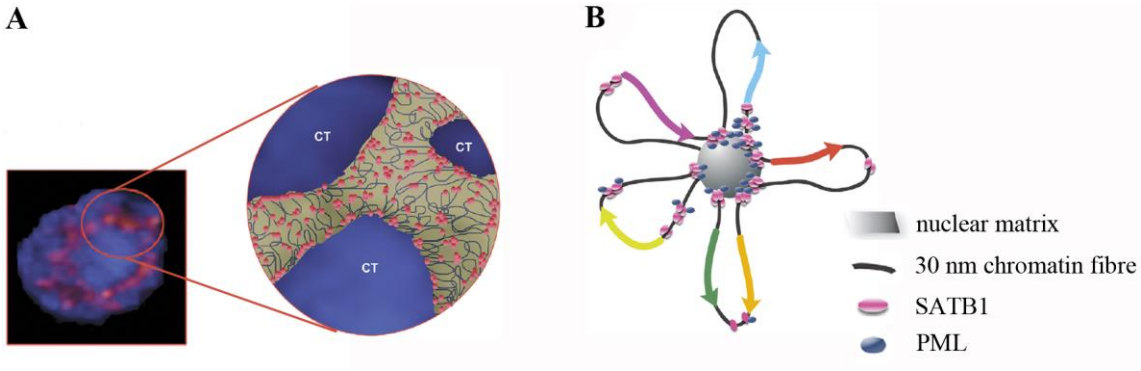

Figure 1.7 Organisation of chromatin architecture by SATB1. (A) Immunofluorescence in mouse thymocytes for DAPI, which reveals the chromatin territories (CTs) and SATB1, which surrounds the heterochromatin CTs, forming a characteristic cage-like network. **(B)** Schematic representation of the chromatin loop organisation of the MHC-I locus when SATB1, along with its interacting partner PML, binds on MARs and recruits them to the nuclear matrix. Apart from the base of chromatin loops, SATB1 can also be found at regulatory sequences upstream of various genes. Coloured arrows indicate genes within a 300 kb region of the MHC-I locus. Adapted with permission from Galande *et al*., 2007.

1.5.2.1 Regulation of SATB1 function by posttranslational modifications

Recent lines of evidence suggest that the ability of SATB1 to function as a repressor or activator of gene expression is controlled by posttranslational modifications. Depending on the phosphorylation status of its PDZ-like domain, SATB1 acts to either repress or derepress gene expression (Pavan Kumar *et al*., 2006). Phosphorylation of SATB1 by protein kinase C (PKC) increases its DNA binding affinity and allows the recruitment of HDAC1, which deacetylates histones at the bound loci thereby repressing transcription. On the contrary, dephosphorylated SATB1 interacts *via* its PDZ-like domain with the histone acetyltransferase PCAF, resulting in its acetylation, loss of its DNA binding activity and derepression of associated genes (Pavan Kumar *et al*., 2006).

The ability of SATB1 to interact with different cofactors depending on its

posttranslational modification status was confirmed by subsequent studies. SATB1 was shown to interact with CtBP1 (Purbey *et al*., 2009), a corepressor which acts in an HDAC1-dependent or independent way (reviewed in Chinnadurai, 2002). However upon acetylation of SATB1 the CtBP1/HDAC1 corepressor complex gets dislocated and PCAF coactivator complexes are recruited instead, leading to histone acetylation and activation of target gene expression (Purbey *et al*., 2009).

1.5.3 Expression and function of *Satb1* in the CNS

The first study to offer insight into the expression pattern of *Satb1* in the developing CNS reported Satb1 mRNA expression in the spinal cord of the E13.5 mouse embryo. By E15.5, Satb1 transcripts were detected within the neocortex, the hippocampus and the piriform cortex (Britanova *et al.*, 2005). Moreover, immunofluorescence studies reported robust SATB1 expression in the adult mouse neocortex, hippocampus, amygdala, midbrain tegmental area and spinal cord, while areas of the subpallium such as the striatum and ventral pallidum were devoid of SATB1 (Huang *et al.*, 2011). Within the neocortex, SATB1 protein was found in both cortical interneurons and pyramidal cells, across layers II-VI (Huang *et al.*, 2011; Balamotis *et al.*, 2012). Notably, SATB1 was detected exclusively in neurons and not glial cells (Huang *et al.*, 2011; Balamotis *et al.*, 2012).

The function of SATB1 in the cerebral cortex was first examined by using the same *Satb1*$^{-/-}$ mutants that were initially described in the immune system (Alvarez *et al*., 2000), at an independent study (Balamotis *et al.*, 2012). *Satb1* deficiency resulted in altered timing and levels of expression of several immediate early genes (IEGs) associated with brain plasticity, in the cortex of mutant animals. For example, expression of *Bdnf*, *Fos*, and *Arc* initiated three days earlier than normal and declined rapidly thereafter. Loss of *Satb1* activity also affected the levels of genes encoding

neuropeptides found in cortical interneurons, such as SST and CRH (section 1.2.1.2) and in fact, urea-ChIP experiments proved the direct binding of SATB1 to regulatory elements of these genes. Notably, dendritic spine density was significantly reduced in pyramidal cells of *Satb1*$^{-/-}$ mice, indicating a possible role of SATB1 in controlling synapse formation in the postnatal mouse cortex (Balamotis *et al.*, 2012).

1.5.3.1 SATB1 in cortical interneurons

The latest studies in the field report that SATB1 expression in cortical interneurons is restricted exclusively in the MGE-derived lineage, suggesting specific roles of this transcription factor in certain interneuron subsets. Two parallel studies, one from our laboratory (Denaxa *et al*., 2012) and one from the Fishell group (Close *et al*., 2012), demonstrated the presence of SATB1 protein in nearly all PV^+ and SST^+ interneurons, which are MGE-derived, and its exclusion from their VIP^+ or $5HT3aR^+$ CGE-derived counterparts. Furthermore, both studies noted a lack of SATB1 protein within the MGE and in tangentially migrating interneurons. SATB1 expression initiated only when interneurons started populating the CP, becoming more robust and apparent in increasing numbers of cells at late embryonic stages.

Interestingly, Denaxa and colleagues noticed that the temporal profile of SATB1 expression in the developing neocortex coincides with the appearance of spontaneous cortical activity, which starts from E16.5 and peaks at early postnatal life (Corlew *et al*., 2004). To investigate a possible connection between the two, dissociated cultures from E14.5 mouse cortices were established and treated with KCl after 24 hours, to depolarise neurons. KCl treatment resulted in a significant increase in the number of $SATB1^+$ GABAergic interneurons, compared to untreated controls. Conversely, treatment with a Ca^{2+} channel blocker or $GABA_A$ receptor antagonists resulted in a reduction in the number of SATB1-expressing interneurons indicating that Ca^{2+} activity

can induce SATB1 expression, partly through $GABA_A$ receptors (Denaxa *et al*., 2012). Similarly, *in vivo* attenuation of neuronal activity in cortical interneurons, by electroporation of the inward-rectifying channel Kir2.1, resulted in the downregulation of *Satb1* expression levels (Close *et al*., 2012).

Additional findings from these studies provide evidence for the involvement of SATB1 in cortical interneuron development and will be discussed in Chapters 3 and 4 of this thesis.

1.6 Aims of the present work

Previous work from our laboratory has established that the LIM-homeodomain transcription factor LHX6 is intrinsically required in MGE-derived cortical interneurons to regulate their specification during early embryonic development, migration into the cortex and differentiation into mature subtypes. However, the region- and stage-specific factors operating downstream of LHX6 to regulate cortical interneuron maturation in the cortex remain largely unknown. The latest studies from our group established that the genome organiser protein SATB1 is genetically downstream of LHX6 and demonstrated that this factor is expressed specifically in MGE-derived SST^+ and PV^+ interneurons upon invasion of the cortical plate, where terminal differentiation of these cells takes place.

The overall objective of our studies is to investigate the role of SATB1 in the development of inhibitory circuits in the mammalian cortex. In particular, as part of our efforts to understand the molecular/genetic mechanisms underpinning the generation of cortical interneuron diversity, we will examine the role of SATB1 in the terminal differentiation and maturation of MGE-derived interneurons. To this end, we will examine the differentiation of PV^+ and SST^+ interneurons in the postnatal cortex of *Satb1*-null or conditional *Satb1* floxed mice, using a battery of molecular markers that identify mature interneuron subsets. With these studies we will determine the potential differential requirements of *Satb1* activity in the differentiation of SST^+ and PV^+ interneurons. Finally, we wish to explore the mechanisms by which *Satb1* expression is regulated in the cortex by investigating its functional relationship with KCC2, a molecule implicated in the maturation of diverse groups of CNS neurons. We will examine the coexpression of SATB1 and KCC2 in the mouse cortex at different developmental stages and address their epistatic relationship by using an ectopic overexpression system in embryonic brain slices, maintained in culture.

Chapter 2

Materials and Methods

2.1 Animals

2.1.1 Mouse lines

Satb1$^{-/-}$ mice used in the present study were established in our laboratory, using targeted embryonic stem (ES) cells from EUCOMM. *Satb1*^{flox} mice were generated from *Satb1*$^{+/-}$ stocks combined with the *ACTB:FLPe* line (S. Dymecki, Harvard Medical School, USA; Rodriguez *et al*., 2000), as shown in Figure 4.1. Constitutive *Nkx2.1-Cre* transgenic (Kessaris *et al*., 2006) and inducible *Nkx2.1-CreER*^{T2} mice were kindly provided by N. Kessaris, University College London, UK. The *R26ReYFP* line (Srinivas *et al*., 2001) was obtained from S. Srinivas, University of Oxford, UK. *PV-Cre* mice (Hippenmeyer *et al*., 2005) were imported from the Jackson Laboratory (stock number: 008069; donating investigator: Silvia Arber, Friedrich Miescher Institute, Switzerland). The *Lhx6-CreER*^{T2}, *SST-CreER*^{T2} and *Pv-CreER*^{T2} inducible lines (Taniguchi *et al*, 2011) were also imported from the Jackson Laboratory (stock numbers: 010776, 010708, 010777 respectively; donating investigator: Josh Huang, Cold Spring Harbor Laboratory, USA). For wild type studies, Parkes mice (established at the Biological Services department of the National Institute for Medical Research, UK) were used.

2.1.2 Animal husbandry

Mice were housed, bred and handled according to the guidelines approved by the UK Home Office, under the Animals (Scientific Procedures) Act 1986. Matings were set up after 04:00 pm in the afternoon and the presence of a vaginal plug (VP) was checked the next morning. The day of VP detection was defined as embryonic day 0.5 (E0.5). For postnatal animals the day of birth was considered as postnatal day 0 (P0).

2.1.3 *In vivo* administration of 4-OHT

4-hydroxytamoxifen (4-OHT; Sigma, H6278) was dissolved in a mixture of ethanol:sunflower oil (1:9) at a final concentration of 10 mg/ml and stored at 4°C for up to 2 weeks, or at -20°C for long-term (months) usage. To label cortical interneurons at P30 or adult (P90 or older) stages, animals were injected intraperitoneally with 3 mg 4-OHT per day for 2 consecutive days. Alternatively, adult animals were injected daily with 2 mg of 4-OHT for a period of 5 consecutive days. Animals were perfused (2.2.2) for analysis 1-2 weeks after induction.

2.2 Tissue manipulation

2.2.1 Dissection of embryos and embryonic brains

Pregnant females were sacrificed at various stages of gestation (from E13.5 to E18.5) by cervical dislocation and their uteri were transferred in pre-chilled phosphate-buffered saline (PBS), unless otherwise stated. The embryos were dissected out of the uterus, the placenta and extra-embryonic membranes, including the yolk sac, were removed and the head was decapitated. Brains were subsequently dissected out of the developing scull and fixed in 4% (w/v) paraformaldehyde (PFA, Sigma-Aldrich, P6148) in PBS at 4^{o}C overnight. A small piece of the tail was collected for genotyping, when required.

2.2.2 Perfusion and adult brain dissection

Adult mice or pups were anaesthetised by intraperitoneal injection of 0.01 ml/g of Pentobarbitone (Pentoject ®, stock of 60 mg/ml) and subsequently transcardially perfused with 0.9% (w/v) NaCl in distilled H_2O (dH_2O), followed by 4% PFA in PBS. Brains were then dissected out of the scull and post-fixed in 4% PFA at 4^{o}C overnight.

2.2.3 Tissue freezing and cryosectioning

Fixed postnatal brains (2.2.2) were washed thoroughly in PBS, and cryoprotected in 15% sucrose (VWR, 27480.294) in PBS overnight at 4^{o}C, followed by 30% sucrose in PBS overnight at 4^{o}C. They were then embedded in a mix of 7.5% gelatin (Sigma-Aldrich, G2500); 15% sucrose in PBS, at 4^{o}C until set, and frozen in Isopentane (Sigma-Aldrich, 154911) cooled at -60 ^{o}C. Serial cryosections at 14 µm were acquired using a cryostat (Leica CM3050S) and mounted on Superfrost Plus glass slides (Thermo Scientific, J1800AMNZ). Sections were left to dry at room temperature for 1 hour and subsequently stored at -80^{o}C, or used directly for immunohistochemistry (2.5.1) or *in situ* hybridisation (2.5.2). The same process was followed for embryonic fixed tissue (2.2.1) with the only difference that brains were cryoprotected directly in 30% sucrose.

2.2.4 Vibratome sectioning

Fixed brains from postnatal animals (2.2.2) were washed thoroughly in PBS, embedded in 4% (w/v) Low Melting Agarose type VII (Sigma-Aldrich, A9045) in PBS and left to set at 4^{o}C. Floating sections were acquired at a thickness of 100 µm using a vibratome (Leica, VT1000S), transferred to 24-well plates (NUNC, 142485) containing PBS and stored at 4^{o}C. For long-term storage 0.05% NaN_3 (Sigma-Aldrich, 13412) was added to the PBS to preserve tissue quality.

2.2.5 Fixation and resectioning of electroporated brain slices

Twenty-four hours after electroporation (2.4.4), brain slices were fixed in 4% PFA for 1 hour on ice, washed 3 times for 10 minutes each time in PBS, cryoprotected in 30% sucrose overnight and embedded in 7.5% gelatin;15% sucrose in PBS for further

sectioning on the cryostat at a thickness of 14 μm. The cryosections acquired were later subjected to standard immunohistochemistry procedures (2.5.1).

2.2.6 Fluorescence-activated cell sorting (FACS)

Twenty-four hours after electroporation (2.4.4), E14.5 MGEs were dissociated in Leibovitz's L15 medium (L15; PAA, E15-821) with Glutamine, containing 1% penicillin-streptomycin (pen-strep) (Invitrogen, 15140-122) and collected into sterile 1.5 ml tubes. The L15 medium was removed and the tissue was briefly washed in 500 μl of DMEM/F-12 (Gibco, 21331-020) containing 1:10 DNase I (1 mg/ml stock; Sigma-Aldrich, 070M7032V). Samples were then resuspended in 500 μl of Neurobasal medium (Gibco, 21103-049) with 1:10 DNase I and mechanically dissociated by gentle pipetting. After a 5-minute spin-down at 1000 rpm the supernatant was discarded and the cell pellets were resuspended in 500 μl OptiMEM (Gibco, 11058-021) containing 1:10 DNase I. The cell suspension was transferred to a flow cytometry polystyrene tube provided with a cell strainer cap (BD, 352235), through which it was filtered to ensure single cell suspension. Tubes were kept on ice and samples were transferred into a cell sorter (FACS AriaII, Becton-Dickinson). 15-20 electroporated slices, or approximately 40 MGEs, yielded 10,000-20,000 RFP^+ or GFP^+ cells, which were collected into individual RNase-free tubes and immediately processed for RNA extraction (2.3.2).

2.3 Molecular biology techniques

2.3.1 Genomic DNA extraction

Ear biopsies from pups, or tail pieces from embryos, were incubated in 500 μl Proteinase K lysis buffer (100 mM Tris-HCl pH 8.5, 5 mM EDTA pH 8.0, 0.2% SDS, 200 mM NaCl, Proteinase K (0.1 mg/ml; Roche, 03 115 879 001) at 55^{o}C overnight. The following day, DNA was precipitated by adding 500 μl of isopropanol, mixing and

centrifuging at 13000 rpm for 10 minutes at room temperature. The supernatant was discarded and the pellets were left to air-dry and finally resuspended in 50 μl of dH_2O. 1-2 μl of DNA were used in PCR genotyping (2.3.7).

2.3.2 RNA extraction

Total RNA was extracted from FACS purified cells (2.2.6) using an RNeasy Micro Kit (QIAGEN, Cat. No. 74004) following the manufacturer's instructions. Briefly, sorted cells were centrifuged at 200 x g for 15 minutes at room temperature and the supernatant removed. The cell pellet was resuspended in 100 μl of lysis solution and the lysate was then treated with 70% ethanol and applied to an RNeasy MinElute spin column. Proteins, DNA, and other contaminants were removed in a series of washing steps, and the bound RNA was eluted in 20 μl of RNase-free dH_2O and stored at -80^oC.

2.3.3 Plasmid DNA amplification

For plasmid DNA amplification, plasmid DNA (10 pg - 100 ng) was transformed into One Shot® TOP10 chemically competent *E. coli* cells (Invitrogen, C4040). In more detail, a 50 μl aliquot of the competent cells was thawed on ice, combined with the plasmid and incubated on ice for 30 minutes. The cells were then heat-shocked at 42^oC for 30 seconds, to allow uptake of the DNA, and subsequently returned on ice for 30 seconds. Working under the flame of a Bunsen burner, 250 μl of LB medium were added to the cells, which were then allowed to recover in a 37^oC incubator, shaking at 225 rpm for 1 hour. 100 μl of the cell suspension were then plated onto an LB agar plate (pre-warmed at 37^oC) containing 100 μg/ml of ampicillin. The plates were incubated upside down at 37^oC overnight and the following morning they were examined for the presence of antibiotic-resistant colonies.

A single colony was then used to inoculate 5 ml of LB medium containing 100

μg/ml ampicillin and the mini-culture was then incubated at 37^{o}C, shaking at 225 rpm overnight. The next day, the starter mini-culture was diluted 1/500 in LB with 100 μg/ml ampicillin and left to grow for 12-16 hours with shaking at 37^{o}C, in order to produce a bacterial maxi-culture. Bacterial cells were collected by centrifugation at 6000 x g for 15 minutes at 4^{o}C and processed for plasmid DNA extraction (2.3.4).

2.3.4 Plasmid DNA extraction

Plasmid DNA was isolated and purified using a QIAfilter Plasmid Maxi Kit (QIAGEN, Cat. No. 12262), according to the manufacturer's instructions. Briefly, after alkaline lysis of bacterial pellets, the plasmid DNA was allowed to bind to a resin column under low- salt conditions. Proteins, RNA and other impurities were washed off and the DNA was eluted using a high-salt buffer and precipitated using isopropanol. DNA was finally eluted in 500 μl dH_2O and stored at -20^{o}C.

2.3.5 Restriction enzyme digestion

Diagnostic digestions of plasmid DNA were done using 1μg of DNA, 2 μl of enzyme-specific 10x digestion buffer, 0.5 μl of the suitable restriction enzyme (10 U/μl) and dH_2O up to a final volume of 20 μl. Restriction enzymes and their buffers were purchased from Roche. The reactions were incubated for 1 hour at 37^{o}C and loaded on a 1% agarose gel for electrophoresis (2.3.8).

2.3.6 Riboprobe synthesis

Riboprobes used in RNA *in situ* hybridisation (2.5.2) were generated by *in vitro* transcription of linearised plasmid DNA containing the coding sequence of the gene of interest. Approximately 10 μg of plasmid DNA were used for linearisation. The plasmid was mixed with 2.5 μl of the required restriction enzyme, 10 μl of the enzyme-specific

buffer and dH_2O up to a final volume of 100 µl. The reaction was then incubated at 37°C for 2 hours, along with an uncut control reaction, in which no restriction enzyme was added. A few µl of these reactions were then run on a 1% (w/v) agarose gel to determine if the plasmid was successfully linearised. DNA was then purified by phenol/chloroform extraction followed by ethanol precipitation. More specifically, a 1:1 volume of phenol was added to the linearised DNA reaction, centrifuged at 13000 rpm for 5 minutes and the upper phase transferred to a clean tube. A 1:1 volume of chloroform was then added, followed by a spin down at 13000 rpm for 5 minutes. The aqueous phase containing the DNA was pipetted out into a new tube and the DNA was precipitated by adding 10:1 sodium acetate (NaAC) and 1:2 ethanol (EtOH) and incubating the mix at -80°C for 1 hour or at -20°C overnight. The DNA was subsequently centrifuged at 13000 rpm for 10 minutes and the pellet washed with 70% EtOH and left to air dry. The DNA pellet was dissolved in 10 µl of dH_2O and stored at -20°C or used directly for *in vitro* transcription.

In vitro transcription for the generation of digoxigenin (DIG)-labeled riboprobes was performed by combining 1.5 µg of linearised plasmid, 4 µl of 5x transcription buffer (Promega, P118B), 2 µl of 100mM DTT (Promega, P117B), 2 µl of 10x DIG labeling mix (Roche, 11277073910), 0.5 µl of Rnasin RNase inhibitor (Promega, N211B), 1.5 µl of the required RNA polymerase (10 units/µl, T7 Promega, P207B; T3 Promega, P208C) and RNase-free dH_2O up to 20 µl. The reaction was incubated at 37°C for a maximum of 2 hours. Half way through the incubation, 1 µl of the reaction was run on an agarose gel to check for the presence of an RNA transcript. After confirming the presence of RNA, 2 µl of RQ1 DNase I (Promega, M198A) were added to the reaction and incubated at 37°C for 15 minutes, to eliminate any traces of plasmid DNA. The probes were precipitated by adding 100 µl TE, 10 µl 4M lithium chloride (LiCl) and 300 µl of 100% EtOH and incubating at -20°C for at least 30 minutes. The

reaction was then centrifuged at 13000 rpm for 10 minutes and the RNA pellet was washed with 70% EtOH, air-dried, dissolved in 50 µl TE and stored at -20^{o}C. The full list of the antisense riboprobes used in this study, as well as the restriction enzymes and RNA polymerases used for their generation is given in Table 2.1.

Table 2.1 Antisense riboprobes, restriction enzymes and RNA polymerases used for their generation

Riboprobe	Restriction enzyme	RNA polymerase
Lhx6	NotI	T3
Gad1	SalI	T7
Sst	EcorI	T7
Kcnc1	EcorI	T3
Er81	SpeI	T7
Cux2	NotI	T3
Crh	NotI	T3

2.3.7 Polymerase chain reaction (PCR)

PCR was performed using 10x buffer (Invitrogen, P/N y02028), 50 mM $MgCl_2$ solution (Invitrogen, P/N y02016), a mix of 10 mM dNTPs (set of dATP, dCTP, dGTP, dTTP, each at 100 mM, Invitrogen, 10297-018), suitable primers, Taq DNA polymerase (Invitrogen, 18038-026), and dH_2O. Primer stocks (Sigma-Genosys) were ordered in lyophilized form and resuspended in dH_2O to a final concentration of 100 µM. For working solutions, primer stocks were further diluted to 10 µM.

Reactions for the Cre, iCre and R26ReYFP PCRs were performed in a final volume of 25 µl, by adding 1 µl of extracted genomic DNA (2.3.1) in a mixture of 2.5 µl 10x buffer, 0.75 µl $MgCl_2$, 0.5 µl dNTPs, 0.5 µl forward primer, 0.5 µl reverse primer, 0.2 µl Taq polymerase and 19.05 µl dH_2O. For the Satb1 PCR, reactions were set up at a final volume of 20 µl using 1 µl of extracted genomic DNA, 2 µl 10x buffer,

1.6 µl $MgCl_2$, 0.4 µl dNTPs, 0.2 µl of each primer, 0.5 µl Taq and 13.9 µl dH_2O.

Primer sequences, cycling conditions and expected band sizes for each PCR can be found in Table 2.2. The presence or absence of PCR products, as well as their size was determined by agarose gel electrophoresis (2.3.8).

Table 2.2 Primer sequences and PCR cycling conditions used for genotyping

	Primer sequence (5' - 3')	PCR settings						Band size (bp)
		Step 1 1 cycle		Step 2 35 cycles		Step 3 1 cycle		
		°C	T	°C	T	°C	T	
Satb1	(F9) TGCTCATGTGGAATGTCGAG	95	10’	94	30”	72	10’	337 (wt)
	(R10) CAGGCCACATTGTCCTAACTT			60	45”			184 (KO)
	(R11) GAATAGGAACTTCGGTTCCG			72	60”			428 (flox)
Cre	(F) ATCCGAAAAGAAAACGTTGA	94	3’	94	30”	72	10’	550
	(R) ATCCAGGTTACGGATATAGT			53	60”			
				72	90”			
iCre	(F) GAGGGACTACCTCCTGTACC	94	5’	94	45”	72	10’	630
	(R) TGCCCAGAGTCATCCTTGGC			61	60”			
				72	60”			
R26ReYFP	(F) GCTCTGAGTTGTTATCAGTAA	95	6’	95	30”	72	10’	500 (wt)
	(R) GCGAAGAGTTTGTCCTCAACC			55	30”			350 (stop)
	(R) GGAGCGGGAGAAATGGATAG			72	45”			

2.3.8 Agarose gel electrophoresis

Gels for DNA electrophoresis were prepared by dissolving 1% or 2% (w/v) agarose in TAE buffer and heating the solution in a microwave oven until the agarose

was fully dissolved. To visualize the DNA, the fluorescent nucleic acid dye GelRed™ was added to the agarose solution at a concentration of 1:10,000 and the solution was then poured into a suitable mold with the appropriate well comb and left to set. DNA samples were mixed with 10x Orange G loading dye (20% Ficoll, 0.1 M EDTA, 1% SDS, 0.25% Orange G) at a ratio of 9:1, loaded onto the gel and electrophoresed at 100-150 V. The gel was also loaded with a 1 Kb DNA ladder (Invitrogen, 10787-018) which was used to determine the band size of the DNA samples when visualized in an ultraviolet gel documentation system (UVP BioDoc-It™, LM-26E) at 302 nm.

2.3.9 Generation of the KCC2-encoding vector

The complete coding sequence of the mouse *Kcc2* (IMAGE clone ID: 6838880) was cloned into the pCAGGs-GFP vector, in order to generate the pCAGGS-Kcc2-GFP plasmid. More specifically, a SalI/SacI fragment containing the full-length cDNA for *Kcc2* was excised from the host pYX-Asc vector and inserted into the XhoI/SacI sites of the pCAGGS-GFP vector. The cloning was done upstream of an internal ribosome entry site (IRES), followed by a GFP coding sequence. Expression of KCC2 was confirmed by immunostaining transfected P19 embryonal carcinoma cells (2.4.6) and brain slices after electroporation (2.4.4).

2.3.10 Reverse transcription

Reverse transcription was performed using the High-Capacity cDNA Reverse Transcription kit (Applied Biosystems, 4374966) following manufacturer's instructions. Briefly, a reaction containing 25 ng RNA (2.3.2), 2 μl 10x RT reaction buffer, 0.8 μl 25x dNTPs, 2 μl 10x random primers, 1 μl RNAse inhibitor, 1 μl MultiScribeTM MuLV reverse transcriptase and sterile RNAse-free H_2O up to 20 μl was prepared in a RNAse-free tube. A control reaction was set up for each RNA sample by omitting the

MuLV reverse transcriptase (No RT reaction). Reactions were incubated at 25^{o}C for 10 minutes and 37°C for 120 minutes, stopped by heating to 85°C for 5 seconds and then stored at -20°C.

2.3.11 Quantitative real-time PCR

Gene expression was quantified by quantitative real-time PCR. Quantitative PCR (qPCR) was performed by using the TaqMan Gene Expression technology (Applied Biosystems), which provides a mix of pre-made fluorescence TaqMan probe and primers for a specific gene of interest. Reactions were prepared in triplicates in nuclease-free multi-well plates for each cDNA template and negative control (NRT). TaqMan Gene Expression Assays IDs: ß-actin Mm01205647_g1, Kcc2 Mm00803929_m1, Sst Mm00436671_m1, Satb1 Mm 01268940_m1. A reaction containing 1 µl 20x TaqMan Gene Expression Assays, 10 µl 10x TaqMan Fast Universal Master Mix, 2 µl cDNA (diluted 1:5 in dH_2O), and sterile RNase-free H_2O up to 20 µl was prepared in a RNase-free tube. Reactions were performed in a 7500 Real-Time PCR System (Applied Biosystems). An initial denaturation step of 10 minutes at 95°C, was followed by 40 cycles of denaturation (95°C for 15 seconds), annealing (60°C for 1 minute) and elongation (72°C for 1 minute).

The relative quantification approach was used to analyse data, using the $2^{-\Delta\Delta CT}$ formula. Briefly, the amount of target transcript was normalised to the levels of the housekeeping gene *ß-actin* (endogenous reference) and expressed relative to a calibrator (control condition). Data are presented in either of the following two ways: data are shown as the mean of biological triplicate values (3 pairs of control and *Satb1*- or *Kcc2*-overexpressing samples, each of them coming from an independent electroporation experiment) with error bars representing standard error of the mean (SEM). Alternatively, data are shown as the mean of technical triplicate values from 2

representative experiments, chosen out of a total of 7 independent experiments. Error bars in this case represent Δmax and Δmin values calculated using the formulas: Δmin = RQ sample – RQ Min sample and Δmax = RQ Max sample – RQ sample, where RQ Max and RQ Min are the maximum and minimum relative quantities of the sample calculated with a 95% confidence level.

2.4 Tissue and cell culture techniques

2.4.1 Coating of tissue culture plates

For the plating of cortical feeder (2.4.2) or P19 embryonal carcinoma cells (2.4.6) Permanox 8-well chamber slides (Thermo Scientific, 177445) were coated with poly-D-lysine (PDL; Sigma-Aldrich, P6407) and laminin (Sigma-Aldrich, L2020). In more detail, 10 μg/ml PDL in PBS was added in each well and incubated for 1 hour at room temperature. The chambers were then washed once with sterile Dulbecco's PBS (DPBS; Gibco, 14190-094) and coated with 5 μg/ml laminin overnight in a 37^{o}C;5% CO_2 incubator. The following day, laminin was aspirated, the wells were washed once with DPBS and used for seeding.

2.4.2 Preparation of P0 cortical feeder cells

Neonatal mouse pups (P0) were decapitated and their brains dissected out in L15 medium. The cortex was carefully separated from the ventral telencephalic structures and cut further into small pieces which were then transferred into a 15 ml falcon tube containing DMEM/F-12 medium with 0.05% trypsin (Invitrogen, 25200-054) and 1% DNase I in a 37^{o}C waterbath for 15 minutes. Subsequently, DMEM/F-12+FCS (43.5 ml DMEM/F-12, 5 ml fetal calf serum (FCS; PAA, A15-649), 0.5 ml pen/strep, 0.5 ml 50x glutamine) was added at a ratio of 3:1 and the tissue was dissociated by passing through a fire-polished glass pipette. The cells were then spun at 800 rpm for 5 minutes and the

pellet resuspended in Neurobasal+B-27 (47 ml Neurobasal, 1 ml B-27 supplement, 1 ml 25% glucose, 0.5 ml 50x glutamine, 0.5 ml pen-strep). The cell suspension was passed through a 40 µm cell strainer (BD Falcon, 352340), diluted further with Neurobasal+B-27 so that 10^6 cells/ml are present and plated onto PDL/laminin coated Permanox 8-well plates (2.4.1). The cells were incubated at 37^{o}C; 5% CO_2 until the next day when they were seeded with dissociated MGEs (2.4.5).

2.4.3 Embryonic brain slice cultures

Preparation of brain slice cultures was performed as described previously (Anderson *et al*, 1997). Wild type, Parkes, mouse embryos were harvested at E14.5 and brains were dissected out of the forming scull, in ice-cold 1x Krebs buffer (1:10 dilution of 10x Krebs in sterile dH_2O, supplemented with 0.99 g D-(+)-Glucose (Sigma-Aldrich, G7021) and 1.05 g $NaHCO_3$ (Sigma-Aldrich, S5761) and filtered through a 0.2µm pore). The ingredients and concentrations of the 10x Krebs stock solution can be found in Table 2.3. Brains were then embedded in 3% (w/v) Low Melting Agarose type VII (Sigma-Aldrich, A9045) in sterile DPBS kept at 37°C and left to set at 4°C for 1 hour. The agarose embedded brains were then transferred in a vibratome (Leica, VT1000S) chamber containing ice-cold 1x Krebs and 300 µm coronal sections were collected and immediately transferred on to polycarbonate culture membranes (13 mm diameter, 8 µm pore size, SLS, 110414) in Falcon organ tissue culture dishes (Becton Dickinson, 353037) containing 800µl Minimum Essential Medium (MEM) with serum (44 ml MEM (Gibco, 42360-024), 5 ml 100% FCS, 0.5 ml 50% glucose, 0.5 ml 100x Pen-Strep). Sections were then left to recover in a 37^{o}C;5% CO_2 incubator for 1 hour and used for focal electroporations (2.4.4).

Table 2.3 Salts and their molar concentration used to make 10x Krebs buffer

Salt	Molar concentration
NaCl	1.26 M
KCl	25 mM
NaH_2PO_4	12 mM
$MgCl_2$	12 mM
$CaCl_2$	21 mM

2.4.4 Focal injections – electroporations

Focal injection of plasmid DNA and electroporation was performed as described previously (Stühmer *et al.*, 2002). After slice culture (2.4.3), small amounts of either control (pCAGGS-GFP or pCAGGS-RFP) or overexpressing vector (pCAGGS-Kcc2-GFP or pCAGGS-Satb1-RFP) at 1µg/µl, were pressure-injected bilaterally into the medial ganglionic eminence (MGE) with a Pneumatic PicoPump through a very fine glass needle. The culture membrane carrying the injected brain slice was then placed onto a 1% agarose block (1% agarose in 1x Krebs) within a setup of two horizontally orientated platinum electrodes (Protech International Inc., CUY-700-1 and CUY-700-2). A thin (diameter of 0.5-0.8 mm) agarose column (punched with clipped hypodermic needle from a 1% agarose in 1x Krebs gel) was attached to a mobile upper electrode and used to target the injected MGEs. The electrode was lowered so that the agarose plug came into contact with the brain slice and electric pulses of 125V (2 pulses of 15 ms each, with an interval of 500 ms) were passed through the tissue. A square-wave electroporator (VWR, T 820 BTX) was used to power the system. After electroporation, the slices were left to recover in a 37^oC;5% CO_2 incubator for 1 hour, the medium was then changed to serum-free medium (47.5ml Neurobasal medium, 1 ml B-27 supplement (Invitrogen, 17504-044), 0.5 ml 50% glucose, 0.5 ml 100x pen-strep, 0.5 ml 100x Glutamine (Invitrogen, 25300-054)) and finally the cultures were returned to the

incubator overnight. The next morning the density of GFP^+ or RFP^+ cells in the electroporated MGEs was checked under a fluorescent stereomicroscope (Leica, MZFLIII) and brain slices were processed for resectioning (2.2.5), dissociation and plating (2.4.5) or dissociation and FACS analysis (2.2.6).

2.4.5 Dissociation and plating after electroporation

Twenty-four hours after focal electroporation (2.4.4), the MGEs with high densities of GFP^+ or RFP^+ cells were dissected out in L15 medium with 1% pen-strep, collected into sterile 1.5 ml tubes containing DMEM/F-12 with 0.2% trypsin and 4% DNase I and incubated in a 37^{o}C waterbath for 15 minutes. Trypsin was inactivated by adding 50 µl of FCS and samples were then resuspended in 500 µl of Neurobasal+B-27 medium (47 ml Neurobasal, 1 ml B-27 supplement, 1 ml 25% glucose, 0.5 ml 50x glutamine, 0.5 ml pen-strep) and mechanically dissociated by pipetting. After a 5-minute spin-down at 800 rpm the supernatant was discarded and the cell pellets were resuspended in Neurobasal+B-27. Cell number was counted on a haemocytometer and plated on cortical feeder layers at a density of 500 cells/well in 8-well chamber slides. Feeder cells were prepared and plated the day before (2.4.2). Electroporated cells were then cultured in a 37^{o}C;5% CO_2 incubator for 2-7 days and subsequently fixed and processed for immunofluorescence (2.5.1). One day after plating, the medium was changed to Neurobasal+B-27 supplemented with 10 ng/ml of basic fibroblast growth factor (bFGF; R&D systems, 233-FB-025).

2.4.6 P19 cell culture and transfection

Mouse embryonal carcinoma P19 cells were grown in DMEM supplemented with 10% FCS, 2 mM glutamine and 1% pen/strep and transfected with lipofectamin according to the manufacturer's protocol (Lipofectamin® 2000, Invitrogen).

2.4.7 Fixation of cell cultures

Dissociated MGE cells or P19 embryonal carcinoma cells were fixed in 4% PFA in PBS for 10 minutes at room temperature, washed three times for 5 minutes each in PBT (0.1% Triton X-100 in PBS) and processed for immunostaining (2.5.1).

2.5 Histochemistry and Cytochemistry techniques

2.5.1 Immunofluorescence

Cryostat sections (2.2.3) from embryonic and postnatal animals were permeabilised by washing in PBT for 3 times, 10 minutes each, at room temperature and incubated in blocking solution (1% BSA (Sigma-Aldrich, A9647), 0.15% glycine (VWR, 101196X) in PBT) for at least 1 hour at room temperature. Primary antibodies were diluted in blocking solution and applied on the slides at 4°C overnight. The next day, after 3 washes with PBT, sections were incubated with secondary antibodies diluted in blocking solution at room temperature for 2 hours, washed in PBT, and mounted using Vectashield (Vector) medium which contained DAPI to stain the cell nuclei. The same protocol was followed for immunostaining of dissociated MGE (2.4.5) and P19 (2.4.6) cell cultures after fixation of the cells (2.4.7).

Vibratome floating sections (2.2.4) were permeabilised in 0.3% Triton X-100 in PBS for 1 hour at room temperature and incubated in blocking solution (10% FCS, 1% BSA in PBT) for the same amount of time. Primary antibodies were diluted in antibody solution (1% FCS, 0.1% BSA, in PBT) and incubated at 4°C overnight. The next day, they were thoroughly washed in 0.3% Triton X-100 in PBS and incubated with secondary antibodies diluted in antibody solution at room temperature for 2 hours. After a final wash in 0.3% Triton X-100 in PBS the sections were transferred on to slides with the help of a paintbrush, left to dry and mounted with Vectashield medium which contained DAPI.

The primary antibodies used in this study as well as their working concentrations are mentioned in Table 2.4. Secondary antibodies were donkey Alexa Fluor® 488-, 568- and 647-conjugates (Molecular Probes), used at a concentration of 1:500.

Table 2.4 Primary antibodies and their working concentration used in immunofluorescence

Primary Antibody	Host	Dilution	Source
SST	Rat	1:500	Millipore
PV	Rabbit	1:1,000	Swant
CR	Rabbit	1:1,000	Chemicon
NPY	Rabbit	1:1,000	Peninsula Laboratories
nNOS	Rabbit	1:1,000	BD Biosciences
VIP	Rabbit	1:1,000	Immunostar
SATB1	Goat	1:500	Santa Cruz
SATB2	Rabbit	1:1,000	Abcam
KCC2	Rabbit	1:1,000	Millipore
GFP	Rabbit	1:1,000	Molecular Probes
GFP	Rat	1:500	Nacalai Tesque

2.5.2 RNA *in situ* hybridisation

Non-radioactive *in situ* hybridisation was performed as described previously (Schaeren-Wiemers and Gefrin-Moser, 1993), on 14 µm thick cryosections (2.2.3) from P15 animals. Sections were fixed in 4% PFA in PBS for 10 minutes at room temperature and washed 3 times in PBS with 0.1% Tween 20, for 10 minutes each time. Slides were then incubated in acetylation solution (0.1 M Triethanolamine, 0.65% of 37% HCl, and 0.375% acetic anhydride in dH_2O) for 10 minutes at room temperature and washed 3 times for 10 minutes each in PBT. Pre-hybridisation solution (50% v/v deionised formamide (SIGMA, F9037), 5x SSC, 5x Denhardt's (Invitrogen, 750018), 250 µg/ml yeast tRNA (SIGMA, R6750) and 500 µg/ml herring sperm DNA (Promega,

D1816)) was then applied on the sections and incubated for 4 hours at room temperature. Hybridisation buffer was prepared by mixing pre-hybridisation solution with 1:100 of the DIG-labelled riboprobe (2.3.6) of choice, heating at 80^{o}C for 5 minutes and then transferring on ice. Subsequently, 100 µl of hybridisation solution were applied on each slide, coverslipped and incubated in a humidified chamber placed in an oven set at 72^{o}C overnight.

The following day, the slides were immersed briefly in 5x SSC solution, which was pre-warmed at 72^{o}C overnight, to remove coverslips, then transferred in 0.2x SSC at 72^{o}C for 1 hour, followed by 5 minutes in 0.2x SSC at room temperature and finally equilibrated in buffer B1 (0.1 M Tris pH 7.5, 0.15 M NaCl) for 5 minutes at room temperature. Slides were then blocked in buffer B2 (buffer B1 + 10% heat inactivated sheep serum) for 2 hours at room temperature and after this, incubated with alkaline phosphatase (ALP) conjugated sheep anti-DIG antibody (Roche, 11 093 274 910) which was diluted 1:2000 in buffer B1 + 1% heat inactivated sheep serum, in a humidified chamber at 4^{o}C overnight.

The next day, the sections were washed with buffer B1 for 3 times, 5 minutes each, at room temperature and then incubated in buffer B3 (0.1 M Tris pH 9.5, 0.1 M NaCl, 50 mM $MgCl_2$) for 10 minutes on the bench. The staining solution for colorimetric detection of the AP-conjugated anti-DIG antibody was prepared by mixing 4.5 µl/ml of 75 mg/ml Nitrotetrazolium Blue chloride (NBT; Sigma-Aldrich, N6639, diluted in 70% dimethylformamide) and 3.5 µl/ml of 50 mg/ml 5-Bromo-4-chloro-3-indolyl phosphate disodium (BCIP; Sigma-Aldrich, B6149, diluted in dH_2O) in buffer B3. Slides were incubated in staining solution, in a humidified chamber kept in the dark at room temperature, until satisfactory staining was acquired. To stop the reaction, slides were washed in PBS. They were then air-dried and mounted with Aquatex® aqueous mounting agent (Merck Millipore, 108562).

2.6 Image processing and analysis

Bright field images of *in situ* hybridised sections were acquired with a digital colour camera (ProgRes C14) attached to an Axioplan 2 microscope (Zeiss) and processed with Openlab software (Improvision). All fluorescent images were captured with a confocal laser-scanning microscope (Leica TCS SP5 II MP) using standard excitation and emission filters to visualise DAPI, Alexa Fluor 488, Alexa Fluor 568 and Alexa Fluor 647. Figures of both bright field and fluorescence images were composed using the Adobe Photoshop CS4 (Adobe Systems) software.

2.7 Quantification and statistical analysis

Cell countings were performed on coronal cortical sections from 3 independent embryos per genotype, each embryo coming from a different litter. The number of Gad1-, Lhx6-, Sst- and Kcnc1- mRNA expressing cells was determined in the primary motor (M1, Br 0.38 mm), somatosensory barrel field (S1BF, Br 0.38 mm and -1.94 mm) and primary visual (V1, Br -2.92 mm) cortex of P15 *Satb1*$^{-/-}$ and *Satb1*$^{+/+}$ animals. For each region we counted cells present in 675.66 µm–wide columns, spanning the whole cortical depth (white matter-pial surface) on 14 µm cryosections. For confocal images, we counted cells from 775 µm–wide columns spanning the whole cortical depth on 14 µm cryosections focusing on S1BF, Br 0.38 mm. For the SST subset (CR, NPY and nNOS stainings) and VIP analyses, we counted cells from 4 serial sections of the somatosensory cortex (from Br 0.38 to 0.14 mm). For both the *in situ* hybridisation and immunofluorescence countings, data are given as means ± standard deviation (STDEV) of the mean. Statistical significance between data sets was determined using the Student's t-test function (two-tailed distribution, two-sample equal variance) in Excel (Microsoft) and they were considered significant when $p<0.05$ (*), $p<0.01$ (**) and $p<0.001$ (***). Histograms and survival curves were generated in Excel.

Chapter 3

Characterisation of cortical GABAergic interneuron development in a new *Satb1*-null mutant

3.1 Results

The latest studies from our laboratory have identified the genome organiser protein SATB1 genetically downstream of LHX6, in MGE-derived cortical interneurons (Denaxa *et al*., 2012). We therefore reasoned that SATB1 could play a role in regulating certain aspects of the development of this cellular network. Indeed, our work has demonstrated that SATB1 can promote the acquisition of mature characteristics, such as termination of migration and expression of the SST protein, in MGE progenitors *in vitro* (Denaxa *et al*., 2012).

To investigate the *in vivo* role of SATB1 in cortical interneuron development I have herein made use of a *Satb1* knockout (KO) allele that was established in our laboratory. In this chapter, I will present the generation and characterisation of this new *Satb1*$^{-/-}$ mutant. Independently-generated *Satb1*-null mice have been previously described in the literature, although these reports have focused exclusively on the role of SATB1 in T-cell (Alvarez *et al*., 2000) or projection neuron (Balamotis *et al*., 2012) development. Therefore, the possible *in vivo* requirement for SATB1 in cortical interneuron development remains in question. The main objective of the work presented in this chapter will be to address this question, although the overall physiology, brain anatomy and cortical lamination of *Satb1*$^{-/-}$ mice will also be addressed. With regards to cortical interneuron development, I will first investigate the specification of GABAergic identity and will then go on to examine the differentiation of cortical interneurons into mature, MGE-derived, PV^{+} and SST^{+} subsets, in the absence of *Satb1* activity.

3.1.1 A new *Satb1*-null mouse line

Satb1 loss of function mutant mice were generated using ES cells from the European Conditional Mouse Mutagenesis (EUCOMM) program, in which one locus of *Satb1* was targeted with a "knockout first, conditional ready" cassette (allele ID:

Satb1$^{tm1a(EUCOMM)Hmgu}$, herein referred to as *Satb1*$^{-}$). A detailed schematic representation of the targeted *Satb1* locus is given in Figure 3.1, A. The main elements of the targeting cassette include a ß-galactosidase (ß-gal) gene trap cassette, which consists of a splice acceptor (SA) site upstream of a promoterless IRES-ß-gal reporter, followed by a polyadenylation (polyA) sequence. The targeting cassette also includes the selectable marker Neo downstream of the phosphoglycerate 1 (PGK1) promoter and upstream of a polyA sequence (Figure 3.1, A). Upon integration into intron 3 of the *Satb1* gene the gene trap cassette will be transcribed from the *Satb1* promoter, forming a fusion transcript between *Satb1* exons 1-3 and the IRES-ß-gal reporter. Transcription will terminate early at the polyA signal, rendering the translation product of this transcript shorter and non-functional compared to the wt SATB1 protein. The mutant SATB1 protein will only contain aa 1-171, which correspond to the N-terminal ULD domain, and will lack aa 172-764 corresponding to the MAR-binding domain, CUT domains and HD, which are responsible for target sequence recognition and increased DNA binding affinity (section 1.5.1). This fusion protein should also be reporting the endogenous *Satb1* expression, allowing for the tracing of mutant cells *in vivo*.

Two independently generated JM8A1.N3 ES cell clones (Aa genotype) with the *Satb1*$^{-}$ allele, E11 and F12 (ES cell cultures were carried out by Reena Lasrado and Anna Garefalaki), were microinjected into either C57BL/6 or BALB/c blastocysts (4 independent injections for clone F12 and 3 independent injections for clone E11, performed by Mauro Tollaini), which were subsequently transferred to pseudopregnant females. Chimeric male offspring, which were identified by agouti/black or agouti/white coat colour respectively, were crossed with wt C57BL/6 females and germline transmission was tested by genotyping. The *Satb1*$^{-/-}$ line used herein came from an agouti/white founder male from clone E11 mated with a wt C57BL/6 female. Pups born from this cross were screened for successful targeting of the *Satb1* locus by

PCR using the F9, R10 and R11 primers (Figure 3.1, B; Table 2.2). Out of the 17 pups born we identified 11 *Satb1*$^{+/-}$ heterozyotes, the wt band given by primers F9-R10 at 337 bp and the mutant band given by primers F9-R11 at 184 bp (Figure 3.1, B), which were subsequently intercrossed to establish the *Satb1*$^{-/-}$ mutant line. Deletion of the *Satb1* locus was confirmed by immunostaining brain sections from P15 *Satb1*-null animals (*Satb1*$^{-/-}$), using a SATB1-specific antibody (Figure 3.1, C-D). Although the targeting cassette contained an IRES-ß-gal sequence, we were unable to detect ß-gal expression in the brains of *Satb1*$^{-/-}$ mice, using either an antibody against ß-gal or by performing an enzymatic X-gal staining assay (data not shown). The exact reason of why this happens is not known. We hypothesise that this could be due to the continued presence of the Neo cassette in our mice, as it can promote inappropriate pre-mRNA splicing or interfere with the stability of the mRNA product. Reduced gene expression levels due to the presence of a Neo cassette is a common phenomenon reported in the literature (Wang *et al*., 1998; Rucker *et al*., 2000). Alternatively, activation of a cryptic splice acceptor site within the ß-gal cassette could result in splicing out of a part of the reporter and formation of a truncated non-functional protein.

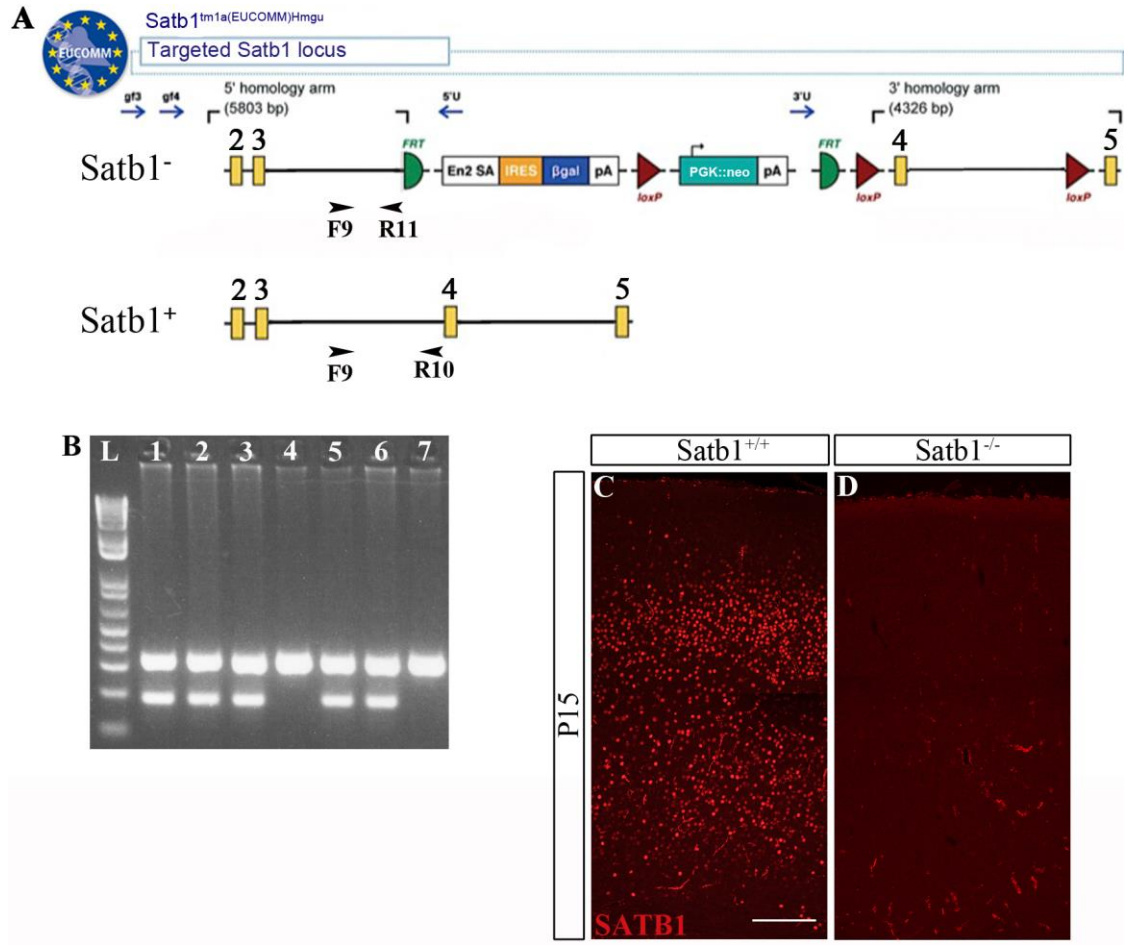

Figure 3.1 A new *Satb1*-null allele. (A) The targeted *Satb1* locus (top) and part of the wt *Satb1* locus that was targeted (bottom). Primers F9, R10 and R11 used for genotyping are indicated by black arrowheads at the bottom of each locus. The *Satb1*$^{-}$ allele is genotyped by primers F9-R11. Primer F9 anneals at the 5' homology arm and primer R11 anneals at the end of the 5' homology arm, just before the first FRT site. The *Satb1*$^{+}$ allele is genotyped by primers F9-R10. Primer R10 anneals just before exon 4. Note that primers F9-R10 do not generate a product when annealed at the *Satb1*$^{-}$ locus, as they are spaced too far apart (approximately 7.5 kb). Yellow rectangles represent exons of *Satb1*. **(B)** Representative lanes of PCR genotyping of a total of 17 pups used to establish the *Satb1*$^{-/-}$ line. Lanes 4 and 7 correspond to *Satb1*$^{+/+}$ mice and lanes 1, 2, 3, 5 and 6 correspond to *Satb1*$^{+/-}$ mice. The wt band is at 337 bp (primers F9-R10) and the mutant band is at 184 bp (primers F9-R11). L= 1 kb ladder. **(C-D)** Immunofluorescence on coronal cortical sections from P15 *Satb1*$^{+/+}$ (C) and *Satb1*$^{-/-}$ (D) mice. SATB1 protein is undetectable in the brains of *Satb1*-deficient animals. Scale bars 200 μm.

3.1.2 *Satb1*-null mutants exhibit growth defects and die shortly after weaning

Mice heterozygous for the *Satb1*$^{-}$ allele developed normally and were fertile, thus were intercrossed in order to generate *Satb1*$^{-/-}$ homozygous mutants. Of the total 131 pups that were born from *Satb1*$^{+/-}$ x *Satb1*$^{+/-}$ crosses and weaned at P21, we identified by PCR genotyping 35 *Satb1*$^{+/+}$ (27%), 74 *Satb1*$^{+/-}$ (56%) and 22 *Satb1*$^{-/-}$ (17%) progeny. Although wt and heterozygous mice were generated at the expected Mendelian ratio for autosomal recessive mutations, *Satb1*-null mutants were slightly underrepresented, indicating that a small fraction of mutant pups die before weaning.

Homozygous *Satb1*$^{-/-}$ mice were initially indistinguishable from their wt littermates. However, within a few days after birth they failed to thrive and grew to be smaller in size (Figure 3.2, A), weaker and less active than their wt and heterozygous siblings. Eventually, *Satb1*$^{-/-}$ mutants died 2-4 days after weaning, i.e. at P23-25 (Figure 3.2, B). Control animals picked up by the tail extended their limbs as a reflex in anticipation of contact with a horizontal surface (Figure 3.2, C). However, when this simple neurological assay was performed on *Satb1*$^{-/-}$ mutants they exhibited crossing of the hindlimbs and paw clasping (Figure 3.2, D), which is described in the literature as the clasping reflex. This is a neurological defect often observed in mice with lesions in the cerebellum, basal ganglia and neocortex (reviewed in Lalonde and Strazielle, 2011) that has also been observed in another *Satb1*-null mutant described in the literature (Alvarez *et al.*, 2000). Moreover, dissection of *Satb1*$^{-/-}$ mice revealed a dramatic difference in spleen size compared to wild-type littermates (Figure 3.2, E-F), in consistence with the studies of Alvarez *et al.*, which report that *Satb1*-null spleens had shrunken white pulp and contained fewer T cells (Alvarez *et al.*, 2000). In summary, our findings demonstrate that loss of *Satb1* activity leads to developmental and neurological defects and eventually results in death after weaning.

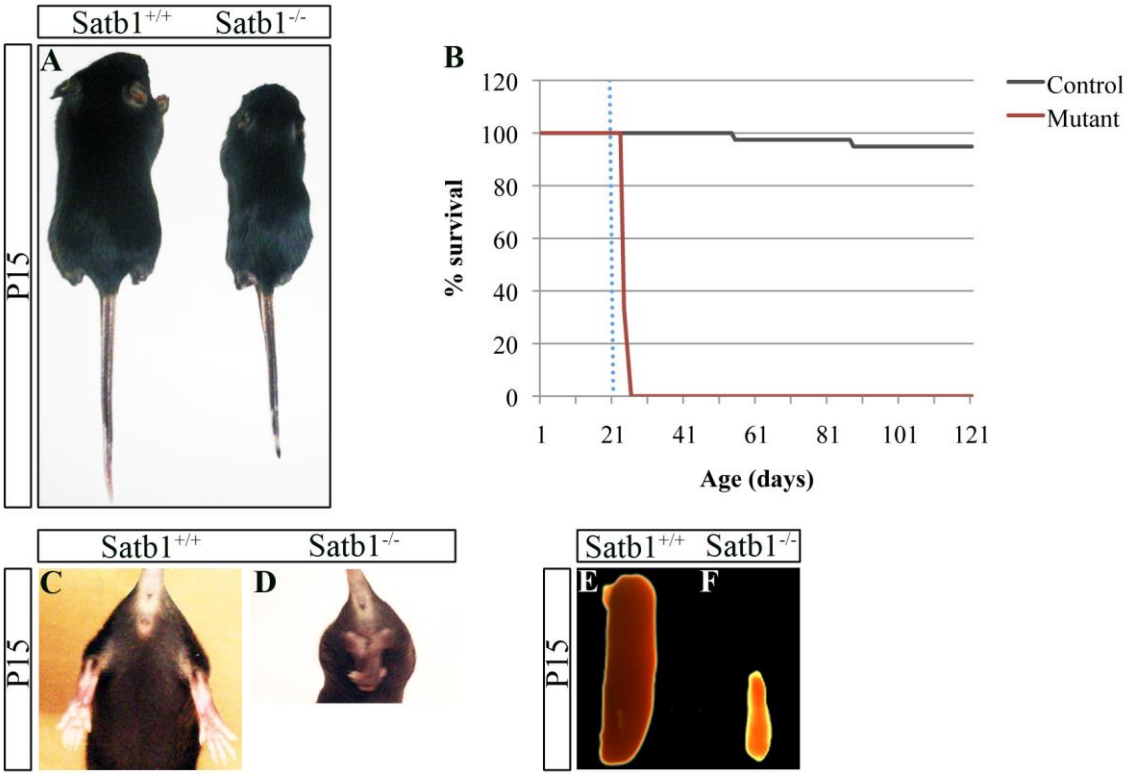

Figure 3.2 Abnormal development and compromised survival of *Satb1*$^{-/-}$ mutants. **(A)** P15 *Satb1*-null mutants are considerably smaller compared to control littermates of the same age. **(B)** Kaplan-Meier survival graph of mutant animals (red line) compared to controls (grey line) showing lethality of the former 2-4 days after weaning. n=6 for mutants, n=39 for controls. **(C-D)** Neurological assay of tail suspension performed at P15 *Satb1*$^{+/+}$ (C) and *Satb1*$^{-/-}$ mice (D). Control animals extend their limbs whereas mutants cross their hindlimbs. **(E-F)** Spleen size is dramatically reduced in *Satb1*$^{-/-}$ animals (F) compared to *Satb1*$^{+/+}$ littermates (E). Images of live mice were taken by authorised personnel at the NIMR biological services facility.

3.1.3 Normal brain development and cortical layer formation in *Satb1*-deficient mice

On the basis that *Satb1* is expressed in both cortical pyramidal neurons and interneurons (Denaxa *et al*., 2012; Balamotis *et al*., 2012), we searched for alterations in cortical layer development of *Satb1*-deficient mice. Given the lethality of *Satb1*$^{-/-}$ mutants immediately after weaning we performed all our analyses at P15. Dissected brains of P15 *Satb1*$^{-/-}$ mice appeared macroscopically normal (Figure 3.3, A-B) and Nissl staining of coronal sections from these brains revealed no gross anatomical abnormalities compared to controls (Figure 3.3, C-J). Moreover, cortical lamination markers such as *Cux2* and *Er81*, specific for layers II-IV (Zimmer *et al.*, 2004) and V (Hevner *et al.*, 2003) respectively, showed similar expression patterns between control (Figure 3.3, K and M) and mutant animals (Figure 3.3, L and N), suggesting that although *Satb1* is expressed in pyramidal neurons its deletion does not affect cortical layering. Similarly, examination of layer VI and layer V/VI markers *Tbr1* and *Ctip2* respectively, at an independently generated *Satb1*-null mouse, showed no marked difference compared to controls (Balamotis *et al*., 2012). Finally, expression of *Satb2*, a close homologue of *Satb1* detected in layers II-VI that regulates cortical layer development (Alcamo *et al.*, 2008; Britanova *et al.*, 2008), remains unaffected upon loss of *Satb1* activity (Figure 3.3, O-P) and cortical thickness is comparable between controls and mutants, again in accordance with what has been reported in the literature (Balamotis *et al*., 2012). In summary, no anatomical or cortical layering defects were observed in our *Satb1*$^{-/-}$ mutants that could influence our subsequent cortical interneuron analysis.

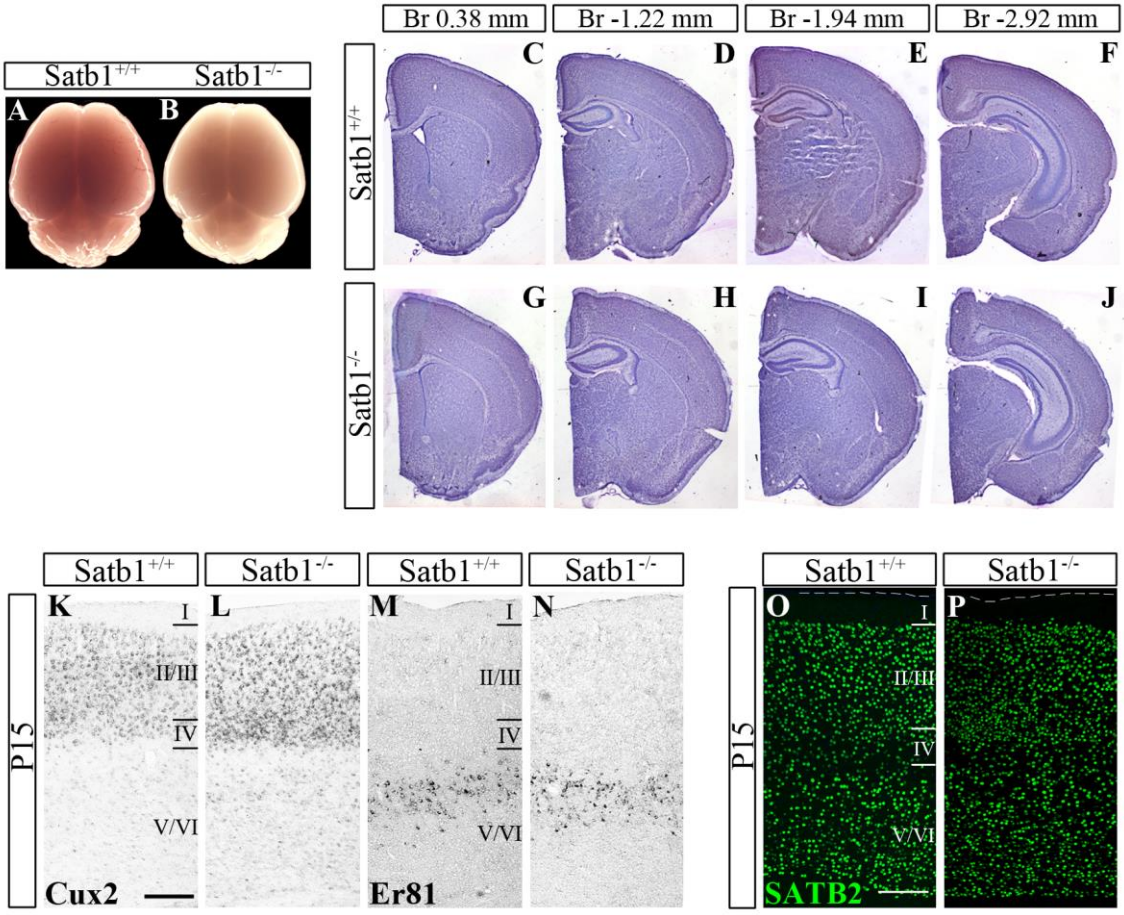

Figure 3.3 Brain anatomy and cortical lamination are unaffected in *Satb1*$^{-/-}$ mice. **(A-B)** Dissected P15 brains from *Satb1*$^{+/+}$ (A) and *Satb1*$^{-/-}$ (B) mice appear similar. **(C-J)** Nissl staining on P15 coronal hemisections from *Satb1*$^{+/+}$ (C-F) and *Satb1*$^{-/-}$ (G-J) mice reveals no gross anatomical differences between the two. **(K-N)** *In situ* hybridisation of cortical sections from P15 control (K, M) and *Satb1*-deficient (L, N) mice with riboprobes specific for Cux2 (K, L) and Er81 (M, N), which labell layers II-IV and V respectively. **(O-P)** Immunofluorescence for SATB2, which marks layers II-VI, in P15 controls (O) and mutants (P). Overall, cortical layer formation remains unaffected upon loss of *Satb1* activity. Scale bars 200 µm. Nissl staining performed by Radhika Anand at the NIMR histology facility.

3.1.4 GABAergic interneurons are correctly specified in *Satb1*-deficient mutants

Satb1 is expressed in GABAergic cortical interneurons and specifically in the MGE-derived population (Denaxa *et al*., 2012; Close *et al*., 2012). We therefore set out to investigate whether the loss of *Satb1* function had any effect on this group of cells. The total number of cortical interneurons was assessed by RNA *in situ* hybridisation for the mRNA transcript of *Gad1*, the gene encoding for GAD67, which participates in the rate-limiting step of GABA biosynthesis (section 1.2.1.2) and the transcript of *Lhx6*, to specifically label GABAergic interneurons of MGE origin (Liodis *et al.*, 2007). The number of these cells in the cortex of P15 *Satb1*$^{+/+}$ and *Satb1*$^{-/-}$ animals was counted in columns spanning the whole depth (white matter-pial surface) of the cortex and 675.66 μm in width, in four different cortical areas along the anteroposterior (AP) axis, namely the primary motor cortex (M1, Br 0.38 mm), the somatosensory cortex barrel field (S1BF, Br 0.38 mm and Br -1.94 mm) and the primary visual cortex (V1, Br -2.92 mm).

Comparison of equivalent bregma positions in control and mutant cortices revealed no significant change in the total number of Gad1^{+} interneurons in any of the four areas examined (Figure 3.4, A-H and Q; M1, 143±35.5 in controls, 135±33.5 in mutants; S1BF Br 0.38 mm, 161±36.1 in controls, 151±31 in mutants; S1BF Br -1.94 mm, 84±20.8 in controls, 80±14.5 in mutants; V1, 80±22.6 in controls, 71±7.5 in mutants). Moreover, we observed no difference in the number of Lhx6^{+} cells between controls and mutants in three out of four areas examined (Figure 3.4, I-J, M-P and Q; M1, 128±7.6 in controls, 123±11 in mutants; S1BF Br -1.94 mm, 88±26.2 in controls, 94±5.2 in mutants; V1, 84±7.4 in controls, 77±6.7 in mutants) with the exception of a subtle but yet statistically significant reduction of 17.5% in anterior levels of the somatosensory cortex (Figure 3.4 K-L and Q; S1BF Br 0.38 mm, 149±2.1 in controls, 123±5.1 in mutants) of *Satb1*$^{-/-}$ animals.

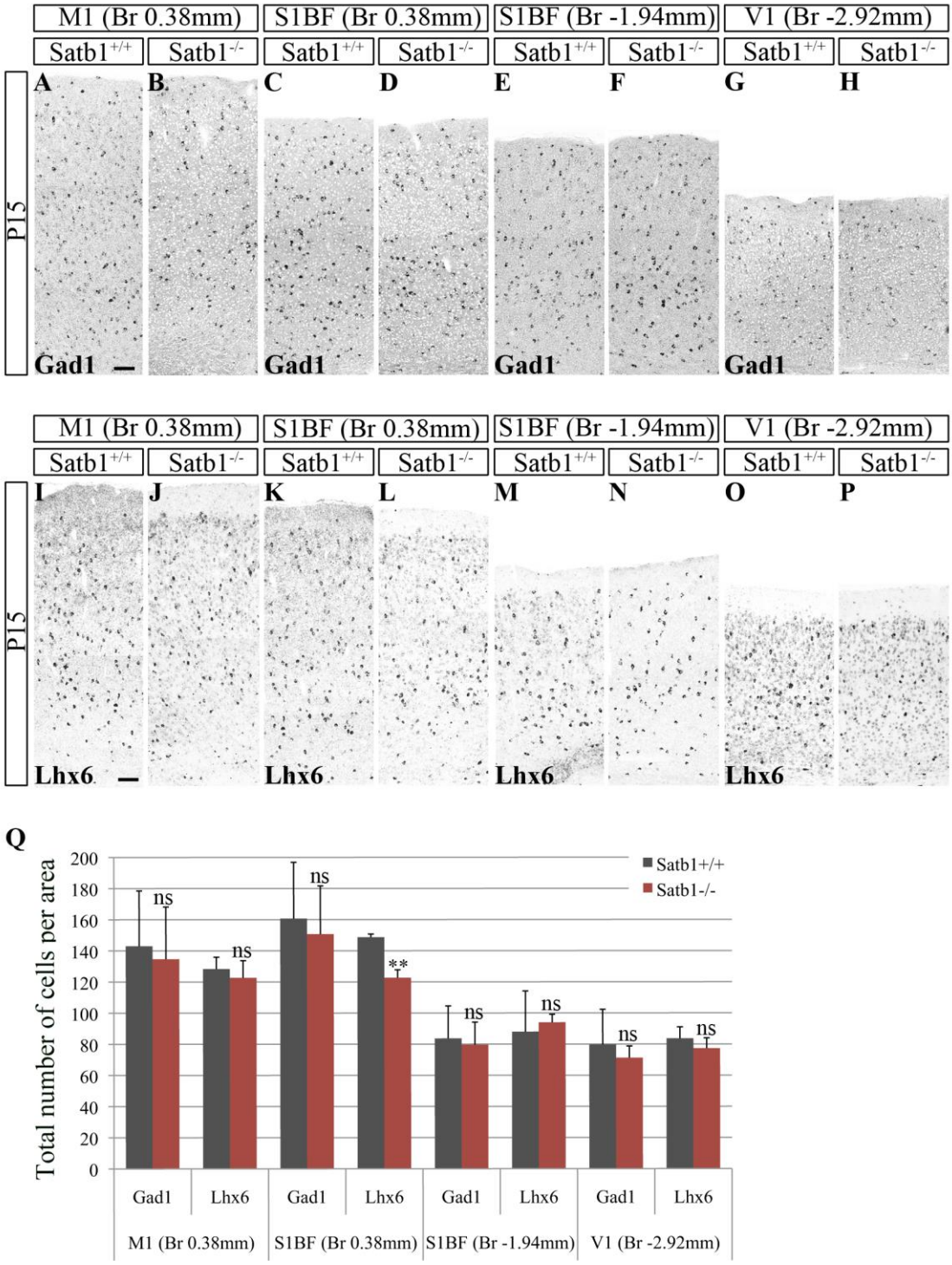

Figure 3.4 Normal specification of cortical GABAergic interneurons in the absence of *Satb1* activity. (A-H) *In situ* hybridisation of P15 cortical sections from wt (A, C, E and G) and *Satb1*-deficient (B, D, F and H) mice with a Gad1-specific riboprobe. **(I-P)** *In situ* hybridisation of P15 cortical sections from wt (I, K, M and O) and *Satb1*-deficient (J, L, N and P) mice with an Lhx6-specific riboprobe. **(Q)** Quantification of $Gad1^+$ and $Lhx6^+$ interneurons in the primary motor (M1, Br 0.38 mm), somatosensory

barrel field (S1BF, Br 0.38 and -1.94 mm) and primary visual (V1, Br -2.92 mm) cortex of P15 wt (grey bars) and *Satb1*-deficient (red bars) mice. The number of Gad1 or Lhx6 mRNA-expressing interneurons is not significantly reduced in any of the areas examined, the only exception being a significant reduction of 17.5% in $Lhx6^+$ cells in S1BF Br 0.38 mm (K-L and Q). n=3 animals per genotype. ns indicates no statistical significance, ** indicates $p<0.01$, Student's t test (two-tailed distribution, two-sample equal variance). Error bars, standard deviation of the mean (STDEV). Scale bars 100 μm.

Given the fact that we do not see a change in the number of $Gad1^+$ cells in S1BF Br 0.38 mm, we interpret the small reduction of $Lhx6^+$ cells in this area of *Satb1* mutants in two ways: either a small subset of GABAergic interneurons loses expression of *Lhx6* in *Satb1*-deficient mice, or the Lhx6 countings, as they target only a subset of interneurons, reveal an increased propensity of cells in this area for apoptotic cell death. However, we failed to detect any difference in the number of apoptotic cells, as assessed by TUNEL assay, at P15 between controls and mutants (data not shown), consistent with the findings of another $Satb1^{-/-}$ mutant analysis (Balamotis *et al*., 2012). It is worth mentioning that a recent *Satb1* conditional loss of function study reports SST^+ interneuron death in the somatosensory cortex of mutants from P5 onwards, attributed to the reduced excitatory input received by these cells (Close *et al*., 2012). This could also be exacerbated by seizure activity reported in the cortex of these mutants, as SST-expressing interneurons are sensitive to epileptic seizures (Choi *et al*., 2007).

Taken together our results demonstrate that GABAergic identity is correctly specified in *Satb1*-deficient mice, similarly to *Lhx6*-null mutants (Liodis *et al*., 2007; Zhao *et al*., 2008). Moreover, these findings are consistent with the observation that *Satb1* is expressed at relatively late stages of cortical interneuron development, following their specification in the subpallium (Denaxa *et al*., 2012; Close *et al*., 2012).

3.1.5 Cortical interneuron differentiation defects in the absence of *Satb1* activity

Although GABAergic identity is specified at the progenitor level, at the very early stages of cortical interneuron development and some subtype-specific features are acquired by the influence of genetic determinants in the GEs of the ventral forebrain, mature properties such as the expression of specific molecular markers, the acquisition of characteristic morphology and electrophysiological features as well as the selection of synaptic partners are only acquired later on, when cells settle in the cortex and are exposed to extrinsic, environmental influences, including neuronal activity (reviewed in Cossart, 2011).

Analyses of *Satb1* expression during embryonic development have demonstrated that it is excluded from the MGE and tangentially migrating interneurons but instead is expressed specifically in MGE-derived cortical interneurons following invasion of the cortical plate (Denaxa *et al*., 2012; Close *et al*., 2012) and persists in these cells throughout life. We thus reasoned that SATB1 could play a specific role in regulating the maturation and terminal differentiation of these cells in the cortex. Moreover, ectopic overexpression of *Satb1* in MGE precursors, in a brain slice culture system, demonstrated that SATB1 can induce the expression of *Sst* not only at the mRNA level but also at the protein level (Denaxa *et al*., 2012), strengthening our hypothesis for a role of SATB1 in cortical interneuron maturation, since SST protein is detected within the cortex only in postnatal stages (Gonchar *et al*., 2008).

To investigate cortical GABAergic interneuron differentiation in the *Satb1*$^{-/-}$ mutant cortex we focused on a series of molecular markers that define subsets of cortical interneurons and performed *in situ* hybridisation and immunofluorescence experiments on P15 coronal cortical sections.

First, we examined the non-overlapping groups of SST- and PV-expressing cortical interneurons (Gonchar *et al*., 2008) of the MGE lineage, which represent the

two largest populations of interneurons in the cortex (Butt *et al*., 2005; Fogarty *et al*., 2007; reviewed in Gelman and Marín, 2010). We investigated the development of these two major interneuron subsets in P15 brains by *in situ* hybridisation using riboprobes specific for Sst (Figure 3.5, A-B) and Kcnc1 (Figure 3.5, C-D) transcripts, focusing on the same four cortical regions examined in our previous studies. *Kcnc1*, otherwise known as *Kv3.1*, encodes a voltage-gated K^+ channel specifically found in PV^+ interneurons (Weiser *et al*., 1995; Chow *et al*, 1999) and required for the fast-spiking properties of these cells (Erisir *et al*., 1999). Quantification of the absolute number of cells per area revealed a dramatic reduction in the number of Sst mRNA-expressing interneurons in all areas examined (Figure 3.5, A-B and E; M1, 57±16.1 in controls, 24±10.1 in mutants; S1BF Br 0.38 mm, 72±17.9 in controls, 27±3.4 in mutants; S1BF Br -1.94 mm, 42±15.1 in controls, 18±5.5 in mutants; V1, 36±1.5 in controls, 17±6.3 in mutants). The number of Kcnc1 mRNA-expressing cells was unaffected in the primary motor and visual cortex (Figure 3.5, E; M1, 115±25.2 in controls, 74±16.9 in mutants; V1, 79±37 in controls, 44±2.6 in mutants) but was significantly reduced in the somatosensory cortex, at both bregma positions examined (Figure 3.5, C-D and E; S1BF Br 0.38 mm, 123±6 in controls, 87±8 in mutants; S1BF Br -1.94 mm, 98±19.3 in controls, 63±4.4 in mutants). Focusing on the somatosensory cortex barrel field (S1BF, Br 0.38 mm), a well-studied and commonly used area in the literature, the reduction in Sst and Kcnc1 mRNA-expressing interneurons was 63% and 29% respectively.

We then assessed the expression of the SST neuropeptide (Figure 3.5, F-G) and the calcium-binding protein PV (Figure 3.5, H-I), in this area (S1BF, Br 0.38 mm). Expression of both peptides initiates in the mouse cortex at the first weeks of postnatal life (del Río *et al*., 1994; Gonchar *et al*., 2008), thus allowing us to use SST- and PV-specific antibodies for our analysis at P15. We observed a dramatic reduction of 62% in the number of SST^+ interneurons in *Satb1*$^{-/-}$ mice compared to wt littermates (Figure

3.5, J; 66±9.5 in controls, 25±2 in mutants), which is very close to the 63% reduction in Sst mRNA-expressing cells, and a less pronounced but significant reduction of 14% in the PV^+ population (Figure 3.5, J; 107±4 in controls, 93±4.9 in mutants). The smaller reduction in PV^+ cells compared to that observed in Kcnc1 mRNA-expressing cells could perhaps be explained by a differential requirement for SATB1 in the regulation of *Pv* and *Kcnc1* gene expression. Alternatively, our countings at P15 could be underestimating the PV^+ interneuron defect, as expression of *Pv* begins shortly before this stage (del Río *et al*., 1994), whereas *Kcnc1* expression is thought to initiate during late embryonic stages (Boda *et al*., 2012).

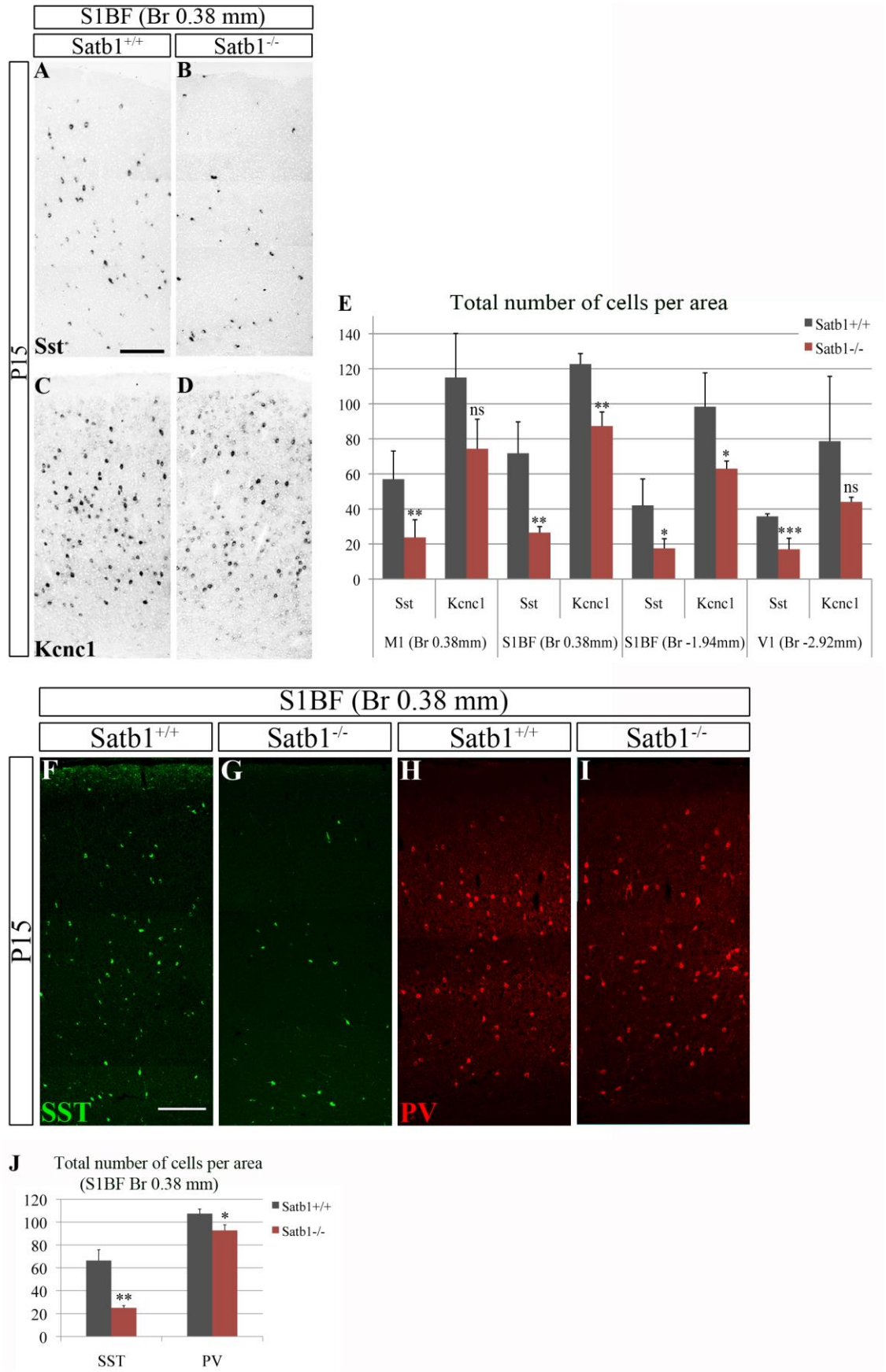

Figure 3.5 (legend at following page)

Figure 3.5 Impaired differentiation of MGE-derived interneurons in *Satb1*-deficient mice. (A-D) *In situ* hybridisation on P15 cortical sections from wt (A, C) and *Satb1*-null (B, D) mice with riboprobes specific for Sst (A-B) and Kcnc1 (C-D). **(E)** Quantification of Sst^+ and $Kcnc1^+$ interneurons in the primary motor (M1, Br 0.38 mm), somatosensory barrel field (S1BF, Br 0.38 and -1.94 mm) and primary visual (V1, Br -2.92 mm) cortex of P15 wt (grey bars) and *Satb1*-null (red bars) mice. The number of Sst mRNA-expressing interneurons is dramatically reduced in all areas examined, whereas Kcnc1 mRNA-expressing cells were significantly reduced in S1BF, at both Br 0.38 mm and -1.94 mm. **(F-I)** Immunofluorescence on P15 cortical sections from wt (F and H) and *Satb1*-deficient (G and I) mice with antibodies specific for SST (F-G) and PV (H-I). **(J)** Quantification of SST^+ and PV^+ cells in the somatosensory cortex (S1BF, Br 0.38 mm) of wt (grey bars) and *Satb1*-deficient animals (red bars). The number of SST^+ interneurons is reduced by 62% and the number of PV^+ interneurons is reduced by 14% in $Satb1^{-/-}$ mice compared to controls. n=3 animals per genotype. ns indicates no statistical significance, * indicates $p<0.05$, ** indicates $p<0.01$, *** indicates $p<0.001$, Student's t test (two-tailed distribution, two-sample equal variance). Error bars, STDEV. Scale bars 200 µm.

Last, we examined the expression of the neuropeptide VIP, a CGE-specific marker (Butt *et al*., 2005; Miyoshi *et al*., 2010), by immunofluorescence on P15 cortical sections (Figure 3.6, A-B). To increase the number of cells counted, we performed our analysis at four serial sections of the somatosensory cortex (between Br 0.38 mm and 0.14 mm) in each of the three animals per genotype. In line with *Satb1* being restricted to MGE-derived interneurons, we were unable to detect any significant difference in the number of VIP^+ cells between control and *Satb1*-null animals (Figure 3.6, C; 100±20.6 in controls, 88±9.3 in mutants), which argues against the possibility of a non-cell autonomous effect caused in CGE interneurons by loss of *Satb1* activity in their MGE counterparts.

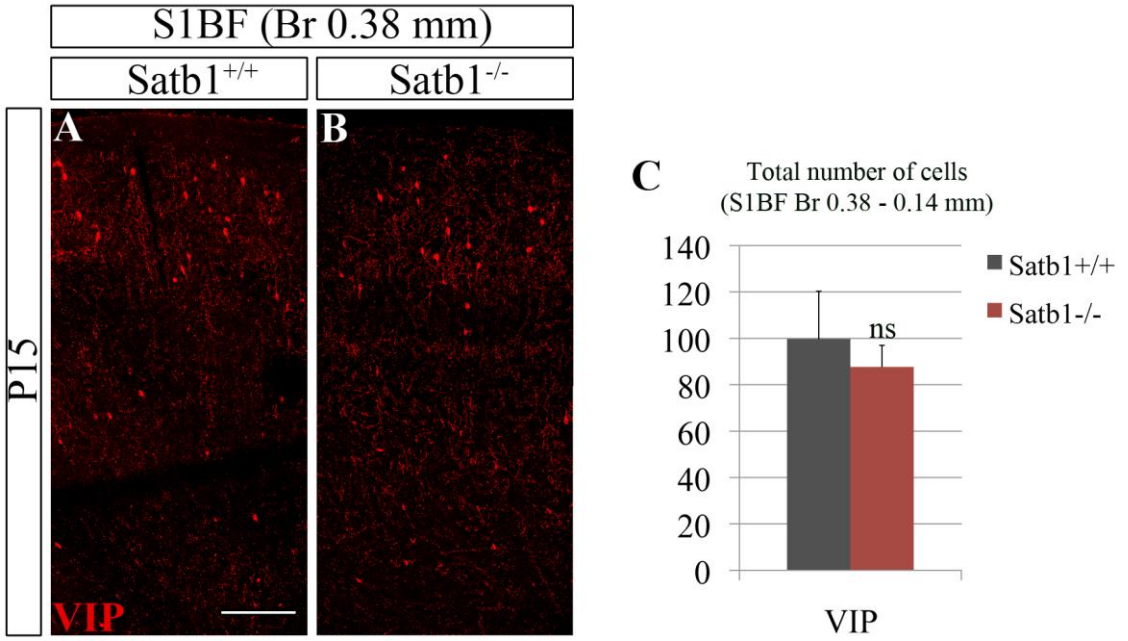

Figure 3.6 Loss of *Satb1* activity does not affect the differentiation of VIP$^+$, CGE-derived interneurons. (A-B) Immunofluorescence on P15 cortical sections from wt (A) and *Satb1*-deficient (B) mice with a VIP-specific antibody. **(C)** Quantification of VIP$^+$ cells in the somatosensory cortex (S1BF, Br 0.38 – 0.14 mm) of wt (grey bars) and *Satb1*-deficient mice (red bars) reveals no significant change in the number of CGE-derived VIP$^+$ interneurons upon loss of *Satb1* activity. n=3 animals per genotype, 4 sections per animal (Br 0.38 mm - 0.14 mm). ns indicates no statistical significance, Student's t test (two-tailed distribution, two-sample equal variance). Error bars, STDEV. Scale bar 200 µm.

Overall, our *in vivo* findings demonstrate that *Satb1* is intrinsically required to regulate primarily the differentiation of the SST-expressing subset of cortical interneurons. Moreover, taking into account the fact that the expression pattern of three cortical lamination markers (Figure 3.3, K-P) remains unaltered between controls and mutants we conclude that the differentiation defects observed in our *Satb1*$^{-/-}$ mice are not secondary to impaired cortical lamination.

3.1.6 *Satb1* regulates multiple aspects of SST-expressing interneuron differentiation

In agreement with our finding that *Satb1* controls the differentiation of SST^+ interneurons, a recent study has provided evidence for direct regulation of the *Sst* genomic locus by SATB1, via direct binding of the latter to upstream regulatory elements of the *Sst* gene (Balamotis *et al*., 2012). We therefore sought to elucidate whether SATB1 plays a specific role in exclusively controlling the expression of *Sst* or whether it has a wider function in regulating the maturation of SST-expressing interneurons. For this purpose we analysed the expression of markers that are coexpressed with SST in certain cortical interneuron subsets. These include the calcium-binding protein CR (Xu *et al.*, 2006; Miyoshi *et al*., 2007; Fogarty *et al*., 2007), the neuropeptides NPY (Ma *et al*., 2006; Karagiannis *et al.*, 2009) and CRH (Kubota *et al.*, 2011) and the nNOS protein (Magno *et al.*, 2012; Jaglin *et al.*, 2012; Perrenoud *et al.*, 2012).

In the mouse cortex, approximately 30% of SST^+ interneurons coexpress CR, with the majority of these cells located in layers II/III (Xu *et al.*, 2006; Miyoshi *et al*., 2007), and close to 50% of SST^+ interneurons coexpress NPY (as deducted from the combined studies of Fogarty *et al*., 2007 and Gelman *et al*., 2009). The total CR^+ and NPY^+ populations were reduced by 31% and 21% respectively, across all cortical layers in the somatosensory cortex (S1BF between Br 0.38 mm and 0.14 mm) of mutants (Figure 3.7, B1, D1 and E) compared to controls (Figure 3.7, A1, C1 and E). Notably, double immunofluorescence for CR;SST or NPY;SST revealed a pronounced decrease in the number of both CR^+;SST^+ (Figure 3.7, A-B and E; 89% reduction, 67±4.7 in controls, 7±3.2 in mutants) and NPY^+;SST^+ interneurons (Figure 3.7, C-D and E; 54% reduction, 116±32.7 in controls, 41±2.6 in mutants) in *Satb1*$^{-/-}$ animals but no change in

the number of $CR^+;SST^-$ (Figure 3.7, E; 126±21.5 in controls, 129±8.6 in mutants) or $NPY^+;SST^-$ (Figure 3.7, E; 193±3 in controls, 202±18.8 in mutants) cells.

According to a recent study performed in the rat frontal cortex, 20-25% of the SST^+ cells in cortical layers V and VI coexpress the neuropeptide CRH (Kubota *et al.*, 2011). In the lack of a CRH-specific antibody, we generated a Crh-specific riboprobe and counted the total number of Crh^+ cells in layers I-IV, layers V-VI, as well as across all cortical layers at S1BF Br 0.38 mm (Figure 3.7, F-G and H). We observed a tendency for reduced numbers of Crh^+ cells across all layers in *Satb1*-null cortices (all layers, 29±5.5 in controls, 19±4.5 in mutants; layers I-IV, 18±4.9 in controls, 15±3.4 in mutants), although a statistically significant decrease in the number of these cells was noted only in layers V-VI (10±1.1 in controls, 4±1.7 in mutants), which is where the $CRH^+;SST^+$ double positive interneurons are mainly found (Kubota *et al.*, 2011). Notably, our results are in agreement with a recent study describing another $Satb1^{-/-}$ mutant strain, which reports downregulation of Crh mRNA levels in this mutant and binding of SATB1 to regulatory regions of the *Crh* locus (Balamotis *et al*., 2012).

Finally, we counted the number of type I $nNOS^+$ projection interneurons, which are mainly located in bottom cortical layers (V-VI) and express high levels of the nNOS peptide along with SST (Magno *et al.*, 2012). No significant change in the percentage of type I $nNOS^+;SST^+$ interneurons was documented between controls (Figure 3.7, I and K; 97±2.5%) and $Satb1^{-/-}$ mutants (Figure 3.7, J and K; 89±6.9%) at Br 0.38 mm - 0.14 mm of the P15 somatosensory cortex.

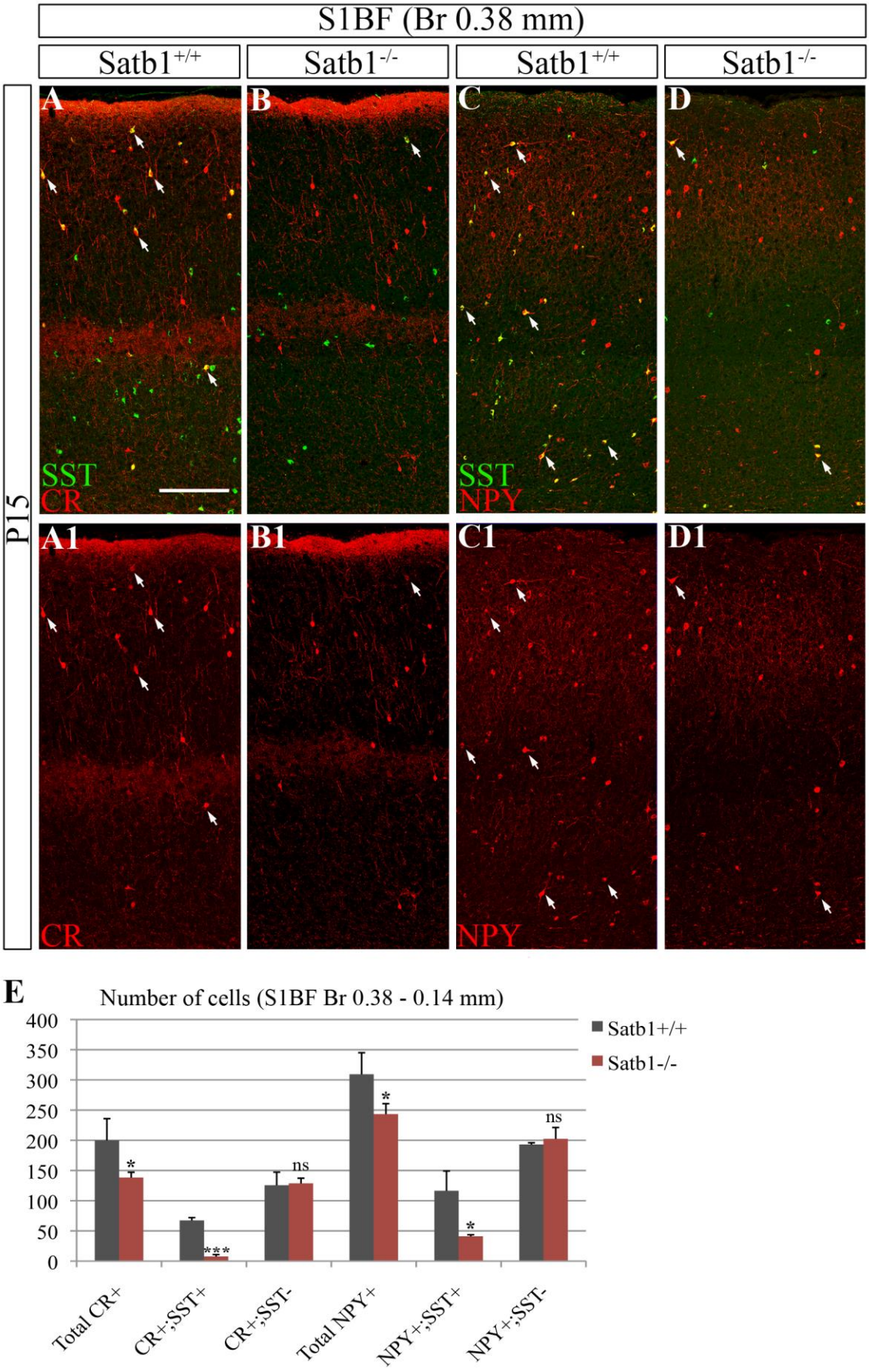

Figure 3.7 (continues at following page)

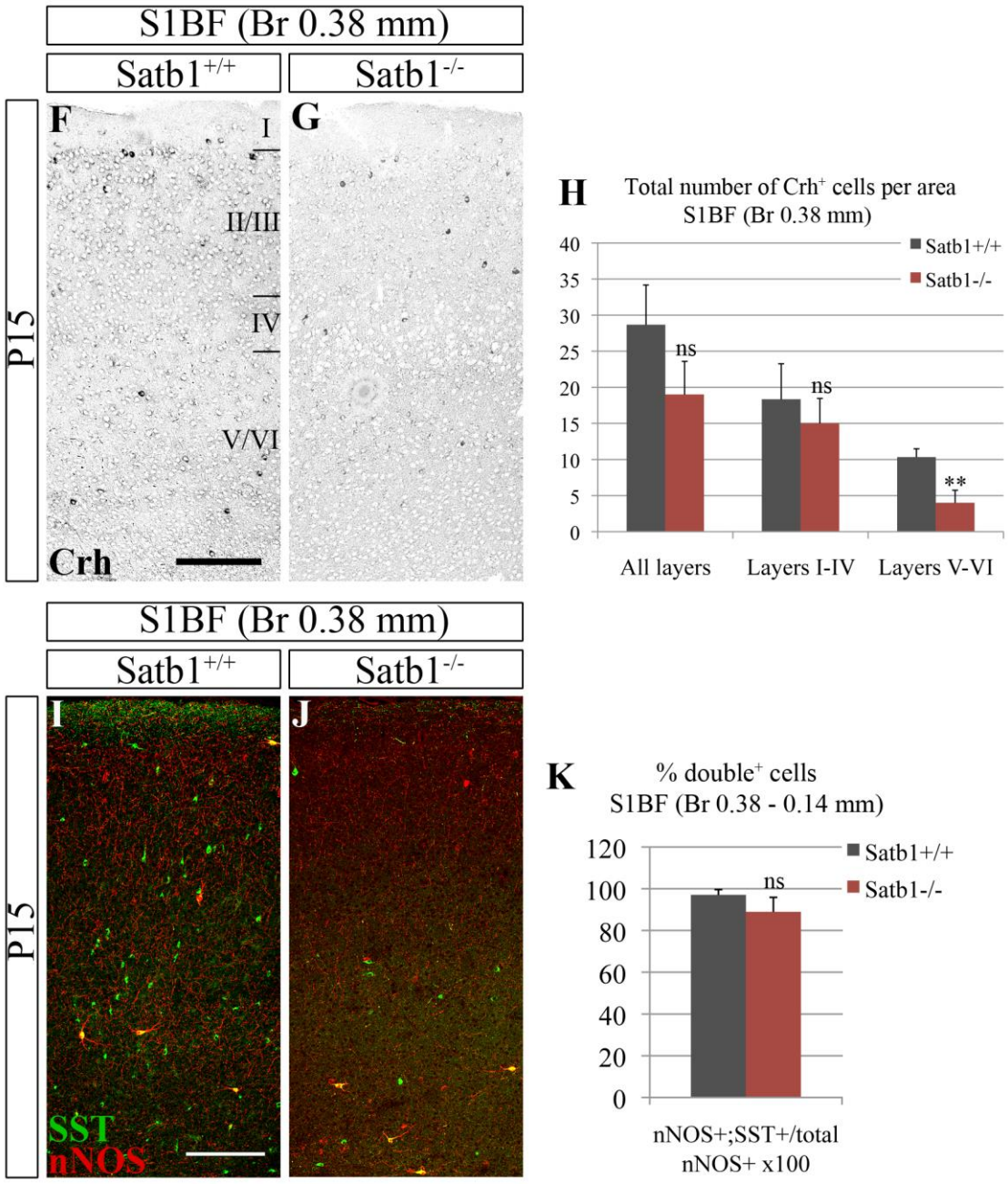

Figure 3.7 SATB1 is required for the expression of additional markers defining SST$^+$ interneuron subsets. (A-D) Double immunofluorescence on P15 coronal cortical sections from wt (A and C) and *Satb1*-deficient (B and D) mice with antibodies specific for SST and CR (A-B) or SST and NPY (C-D). **(A1-D1)** Panels showing the CR (A1-B1) or NPY (C1-D1) staining alone. **(E)** Quantification of the total number of total CR$^+$, CR$^+$;SST$^+$, CR$^+$;SST$^-$, total NPY$^+$, NPY$^+$;SST$^+$ and NPY$^+$;SST$^-$ cells in the somatosensory cortex (S1BF, Br 0.38 – 0.14 mm) of wt (grey bars) and *Satb1*-deficient mice (red bars). The number of CR$^+$;SST$^+$ interneurons is reduced by 89% and the number of NPY$^+$;SST$^+$ interneurons is reduced by 54% in *Satb1*$^{-/-}$ mice compared to

controls. **(F-G)** *In situ* hybridisation for Crh on P15 coronal cortical sections from wt (F) and *Satb1*-deficient (G) mice. **(H)** Quantification of the total number of Crh^+ cells in upper and lower cortical layers in S1BF, Br 0.38 mm. Notice the significant reduction of Crh-expressing cells only in layers V-VI. **(I-J)** Double immunofluorescence on P15 cortical sections from wt (I) and *Satb1*-deficient (J) animals with antibodies specific for SST and nNOS. **(K)** Quantification of the percentage of $nNOS^+;SST^+$ cells in the $nNOS^+$ population in the somatosensory cortex (S1BF, Br 0.38 – 0.14 mm) of wt (grey bars) and *Satb1*-deficient mice (red bars) revealed no significant change in this population. n=3 animals per genotype. ns indicates no statistical significance, * indicates $p<0.05$, ** indicates $p<0.01$, *** indicates $p<0.001$, Student's t test (two-tailed distribution, two-sample equal variance). Error bars, STDEV. Scale bars 200 µm.

In conclusion, our results demonstrate that SATB1 regulates the expression of *Sst* and has a profound effect in the overall maturation of SST-expressing interneurons, by controlling the expression of a multitude of neuropeptides and proteins that define SST^+ interneuron subsets in the postnatal mouse cortex. Interestingly, the fact that $nNOS^+;SST^+$ long-projection interneurons remain unaffected upon loss of *Satb1* activity could possibly indicate a specific requirement for *Satb1* in local circuit interneuron differentiation in the cortex.

3.2 Discussion

Formation of local inhibitory circuits in the mammalian cortex depends on the function of a vast array of different subtypes of cortical GABAergic interneurons, which are born and specified in the ventral forebrain, reach the cortex by tangential migration and finally integrate into the different cortical layers where they differentiate into mature subtypes. Although considerable progress has been made in understanding the transcriptional cascades that operate in the embryonic subpallium to control the specification of cortical interneurons and the mechanisms by which they reach their final destination in the pallium, our understanding of the terminal differentiation of cortical interneuron subsets in the maturing cortex is limited.

By analysing a new *Satb1*-null mouse we demonstrate here that the chromatin organiser protein SATB1 plays a novel and specific role primarily in the maturation of the SST-expressing subset of MGE-derived cortical interneurons *in vivo*, without affecting the acquisition of GABAergic identity.

3.2.1 Requirement of *Satb1* activity in the terminal differentiation of GABAergic cortical interneurons

The LIM-HD transcription factor LHX6 is expressed throughout the development of MGE-derived GABAergic cortical interneurons, from the moment they exit the cell cycle (Liodis *et al.*, 2007; Du *et al.*, 2008) and initiate tangential migration to the cortex (Lavdas *et al.*, 1999; Liodis *et al.*, 2007), up to adulthood, when LHX6 colocalises with SST and PV in mature interneurons (Liodis *et al.*, 2007; Fogarty *et al.*, 2007). Consistent with this, *Lhx6* loss of function studies have demonstrated an early requirement of *Lhx6* activity for the proper tangential and radial migration of MGE-derived interneurons to the cortex (Alifragis *et al.*, 2004; Liodis *et al.*, 2007; Zhao *et al.*, 2008) and a late role of LHX6 in the differentiation of SST^+ and PV^+ interneurons

(Liodis *et al.*, 2007; Zhao *et al*., 2008). Importantly, studies from our laboratory have demonstrated that this differentiation deficit is independent of the migration defect observed in these mutants (Neves *et al*., 2012). Finally, *Lhx6*-deficiency has no effect on the GABAergic identity of these cells (Alifragis *et al*., 2004; Liodis *et al.*, 2007).

Given that little is known about the terminal differentiation of interneurons in the maturing cortex, the latest studies from our group have focused on identifying genes that act downstream of LHX6 to regulate cortical interneuron differentiation. A genome-wide microarray screen conducted on E15.5 cortices from *Lhx6*$^{+/+}$ and *Lhx6*$^{-/-}$ mice identified the transcription factor and genome organiser protein SATB1 as being downregulated in the absence of *Lhx6* activity (Denaxa *et al*., 2012). To investigate the potential role of SATB1 in cortical interneuron development we generated a *Satb1*$^{-/-}$ mutant mouse and chose postnatal day 15 as our stage of analysis.

Macroscopically, *Satb1*-deficient mice exhibited a similar phenotype to *Lhx6*$^{-/-}$ mutants (Liodis *et al*., 2007), with severely delayed development, weakness and early lethality around weaning. Neither of the two mutant strains developed obvious signs of epileptic seizures and at the cellular level, the total number of Gad1^{+} interneurons, as assessed by *in situ* hybridisation, remained unaffected in the cortex of both *Satb1*- and *Lhx6*-deficient animals. Another common finding between these mutants is the compromised differentiation of MGE-derived interneurons. This is in agreement with *in vitro* studies from our laboratory, which provide evidence that LHX6 and SATB1 operate in the same pathway. In this cascade, SATB1 acts as a mediator of *Lhx6* activity, necessary and sufficient to control the differentiation of GABAergic interneurons (Denaxa *et al*., 2012).

However, there are clear differences between *Lhx6*$^{-/-}$ and *Satb1*$^{-/-}$ mutants. In contrast to the tangential and radial migration defects documented in *Lhx6*-null mice (Liodis *et al*., 2007; Zhao *et al*., 2008), tangential migration of cortical interneurons

proceeds normally in *Satb1*$^{-/-}$ mutants (Denaxa *et al*., 2012) and our results so far do not show a consistent pattern for laminar distribution defects in these mice (analysis in progress). Our findings are in agreement with the fact that expression of *Satb1* is excluded from tangentially migrating interneurons and only starts once these cells have reached the cortical plate (Denaxa *et al*., 2012; Close *et al*., 2012). Moreover, the studies of Liodis *et al*. report a dramatic reduction of both SST^{+} and PV^{+} interneurons (Liodis *et al*., 2007) in *Lhx6*-deficient mice, whereas our *Satb1*$^{-/-}$ analysis demonstrates a greater deficit in the differentiation of the SST^{+} subset and a smaller but still significant defect in the PV^{+} subset of cortical interneurons. These data point towards the existence of distinct cascades operating downstream of LHX6 to regulate the differentiation of SST- and PV-expressing interneurons.

3.2.2 Differential roles of SATB1 in SST^{+} and PV^{+} cortical interneuron development

Colocalisation studies in the postnatal mouse cortex revealed that virtually all SST^{+} and PV^{+} cortical interneurons express the SATB1 protein (Denaxa *et al*., 2012; Close *et al*., 2012). However, we present here the first constitutive *Satb1* KO study that provides evidence for the differential requirement of SATB1 in the maturation of these two major MGE-derived interneuron populations. Although there was a profound decrease in the number of cortical interneurons expressing the SST neuropeptide in our *Satb1*$^{-/-}$ mice, loss of PV protein expression was documented in a much smaller population of cells in the cortex of these mutants. Along the same lines, a conditional *Satb1* mutant study, published at the same time as our work, reports that specific loss of *Satb1* activity from postmitotic interneurons has a greater effect on the SST-expressing subset compared to their PV-expressing counterparts (Close *et al*., 2012). Moreover, the idea that SATB1 does not play an instructive role for the differentiation of PV^{+}

interneurons is further supported by *in vivo* transplantation experiments conducted in our laboratory, which demonstrate that SATB1-overexpressing MGE progenitors grafted into the neonatal mouse cortex predominantly differentiate into SST^+, rather than PV^+ interneurons (Denaxa *et al*., 2012).

The above findings argue that other genes, besides *Satb1*, must be operating downstream of LHX6 to instruct the differentiation of PV^+ cortical interneurons. One of these genes is *Sox6*. Conversely to the *Satb1*-null findings, examination of *Sox6* mutant mice demonstrated that the transcription factor SOX6, although being expressed in both SST- and PV-expressing interneurons, is required primarily for the differentiation of the latter (Batista-Brito *et al*., 2009). GABAergic interneurons were specified normally in *Sox6*-deficient mice but were mispositioned in the cortex and the number of cells expressing the PV protein was drastically reduced by 94%, as opposed to a 30% reduction in the population expressing SST. The firing properties of PV^+ interneurons were also altered towards a less mature state in these mutants (Batista-Brito *et al*., 2009).

Collectively, the data gathered so far indicate the existence of two distinct pathways that operate downstream of LHX6 to control the differentiation of the two major cortical interneuron populations: one cascade governed by SOX6 regulating development of the PV^+ subset and a second, novel cascade driven by SATB1 regulating development of the SST^+ subset, as summarised in Figure 3.8.

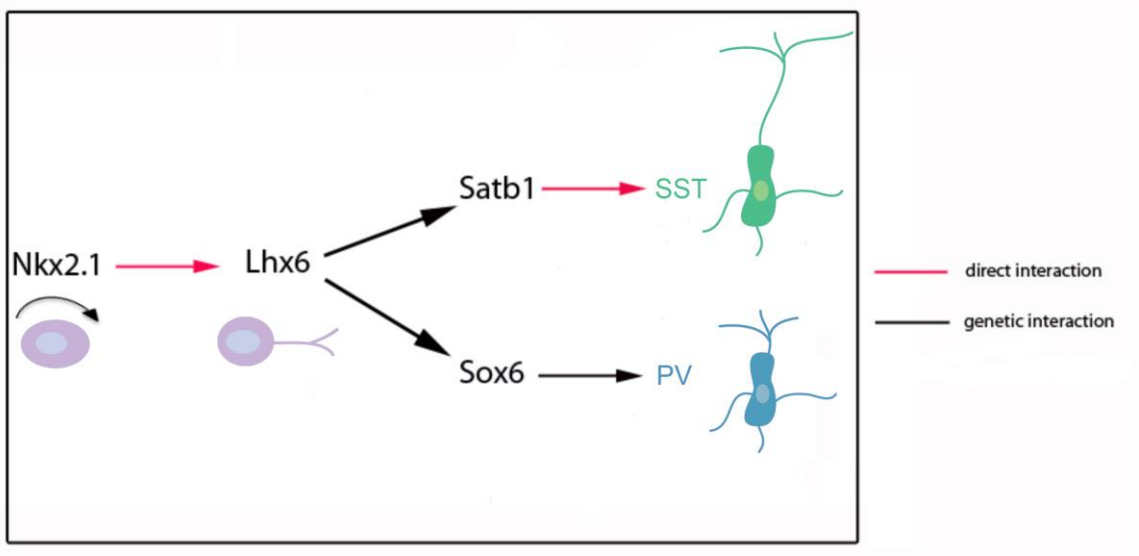

Figure 3.8 Proposed model of the divergent pathways downstream of LHX6 that regulate SST$^+$ and PV$^+$ interneuron differentiation. The literature provides evidence for direct regulation of *Lhx6* expression by NKX2.1, as soon as MGE progenitors exit the cell cycle (Du *et al.*, 2008). Data from our laboratory (Denaxa *et al*., 2012) show that SATB1 is genetically downstream of LHX6, and the findings of this thesis demonstrate that SATB1 directs the differentiation of SST$^+$ interneurons, in agreement with observations from another group (Close *et al*., 2012). In fact, direct binding of SATB1 to the *Sst* locus has been shown in the literature (Balamotis *et al*., 2012). In a parallel pathway, SOX6 functions genetically downstream of LHX6 to regulate PV$^+$ interneuron differentiation (Batista-Brito *et al*., 2009). Red arrows indicate direct regulation. Black arrows indicate genetic interaction.

3.2.3 SATB1 coordinately regulates the expression of multiple genes, whose protein products are associated with mature SST$^+$ interneurons

The SST$^+$ subset of cortical interneurons is extremely heterogeneous and includes "SST$^+$ only" cells, SST$^+$ cells coexpressing CR, NPY, or Reelin (reviewed in Gelman and Marín, 2010) as well as a small percentage of SST$^+$;CRH$^+$ cells (Kubota *et al*., 2011). Moreover, SST colocalises with nNOS in type I long-projection interneurons (Magno *et al.*, 2012; Jaglin *et al.*, 2012; Perrenoud *et al.*, 2012), a distinct group of cortical GABAergic interneurons, which differ from the local circuit interneurons

mainly in that they extend long horizontal projections to distant cortical areas (Tomioka *et al.*, 2005).

We provide evidence herein for a novel role of SATB1 in controlling the expression of a set of these factors, which characterise mature cortical interneurons of the SST^+ subset. Analysis of our *Satb1*$^{-/-}$ mutants at P15 revealed no change in the total population of GABAergic interneurons but a dramatic decrease in the number of interneurons expressing the neuropeptide SST along with a significant reduction in the numbers of CR^+, NPY^+ and Crh^+ cells. No change was observed in the long-projection population of type I nitrinergic interneurons between controls and mutants. Our findings are consistent with the analysis of an independently generated *Satb1* KO mouse, which presents a significant downregulation of the Sst, Crh and Calb2 mRNA levels, the latter being the gene that encodes for the calcium-binding protein CR, in the cortices of P13-P14 *Satb1*-null mice (Balamotis *et al*., 2012). We provide additional evidence for the regulation of *Npy* expression by SATB1. Notably, the Balamotis *et al*. study also demonstrates binding of SATB1 to upstream regulatory elements of the *Sst, Crh* and *Calb2* genomic loci. This suggests direct transcriptional regulation of these genes by SATB1 and thereby explains the reduced expression of these markers observed in *Satb1*-deficient mutants.

However, the exact mechanism by which SATB1 orchestrates the expression of multiple cortical interneuron-specific genes in a coordinated manner has not been elucidated. Similarly to our results, synchronous regulation of multiple genes by SATB1 has been demonstrated in cells of the immune system (Alvarez *et al*., 2000; Yasui *et al*., 2002; Cai *et al*., 2003), as well as in breast cancer cells, where SATB1 controls the expression of more than 1,000 genes to promote cancer growth and metastasis (Han *et al*., 2008). Therefore, studying these examples could offer insight into how SATB1 might be functioning in our context. One hypothesis, based on the above-mentioned

studies, is that it all begins with the higher order organisation of chromatin structure: SATB1 recognises its target MARs sequences in a multitude of genomic loci and tethers them to the nuclear matrix resulting in the formation of chromatin loops with SATB1 and its bound sequences located at the base of these loops. This chromatin looping brings distant *cis*-regulatory elements physically closer to promoters of genes thus allowing for transcriptional activation or repression (reviewed in Galande *et al*., 2007). In addition, following the formation of this complex network, SATB1 recruits chromatin-remodelling factors, histone-modifying enzymes and transcription factors at the base of chromatin of loops, allowing them to act on the genomic loci tethered onto this common "transcription hub" (reviewed in de la Serna *et al*., 2006). One could imagine a similar model for the coordinated regulation of cortical interneuron maturation-promoting genes by SATB1.

Chapter 4

Cortical interneuron-specific deletion of *Satb1*

4.1 Results

The results obtained from our *Satb1*$^{-/-}$ analysis demonstrate a marked requirement for *Satb1* activity for the maturation of SST^{+} cortical interneurons and a less clear, if any, role in the differentiation of PV^{+} interneurons. Consistent with *Satb1* expression in both cortical interneurons and pyramidal cells (Balamotis *et al*., 2012; Denaxa *et al*., 2012) we wished to determine whether the effect of *Satb1* deletion is secondary to its role in pyramidal neurons. For this, we characterised the expression of three cortical lamination markers in our *Satb1*-null mutants and observed no difference in cortical layer formation, compared to controls (section 3.1.3). However, analysis of another *Satb1*$^{-/-}$ mouse revealed that dendritic spine density of pyramidal neurons is reduced by half, thereby affecting their ability to form synapses and receive input (Balamotis *et al*., 2012). We therefore decided to delete *Satb1* exclusively in cortical interneurons by generating a *Satb1* floxed allele and combining it with interneuron-specific Cre lines.

The overall aim of the work presented in this chapter is to distinguish between the cell-autonomous and non-cell-autonomous roles of SATB1 in cortical interneuron development. First, I will present the generation of *Satb1* floxed mice, as well as the characterisation of several inducible Cre lines that could potentially be combined with these mice to achieve cortical interneuron-specific deletion of *Satb1*. Next, I will mainly focus on the conditional deletion of *Satb1* from MGE-derived interneurons using the *Nkx2.1-Cre* transgenic line. *Nkx2.1-Cre;Satb1-flox* mutants will be examined for SST and PV differentiation defects and their phenotype will be compared to that of *Satb1*$^{-/-}$ mutants. Finally, I will investigate whether SATB1 is intrinsically required for the maturation of PV-expressing interneurons, by combining *Satb1* floxed with *PV-Cre* mice, in an attempt to address the subtle but significant PV^{+} interneuron deficit observed in our *Satb1*-null mutants (section 3.1.5).

4.1.1 Generation of a *Satb1* floxed mouse

For the generation of the *Satb1* floxed mouse we took advantage of the fact that the targeted *Satb1* allele of our $Satb1^{-/-}$ mice contains two LoxP recombination sites flanking exon 4 (Figure 4.1, A top panel). Therefore, the $Satb1^{-}$ allele has the potential to be converted into a conditional allele by simply excising the first part of the targeting cassette by recombination at the FRT sites that flank it. To this aim, we crossed $Satb1^{+/-}$ mice with the *ACTB:FLPe* deleter line (Figure 4.1, A top panel) in which the improved Flpe recombinase is under the control of the human *ß-actin* promoter and drives recombination at both somatic and germ-line lineages (Rodriguez *et al*., 2000). Excision of the FRT-flanked cassette and thus successful generation of the floxed *Satb1* allele (referred to from now on as $Satb1^{flox}$; Figure 4.1, A middle panel) was confirmed by PCR genotyping with the same primers used to genotype the wt *Satb1* allele. Primers F9 and R10 give the wt band at 337 bp and the floxed band slightly higher, at 428 bp (Figure 4.1, B). The size difference between the wt and floxed bands comes from the remaining FRT site in the $Satb1^{flox}$ allele. Importantly, had the FRT-flanked cassette not been removed, primers F9-R10 would not be able to generate a product as they would be spaced too far apart. $Satb1^{flox/+}$ mice born from $Satb1^{+/-}$ x $ACTB^{flpe/flpe}$ matings were then intercrossed to generate the $Satb1^{flox/flox}$ colony. As anticipated, $Satb1^{flox/flox}$ mice developed normally and were indistinguishable from wt mice, as after successful removal of the FRT-flanked cassette the resulting allele no longer contains the splice acceptor and therefore cannot function as a loss-of function allele. Since exon 4 of *Satb1* is flanked by LoxP recombination sites in our $Satb1^{flox/flox}$ mice, crossing with a Cre line should result in Cre-mediated recombination and deletion of exon 4 (Figure 4.1, A bottom panel). Excision of exon 4 will create several in-frame stop codons, resulting in early termination of Satb1 mRNA translation and a shorter protein, and will thereby generate a loss of function allele.

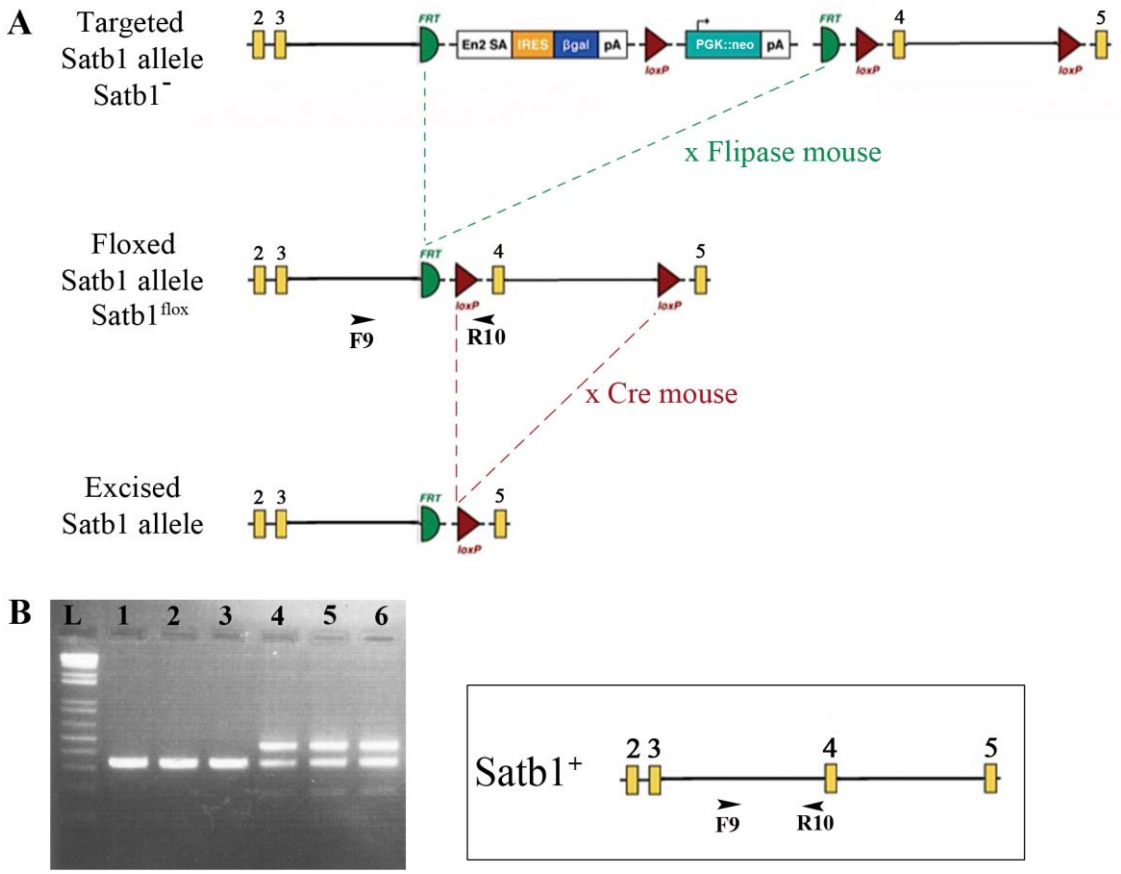

Figure 4.1 Generation of the floxed *Satb1* allele. (A) From top to bottom: the targeted *Satb1* allele (*Satb1*$^{-}$), the floxed *Satb1* allele (*Satb1*^{flox}) and the recombined *Satb1* allele, after exon 4 deletion. Matings between *Satb1*$^{+/-}$ and *ACTB*$^{flpe/flpe}$ mice result in recombination at the FRT sites flanking the *Satb1* targeting cassette and excision of the first part of the cassette. What remains is one FRT site and two LoxP sites that flank exon 4 of *Satb1* (*Satb1*^{flox} allele). Matings between mice carrying the *Satb1*^{flox} allele and a Cre line should culminate in Cre-mediated recombination at the LoxP sites and excision of exon 4. Yellow rectangles represent exons of *Satb1*. **(B)** PCR genotyping results for *Satb1*$^{flox/+}$ (lanes 4-6) and *Satb1*$^{+/+}$ mice (lanes 1-3) born from a *Satb1*$^{+/-}$ x *ACTB*$^{flpe/flpe}$ mating. The *Satb1*^{flox} allele is identified by the upper 428 bp band, while the lower 337 bp band corresponds to the wt *Satb1* allele (boxed area in B). Both the wt and floxed bands are given by the same set of primers, F9 and R10, indicated by black arrowheads. The floxed band is slightly bigger than the wt one because of the FRT site that remained after Flpe recombination that generated the floxed allele. L= 1 kb ladder.

4.1.2 Characterisation of Cre lines for the conditional deletion of *Satb1* in cortical interneurons

We decided to follow two approaches for the selective deletion of *Satb1* in cortical interneurons: first, removal of *Satb1* from the MGE lineage, which includes both the SST- and PV-expressing cells. Second, subtype-specific deletion of *Satb1* in the SST^+ and PV^+ subsets separately, which would help us distinguish between differential requirements of *Satb1* in these two non-overlapping populations of cells.

To achieve deletion of *Satb1* in the MGE we selected the *Nkx2.1-CreER^{T2}* (Kessaris N., unpublished) and *Lhx6-CreER^{T2}* (Taniguchi *et al*., 2011) lines, whereas for subtype-specific studies we focused on the *SST-CreER^{T2}* and *Pv-CreER^{T2}* inducible mice (Taniguchi *et al*., 2011). The latter three lines are publicly available through the JAX mice database but had not been described in the literature at the time we obtained them. In all the above-mentioned mice the catalytic domain of the bacterial Cre recombinase is fused to a Tamoxifen-responsive Estrogen Receptor ligand-binding domain from the human gene (ER^{T2}) (Feil *et al*., 1997). $CreER^{T2}$ is sequestered in the cytoplasm and only when Tamoxifen, or its analog 4-Hydroxytamoxifen (4-OHT), is administered, CreER can be translocated to the nucleus and induce recombination between LoxP sites. Recombination generally occurs within 6-12 hours and continues for up to 36 hours. (reviewed in Joyner and Zervas, 2006). The advantage of these lines would be the temporal regulation of *Satb1* deletion, allowing us to investigate the early versus late requirements of *Satb1* in cortical interneuron development.

Before crossing with the *Satb1$^{flox/flox}$* mice, the *Nkx2.1-CreER^{T2}*, *Lhx6-CreER^{T2}*, *SST-CreER^{T2}* and *Pv-CreER^{T2}* lines were combined with the *R26ReYFP* reporter (Srinivas *et al*, 2001) in order to test their recombination efficiency after 4-OHT administration. We concentrated on establishing a protocol for successful recombination of the *R26ReYFP* locus at P30 pups or adult (P90 or older) mice, by intraperitoneally

administering 3 mg of 4-OHT per animal, daily, for two consecutive days, or by injecting 2 mg of 4-OHT per animal, daily for a period of five consecutive days. The latter protocol was only followed in adult stages, to avoid adverse effects in younger animals. One or two weeks after the last dose of 4-OHT was given, the mice were perfused and their brains analysed for expression of YFP by immunofluorescence using a GFP-specific antibody on 100 µm vibratome coronal sections.

After 4-OHT administration, a total of six *Nkx2.1*$^{CreERT2/+}$*;R26ReYFP*$^{stop/+}$ and five *Lhx6*$^{CreERT2/+}$*;R26ReYFP*$^{stop/+}$ animals were analysed for YFP expression. Representative examples of the best induction efficiency and the protocol used to achieve this are summarised in Figure 4.2. Both lines gave consistent labelling in ventral regions, such as the piriform cortex (Figure 4.2, E and K), the hypothalamus (Figure 4.2, F) and the amygdala (Figure 4.2, G) but only sparse and inconsistent labelling in the motor and somatosensory cortices (Figure 4.2, B and C), which are our areas of interest. The *Nkx2.1*$^{CreERT2/+}$*;R26ReYFP*$^{stop/+}$ line gave relatively good labelling in the hippocampus (Figure 4.2, J) and auditory cortex (Figure 4.2, I)

Figure 4.2 (next page) The *Nkx2.1-CreER*^{T2} and *Lhx6-CreER*^{T2} lines show poor recombination efficiency in the adult mouse forebrain. (A) Schema of the 4-OHT administration protocol followed at P120 *Lhx6*$^{CreERT2/+}$*;R26ReYFP*$^{stop/+}$ mice. **(B-G)** GFP staining at coronal brain sections from *Lhx6*$^{CreERT2/+}$*;R26ReYFP*$^{stop/+}$ mice 2 weeks after induction with 4-OHT reveals very sparse labelling in the somatosensory cortex (B), motor cortex (C) and hippocampus (D). Better efficiency was observed in ventral areas such as the piriform cortex (E), the hypothalamus (F) and the amygdala (G). **(H)** Schema of the 4-OHT administration protocol followed at P90 *Nkx2.1*$^{CreERT2/+}$*;R26ReYFP*$^{stop/+}$ mice. **(I-K)** Representative images of brain regions with the best labelling after GFP immunostaining at *Nkx2.1*$^{CreERT2/+}$*;R26ReYFP*$^{stop/+}$ mice, 1 week after induction with 4-OHT. The dorsal-most areas with GFP^{+} cells were the auditory cortex (I) and hippocampus (J). Ventrolateral areas showed consistently the best induction (K). Scale bars 100 µm for B-F, and 200 µm for G and I-K.

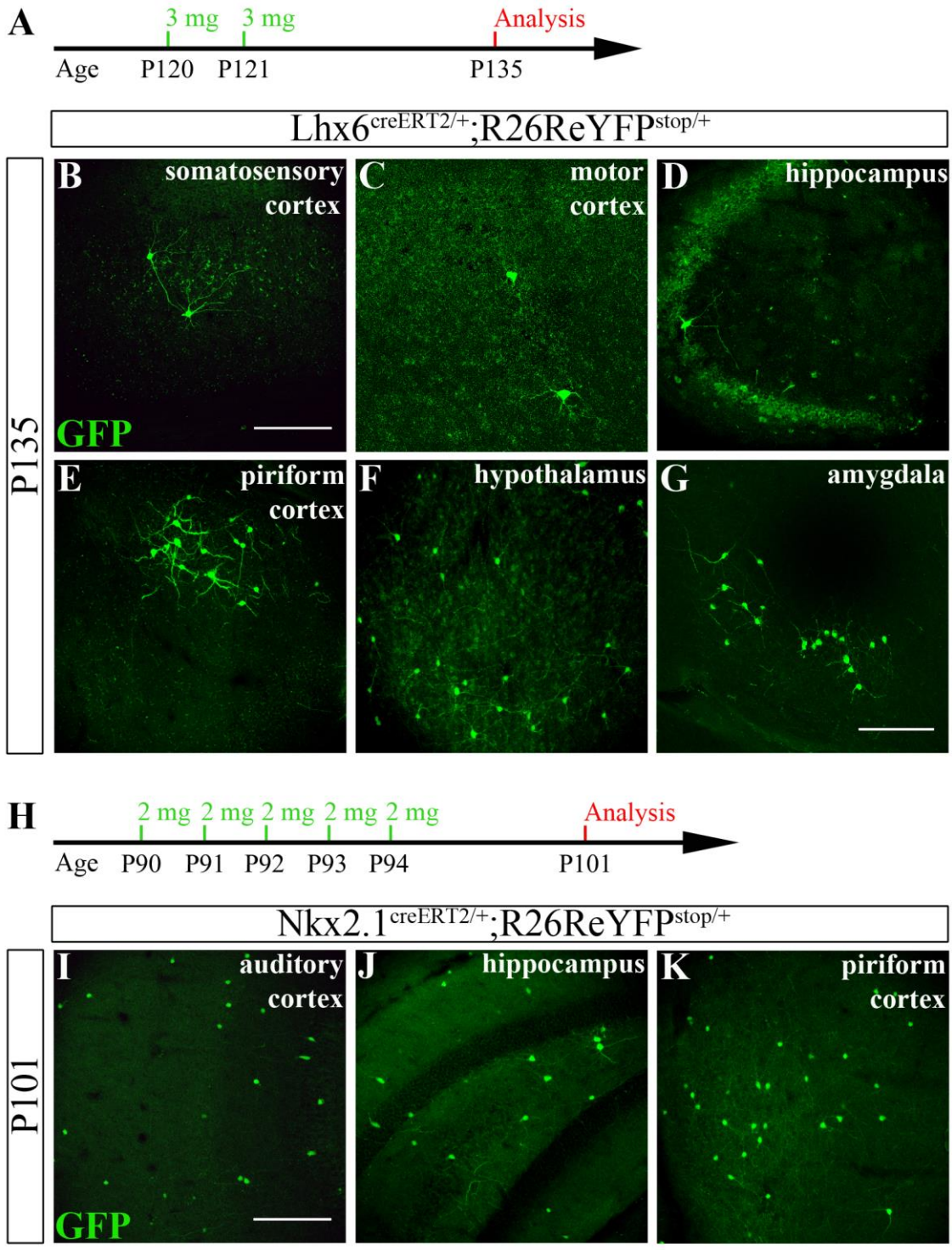

Figure 4.2 (legend at previous page)

Repeated efforts to activate Cre and the YFP reporter in a total of six animals from the *SST*$^{CreERT2/+}$*;R26ReYFP*$^{stop/+}$ and six animals from the *Pv*$^{CreERT2/+}$*;R26ReYFP*$^{stop/+}$ line, resulted in failure to detect YFP^{+} cells anywhere within the brain of these mice (data not shown). An alternative approach would be to inject

mice with 1 mg of 4-OHT twice a day for five consecutive days, thus achieving accumulation of higher systemic concentrations of the substance and therefore improved recombination efficiency (Leone *et al*., 2003). However, we decided not to pursue this protocol as our findings were confirmed by a publication from the group that generated the *Lhx6-CreER*^{T2}, *SST-CreER*^{T2} and *Pv-CreER*^{T2} inducible lines (Taniguchi *et al*, 2011). This study reports labelling of less than five cells within the cortex after Tamoxifen administration in all three lines and attributes this to possible changes in the sequences at the translation initiation codon of these genes, where the CreER cassette was targeted to, which could result in low transcription levels from this locus and consequently inefficient CreER induction.

We therefore explored alternative tools and turned our attention to the constitutive *Nkx2.1-Cre* (Kessaris *et al*., 2006), *SST-ires-Cre* (Taniguchi *et al.*, 2011) and *PV-Cre* (Hippenmeyer *et al.*, 2005) lines. While working on generating the *Nkx2.1-Cre;Satb1-flox, SST-Cre;Satb1-flox* and *PV-Cre;Satb1-flox* conditional mutants, a parallel study from the Fishell group came to our attention, which included the description of a *Satb1* conditional mutant using the SST-*ires*-Cre line (Close *et al*., 2012). For this reason, we focused on the *Nkx2.1-Cre;Satb1-flox* and *PV-Cre;Satb1-flox* strains, the analysis of which is presented in the following sections.

4.1.3 Conditional deletion of *Satb1* in MGE-derived cortical interneurons results in cell death and development of epileptic seizures

In order to selectively inactivate *Satb1* in cortical interneuron progenitors and be able to trace mutant cells at the same time, we combined the *Nkx2.1-Cre* transgene (Kessaris *et al*., 2006) with the *R26ReYFP* reporter allele (Srinivas *et al*., 2001). In the *Nkx2.1*$^{Cre/+}$*;R26ReYFP*$^{stop/+}$ double transgenic mice, Cre is expressed in AEP, POA and MGE progenitors, apart from those in the dorsal-most MGE (Fogarty *et al*., 2007), and

mediates recombination of the *R26ReYFP* reporter allele resulting in permanent labelling of progenitor cells and their descendants. We then crossed these mice with our newly generated *Satb1*$^{flox/flox}$ line to achieve conditional inactivation of *Satb1* in the MGE lineage and permanent tracing of the mutant cells. The detailed breeding scheme used to generate the experimental *Nkx2.1*$^{Cre/+}$;*R26ReYFP*$^{stop/+}$;*Satb1*$^{flox/+}$ (control) and conditional KO (cKO) *Nkx2.1*$^{Cre/+}$;*R26ReYFP*$^{stop/+}$;*Satb1*$^{flox/flox}$ genotypes, the latter referred to as *Satb1|Nkx2.1* cKO, is shown in Figure 4.3.

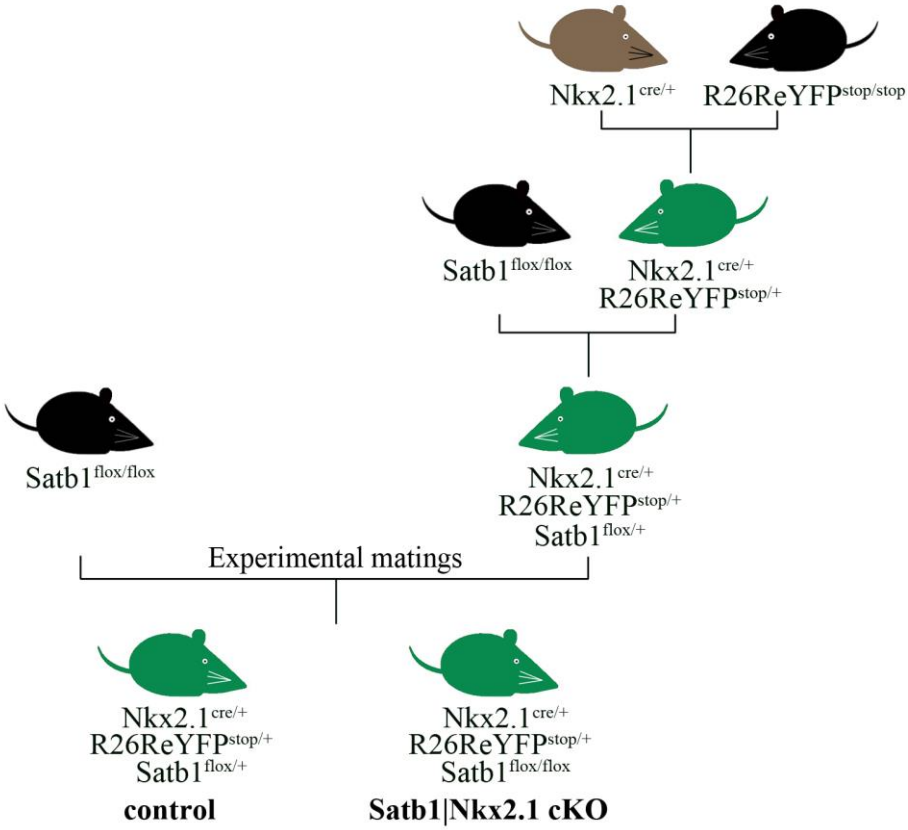

Figure 4.3 Breeding strategy for the generation of *Satb1|Nkx2.1* conditional mutants. The *R26ReYFP* reporter was combined with the *Nkx2.1-Cre* transgenic line, by breeding *R26ReYFP*$^{stop/stop}$ with *Nkx2.1*$^{cre/+}$ mice. The resulting *Nkx2.1*$^{cre/+}$;*R26ReYFP*$^{stop/+}$ double transgenics were then crossed with the *Satb1*$^{flox/flox}$ mice to generate a stock of *Nkx2.1*$^{cre/+}$;*R26ReYFP*$^{stop/+}$;*Satb1*$^{flox/+}$ animals. Finally, this stock colony was combined with *Satb1*$^{flox/flox}$ mice to generate the control *Nkx2.1*$^{cre/+}$;*R26ReYFP*$^{stop/+}$;*Satb1*$^{flox/+}$ and *Nkx2.1*$^{cre/+}$;*R26ReYFP*$^{stop/+}$;*Satb1*$^{flox/flox}$ (*Satb1|Nkx2.1*) triple transgenic mice used in our experiments.

Satb1|Nkx2.1 cKO mice were born alive, at the expected Mendelian ratio for triple transgenics (1/8) and were initially indistinguishable from control littermates. Within the first postnatal week though, a developmental delay became evident and by P15 *Satb1|Nkx2.1* cKO pups were noticeably smaller and weaker compared to controls. Upon observation in their home cage or minor handling, *Satb1|Nkx2.1* cKO mutants developed signs of epileptic seizures, such as loss of postural control and forelimb clonus (data not shown). Among the four conditional mutants that were allowed to survive beyond P15, which is the stage of analysis, two died at P23 (two days after weaning) and two managed to survive until adulthood.

Given the early lethality of the *Satb1|Nkx2.1* pups and for consistency with our *Satb1*-null mutant characterisation, we chose P15 as the analysis stage. We first sought to determine the functionality of our $Satb1^{flox}$ allele and to this aim we examined whether *Satb1* expression is abolished in the *Nkx2.1* progeny, which is faithfully labelled by the YFP reporter. Our analysis was conducted in S1BF (4 sections per brain, Br 0.38 - 0.14 mm) by double immunofluorescence for GFP, to detect the YFP reporter-expressing cells, and SATB1. We observed a dramatic reduction of 87% in the percentage of GFP^+;$SATB1^+$ cells in the total GFP^+ population of *Satb1|Nkx2.1* mutants (10±0.3%; Figure 4.4, C-D and E red bar) compared to controls (83±1.3%; Figure 4.4, A-B2 and E grey bar), indicating successful deletion of *Satb1*. Interestingly, we observed a significant reduction of 26% in the absolute number of GFP^+ cells in *Satb1|Nkx2.1* cKOs (488±57.2; Figure 4.4, F red bar) versus controls (660±39.1; Figure 4.4, F grey bar), which suggests increased cell death in the mutants, possibly as a consequence of seizure activity. It should be noted that the *Nkx2.1-Cre* line also labells oligodendrocytes, although the majority of these are eradicated in the cortex by P10 (Kessaris *et al*., 2006). The few GFP^+ oligodendrocytes identified in our sections, based on their highly branched morphology, were excluded from our countings.

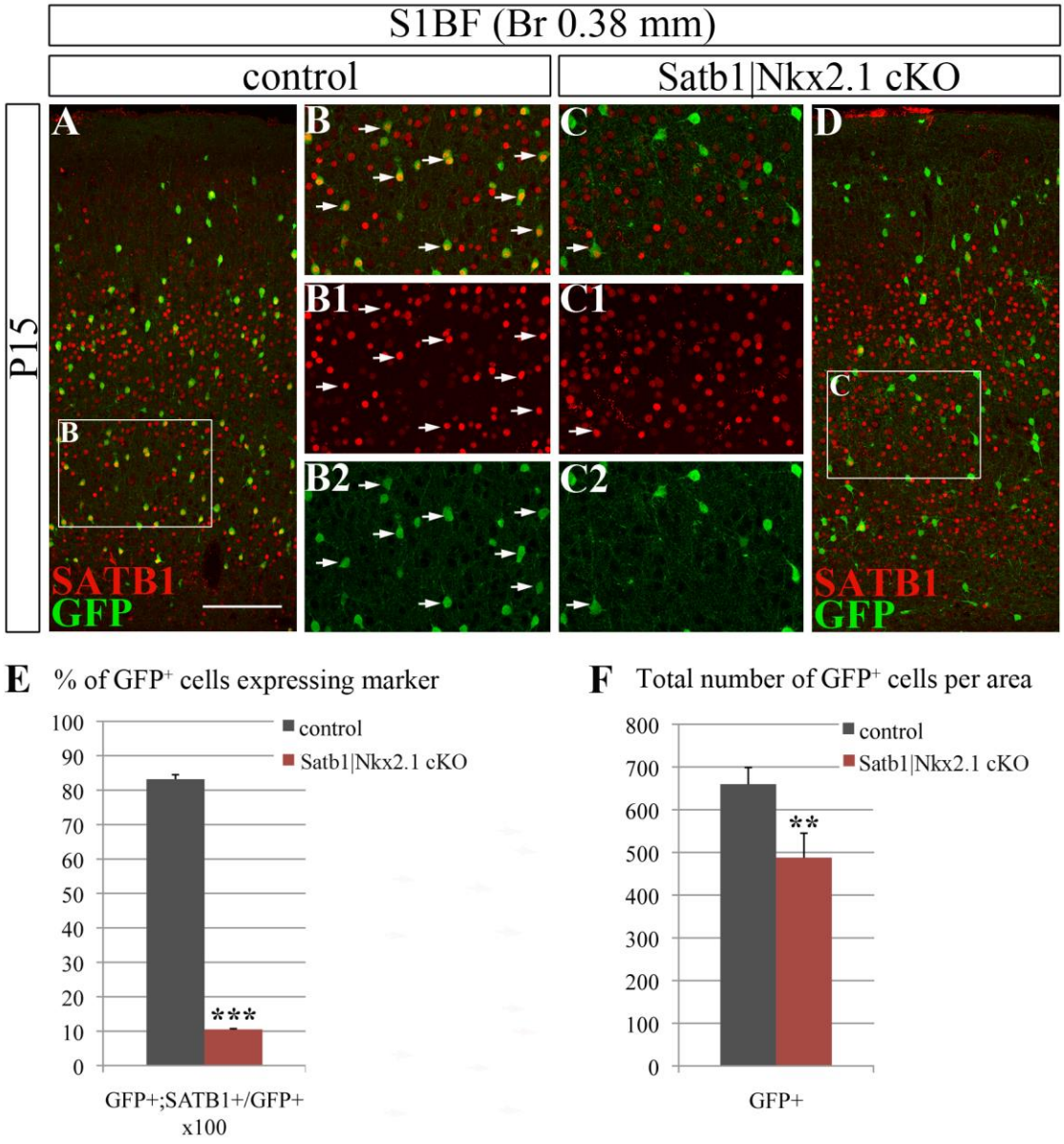

Figure 4.4 The *Satb1^{flox}* allele functions as a null allele. (A-D) Double immunofluorescence for SATB1 and GFP at P15 control (A-B2) and *Satb1|Nkx2.1* mutants (C-D). Panels B and C are magnifications of the boxed areas in A and D respectively and merged images of panels B1-B2 and C1-C2. Arrows indicate double labelled cells. **(E)** Quantification of the percentage of GFP$^+$ cells expressing SATB1 in controls (grey bars) compared to *Satb1|Nkx2.1* littermates (red bars) reveals a dramatic reduction in mutants. **(F)** Quantification of the absolute number of GFP$^+$ cells in controls (grey bars) versus *Satb1|Nkx2.1* cKOs (red bars) shows a significant reduction of 26% in the latter. n=3 animals per genotype, 4 sections per animal (Br 0.38 - 0.14 mm). ** indicates $p<0.01$, *** indicates $p<0.001$, Student's t test (two-tailed distribution, two-sample equal variance). Error bars, STDEV. Scale bars 200 µm.

We next examined the expression of the SST neuropeptide in the *Satb1|Nkx2.1* cKO mutants, as we know from our *Satb1*$^{-/-}$ analysis that *Satb1* regulates SST^{+} interneuron differentiation. By performing double immunofluorescence with antibodies against GFP and SST, we documented a marked decrease of 50% in the percentage of GFP^{+};SST^{+} cells within the total GFP^{+} population of *Satb1|Nkx2.1* cKOs (17±0.1%; Figure 4.5, C-D and I red bar) compared to control littermates (34±0.6%; Figure 4.5, A-B2 and I grey bar), which is close to the 62% reduction of SST^{+} interneurons observed in our constitutive *Satb1*$^{-/-}$ animals. We performed the same analysis with GFP and PV double immunostaining, in order to examine if the PV^{+} population is affected after interneuron-specific deletion of *Satb1*. Our results show a 24% reduction in the percentage of GFP^{+};PV^{+} cells within the total GFP^{+} population of *Satb1|Nkx2.1* cKO animals (35±5.7%; Figure 4.5, G-H and I red bar) compared to controls (45±2.4%; Figure 4.5, E-F2 and I grey bar), which is greater than the 14% reduction seen in constitutive *Satb1*$^{-/-}$ mice. Notably, our data suggest that the PV^{+} interneuron deficit observed in our mutants is not secondary to abnormal pyramidal neuron physiology, as *Satb1* activity was not affected in pyramidal cells. Taken together, the combined reduction in SST^{+} and PV^{+} cells accounts for the 26% loss of GFP^{+} cells in *Satb1|Nkx2.1* cKO mutants, indicating that this reduction is due to cell death rather than loss of SST and PV protein expression. However, based on our *Satb1*$^{-/-}$ findings we have reasons to believe that SST^{+} interneuron differentiation defects precede the death of these cells. Analysis of our *Satb1|Nkx2.1* cKO mutants at early postnatal stages should elucidate this. This hypothesis is supported by recently published work, which reports that *Satb1*-deficient SST^{+} interneurons exhibit maturation defects, receive reduced excitatory input, fail to integrate into cortical networks and are vulnerable to apoptosis (Close *et al*., 2012).

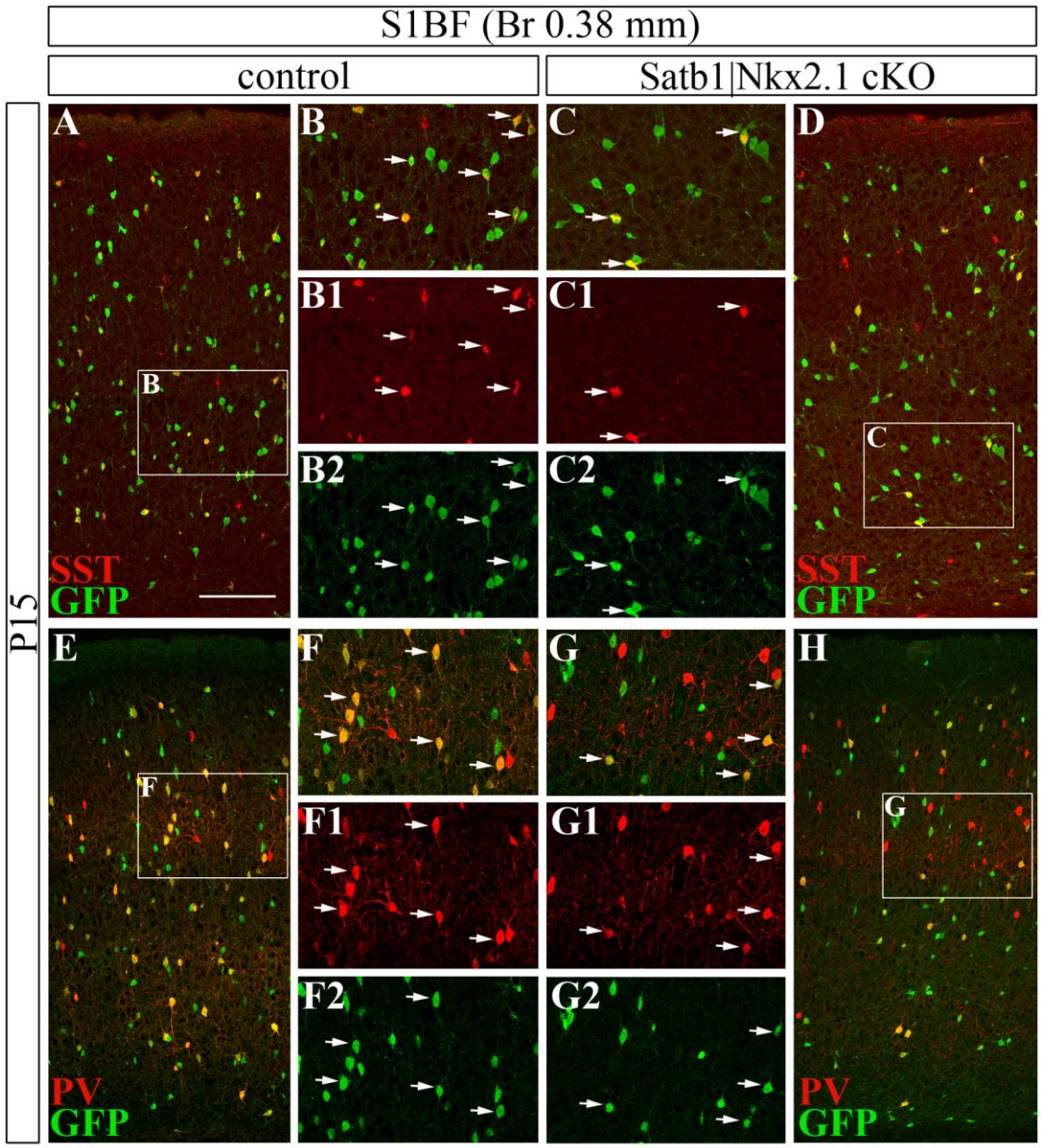

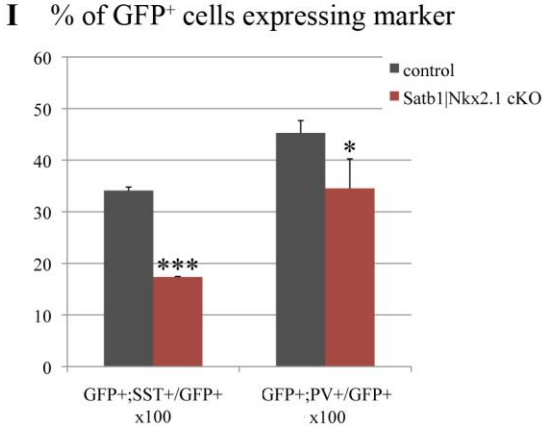

Figure 4.5 (legend at following page)

Figure 4.5 SST$^+$ and PV$^+$ interneurons are significantly affected in *Satb1|Nkx2.1* cKO mutants. (A-D) Double immunofluorescence for SST and GFP at P15 control (A-B2) and *Satb1|Nkx2.1* cKO mutants (C-D). Panels B and C are magnifications of the boxed areas in A and D and merged images of panels B1-B2 and C1-C2 respectively. Arrows indicate double labelled cells. **(E-H)** Double immunofluorescence for PV and GFP at P15 control (E-F2) and *Satb1|Nkx2.1* mutants (G-H). Panels F and G are magnifications of the boxed areas in E and H and merged images of panels F1-F2 and G1-G2 respectively. Arrows indicate double labelled cells. **(I)** Quantification of the percentages of GFP$^+$ cells expressing SST or PV in controls (grey bars) compared to *Satb1|Nkx2.1* littermates (red bars). Notice the significant reduction in both the GFP$^+$;SST$^+$ and GFP$^+$;PV$^+$ percentages in mutants. n=3 animals per genotype, 4 cortical sections per animal (Br 0.38 - 0.14 mm). * indicates $p<0.05$, *** indicates $p<0.001$, Student's t test (two-tailed distribution, two-sample equal variance). Error bars, STDEV. Scale bars 200 µm.

In summary, the analysis of *Nkx2.1$^{cre/+}$;R26ReYFP$^{stop/+}$;Satb1$^{flox/flox}$* conditional mutants reveals that specific deletion of *Satb1* in cortical interneuron progenitors results in a more severe phenotype compared to that observed in the constitutive *Satb1*-null mice, at which *Satb1* activity is abolished in both inhibitory cortical interneurons and excitatory pyramidal cells. Our *Satb1* conditional studies thus indicate an important function of SATB1 in regulating the balance between excitation and inhibition in the brain, similarly to what has been described in the literature for another *Satb1* conditional mutant generated using the *Dlx5/6-Cre* line (Close *et al*., 2012), as will be discussed in section 4.2.1.

4.1.4 *Satb1* activity is not intrinsically required for the maturation of PV$^+$ interneurons

Analysis of our constitutive *Satb1* KO mutants demonstrated a dramatic reduction of 62% in the number of SST-expressing interneurons in the P15 mouse cortex and a less pronounced reduction of 14% in their PV-expressing counterparts (section 3.1.5). Examination of *Satb1|Nkx2.1* conditional mutants excluded the possibility that the PV$^+$ interneuron deficit is due to perturbation of pyramidal neuron development, therefore two possible interpretations remain: either *Satb1* is intrinsically required in a small subset of PV$^+$ interneurons, or alternatively, the modest reduction in this population could be secondary to the impaired development of SST$^+$ interneurons. Having established that the newly generated *Satb1^{flox}* allele can be used to successfully abolish *Satb1* expression in a conditional, tissue-specific manner, we reasoned that by combining it with a constitutive *PV-Cre* knockin line (Hippenmeyer *et al*., 2005) we could specifically delete *Satb1* in PV-expressing cortical interneurons and explore the possibility of *Satb1* activity being required for the maturation of a subset of these cells.

Expression of Cre in the *PV-Cre* mice is driven by the endogenous *Pv* promoter and therefore should initiate approximately after P10 (del Rio *et al.*, 1994). A recent study that has used this line reports more than 90% recombination in PV$^+$ interneurons of the visual cortex (Runyan *et al*., 2010). We therefore set out to investigate how the *PV-Cre* line behaves in the somatosensory cortex, which is our area of interest, by combining it with the *R26ReYFP* reporter line and analysing YFP and PV expression at various postnatal stages.

As anticipated, immunofluorescence for PV and GFP revealed no expression of either the endogenous PV protein, or the YFP reporter in the P8 cortex (Figure 4.6, A). Notably, PV$^+$ and GFP$^+$ cells were observed in the P8 thalamus (Figure 4.6, inset in A), in accordance with what has been reported in the literature (Tanahira *et al*., 2009), thus

providing an internal control for our staining. Examination of the P15 somatosensory cortex revealed the anticipated expression of PV protein for this developmental stage, but YFP reporter activation was quite limited (Figure 4.6, B). We therefore focused at a later stage, namely P30, and observed an increase in the total number of PV^+ cells as well as more efficient activation of the reporter (Figure 4.6, C). In detail, the fraction of PV^+ cells that were also labelled with GFP (efficiency) was 79% and the percentage of GFP^+ cells expressing PV (specificity) was 73%, in a total of three animals examined. We also noticed a fraction of $GFP^+;PV^-$ cells, which could likely correspond to cells that expressed PV at some earlier point and downregulated its expression later on. The possibility that these cells are SST^+ interneurons was ruled out, as double staining with antibodies against GFP and SST revealed that reporter activation in the *PV-Cre* line is excluded from SST-expressing cells (Figure 4.6, D). This is in consistence with the fact that the PV^+ and SST^+ subsets of cortical interneurons are non-overlapping (Gonchar *et al*., 2008).

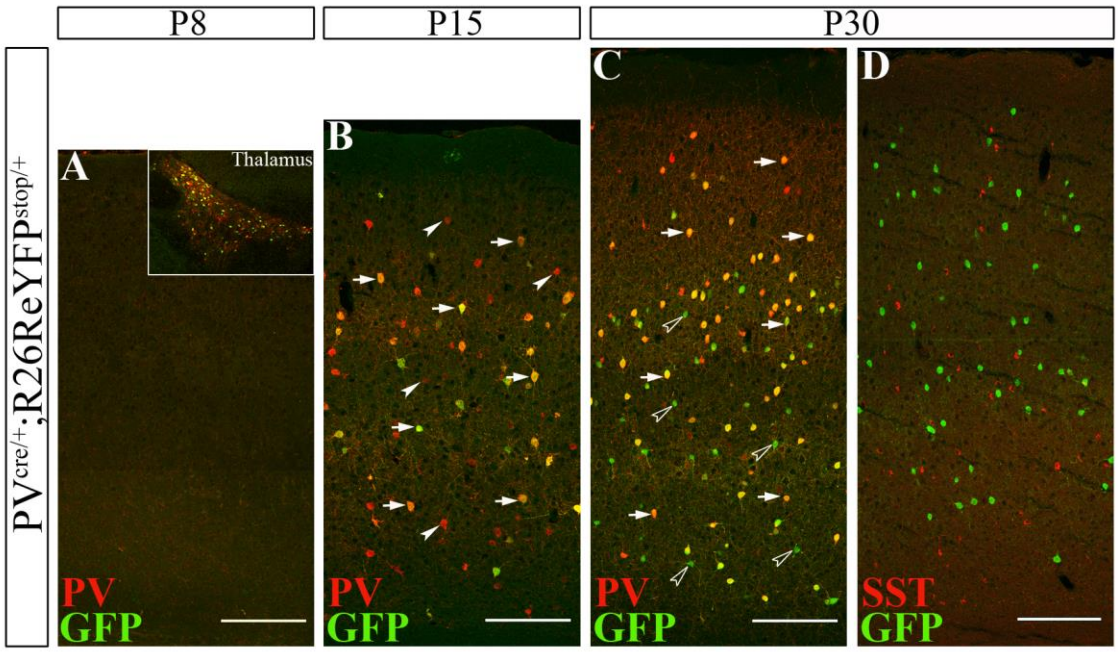

Figure 4.6 The *PV-Cre* line efficiently and specifically labells PV$^+$ cortical interneurons when combined with the *R26ReYFP* reporter. (A-C) Double immunofluorescence for PV and GFP on coronal cortical sections from P8 (A), P15 (B) and P30 (C) *PV$^{cre/+}$;R26ReYFP$^{stop/+}$* animals. Inset in (A) depicts GFP and PV staining in the thalamus of P8 animals. Arrows indicate double positive cells (B and C), filled arrowheads (B) indicate PV$^+$ cells that have not turned on reporter expression and empty arrowheads (C) indicate GFP$^+$;PV$^-$ cells. **(D)** Double immunofluorescence for SST and GFP at P30 *PV$^{cre/+}$;R26ReYFP$^{stop/+}$* cortical sections. Notice that GFP expression is excluded from SST$^+$ interneurons. Scale bars 200 μm.

Based on the above findings, we decided to perform all our analyses at P30 and proceeded with combining the *PV$^{cre/+}$;R26ReYFP$^{stop/+}$* line with the *Satb1* conditional allele. For increased recombination efficiency we first introduced the *Satb1*-null allele to the *PV$^{cre/+}$;R26ReYFP$^{stop/+}$* line, generating *PV$^{cre/+}$;R26ReYFP$^{stop/+}$;Satb1$^{+/-}$* triple transgenic animals that were then crossed with *Satb1$^{flox/flox}$* mice to generate the *PV$^{cre/+}$;R26ReYFP$^{stop/+}$;Satb1$^{flox/+}$* (control) and *PV$^{cre/+}$;R26ReYFP$^{stop/+}$;Satb1$^{flox/-}$* (*Satb1|Pv* cKO) experimental genotypes (Figure 4.7). *Satb1|Pv* cKO and control mice were born at the expected Mendelian ratio for triple transgenics (1/8 or 12.5%).

Specifically, in a total of 83 pups genotyped at P21, 14% were controls and 12% were *Satb1|Pv* cKOs. Development of these conditional mutants proceeded normally, in terms of both growth and behaviour, and pups survived after weaning at P21 and thrived until adulthood, just like their wt littermates.

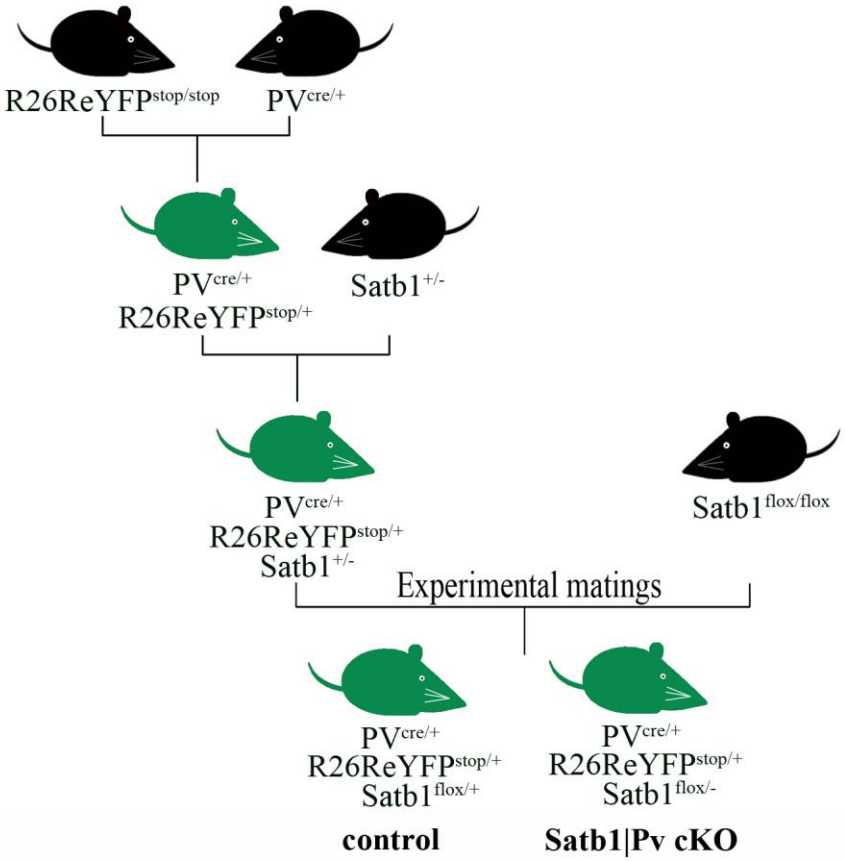

Figure 4.7 Breeding strategy for the generation of *Satb1|Pv* conditional mutants. The *R26ReYFP* reporter was combined with the *PV-Cre* knockin line by breeding *R26ReYFP*$^{stop/stop}$ with *PV*$^{cre/+}$ mice. The resulting *PV*$^{cre/+}$*;R26ReYFP*$^{stop/+}$ double transgenics were then crossed with the *Satb1*$^{+/-}$ mice to generate a stock of *PV*$^{cre/+}$*;R26ReYFP*$^{stop/+}$*;Satb1*$^{+/-}$ animals. Finally, this colony was combined with *Satb1*$^{flox/flox}$ mice to generate the *PV*$^{cre/+}$*;R26ReYFP*$^{stop/+}$*;Satb1*$^{flox/+}$ (control) and *PV*$^{cre/+}$*;R26ReYFP*$^{stop/+}$*;Satb1*$^{flox/-}$ (*Satb1|Pv*) triple transgenic mice used in our experiments.

As in our previous analyses, we examined the S1BF area (4 sections per brain, between Br 0.38 and 0.14 mm). We first confirmed the deletion of *Satb1* in PV-expressing cells by performing double immunofluorescence for GFP and SATB1 and observed a nearly 100% reduction of the percentage of GFP^+;$SATB1^+$ cells in the total GFP^+ population of *Satb1|Pv* animals (0.73±0.2%; Figure 4.8, C-D and I, left panel, red bar) compared to controls (64±9.9%%; Figure 4.8, A-B2 and I, left panel, grey bar). To address a possible requirement of *Satb1* for the maturation of PV^+ interneurons we quantified the percentage of GFP^+;PV^+ cells within the GFP^+ population of controls and *Satb1|Pv* conditional mutants, after staining with antibodies against GFP and PV. Our findings demonstrate no significant difference between *Satb1|Pv* cKO mutants (73±6.8%; Figure 4.8, G-H and I, right panel, red bar) and control littermates (73±5.7%; Figure 4.8, E-F2 and I, right panel, grey bar). It should also be noted that the total GFP^+ population was not significantly affected in the *Satb1|Pv* cKO mice (404±43 in mutants, 336±27 in controls; Figure 4.8, J).

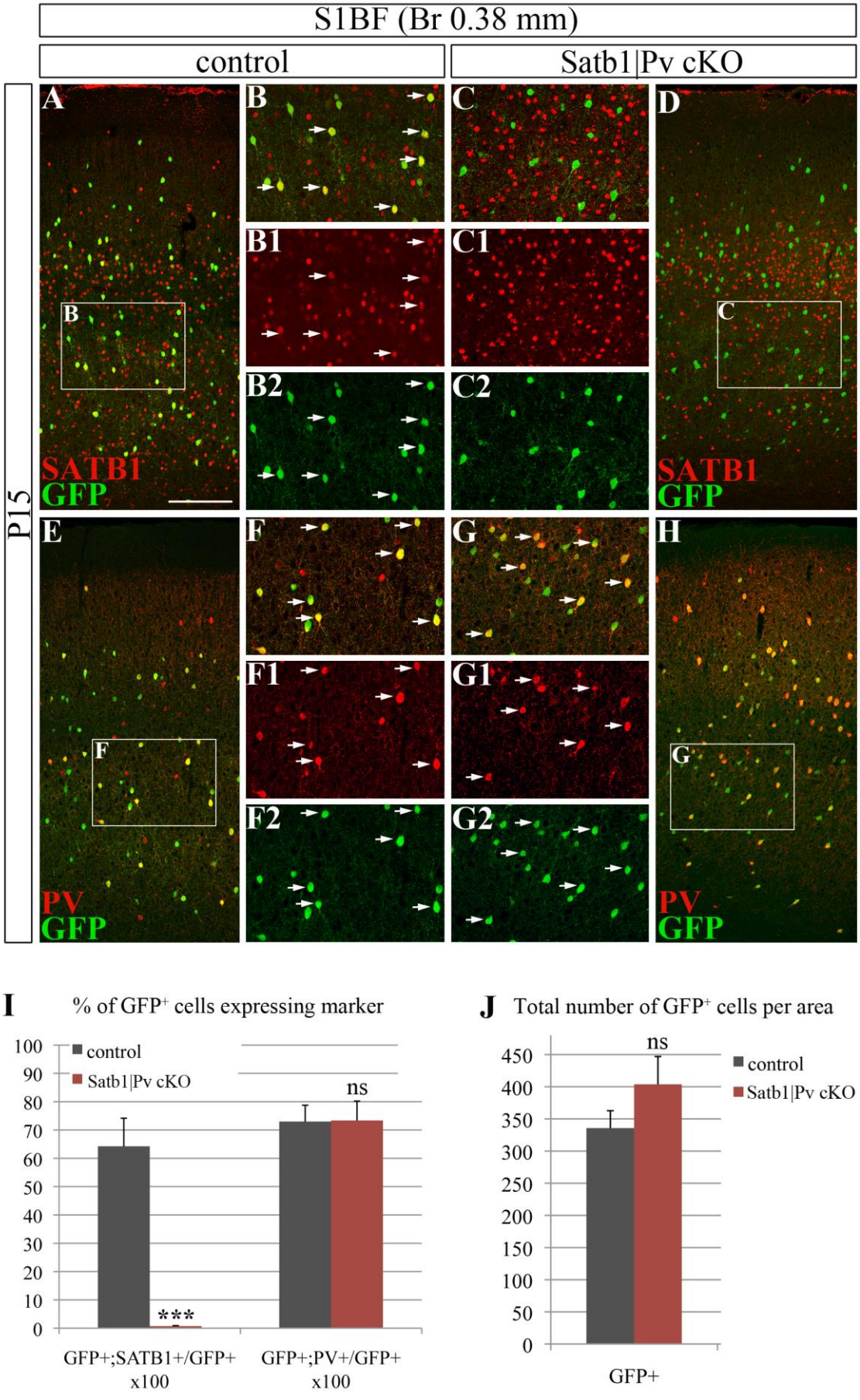

Figure 4.8 (legend at following page)

Figure 4.8 Conditional deletion of *Satb1* in PV$^+$ cortical interneurons does not affect their maturation. (A-D) Double immunofluorescence for SATB1 and GFP on coronal cortical sections from P30 control (A-B2) and *Satb1|Pv* cKOs (C-D). Panels B and C are magnifications of the boxed areas in A and D, and merged images of panels B1-B2 and C1-C2 respectively. Arrows indicate double labelled cells. **(E-H)** Double immunofluorescence for PV and GFP at P30 control (E-F2) and *Satb1|Pv* cKOs (G-H). Panels F and G are magnifications of the boxed areas in E and H, and merged images of panels F1-F2 and G1-G2 respectively. Arrows indicate double labelled cells. **(I)** Percentages of GFP$^+$ cells expressing SATB1 or PV in controls (grey bars) compared to *Satb1|Pv* cKOs (red bars). The percentage of GFP$^+$;SATB1$^+$ cells is almost totally abolished in mutants, however the percentage of GFP$^+$;PV$^+$ cells is unaffected, indicating that loss of *Satb1* activity does not affect the expression of PV in these cells. **(J)** Quantification of the total number of GFP$^+$ cells in controls (grey bars) versus *Satb1|Pv* mutants (red bars) shows no significant reduction in the GFP$^+$ population of the latter. n=3 animals per genotype, 4 cortical sections per animal. ns indicates no statistical significance, *** indicates $p<0.001$, Student's t test (two-tailed distribution, two-sample equal variance). Error bars, STDEV. Scale bars 200 μm.

Taken together, our preliminary results from the conditional deletion of *Satb1* in the PV$^+$ subset of cortical interneurons during the second postnatal week, demonstrate that *Satb1* function is not intrinsically required to regulate expression of *Pv* in these cells. Nevertheless, analysis of the expression of more molecular markers and further investigation of the firing and connectivity properties of PV$^+$ interneurons in *Satb1|Pv* cKO mutants, is needed in order to further elucidate the possible role of SATB1 in controlling their maturation.

4.2 Discussion

Analysis of *Satb1* KO mutants revealed an important function of *Satb1* in regulating the maturation of MGE-derived cortical interneurons in the postnatal mouse neocortex. However, as *Satb1* is expressed in both cortical interneurons and pyramidal cells, selective deletion in the former is needed in order to tease apart the specific effects of loss of *Satb1* function in GABAergic interneurons. Furthermore, the results presented in Chapter 3 demonstrated a pronounced requirement for *Satb1* function in the terminal differentiation of SST^+ cortical interneurons but a less clear role in the maturation of the PV^+ population. *Satb1* ablation within the PV^+ subset should elucidate if *Satb1* is intrinsically required in these cells.

We have generated here a novel *Satb1* floxed allele and combined it with the *Nkx2.1-Cre* and *PV-Cre* lines to conditionally delete *Satb1* in MGE progenitors and in the PV^+ subset of cortical interneurons respectively. Our findings are the first to report the effects of conditional *Satb1* removal on cortical interneuron development using the *Nkx2.1-Cre* and *PV-Cre* lines. An independent study that addressed the same question, although by using different Cre-driver lines (Close *et al*., 2012), came out in the literature during the course of our studies. We provide evidence for a more severe phenotype of *Satb1|Nkx2.1* cKO mice compared to constitutive *Satb1*$^{-/-}$ mutants, with signs of seizure activity and significant loss of both SST^+ and PV^+ interneurons attributed to cell death. Moreover, our results from the PV^+ interneuron-specific deletion of *Satb1* argue against an intrinsic requirement for this transcription factor for the maturation of these cells.

4.2.1 Indications for altered excitation/inhibition balance after interneuron-specific deletion of *Satb1*

Inhibitory cortical GABAergic interneurons are bestowed with the critical role of maintaining the fine balance between excitation and inhibition in the brain, which prevents hyperexcitability and at the same time allows the processing of information. It has long been appreciated that deficits in the development and/or function of cortical interneurons disrupt the excitation/inhibition balance with severe consequences, manifested as neuropsychiatric disorders such as epilepsy, schizophrenia and autism spectrum disorders (reviewed in Rossignol, 2011). Epilepsy in particular has been described in a plethora of mouse models carrying mutations in genes involved in cortical interneuron development, including *Lhx6* (Neves *et al*., 2012), *Sox6* (Batista-Brito *et al*., 2009), *Nkx2.1* (Butt *et al*., 2008), *Dlx5/6* (Wang *et al*., 2010), *Dlx1* (Cobos *et al*., 2005) and *Arx* (Kitamura *et al*., 2002).

Inspection of our constitutive *Satb1*$^{-/-}$ mutants in their home cage and minor handling or tail suspension did not reveal any signs of seizure activity in these animals, at least up to P23-P25 which is the latest stage we could examine. In contrast though, *Satb1|Nkx2.1* cKO mutants examined at the same developmental stages demonstrated characteristic traits of epileptic seizures such as loss of balance and myoclonic spasms (Neves *et al*., 2012). It is presently unclear what causes this difference in phenotype severity between constitutive *Satb1* KO and *Satb1|Nkx2.1* cKO mutants. A plausible hypothesis would be the following: *Satb1* is expressed in both inhibitory cortical interneurons and excitatory pyramidal cells and its ubiquitous deletion perturbs both cortical interneuron differentiation, as our studies show, as well as pyramidal neuron connectivity (Balamotis *et al*., 2012). Specifically, cortical pyramidal cells of *Satb1* KO animals show reduced dendritic spine density, an indication that synapse formation is compromised, as dendrites represent postsynaptic entities where excitatory input is

received (reviewed in Nimchinsky *et al*., 2002). Therefore, both components of the excitation/inhibition balance are compromised in *Satb1*$^{-/-}$ mutants. On the contrary, conditional deletion of *Satb1* using the *Nkx2.1-Cre* transgenic line only affects cortical interneurons, leaving the expression of *Satb1* intact in pyramidal cells and consequently could have a greater impact on the excitation/inhibition ratio in the brain, shifting it towards excitation and thus epilepsy.

Although the findings presented herein do not include histopathological or electroencephalogram (EEG)-based evidence to clearly demonstrate epileptic activity, we have documented a significant reduction in the number of YFP-expressing cells in the cortices of *Satb1|Nkx2.1* cKO animals, which indicates cell death. Interestingly, the combined decrease in the numbers of SST^{+} and PV^{+} cells in our *Satb1|Nkx2.1* conditional mutants can account for the total reduction seen in the YFP^{+} population. One hypothesis is that increased cell death occurrence in these animals could be a consequence of seizure activity, as neuronal loss is a common histopathological finding in human patients and rodent models of epilepsy (Henshall and Meldrum, 2012), with SST^{+} interneurons known to be particularly affected by seizures (Cossart *et al*., 2001; Choi *et al*., 2007). However, an alternative possibility is that the loss of cortical interneurons precedes the onset of seizures (Neves *et al*., 2012; Cobos *et al*., 2005). The latter hypothesis is supported by findings from the Fishell group, which demonstrate that loss of *Satb1* activity in *Dlx5/6-Cre;Satb1-flox* conditional mutants results in SST^{+} interneuron maturation defects and apoptosis, the functional implications of which are reduced synaptic inhibition on layer IV pyramidal neurons and development of cortical interictal seizures (Close *et al*., 2012). Analysis of our *Satb1|Nkx2.1* cKO animals at early postnatal stages will help us determine if a differentiation defect precedes the death of cortical interneurons and quantification of the number of YFP^{+} cells at different

stages will elucidate whether the loss of cortical interneurons precedes the onset of seizures or vice versa.

4.2.2 Evidence for non-cell-autonomous effects of the *Satb1* mutation in PV^+ interneuron development

The data presented in Chapters 3 and 4 of this thesis provide evidence for subtle but reproducible defects in PV-expressing cortical interneurons of *Satb1*-deficient mice. Analysis of P15 constitutive *Satb1* KO animals revealed a 14% reduction in the number of PV^+ interneurons, while the total GABAergic population remained unaffected, thus indicating a differentiation defect in a small subset of this population. We therefore aimed to elucidate whether this defect was due to a cell-intrinsic requirement for *Satb1* activity in these cells, or secondary to the SST^+ population deficit or the pyramidal spine density and synapse formation defects of pyramidal neurons (Balamotis *et al*., 2012).

We first addressed this question by selective deletion of *Satb1* in cortical interneuron progenitors using the $Nkx2.1^{cre/+};R26ReYFP^{stop/+}$ transgenic line. When *Satb1* was deleted in interneurons but unaffected in pyramidal cells, we observed a significant reduction of 24% in the percentage of $PV^+;GFP^+$ cells in P15 cKO animals compared to control littermates, which is more pronounced than the 14% reduction in PV^+ interneurons in constitutive $Satb1^{-/-}$ mutants. Therefore, the PV^+ interneuron deficit is unlikely to result from a cell-autonomous activity of the *Satb1* mutation in pyramidal cells. We next investigated a possible intrinsic requirement for *Satb1* function in PV^+ cortical interneuron maturation by combining our newly generated $Satb1^{flox}$ allele with the $PV^{cre/+};R26ReYFP^{stop/+}$ line. Our findings argue against a requirement for *Satb1* in regulating expression of *Pv* in cortical interneurons, although the full maturation features, such as membrane properties, firing pattern and connectivity, of these cells

have not yet been addressed in our study. It should also be noted that deletion of *Satb1* in our experimental system occurs in differentiated PV^+ cells and therefore we cannot definitively exclude an intrinsic requirement for *Satb1* activity in PV^+ interneuron differentiation.

A plausible hypothesis to explain our findings could be that the observed PV^+ interneuron deficits in both constitutive *Satb1* KO and conditional *Satb1* KO mice can be attributed to the dramatic defects observed in SST^+ interneurons. This idea is supported by the latest views in the field, proposing that abnormal development of a particular interneuron subset can affect other populations within the network, as these cells are interconnected and in constant communication with each other (Cossart, 2011). Moreover, we hypothesise that the exacerbated PV^+ cell deficit in *Satb1|Nkx2.1* conditional mutants could be attributed to the overall altered state of excitation/inhibition in the brain of these animals. Indeed, loss of PV-expressing interneurons has been described in mouse (Batista-Brito *et al*., 2009; Neves *et al*., 2012) and rat (Kobayashi and Buckmaster, 2003; van Vliet *et al*., 2004) mutants with epilepsy phenotypes. In addition, it was recently proposed that electrical activity that emerges at postnatal stages has a greater impact on the late-maturing population of PV^+ interneurons compared to earlier-maturing subsets (reviewed in Cossart, 2011).

Notably, the effects of *Satb1* deletion in PV-expressing interneurons have also been described elsewhere, using an independently generated *Satb1* floxed allele (Close *et al*., 2012). However, in contrast to our approach, which ablated *Satb1* from differentiated PV^+ cells, the Close *et al*. study examined the effect of *Satb1* ablation in PV precursors by combining the *Satb1* floxed allele with the *Dlx6a-Cre* line and the G42 reporter, which exclusively labells PV^+ interneurons (Chattopadhyaya *et al*., 2004). This complementary to ours work shows that although the membrane properties and connection probability with pyramidal cells of *Satb1*-deficient PV^+ cortical interneurons

remain largely unaltered, the synapses formed onto pyramidal cells by these cells are less functional, as indicated by smaller inhibitory postsynaptic currents (IPSCs) recorded in the former population (Close *et al*., 2012). Therefore, SATB1 plays a small but important role in regulating some maturation aspects of PV-expressing interneurons. It would be interesting to investigate how these properties are affected in our experimental system, when *Satb1* function is lost in differentiated PV^+ cells, by electrophysiological recordings and examination of the expression levels of a battery of PV^+ interneuron maturation markers published in the literature (Okaty *et al*., 2009) by qPCR.

Chapter 5

Investigation of the functional relationship between SATB1 and the K^+-Cl^- cotransporter KCC2

5.1 Results

The findings described in Chapter 3 of this thesis, as well as additional data presented in our published work (Denaxa *et al*., 2012), clearly demonstrate a role for SATB1 in the maturation of the SST-expressing subset of GABAergic interneurons in the mouse cortex. Our *in vivo* data so far come from the postnatal cortex, at two weeks after birth. However, given the fact that expression of SATB1 in the cortex initiates much earlier, from E15.5 onwards, we wished to examine prior stages of cortical interneuron maturation. To this aim we turned our attention to the K^+-Cl^- cotransporter KCC2, the upregulation of which has been linked to the maturation of neuronal cells during late embryonic/early postnatal stages, as is briefly discussed below.

KCC2 belongs to the Slc12a family of K^+-Cl^- cotransporters and constitutes the only member of this family to be exclusively expressed in neurons (Payne *et al*., 1996). It is widely distributed in the CNS, expressed from the spinal cord all the way to the olfactory bulbs, and is best known for its function in regulating intracellular Cl^- concentrations: KCC2 uses the electrochemical gradient of K^+, generated by the Na^+-K^+ ATPase, to extrude $1K^+$ and $1Cl^-$ from the cell, thus shifting the Cl^- equilibrium potential to more negative values and governing the switch of GABA from excitatory to inhibitory signal (reviewed in Ben-Ari *et al*., 2007; section 1.3.3.3 herein). During embryonic and early postnatal stages KCC2 is found as a monomer in an inactive phosphorylated form, whereas its ion transport function in mature neurons is associated with a dephosphorylated, multimeric form (Blaesse *et al*., 2006; Rinehart *et al*., 2009).

Kcc2 genetic loss of function studies have revealed a critical role for this cotransporter in synapse formation and regulation of neuronal activity. *Kcc2*$^{-/-}$ mice exhibit abnormal spontaneous activity in motor neurons recorded from the E18.5 spinal cord (Hübner *et al*., 2001) and spontaneous epileptic seizures in the hippocampus at the same age (Khalilov *et al*., 2011), although the latter seem to be independent of the ion

transport function of KCC2. Notably, loss of *Kcc2* activity resulted in a pronounced increase in the number of synapses formed in the CA3 region of the hippocampus and enhanced occurrence of GABAergic and glutamatergic spontaneous postsynaptic currents (Khalilov *et al*., 2011). However, contradicting results have emerged from studies in cultured hippocampal neurons where reduced levels (Li *et al*., 2007) or complete loss (Gauvain *et al*., 2011) of *Kcc2* lead to formation of fewer synapses and reduction in glutamatergic synaptic transmission. Such discrepancies could be attributed to the different experimental settings and/or analysis time-points used in different studies or could possibly reflect differential roles of KCC2 in synaptogenesis at different stages.

Upregulation of *Kcc2* expression has been associated with the maturation of pyramidal cells (Rivera *et al*., 1999) and GABAergic interneurons in the cortex (Bortone and Polleux, 2009; Miyoshi and Fishell, 2011) as well as in other brain areas, such as the cerebellum (Simat *et al*., 2007). With regards to cortical interneurons, increased levels of KCC2 protein herald the onset of maturation and radial sorting of MGE and CGE cells within the cortical plate, a step that is critical for the integration of these cells into cortical networks (Miyoshi and Fishell, 2011). Recent findings suggest that although MGE- and CGE-derived interneurons are initially distributed uniformly in the cortical plate, the former start maturing earlier than the latter, as evidenced by the prompt upregulation of *Kcc2*, and hence initiate their radial sorting at an earlier time point (Miyoshi and Fishell, 2011). In addition, variable levels of *Kcc2* expression within the cortical plate have been reported by other studies, which demonstrated that upregulation of *Kcc2* expression in interneurons of the cortical plate facilitates the termination of their migration (Bortone and Polleux, 2009; section 1.3.3.3 herein).

The main objective of this chapter will be to ascertain the functional relationship between SATB1 and KCC2, in the context of the developing mouse telencephalon.

Initially, I will examine the possible regulation of *Kcc2* expression by SATB1, both during *in vitro* overexpression experimental conditions and *in vivo*, to elucidate whether SATB1 can control general maturation properties of cortical interneurons. I will then investigate a possible reciprocal regulation of *Satb1* by KCC2, as part of an effort to address the question of which are the factors that induce or maintain expression of SATB1 within the late embryonic cortical plate.

5.1.1 SATB1 is necessary and sufficient to regulate *Kcc2* expression

Focal electroporations in organotypic brain slice cultures have been widely used and now constitute an established method for ectopic expression and gain or loss of function studies in the developing forebrain (Stühmer *et al*., 2002; Alifragis *et al*., 2004; Nóbrega-Pereira *et al*., 2008). We therefore decided to adopt this experimental strategy in order to heterochronically express SATB1 in MGE progenitors, which do not normally express this transcription factor (Denaxa *et al*., 2012; Close *et al*., 2012), and examine the effect on *Kcc2* expression.

To this aim we used a SATB1-encoding pCAGGS-Satb1-RFP vector and a control pCAGGS-RFP vector that were generated in our lab (Denaxa *et al*., 2012). The pCAGGS plasmid has the ability to drive high expression levels of a gene of interest by combining the cytomegalovirus (CMV) early enhancer element with the chicken *ß-actin* promoter (collectively referred to as the CAG promoter; Niwa *et al*., 1991). Moreover, the presence of an IRES-RFP sequence downstream of the multi-cloning site (MCS) results in bicistronic expression of both the gene of interest (cloned into the MCS) and the RFP reporter, thus enabling the tracing of overexpressing cells. Each vector was electroporated into the MGEs of a total of 15-20 slices from E14.5 wt brains, as described in the literature (Stühmer *et al*., 2002) and 24 hours later the levels of RFP fluorescence were evaluated under a fluorescence stereomicroscope. The MGEs

expressing high levels of RFP were subsequently dissociated and FACS purified, yielding 10,000-20,000 cells for each condition. The cells were immediately processed for RNA extraction and RNA samples were subsequently reverse-transcribed into cDNA, which was used in qPCR following the TaqMan methodology (Figure 5.1, A). Kcc2 mRNA levels were upregulated in MGE progenitors electroporated with the pCAGGS-Satb1-RFP vector, compared to control pCAGGS-RFP electroporated ones (Figure 5.1, B) and importantly, the relative amount of Sst mRNA transcript was also considerably elevated in the SATB1-overexpressing cells (Figure 5.1, B), providing a positive control in our assay since our studies (Chapter 3 herein; Denaxa *et al*., 2012) as well as the literature (Balamotis *et al*., 2012) give evidence for the regulation of *Sst* expression by SATB1.

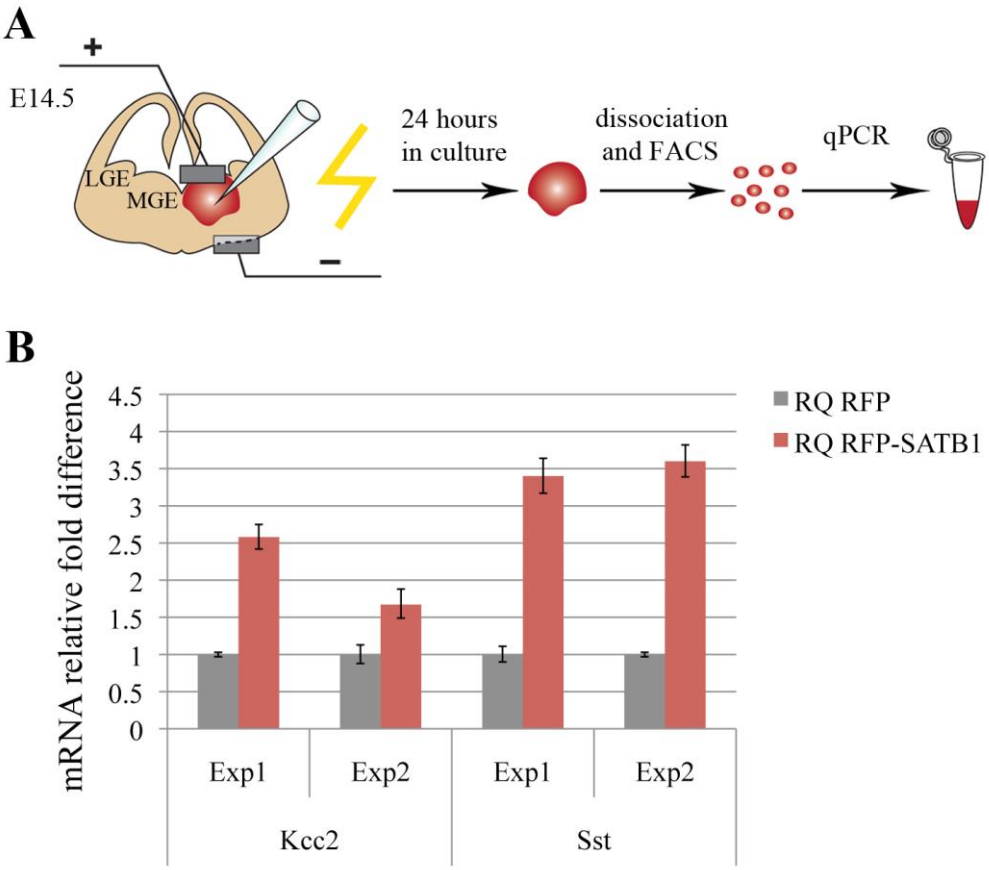

Figure 5.1 Overexpression of SATB1 is sufficient to induce *Kcc2* expression in MGE progenitors. (A) Schematic representation of the experimental approach. Electroporation of E14.5 wt MGEs with pCAGGS-RFP or pCAGGS-Satb1-RFP vectors was followed by dissociation and FACS 24 hours later. RNA was extracted from the purified cells, reverse transcribed into cDNA and used in TaqMan qPCR assays. **(B)** The relative amount of Kcc2 mRNA is enriched in pCAGGS-Satb1-RFP-electroporated cells (red bars) compared to pCAGGS-RFP-electroporated controls (grey bars). Upregulation of Sst in the pCAGGS-Satb1-RFP-electroporated cells provides a positive control. Data are presented as fold change in amounts of mRNA transcript, normalised to the housekeeping gene *ß-actin*, between SATB1-expressing cells and controls, from 2 representative experiments for each gene, chosen out of a total of 7 independent experiments. Error bars represent Δmax and Δmin values calculated as described in section 2.3.11. Schematic in A was generated by Hayley Wood, NIMR photographics.

Given the ability of SATB1 to induce expression of *Kcc2* in our *in vitro* assay, we wished to examine the *in vivo* hierarchical relationship between these two factors in cortical interneurons. To this aim, we used the *Gad67-GFP* knock-in mouse line in which all cortical GABAergic neurons are labelled by the GFP reporter (Tanaka *et al*., 2003) and performed immunofluorescence with antibodies specific for SATB1, KCC2 and GFP at E18.5 coronal brain sections. We observed that virtually all $KCC2^+$ interneurons ($KCC2^+$;GFP^+) within the cortical plate express SATB1 (Figure 5.2, A-B3), consistent with a possible regulation of *Kcc2* expression by SATB1 *in vivo*. To further explore this possibility we analysed *Satb1*$^{-/-}$ mutants by immunostaining E18.5 coronal brain sections for KCC2. We observed a marked downregulation of KCC2 protein levels (Figure 5.2, D-D1) in the cortical plate of *Satb1*-deficient mice, compared to controls (Figure 5.2, C-C1).

In summary, our *in vivo* and organotypic slice culture data demonstrate that SATB1 is necessary and sufficient to induce expression of *Kcc2*.

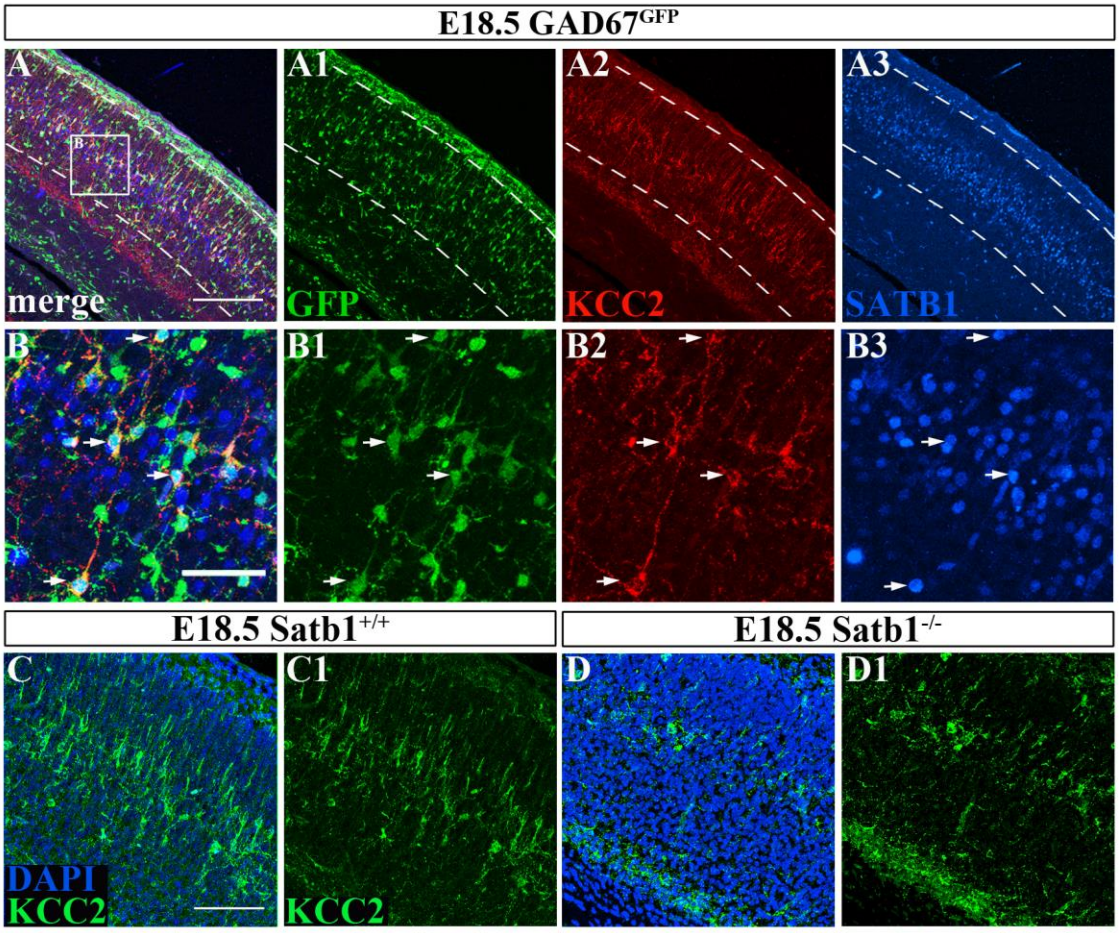

Figure 5.2 SATB1 regulates *Kcc2* expression *in vivo*. (A-B3) Triple immunostaining, on E18.5 coronal brain sections from *GAD67-GFP* embryos, for GFP (A1, B1), KCC2 (A2, B2) and SATB1 (A3, B3). Dashed white lines mark the cortical plate. Panel B is a high magnification image of the boxed area in A. Panels A and B are merged images of A1-A3 and B1-B3 respectively. Note that virtually all $KCC2^{+}$;GFP^{+} interneurons are also $SATB1^{+}$ (arrows in B-B3). **(C-D1)** Immunofluorescence for KCC2 on brain sections from *Satb1*$^{+/+}$ (C-C1) and *Satb1*$^{-/-}$ (D-D1) E18.5 embryos. Cell nuclei are stained with DAPI. Panels C1 and D1 show just the KCC2 signal, without the DAPI counterstain. Note the pronounced reduction in $KCC2^{+}$ cells in the cortical plate of *Satb1*-null mutants (D-D1). Scale bar 200 μm for A-A3, 50 μm for B-B3, 100 μm for C-D1. Data collected by Myrto Denaxa.

5.1.2 Spatio-temporal expression pattern of SATB1 and KCC2 in the embryonic cortex

The colocalisation of SATB1 and KCC2 proteins in cortical interneurons (Figure 5.2, A-B3), as well as the fact that SATB1 regulates the expression of *Kcc2* (Figures 5.1, B and 5.2, C-D1) prompted us to investigate the possibility that KCC2 regulates the expression of *Satb1* in the cortical plate. This would elucidate the bigger question of what are the factors that induce *Satb1* expression in the cortical plate during late embryonic stages. One possibility would be that KCC2 induces *Satb1* and then SATB1 feeds back on *Kcc2* to upregulate its expression levels. Alternatively, SATB1 could induce *Kcc2* expression in the cortical plate and reciprocally, KCC2 could act to upregulate the levels of *Satb1*. A third possibility of course could be that KCC2 has no effect on *Satb1*.

To gain a better understanding of who might be regulating whom, we investigated the expression pattern of the SATB1 and KCC2 proteins in the developing embryonic cortex, before E18.5 when we already see quite a big overlap between the two (Figure 5.2, A-B3). To this aim we performed immunofluorescence experiments on coronal brain sections from E13.5 to E16.5 wt embryos, using antibodies against SATB1 and KCC2. SATB1 and KCC2 were first observed in the cortex at E15.5, with highly overlapping expression patterns at the marginal zone and the subplate, bordering the cortical plate (Figure 5.3, C). A few $SATB1^{+}$;$KCC2^{+}$ cells were located within the cortical plate at this stage (Figure 5.3, E-E2). A day later, at E16.5, there was a significant increase in the number of $SATB1^{+}$ cells in the cortical plate, the majority of which were $KCC2^{-}$ (Figure 5.3, D and open arrowheads in F-F2). Although our data do not distinguish between expression of SATB1 and KCC2 in interneurons or pyramidal cells, they clearly demonstrate that, specifically within the cortical plate, expression of SATB1 initiates before that of KCC2. Based on studies from our lab, we can comment

that strongly-labelled SATB1^{+};KCC2^{+} cells (Figure 5.3, arrows in F-F2) are interneurons (Denaxa *et al.*, 2012), while SATB1^{+};KCC2^{-} cells (Figure 5.3, open arrowheads in F-F2) are possibly cortical plate neurons.

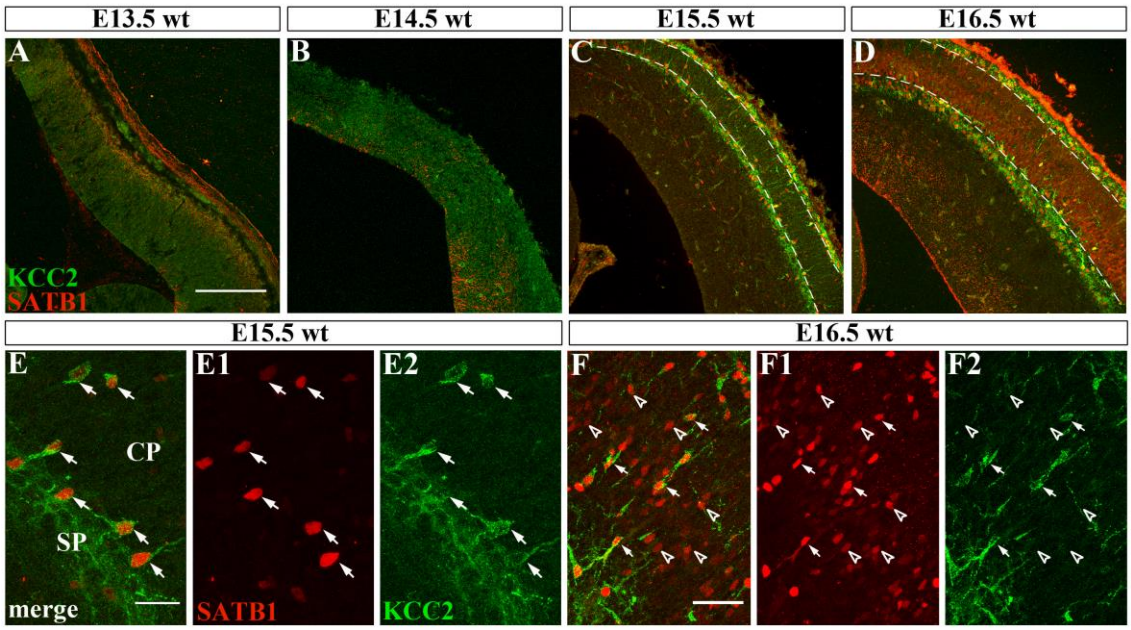

Figure 5.3 Expression of SATB1 in the cortical plate precedes that of KCC2. (A-D) Double immunofluorescence for SATB1 and KCC2 at E13.5 (A), E14.5 (B), E15.5 (C) and E16.5 (D) wt coronal brain sections. Expression of both SATB1 and KCC2 proteins is first detected in the neocortex at E15.5 (C) and is greatly overlapping, in two streams of cells flanking the cortical plate, which is indicated by dashed white lines. By E16.5, the expression of SATB1 is upregulated within the cortical plate (D). **(E-E2)** High magnification images of the subplate-cortical plate border at E15.5, stained with SATB1 and KCC2 antibodies. Arrows indicate SATB1^{+};KCC2^{+} cells, some of which are within the cortical plate. Panel E is a merged image of E1 and E2. **(F-F2)** High magnification images of the E16.5 cortical plate, stained with SATB1 and KCC2 antibodies. Arrows indicate SATB1^{+};KCC2^{+} cells. Notice however that most cells in the cortical plate at this stage are SATB1^{+};KCC2^{-} (open arrowheads). Panel F is a merged image of F1 and F2. SP= subplate, CP= cortical plate. Scale bars 200 µm for A-D, 25 µm for E-E2 and 50 µm for F-F2.

5.1.3 Generation of the pCAGGS-Kcc2-GFP vector to overexpress KCC2

To investigate the relationship of SATB1 and KCC2 at the functional level, we generated a KCC2-encoding vector with the aim to introduce it ectopically into MGE progenitors at E14.5, utilising our *in vitro* brain slice electroporation assay. The KCC2-encoding construct was generated by cloning the full-length coding region of the mouse *Kcc2* gene (IMAGE clone ID: 6838880) into the pCAGGS-GFP vector. In more detail, a SalI/SacI fragment containing the full-length cDNA for *Kcc2* was excised from the host pYX-Asc vector and inserted into the XhoI/SacI sites of the MCS of pCAGGS-GFP (Figure 5.4, B). Restriction enzyme digests and DNA sequencing (data not shown) confirmed that we generated a construct expressing the full-length *Kcc2* coding sequence. In addition, we verified the functionality of the pCAGGS-Kcc2-GFP vector by transfection into P19 embryonal carcinoma cells, followed by double immunostaining for GFP and KCC2. Cells transfected with pCAGGS-Kcc2-GFP were labelled by both GFP and KCC2 (Figure 5.4, D-D3) and notably, KCC2 protein showed the characteristic distribution in the cell membrane around the soma (Figure 5.4, D1 inset; Gulyás *et al*., 2001; Hübner *et al*., 2001). On the contrary, we were unable to detect KCC2 protein in cells transfected with a control pCAGGS-GFP vector (Figure 5.4, C-C3), as expected.

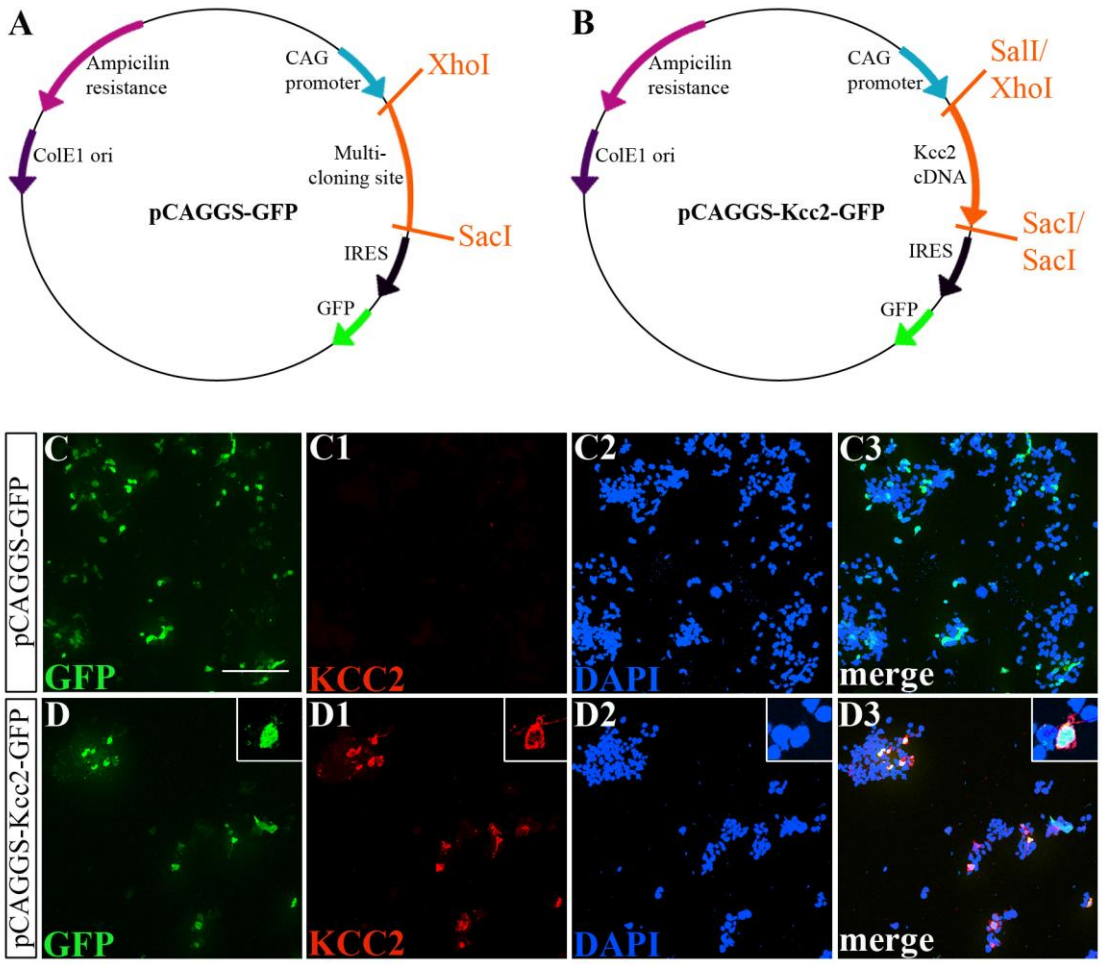

Figure 5.4 The pCAGGS-Kcc2-GFP expression vector can be used to successfully overexpress KCC2. (A-B) Maps of the pCAGGS-GFP (A) and pCAGGS-Kcc2-GFP (B) vectors. A SalI/SacI fragment containing the full-length cDNA of *Kcc2* was cloned into the XhoI/SacI restriction sites of the pCAGGS-GFP vector, upstream of the IRES-GFP sequence to generate the pCAGGS-Kcc2-GFP vector. **(C-D3)** P19 embryonal carcinoma cells transfected with pCAGGS-GFP (C-C3) and pCAGGS-Kcc2-GFP (D-D3), stained with GFP- and KCC2-specific antisera, as well as DAPI to label cell nuclei. Cells transfected with the control pCAGGS-GFP vector do not show any KCC2 immunofluorescence (C-C3), whereas all of the pCAGGs-Kcc2-GFP-transfected cells express the KCC2 protein (D-D3). GFP is localised in the cell nucleus and KCC2 is localised in the cell membrane (insets in D-D1 respectively). Scale bars 200 µm.

5.1.4 KCC2 is not sufficient to induce expression of *Satb1* in MGE progenitors *in vitro*

Having established that the pCAGGS-Kcc2-GFP vector encodes a functional KCC2 protein, we proceeded with ectopic overexpression studies in brain slices. Similarly to the SATB1 overexpression approach (section 5.1.1), the pCAGGS-Kcc2-GFP and the control pCAGGS-GFP vectors were focally electroporated into the MGEs of E14.5 wt brain slices, where KCC2 is not normally expressed (Figure 5.5, B-B3), and 24 hours after electroporation we examined the effects on *Satb1* expression in three different ways.

First, we investigated a possible upregulation of *Satb1* by immunofluorescence on whole brain slices. Specifically, 24 hours after electroporation the slices were fixed, resectioned and immunolabelled (Figure 5.5, A) using an antibody against GFP to detect the targeted cells, as well as KCC2- and SATB1-specific antibodies. Introduction of the control vector, as well as forced expression of KCC2 in MGE progenitors gave similar results: SATB1 protein showed diffuse, non-specific expression around the electroporation area (Figure 5.5, B2 and C2) and we were unable to detect nuclear SATB1 localisation within the targeted GFP^+ cells (Figure 5.5, insets in C-C3). We excluded the possibility that this could result from a technical limitation of the SATB1 antibody by introducing the pCAGGS-Satb1-RFP vector, which is known to drive expression of SATB1 protein (Denaxa *et al*., 2012), in brain slices adjacent to the ones electroporated with the KCC2-expressing vector. SATB1-overexpressing cells showed robust nuclear expression of SATB1 protein (Figure 5.5, E-E1), compared to pCAGGs-RFP-electroporated controls which were devoid of SATB1 expression (Figure 5.5, D-D1), indicating that the SATB1 antibody used in our studies can reliably detect nuclear localised SATB1 in the MGE.

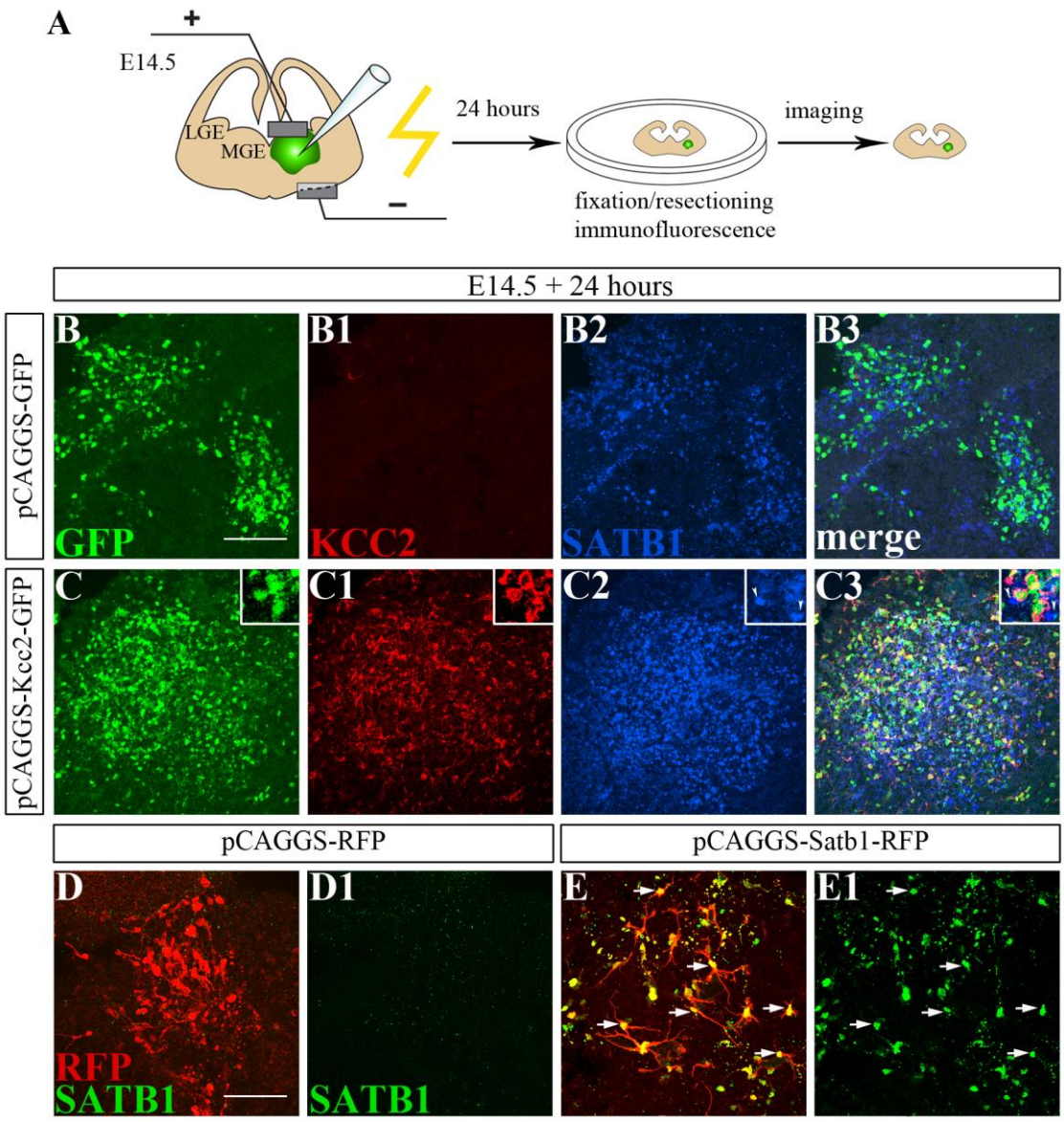

Figure 5.5 KCC2 is not sufficient to induce expression of *Satb1* in MGE progenitors. (A) Schematic representation of the experimental strategy. **(B-C3)** MGE progenitors were electroporated with the pCAGGS-GFP (B-B3) or pCAGGS-Kcc2-GFP (C-C3) vectors and stained 24 hours later with antibodies against GFP (B, C), KCC2 (B1, C1) and SATB1 (B2, C2). Panels B3 and C3 are merged images of B-B2 and C-C2 respectively. Unspecific SATB1 staining was observed in both control and KCC2-overexpressing areas. $SATB1^{+}$ cells were frequently found next to GFP^{+};$KCC2^{+}$;$SATB1^{-}$ cells (arrows in insets at C-C3). **(D-E1)** MGE electroporations with pCAGGS-RFP (D-D1) or pCAGGS-Satb1-RFP (E-E1) vectors, stained 24 hours later with antibodies against RFP and SATB1. Panels D and E represent the overlay of RFP and SATB1 stainings, whereas panels D1 and E1 show SATB1 alone. Notice the absence of SATB1 in control electroporated slices (D-D1) and the characteristic nuclear

SATB1 localisation in pCAGGS-Satb1-RFP electroporated cells (arrows in E-E1). n=3 independent electroporations, 10 slices electroporated bilaterally with each vector per experiment. Scale bars 100 μm. Schematic in A was generated by Hayley Wood, NIMR photographics.

Second, we decided to proceed with single-cell cultures of the electroporated tissue in order to have a clearer view of the expression of SATB1 protein and distinguish between a possible cell-autonomous or non cell-autonomous effect of KCC2 on SATB1 expression. Another advantage of this approach is that the dissociated tissue can be cultured for longer periods, compared to the 48-hour time-window that the brain slices can be kept for before they start degrading, therefore allowing KCC2 to act for a prolonged period of time. To this aim, we dissociated the GFP-expressing MGEs 24 hours post-electroporation, plated the cells on top of a P0 cortical feeder layer and cultured them for 2 or 7 days *in vitro* (DIV) (Figure 5.6, A). Cells were subsequently fixed and processed for immunofluorescence using antibodies for GFP, KCC2 and SATB1. We were able to detect SATB1 in both our pCAGGS-GFP and pCAGGS-Kcc2-GFP cultures already at 2 DIV (Figure 5.6, B-C3) and observed that by 7 DIV the number of $SATB1^+$ cells had increased (Figure 5.6, D). However, quantification of the number of GFP^+ cells coexpressing SATB1 revealed that the percentage of GFP^+;$SATB1^+$ cells was not increased in cultures of MGEs electroporated with the KCC2-expressing vector compared to control vector electroporated ones after either 2 DIV (Figure 5.6, D; 1.9% pCAGGS-control, 2.7% pCAGGS-Kcc2, n=1) or 7 DIV (Figure 5.6, D; 62.5% pCAGGS-control, 62% pCAGGS-Kcc2, n=1). The above findings suggest that KCC2 is not sufficient to drive SATB1 expression in a cell-autonomous manner, even after a period of 7 DIV. We are currently repeating this experiment to obtain larger number of cells and perform statistics.

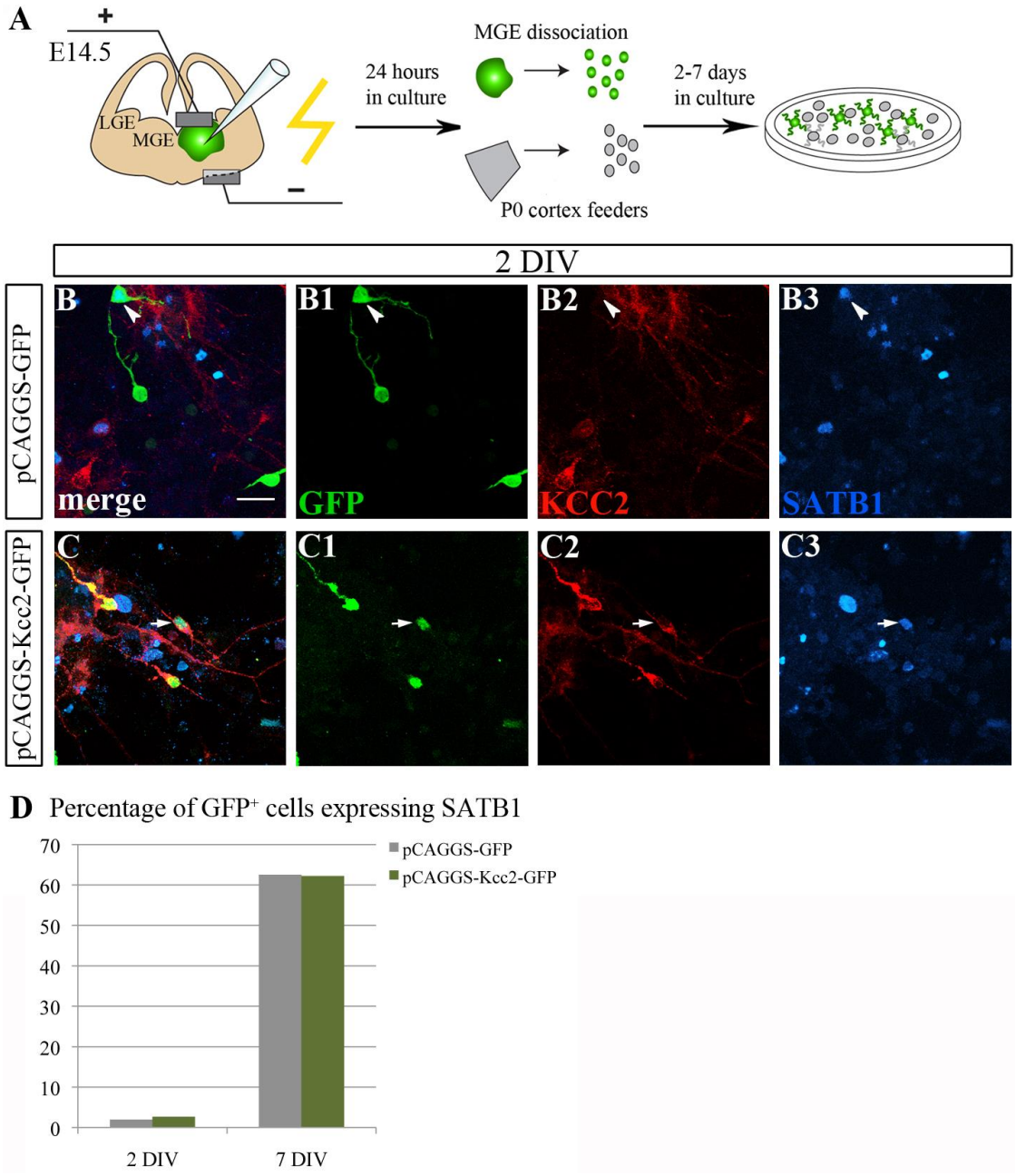

Figure 5.6 Forced expression of KCC2 fails to cell-autonomously upregulate SATB1. **(A)** Schematic representation of the experimental strategy. **(B-C3)** Triple immunofluorescence for GFP (B1, C1), KCC2 (B2, C2) and SATB1 (B3, C3) on dissociated MGEs after electroporation with pCAGGS-GFP (B-B3) or pCAGGS-Kcc2-GFP (C-C3), at 2 DIV. Panels B and C are merged images of panels B1-B3 and C1-C3 respectively. Arrowheads in B-B3 indicate a GFP^+ cell that expresses SATB1 but is negative for KCC2. Arrows in C-C3 point to a GFP^+ cell positive for both KCC2 and SATB1. **(D)** Quantification of the percentage of $SATB1^+;GFP^+$ cells within the GFP^+ population in control electroporations (grey bars) compared to KCC2 overexpression

electroporations (green bars), at 2 and 7 DIV. n=1 electroporation experiment, 15 slices electroporated bilaterally with each vector. Scale bar 25 μm. Schematic in A was generated by Hayley Wood, NIMR photographics. Data collected jointly with Myrto Denaxa.

Our third and final approach was to examine the effect of KCC2 overexpression on Satb1 mRNA levels, by performing highly sensitive qPCR on material collected from three independent electroporation experiments. For this purpose, we followed the same procedure as described in section 5.1.1 to isolate mRNA from FACS purified dissociated MGEs 24 hours after electroporation with pCAGGS-GFP or pCAGGS-Kcc2-GFP and proceeded with quantitation of the Satb1 mRNA transcript levels (Figure 5.7, A) using again the TaqMan methodology. In parallel, we quantified the transcript levels of Kcc2 as a positive control for its successful upregulation in our electroporations. Unfortunately, there is no known target of KCC2 that we could use as a positive control for the functionality of the protein produced by the pCAGGS-Kcc2-GFP vector. We observed that although the Kcc2 mRNA levels were dramatically upregulated (1000-fold) 24 hours post-electroporation with the pCAGGS-Kcc2-GFP vector there was no significant upregulation in the levels of Satb1 mRNA transcript (Figure 5.7, B).

Taken together the results from the three different experimental strategies described above demonstrate that KCC2 is not sufficient to drive expression of *Satb1* in MGE progenitors and is therefore unlikely to be the factor inducing expression of *Satb1* in the cortical plate of the mouse telencephalon. Our proposed model therefore is that SATB1 is necessary and sufficient to positively regulate expression of *Kcc2* but KCC2 does not feedback to upregulate the levels of *Satb1*.

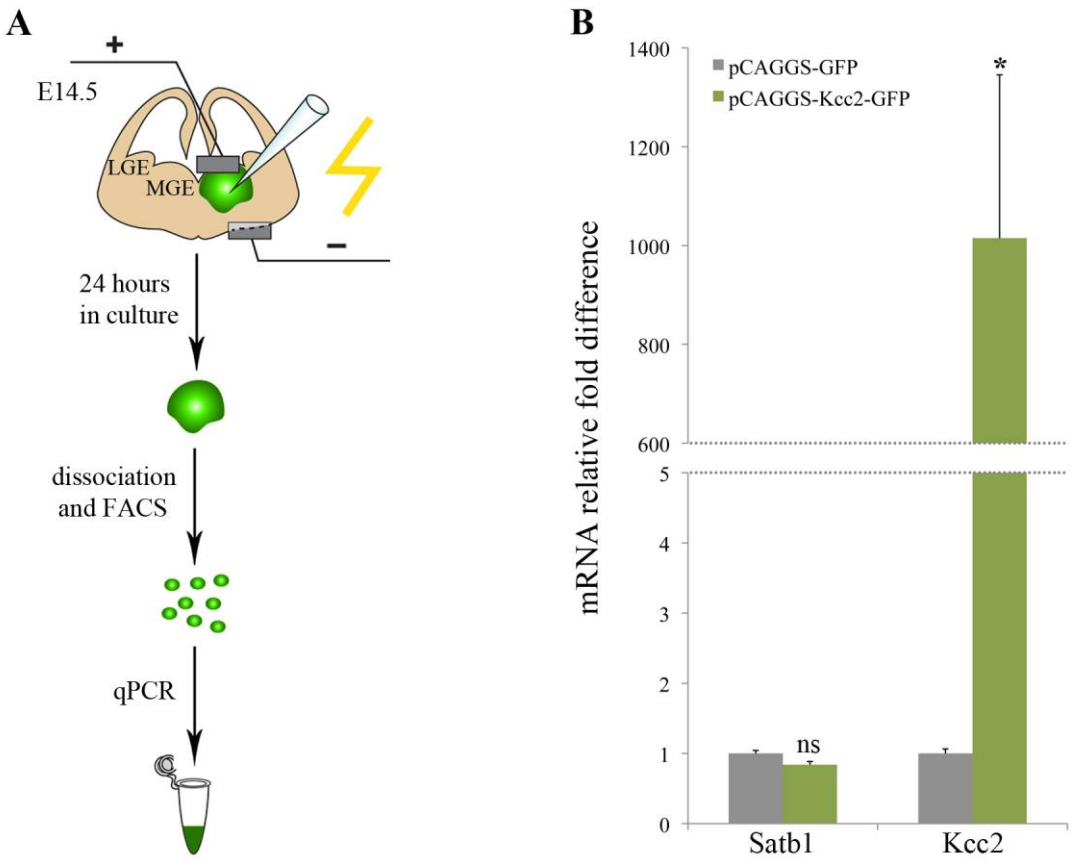

Figure 5.7 Ectopic expression of KCC2 in MGE progenitors is not sufficient to upregulate the mRNA levels of *Satb1*. (A) Schematic representation of the experimental approach. **(B)** The relative amount of Satb1 mRNA is not significantly enriched in pCAGGS-Kcc2-GFP-electroporated cells (green bars) compared to pCAGGS-GFP-electroporated controls (grey bars). The dramatic upregulation of Kcc2 in the pCAGGS-Kcc2-GFP-electroporated cells provides a positive control in our assay. Data are presented as fold change in amount of mRNA transcript, normalised to the housekeeping gene *ß-actin*, between KCC2-overexpressing cells and controls. Values are the mean of biological triplicates for each condition, coming from 3 independent electroporations. ns indicates no statistical significance, * indicates $p<0.05$, Student's t test (two-tailed distribution, two-sample equal variance). Error bars, SEM. The schematic in A was generated by Hayley Wood, NIMR photographics facility.

5.2 Discussion

Upregulation of the expression levels of the K^+-Cl^- cotransporter KCC2, in response to $GABA_A$ receptor-mediated activity and/or the neurotrophic factor BDNF (reviewed in Fiumelli and Woodin, 2007), has been associated with neuronal maturation in the CNS. Our studies have established the regulation of the general neuronal maturation marker KCC2 by SATB1, as we have demonstrated upregulation of Kcc2 mRNA transcript levels in MGE progenitors at an *in vitro* SATB1 overexpression assay and also documented reduced KCC2 protein expression in the cortical plate of *Satb1*-deficient mice. However, we failed to detect a reciprocal regulation of *Satb1* by KCC2 in our attempt to identify the factors that induce *Satb1* expression in cortical GABAergic interneurons. Our study is one of the few to examine the regulation and function of KCC2 specifically in the context of cortical interneuron development, along with recent work by the Polleux group, which correlated the upregulation of *Kcc2* in cortical interneurons with the termination of migration (Bortone and Polleux, 2009; section 1.3.3.3 herein).

5.2.1 SATB1 is necessary and sufficient to regulate expression of *Kcc2*

Excitatory GABA during embryonic development and early postnatal life has been implicated in a wide spectrum of processes including progenitor cell proliferation, migration, synapse formation and maturation (reviewed in Wang and Kriegstein, 2009), as well as control of early network activity (Cherubini *et al*., 2011). The transition of GABA function from excitatory to inhibitory is governed by the developmental upregulation of KCC2 (Rivera *et al*., 1999; reviewed in Ben-Ari *et al*., 20007). Therefore, the time course of *Kcc2* expression has a direct impact on the above processes. Furthermore, the levels of KCC2 are altered in the diseased brain, for example after ischemic brain injury (Papp *et al*., 2008) or during seizure activity (Rivera

et al., 2004; Pathak *et al*., 2007), further highlighting the importance of precise regulation of *Kcc2* expression in the developing and mature CNS.

Data from the literature, based largely on hippocampal cultures, demonstrate that GABA-mediated excitation is the developmental signal that induces the upregulation of *Kcc2* during postnatal stages (Ganguly *et al*., 2001). In addition, the neurotrophic factor BDNF has been shown to positively regulate *Kcc2* in the developing hippocampus, but also negatively regulate *Kcc2* during hyperexcitation in the mature brain (reviewed in Fiumelli and Woodin, 2007). Downregulation of *Kcc2* has also been reported after prolonged postsynaptic spiking activity (reviewed in Fiumelli and Woodin, 2007).

As part of our efforts to investigate the role of SATB1 in promoting the maturation of cortical interneurons, we examined a possible regulatory relationship between SATB1 and KCC2. SATB1 was sufficient to promptly upregulate the Kcc2 mRNA transcript levels, 24 hours after it was introduced by electroporation into E14.5 MGE precursors. Conversely, KCC2 protein expression was evidently reduced in the cortex of *Satb1*-deficient animals, indicating that SATB1 is necessary for normal levels of KCC2 expression. Our findings therefore show that in consistence with the regulation of interneuron-specific maturation markers such as SST, SATB1 can also upregulate the expression of the pan-neuronal maturation marker KCC2. Importantly, we have at the same time identified a novel upstream regulator of *Kcc2* expression.

5.2.2 KCC2 is unlikely to be involved in the initiation of *Satb1* expression in the cortical plate

Despite the well-established role of SATB1 in directing the tissue-specific expression of multiple genes in immune cells (Alvarez *et al*., 2000; Cai *et al*., 2006), cancer cells (Han *et al*., 2008) and interneurons, as our study has shown, very little is

known with regards to its upstream regulators. Recent studies have identified the p63 transcription factor as a direct positive regulator of *Satb1* expression in primary keratinocytes (Fessing *et al*., 2011) and FOXP3 as a repressor of *Satb1* in both regulatory T-cells (Beyer *et al*., 2011) and breast cancer cells (McInnes *et al*., 2012).

Work from our laboratory initiated an attempt to identify factors that could be driving expression of *Satb1* in cortical interneurons. This work first demonstrated that although necessary, LHX6 is not sufficient to induce expression of *Satb1* after overexpression in MGE progenitors or coelectroporation with MASH1 in cortical projection neuron progenitors (Denaxa *et al*., 2012). The latter assay is known to induce interneuron characteristics to dorsal forebrain progenitors (A. Achimastou, V. Pachnis unpublished observations). The above findings are in agreement with the fact that *Satb1* expression begins late and is limited to the cortex (Denaxa *et al*., 2012; Close *et al*., 2012), compared to the early and more widespread expression of *Lhx6* (Grigoriou *et al*., 1998; Liodis *et al*., 2007).

Given the fact that the expression of KCC2 in E18.5 cortical interneurons correlates well with that of SATB1, we investigated the possibility of KCC2 being an upstream regulator of *Satb1*. We began by examining how the expression of SATB1 and KCC2 proteins develops in the embryonic mouse cortex before E18.5, in order to elucidate which one of the two comes on first. Our data are the first in the literature to describe the developmental course of SATB1 and KCC2 coexpression in the cortex by demonstrating that SATB1 and KCC2 proteins greatly overlap in the E15.5 marginal zone and subplate. However, at E16.5 SATB1 was evidently upregulated in the cortical plate, whereas KCC2 was observed in very few cells in this area. Our findings, although they do not distinguish between expression of SATB1 in pyramidal cells or interneurons, are in agreement with the expression pattern of SATB1 in cortical interneurons that was recently described in work from our laboratory (Denaxa *et al*.,

2012) and from the Fishell group (Close *et al*., 2012). With regards to the expression of KCC2 in the embryonic mouse cortex, our data mostly agree with what has been reported in the literature (Bortone and Polleux, 2009). Similarly to the Bortone and Polleux study, we observed no KCC2 immunoreactivity in the E13.5-14.5 cortex. However, our results show more robust KCC2 expression in the marginal zone and cortical plate at E16.5. This could be possibly due to the different mouse lines or KCC2 antibodies used between the two studies. Our data are confirmed by gene expression analysis for *Kcc2* in the E15.5 cortex presented in the GENSAT mouse brain atlas.

The fact that expression of SATB1 precedes that of KCC2 in the cortical plate argues against KCC2 being the factor that initiates *Satb1* expression in cortical interneurons. Nonetheless, we reasoned that KCC2 could be acting to maintain or further upregulate the levels of *Satb1* in the cortical plate. This is the first effort to our knowledge to examine such a functional relationship between KCC2 and SATB1. We tested our hypothesis by generating a pCAGGS-Kcc2-GFP expression vector and introducing it into E14.5 wt MGE progenitors in our usual organotypic brain slice culture setup. We were unable to detect upregulation of SATB1 protein expression in whole brain slices or dissociated cultures after electroporation with the KCC2-encoding vector and similar results were obtained when we quantified the relative Satb1 mRNA levels between pCAGGS-GFP and pCAGGS-Kcc2-GFP electroporated cells with highly sensitive qPCR. We therefore provide novel evidence that argue against regulation of *Satb1* by KCC2 in cortical interneuron precursors and propose that KCC2 is not the factor inducing *Satb1* in the cortical plate. With the role of *Satb1* in neuronal development being newly discovered, examination of *Satb1* expression in $Kcc2^{-/-}$ mutants (Hübner *et al.*, 2001; Woo *et al*., 2002; Khalilov *et al*., 2011) has not been described in the literature. We wished to assess our *in vitro* findings in *Kcc2*-deficient animals, however we were unable to obtain these mice during the course of our studies.

Our prediction is that no change would be observed in the expression of *Satb1* in the cortex of these mutants.

Notably, parallel studies conducted in our laboratory (Denaxa *et al*., 2012) identified neuronal activity as the driving force behind the induction of *Satb1* in cortical interneurons, using a dissociated cortical culture experimental setup. Specifically, addition of KCl, which is commonly used to induce neuronal depolarisation (Ebert *et al*., 2013; Maharana *et al*., 2013), resulted in a significant upregulation of *Satb1* expression, partly through $GABA_A$ receptor activation (Denaxa *et al.*, 2012). Published shortly after our work, the Close *et al*. study provided further, *in vivo*, evidence for the regulation of *Satb1* expression by neuronal activity by demonstrating that *Satb1* levels were downregulated in cortical interneurons in which neuronal activity was attenuated by expression of the Kir2.1 channel (Close *et al*., 2012).

Taken together, our findings, along with data from the literature, can be incorporated into the following model: neuronal activity at the late embryonic cortical plate induces the expression of both *Satb1* and *Kcc2*. SATB1 then functions to maintain or further upregulate the expression levels of *Kcc2* (Figure 5.8). Therefore, activity regulates *Kcc2* in two ways: both directly, as shown in the literature, and indirectly via the induction of *Satb1* in the cortical plate, as we have demonstrated with our studies. There is no indication for reciprocal regulation of *Satb1* by KCC2.

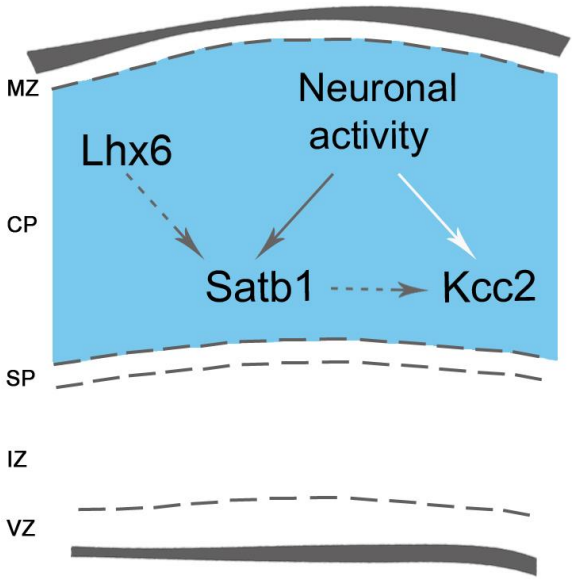

Figure 5.8 Model for the regulation of *Kcc2* and *Satb1* expression in the late embryonic/early postnatal cortex. Neuronal activity in the form of GABA acting through $GABA_A$ receptors induces expression of both *Satb1* and *Kcc2* in the cortical plate. In turn, SATB1, which is genetically downstream of LHX6, acts to maintain or increase *Kcc2* expression levels. Grey arrows indicate the contribution of our work to the model, whereas white arrows indicate interactions known from the literature. Dashed grey arrows indicate genetic interaction. MZ= marginal zone, CP= cortical plate, SP=subplate, IZ= intermediate zone, VZ= ventricular zone.

Chapter 6

Final discussion and future directions

6.1 Novel factors regulating cortical interneuron maturation and diversity

Cortical GABAergic interneurons constitute a remarkably heterogeneous population in terms of physiology, morphology and neurochemical content. It is now well established that this extreme diversity serves the dual role of preventing hyperexcitability and gating of information that forms the basis of brain function. Therefore, it comes as no surprise that perturbation of cortical interneuron development or function was found to often underlie the aetiology of a wide spectrum of neurodevelopmental disorders including epilepsy, schizophrenia, autism spectrum disorders and mental retardation. Elucidation of the mechanisms by which interneuron diversity is established during normal development will aid the understanding of their function in the healthy brain and provide insight into how interneuron deficits contribute to disease.

Accumulating evidence over the past few years have demonstrated that cortical interneuron diversity is, at least in part, specified during embryonic development in spatially segregated progenitor pools in the ganglionic eminences of the developing forebrain, which express characteristic sets of transcription factors, in a manner analogous to neuronal specification in the spinal cord (reviewed in Gelman and Marín, 2010). Moreover, the timing of birth of interneurons is equally important in specifying distinct identities (Butt *et al*., 2005; Miyoshi *et al*., 2007). However, it is becoming increasingly evident that local factors in the cortical environment, such as neuronal activity, also play an important role in influencing the course of cortical interneuron development, from their laminar positioning within the cortex to morphology and network integration (reviewed in Batista-Brito and Fishell, 2009; De Marco García *et al*., 2011). It seems therefore that cortical interneuron diversity arises from the interplay between intrinsic developmental programs and extrinsic influences, which are important

for the execution of these genetic programs. Although significant progress has been made in deciphering the early steps of GABAergic cortical interneuron specification, the maturation of these cells into different subsets and the mechanisms by which the cortical environment influences this process remain poorly understood.

Work from our group, as well as others, has established that the LIM-HD transcription factor LHX6 is required for the differentiation of PV^+ and SST^+ MGE-derived interneurons (Liodis *et al*., 2007; Zhao *et al*., 2008; Neves *et al*., 2012). However, the differentiation of these two subsets progresses in a distinct spatiotemporal manner, indicating that region- and stage-specific factors could be operating downstream of LHX6 to regulate this process. By performing a microarray screen for these factors, work from our lab has identified the genome organiser protein SATB1, which is induced in the cortical plate by neuronal activity and functions genetically downstream of LHX6 (Denaxa *et al*., 2012). The findings presented in this thesis, along with additional work from our laboratory (Denaxa *et al*., 2012), provide novel insight into the role of SATB1 in promoting MGE-derived cortical interneuron maturation and diversity. Although SATB1 is expressed in both SST^+ and PV^+ cells of the MGE lineage, our data demonstrate a specific requirement for *Satb1* activity mainly in the former, arguing that despite their common origin these two populations follow distinct maturation programs in the postnatal cortex.

Regarding the SST^+ interneuron maturation program, I have shown that SATB1 regulates the expression of multiple proteins associated with the terminal differentiation of SST^+ interneurons, including SST, NPY, CR and CRH. I have also revealed regulation of the pan-neuronal maturation marker KCC2 by SATB1, both at the mRNA and protein level. Beyond the molecular aspects of neuronal terminal differentiation, other maturation properties controlled by SATB1 include the termination of cortical interneuron migration, as revealed by the downregulation of tangential migration-

associated markers such as DCLK2 and ERBB4, and the stalling of SATB1-overexpressing interneurons in the ventral forebrain, in the Denaxa *et al*. study (Denaxa *et al*., 2012). Notably, these interneurons had multipolar morphologies, rather than the characteristic bipolar shape of migrating cells. Additional maturation features such as the active and passive membrane properties, the ion channel and neurotransmitter receptor composition as well as the morphology of *Satb1*-deficient cortical interneurons have not been examined in our work. Notably, the membrane properties of *Satb1*-deficient SST^+ and PV^+ interneurons were assessed at an independent study, which revealed alterations characteristic of less mature cells in both populations (Close *et al*., 2012).

Overall, our data offer new insight into how GABAergic interneuron diversity is regulated within the context of the developing cortex, downstream of LHX6, as summarised in our proposed model (Figure 6.1). Further studies aiming to decipher the downstream targets of SATB1 as well as its function at the level of the epigenome will provide a new basis for understanding the generation of cortical interneuron diversity.

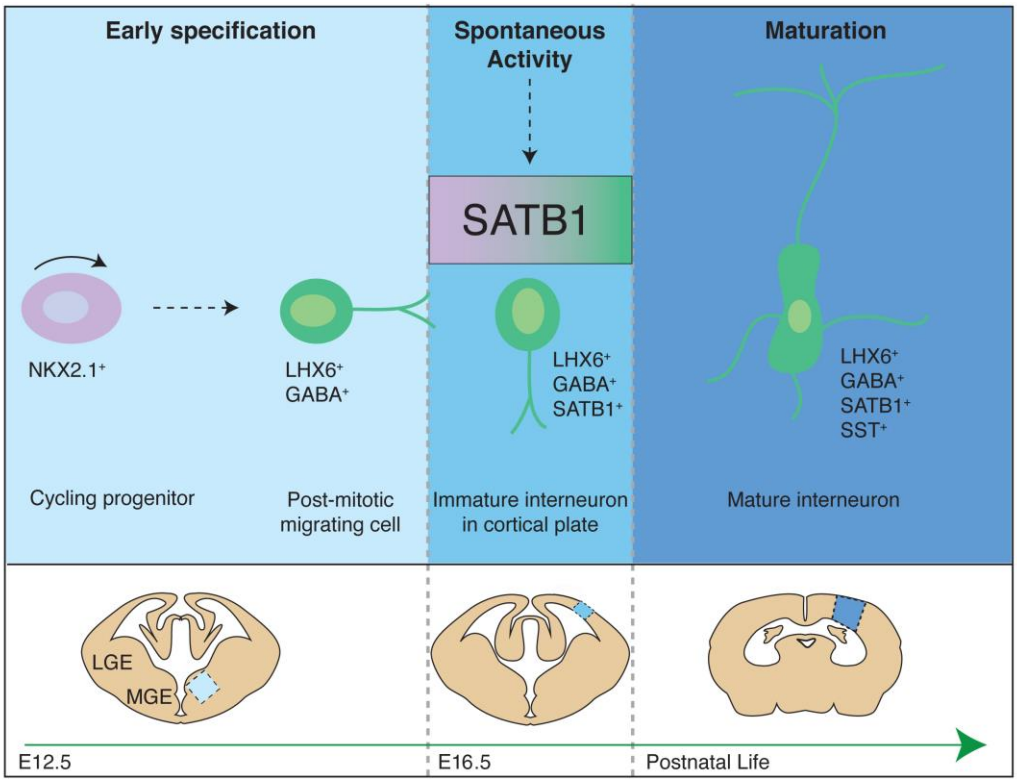

Figure 6.1 Proposed model for the role of SATB1 in cortical interneuron maturation. LHX6 is required in a cell-autonomous manner in MGE precursors as soon as they become postmitotic (left panel) to regulate their migration to the cortex (left and middle panels) and differentiation into SST^+ and PV^+ interneurons (right panel). In the late embryonic cortex (middle panel), spontaneous neuronal activity induces expression of SATB1, which acts genetically downstream of LHX6 to regulate multiple aspects of SST^+ interneuron maturation. In summary, we propose that SATB1 acts as an integrator of the intrinsic genetic program initiated in MGE cortical interneuron progenitors by LHX6 and local cues within the cortex, such as activity, to promote the terminal differentiation of SST^+ interneurons. Schematic generated by Hayley Wood at NIMR photographics for Denaxa *et al*., 2012 and is reproduced herein with permission.

6.1.1 Future aims

Our future experiments will primarily focus on the transcriptional profiling of *Satb1*-deficient cortical interneurons, aiming to elucidate what further cortical interneuron maturation properties are regulated by SATB1. To achieve this we will combine the *Satb1*^{flox} allele with the constitutive *Nkx2.1-Cre* line (Kessaris *et al*., 2006) and perform genome-wide microarray analyses. We will focus at the late embryonic stage of E18.5, when a large proportion of interneurons within the cortical plate upregulate SATB1 (Denaxa *et al*., 2012), as well as at one early postnatal stage, close to birth, during which period a lot of changes in cortical activity patterns occur (reviewed in Cossart, 2011). It would also be of interest to delineate SATB1 targets at a late postnatal stage, from P15 onwards, when synapse formation and maturation take place (reviewed in Batista-Brito *et al*., 2009). Given the role of SATB1 in cortical interneuron maturation, it is of great importance to identify which ion channels, neurotransmitter receptors and synaptic machinery-related genes are regulated by it.

Our work has demonstrated a clear requirement for *Satb1* activity in the terminal differentiation of SST^+ interneurons and a less clear, if any, role in their PV^+ counterparts. Gene expression profiling of cortical interneurons from *SST-ires-Cre;Satb1-flox mice* that we have generated will aid the identification of additional SATB1 targets in SST^+ interneurons and further our understanding of the SATB1-driven maturation program in these cells. With regards to the PV^+ population, we have so far shown that SATB1 is not required for the maintenance of PV expression. However, we lack evidence for the regulation of any other maturation properties in these cells. The literature suggests that PV-expressing cortical interneurons undergo a period of maturation during the first four postnatal weeks, characterised by changes in the expression of various synaptically-localised molecules as well as numerous ionic regulators, which influence the membrane properties of these cells (Okaty *et al*., 2009).

It would therefore be interesting to examine if any of these properties are regulated by SATB1. To this aim, we will perform genome-wide gene expression analyses using the *PV-Cre* line (Hippenmeyer *et al.*, 2005) combined with the *Satb1*^{flox} allele. Overall, elucidation of the downstream effectors of SATB1 will give us invaluable insight on its function in cortical interneurons and the generation of diversity in this cellular network.

So far, we have shown regulation of *Sst*, *Cr*, *Npy* and *Crh* expression by SATB1, based on immunofluorescence, *in situ* hybridisation and qPCR data. Our next goal was then to prove direct regulation of these genes by demonstrating binding of SATB1 with ChIP experiments. However, this evidence actually emerged from another group, which showed direct binding of SATB1 to upstream regulatory regions of the *Sst*, *Calb2* and *Crh* loci (Balamotis *et al*., 2012), coming in support of our observations. Further to providing evidence for direct binding of SATB1 to multiple loci, it is also of great interest to us to understand the three-dimensional, SATB1-tethered transcriptional network in cortical interneurons, similarly to what has been shown in the context of T-cells (Cai *et al*., 2006; Kumar *et al*., 2007). Interestingly, although in the case of the T_H2 cytokine (Cai *et al*., 2006) and the MHC I (Kumar *et al*., 2007) loci SATB1 regulates the coordinated expression of genes positioned on the same chromosome, our work suggests that genes located on different chromosomes can also be transcriptionally coregulated by SATB1, as *Sst*, *Calb2*, *Npy* and *Crh* are found on chromosomes 16, 8, 6 and 3, respectively. In fact, the concept of gene clustering from multiple chromosomes and their shared association with "transcription compartments" within the cell nucleus is not uncommon (reviewed in Misteli, 2007). An example of this model is the close proximity of the human a- and ß-globin genes, located on chromosomes 16 and 11 respectively, when at an active state (Brown *et al*., 2006).

Future studies from our lab will focus on 3D DNA fluorescence *in situ* hybridisation (FISH) to identify the potential association of different genes in the cell

nucleus of isolated cortical interneurons, as well as RNA FISH, so that the colocalisation of transcribed genes is revealed. Both techniques are based on using differentially labelled fluorescent probes to detect the genes or transcripts of interest and are coupled with confocal microscopy to reveal juxtaposition or colocalisation of the fluorescent signals. Moreover, we will examine the 3D chromatin conformation resulting from the interactions between SATB1 and its recruited loci by performing ChIP-3C assays, where 3C stands for "chromatin conformation capture". Briefly, formaldehyde cross-linking will be used to capture chromatin loops, followed by chromatin immunoprecipitation with a SATB1 antibody to allow the analysis of SATB1-bound loops. The basic principle of ChIP-3C is that if distant genomic sites come into proximity by chromatin looping, then they will be isolated from the same cross-linked chromatin fragment (reviewed in Kohwi-Shigematsu *et al*., 2012).

6.2 SATB1 in neurodevelopmental disorders

The role of SATB1 in disease has mostly been examined in relation to cancer, following the discovery that it is highly expressed in metastatic breast cancer cells, where it promotes "aggressive" phenotypes by regulating the expression of more than 1,000 genes (Han *et al*., 2008). Altered SATB1 levels have been correlated with poor prognosis not only in breast cancer (Han *et al*., 2008) but also in a vast number of other malignancies, a few examples of which include glioma (Chu *et al*., 2012), cutaneous malignant melanoma (Chen *et al*., 2011), lung (Selinger *et al*., 2011) and rectal (Meng *et al*., 2012) cancer.

A comprehensive search of the Genetic Association Database, a web-based archive of more than 5,000 genetic association studies, revealed that *Satb1* has been identified as a susceptibility locus in immune, cardiovascular and metabolic diseases, including psoriasis, inflammatory bowel disease, and insulin resistance. However, we

failed to detect any reports on *Satb1* in neuropsychiatric disorders, in the Genetic Association Database, Autism Database (AutDB), Schizophrenia Gene (SzGene) Database and CarpeDB epilepsy gene database. Interestingly, a very recent functional genomics study has put SATB1 forward as a possible regulator of multiple autism spectrum disorder-associated genes (Parikshak *et al*., 2013). Moreover, *Satb2,* the close homolog of *Satb1,* has recently been associated with risk of autism spectrum disorders (Talkowski *et al*., 2012; Jiang *et al*., 2013), as well as intellectual disability (Rauch *et al*., 2012).

Given the very recent discovery of the importance of SATB1 in cortical neuron development and function, it is not surprising that no reports exist yet on its role in neurological disease, apart from the Fishell group findings (Close *et al*., 2012) and our *Satb1|Nkx2.1* cKO analysis (section 4.1.3), which implicate SATB1 in cortical interneuron maturation and epilepsy. Although constitutive *Satb1*$^{-/-}$ mice exhibited signs of the clasping reflex, a general neurological defect (section 3.1.2 and Alvarez *et al*., 2000), no evidence for abnormal behaviour emerged from our studies. In particular, observation of *Satb1*-null mutants in their home cage, or minor handling, did not reveal any traits of hyperactive behaviour, anxiety or epilepsy, at least up to P23-P25 when mutants eventually die. Moreover, we failed to detect histopathological changes indicative of seizure activity (M. Kalaitzidou, M. Denaxa and V. Pachnis, unpublished observations), such as upregulation of the activity-dependent gene *c-fos* (reviewed in Flavell and Greenberg, 2008) or loss of cortical interneurons (Henshall and Meldrum, 2012). In contrast however, our *Satb1|Nkx2.1* conditional mutants show a clear difference in phenotype severity, as they have reduced number of GABAergic interneurons and exhibit behavioural signs of hyperexcitability, such as twitching and loss of postural balance (section 4.1.3). Similarly, conditional *Dlx5/6-Cre;Satb1-flox* and *SST-Cre;Satb1-flox* mutants, described elsewhere, are characterised by

compromised SST^+ interneuron survival and reduced cortical functional inhibition, with the former also displaying epileptiform activity in the motor cortex but not the hippocampus (Close *et al*., 2012).

The behavioural differences between the constitutive and conditional *Satb1* mutants raise the question of what is the underlying cause of this phenomenon. To address this, we started by comparing the cellular and molecular aspects of the two phenotypes. Constitutive $Satb1^{-/-}$ mice show SST^+ interneuron maturation deficits (sections 3.1.5 and 3.1.6), as well as projection neuron dendritic spine defects (Balamotis *et al*., 2012), whereas conditional *Satb1|Nkx2.1* mutants are characterised by compromised SST^+ and PV^+ cell survival but possibly no pyramidal cell defects, if we assume that loss of *Satb1* activity in interneurons does not influence excitatory cortical neuron development. Based on this, our hypothesis for the divergent behavioural phenotypes of the $Satb1^{-/-}$ and *Satb1|Nkx2.1* mutants is that in the former the effects of compromised interneuron development are probably masked by deficits in projection neuron function and therefore the balance between excitation and inhibition is somewhat maintained, while in the latter, cortical interneuron defects drive the excitation/inhibition balance towards abnormally high excitation levels, resulting in epilepsy.

Interestingly, SATB1 is one of the few transcription factors known in the literature to affect cortical interneuron maturation (especially of the SST^+ subset) and function, without disrupting the early development and tangential migration of these cells (our studies and Close *et al*., 2012). Similarly, LHX6 is another transcription factor that plays a role in the maturation of cortical and hippocampal SST^+ interneurons, as demonstrated by recent studies from our lab (Neves *et al*., 2012). Reduced *Lhx6* activity in $Lhx6^{LacZ}$ hypomorph mutants affects the differentiation of SST-expressing interneurons without influencing the migration of these cells (Neves *et al*., 2012). It also

alters the levels of dendritic inhibition in the CA1 area and leads to epileptic activity in hippocampal networks (Neves *et al*., 2012). Along the same lines, *Dlx1*$^{-/-}$ mutants have normal numbers and distribution of GABAergic cortical interneurons up to early postnatal stages, but subsequently show compromised morphological maturation and survival of SST^{+} interneurons. Consequently, there is reduced inhibition in cortical and hippocampal networks and *Dlx1-deficient* mice develop epilepsy (Cobos *et al*., 2005).

Contrary to *Satb1*$^{-/-}$ mutants, mice lacking the DLX5/6 (Wang *et al*., 2010) or SOX6 (Batista-Brito *et al*., 2009; Azim *et al*., 2009) transcription factors show differentiation defects mainly in the PV^{+} subset of cortical interneurons, rather than their SST^{+} counterparts. In particular, *Sox6*-deficient PV^{+} interneurons fail to differentiate and show passive membrane properties characteristic of immature, rather than mature fast-spiking cells (Batista-Brito *et al*., 2009), indicating a role for SOX6 in the functional maturation of cortical basket cells. In contrast to *Satb1*$^{-/-}$ mutants though, *Sox6*-deficient mice exhibit defects in the tangential and radial migration of cortical interneurons (Batista-Brito *et al*., 2009; Azim *et al*., 2009), thus raising the question of whether the immature state of these cells is due to the lack of *Sox6* function or caused by their altered laminar positioning. Notably, both *Dlx5/6- and Sox6*-deficient mutants develop spontaneous seizures (Wang *et al*., 2010; Batista-Brito *et al*., 2009), similarly to our *Satb1|Nkx2.1* conditionals.

6.2.1 Future aims

Intrigued by the development of epileptic seizures in our *Satb1* conditional mutants, we are currently analysing further the *Satb1|Nkx2.1* phenotype by examination of the expression levels of activity-dependent genes such as *c-fos*, *Bdnf* and *Arc* (reviewed in Flavell and Greenberg, 2008) as well as *Npas4* (Lin *et al*., 2008). Our preliminary results from immunofluorescence experiments indicate an upregulation of

c-FOS protein levels in the P15 cortex of *Satb1|Nkx2.1* cKO mice (M. Kalaitzidou and V. Pachnis, unpublished observations) and we are currently validating this result by Western blot analysis.

Regarding the development of cortical projection neurons, we will first investigate their specification into distinct subsets, similarly to the analysis we performed for constitutive *Satb1*$^{-/-}$ mice (section 3.1.3), using layer markers such as *Er81*, *Cux2* and *Tbr1*. Based on our data from *Satb1*$^{-/-}$ mutants, as well as an independent study on other *Satb1*-deficient mice (Balamotis *et al*., 2012), we don't expect cortical layering defects in the *Satb1|Nkx2.1* conditionals. Second, projection neurons will be assessed for dendritic spine development defects, as the literature suggests that *Satb1*$^{-/-}$ mutant pyramidal cells have reduced dendritic spine density (Balamotis *et al*., 2012). However, one assumption is that pyramidal cell dendritic tree complexity could be unaffected after interneuron-specific deletion of *Satb1*, if there are no non-cell autonomous effects on projection neurons. To address this, we will perform the Golgi-Cox staining technique, which is widely used for the detailed visualisation of neuronal morphology, and measure differences in dendrite length, branching pattern as well as spine shape and density between *Satb1|Nkx2.1* mutants and control littermates.

Interestingly, we have noticed an upregulation of SATB1 protein levels in cortical projection neurons of *Satb1|Nkx2.1* mutants (M. Kalaitzidou and V. Pachnis, unpublished observations), a finding that possibly indicates projection neuron hyperactivity when *Satb1* function is abolished in interneurons, as *Satb1* expression is activity-regulated (Denaxa *et al*., 2012; Close *et al*., 2012). Notably, this finding has also been observed in *Lhx6*$^{-/-}$ mice (M. Denaxa and V. Pachnis, unpublished observations), which show reduced inhibitory synaptic current frequencies (Neves *et al*., 2012). These observations, along with the fact that cortical interneuron-specific deletion of *Satb1* results in seizure activity (our observations and Close *et al*., 2012) and

upregulation of activity-dependent markers such as *c-fos,* indicate that SATB1 could play a role in controlling activity levels in the cortex. Knowing that SATB1 is expressed in both cortical interneurons and projection neurons (Denaxa *et al*., 2012; Close *et al*., 2012; Balamotis *et al*., 2012) we decided to focus our future studies in the examination of its role in projection neurons and establish if perturbation of *Satb1* function in these cells will have an effect on cortical network activity levels. To this aim, we will combine our *Satb1*^{flox} mice with the *NEX-Cre* line, in which Cre activity is detected exclusively in postmitotic pyramidal neurons (Goebbels *et al*., 2006) and should therefore drive specific deletion of *Satb1* in these cells.

NEX-Cre;Satb1-flox mutants will be analysed for defects in projection neuron specification and dendritic spine development, similarly to our *Nkx2.1-Cre;Satb1-flox* analysis. One hypothesis is that *Satb1*-deficient projection neurons could potentially have reduced density of dendritic spines, a phenotype observed in constitutive *Satb1*$^{-/-}$ mutants (Balamotis *et al*., 2012). Interestingly, this could have behavioural implications, which we wish to address, as reduced dendritic spine density has been associated with various neuropsychiatric disorders including Alzheimer's disease, schizophrenia and Rett syndrome (reviewed in Penzes *et al*., 2011). Additionally, an interesting and important question to address is whether projection neuron-specific deletion of *Satb1* affects neuronal activity in the cortex. For instance, one possibility could be that loss of *Satb1* function in pyramidal neurons will shift the excitation/inhibition balance towards inhibition, resulting in an opposite phenotype compared to the hyperexcitable state of *Satb1|Nkx2.1* mutants. Behavioural studies to assess social interactions, anxiety levels, as well as learning and memory performance, along with activity-regulated marker analysis, should contribute to the elucidation of this question.

Overall, the role of SATB1 in the regulation of activity in the brain, along with its ability to simultaneously control multiple genetic loci in other systems, and possibly in cortical interneurons, opens up an exciting new era in the field of cortical development that will lead to a better understanding of the function of cortical neuronal networks and the aetiology behind neurodevelopmental disorders.

References

Alcamo, E. A., Chirivella, L., Dautzenberg, M., Dobreva, G., Farinas, I., Grosschedl, R. and McConnell, S. K. (2008). Satb2 regulates callosal projection neuron identity in the developing cerebral cortex. *Neuron* **57**, 364-77.

Alifragis, P., Liapi, A. and Parnavelas, J. G. (2004). Lhx6 regulates the migration of cortical interneurons from the ventral telencephalon but does not specify their GABA phenotype. *J Neurosci* **24**, 5643-8.

Alvarez, J. D., Yasui, D. H., Niida, H., Joh, T., Loh, D. Y. and Kohwi-Shigematsu, T. (2000). The MAR-binding protein SATB1 orchestrates temporal and spatial expression of multiple genes during T-cell development. *Genes Dev* **14**, 521-35.

Alvarez-Dolado, M., Calcagnotto, M. E., Karkar, K. M., Southwell, D. G., Jones-Davis, D. M., Estrada, R. C., Rubenstein, J. L., Alvarez-Buylla, A. and Baraban, S. C. (2006). Cortical inhibition modified by embryonic neural precursors grafted into the postnatal brain. *J Neurosci* **26**, 7380-9.

Anderson, S., Mione, M., Yun, K. and Rubenstein, J. L. (1999). Differential origins of neocortical projection and local circuit neurons: role of Dlx genes in neocortical interneuronogenesis. *Cereb Cortex* **9**, 646-54.

Anderson, S. A., Eisenstat, D. D., Shi, L. and Rubenstein, J. L. (1997a). Interneuron migration from basal forebrain to neocortex: dependence on Dlx genes. *Science* **278**, 474-6.

Anderson, S. A., Kaznowski, C. E., Horn, C., Rubenstein, J. L. and McConnell, S. K. (2002). Distinct origins of neocortical projection neurons and interneurons in vivo. *Cereb Cortex* **12**, 702-9.

Anderson, S. A., Marin, O., Horn, C., Jennings, K. and Rubenstein, J. L. (2001). Distinct cortical migrations from the medial and lateral ganglionic eminences. *Development* **128**, 353-63.

Anderson, S. A., Qiu, M., Bulfone, A., Eisenstat, D. D., Meneses, J., Pedersen, R. and Rubenstein, J. L. (1997b). Mutations of the homeobox genes Dlx-1 and Dlx-2 disrupt the striatal subventricular zone and differentiation of late born striatal neurons. *Neuron* **19**, 27-37.

Andrews, W., Barber, M., Hernadez-Miranda, L. R., Xian, J., Rakic, S., Sundaresan, V., Rabbitts, T. H., Pannell, R., Rabbitts, P., Thompson, H. et al. (2008). The role of Slit-Robo signaling in the generation, migration and morphological differentiation of cortical interneurons. *Dev Biol* **313**, 648-58.

Ang, E. S., Jr., Haydar, T. F., Gluncic, V. and Rakic, P. (2003). Four-dimensional migratory coordinates of GABAergic interneurons in the developing mouse cortex. *J Neurosci* **23**, 5805-15.

Arber, S. and Caroni, P. (1996). Specificity of single LIM motifs in targeting and LIM/LIM interactions in situ. *Genes Dev* **10**, 289-300.

Asbreuk, C. H., van Schaick, H. S., Cox, J. J., Kromkamp, M., Smidt, M. P. and Burbach, J. P. (2002). The homeobox genes Lhx7 and Gbx1 are expressed in the basal forebrain cholinergic system. *Neuroscience* **109**, 287-98.

Ascoli, G. A., Alonso-Nanclares, L., Anderson, S. A., Barrionuevo, G., Benavides-Piccione, R., Burkhalter, A., Buzsaki, G., Cauli, B., Defelipe, J., Fairen, A. et al. (2008). Petilla terminology: nomenclature of features of GABAergic interneurons of the cerebral cortex. *Nat Rev Neurosci* **9**, 557-68.

Azim, E., Jabaudon, D., Fame, R. M. and Macklis, J. D. (2009). SOX6 controls dorsal progenitor identity and interneuron diversity during neocortical development. *Nat Neurosci* **12**, 1238-47.

Bagri, A., Marin, O., Plump, A. S., Mak, J., Pleasure, S. J., Rubenstein, J. L. and Tessier-Lavigne, M. (2002). Slit proteins prevent midline crossing and determine the dorsoventral position of major axonal pathways in the mammalian forebrain. *Neuron* **33**, 233-48.

Balabanian, K., Lagane, B., Infantino, S., Chow, K. Y., Harriague, J., Moepps, B., Arenzana-Seisdedos, F., Thelen, M. and Bachelerie, F. (2005). The chemokine SDF-1/CXCL12 binds to and signals through the orphan receptor RDC1 in T lymphocytes. *J Biol Chem* **280**, 35760-6.

Balamotis, M. A., Tamberg, N., Woo, Y. J., Li, J., Davy, B., Kohwi-Shigematsu, T. and Kohwi, Y. (2012). Satb1 ablation alters temporal expression of immediate early genes and reduces dendritic spine density during postnatal brain development. *Mol Cell Biol* **32**, 333-47.

Banan, M., Rojas, I. C., Lee, W. H., King, H. L., Harriss, J. V., Kobayashi, R., Webb, C. F. and Gottlieb, P. D. (1997). Interaction of the nuclear matrix-associated region (MAR)-binding proteins, SATB1 and CDP/Cux, with a MAR element (L2a) in an upstream regulatory region of the mouse CD8a gene. *J Biol Chem* **272**, 18440-52.

Barber, M., Di Meglio, T., Andrews, W. D., Hernandez-Miranda, L. R., Murakami, F., Chedotal, A. and Parnavelas, J. G. (2009). The role of Robo3 in the development of cortical interneurons. *Cereb Cortex* **19 Suppl 1**, i22-31.

Batista-Brito, R. and Fishell, G. (2009). The developmental integration of cortical interneurons into a functional network. *Curr Top Dev Biol* **87**, 81-118.

Batista-Brito, R., Rossignol, E., Hjerling-Leffler, J., Denaxa, M., Wegner, M., Lefebvre, V., Pachnis, V. and Fishell, G. (2009). The cell-intrinsic requirement of Sox6 for cortical interneuron development. *Neuron* **63**, 466-81.

Ben-Ari, Y., Gaiarsa, J. L., Tyzio, R. and Khazipov, R. (2007). GABA: a pioneer transmitter that excites immature neurons and generates primitive oscillations. *Physiol Rev* **87**, 1215-84.

Bertuzzi, S., Hindges, R., Mui, S. H., O'Leary, D. D. and Lemke, G. (1999). The homeodomain protein vax1 is required for axon guidance and major tract formation in the developing forebrain. *Genes Dev* **13**, 3092-105.

Beyer, M., Thabet, Y., Muller, R. U., Sadlon, T., Classen, S., Lahl, K., Basu, S., Zhou, X., Bailey-Bucktrout, S. L., Krebs, W. et al. (2011). Repression of the genome organizer SATB1 in regulatory T cells is required for suppressive function and inhibition of effector differentiation. *Nat Immunol* **12**, 898-907.

Bird, R. C., Stein, G. S., Lian, J. B. and Stein, J. L. (1997). Nuclear Structure and Gene Expression. 111-141.

Blaesse, P., Guillemin, I., Schindler, J., Schweizer, M., Delpire, E., Khiroug, L., Friauf, E. and Nothwang, H. G. (2006). Oligomerization of KCC2 correlates with development of inhibitory neurotransmission. *J Neurosci* **26**, 10407-19.

Boda, E., Hoxha, E., Pini, A., Montarolo, F. and Tempia, F. (2012). Brain expression of Kv3 subunits during development, adulthood and aging and in a murine model of Alzheimer's disease. *J Mol Neurosci* **46**, 606-15.

Bortone, D. and Polleux, F. (2009). KCC2 expression promotes the termination of cortical interneuron migration in a voltage-sensitive calcium-dependent manner. *Neuron* **62**, 53-71.

Boulikas, T. (1995). Chromatin domains and prediction of MAR sequences. *Int Rev Cytol* **162A**, 279-388.

Brazel, C. Y., Romanko, M. J., Rothstein, R. P. and Levison, S. W. (2003). Roles of the mammalian subventricular zone in brain development. *Prog Neurobiol* **69**, 49-69.

Britanova, O., Akopov, S., Lukyanov, S., Gruss, P. and Tarabykin, V. (2005). Novel transcription factor Satb2 interacts with matrix attachment region DNA elements in a tissue-specific manner and demonstrates cell-type-dependent expression in the developing mouse CNS. *Eur J Neurosci* **21**, 658-68.

Britanova, O., de Juan Romero, C., Cheung, A., Kwan, K. Y., Schwark, M., Gyorgy, A., Vogel, T., Akopov, S., Mitkovski, M., Agoston, D. et al. (2008). Satb2 is a postmitotic determinant for upper-layer neuron specification in the neocortex. *Neuron* **57**, 378-92.

Brown, K. N., Chen, S., Han, Z., Lu, C. H., Tan, X., Zhang, X. J., Ding, L., Lopez-Cruz, A., Saur, D., Anderson, S. A. et al. (2011). Clonal production and organization of inhibitory interneurons in the neocortex. *Science* **334**, 480-6.

Brown, J. M., Leach, J., Reittie, J. E., Atzberger, A., Lee-Prudhoe, J., Wood, W. G., Higgs, D. R., Iborra, F. J. and Buckle, V. J. (2006). Coregulated human globin genes are frequently in spatial proximity when active. *J Cell Biol* **172**, 177-87.

Butt, S. J., Cobos, I., Golden, J., Kessaris, N., Pachnis, V. and Anderson, S. (2007). Transcriptional regulation of cortical interneuron development. *J Neurosci* **27**, 11847-50.

Butt, S. J., Fuccillo, M., Nery, S., Noctor, S., Kriegstein, A., Corbin, J. G. and Fishell, G. (2005). The temporal and spatial origins of cortical interneurons predict their physiological subtype. *Neuron* **48**, 591-604.

Butt, S. J., Sousa, V. H., Fuccillo, M. V., Hjerling-Leffler, J., Miyoshi, G., Kimura, S. and Fishell, G. (2008). The requirement of Nkx2-1 in the temporal specification of cortical interneuron subtypes. *Neuron* **59**, 722-32.

Cai, S., Han, H. J. and Kohwi-Shigematsu, T. (2003). Tissue-specific nuclear architecture and gene expression regulated by SATB1. *Nat Genet* **34**, 42-51.

Cai, S., Lee, C. C. and Kohwi-Shigematsu, T. (2006). SATB1 packages densely looped, transcriptionally active chromatin for coordinated expression of cytokine genes. *Nat Genet* **38**, 1278-88.

Cai, Y., Zhang, Q., Wang, C., Zhang, Y., Ma, T., Zhou, X., Tian, M., Rubenstein, J. L. and Yang, Z. (2013). Nuclear receptor COUP-TFII-expressing neocortical interneurons are derived from the medial and lateral/caudal ganglionic eminence and define specific subsets of mature interneurons. *J Comp Neurol* **521**, 479-97.

Casarosa, S., Fode, C. and Guillemot, F. (1999). Mash1 regulates neurogenesis in the ventral telencephalon. *Development* **126**, 525-34.

Chattopadhyaya, B., Di Cristo, G., Higashiyama, H., Knott, G. W., Kuhlman, S. J., Welker, E. and Huang, Z. J. (2004). Experience and activity-dependent maturation of perisomatic GABAergic innervation in primary visual cortex during a postnatal critical period. *J Neurosci* **24**, 9598-611.

Chen, H., Takahara, M., Oba, J., Xie, L., Chiba, T., Takeuchi, S., Tu, Y., Nakahara, T., Uchi, H., Moroi, Y. et al. (2011). Clinicopathologic and prognostic significance of SATB1 in cutaneous malignant melanoma. *J Dermatol Sci* **64**, 39-44.

Cherubini, E., Griguoli, M., Safiulina, V. and Lagostena, L. (2011). The depolarizing action of GABA controls early network activity in the developing hippocampus. *Mol Neurobiol* **43**, 97-106.

Chiang, C., Litingtung, Y., Lee, E., Young, K. E., Corden, J. L., Westphal, H. and Beachy, P. A. (1996). Cyclopia and defective axial patterning in mice lacking Sonic hedgehog gene function. *Nature* **383**, 407-13.

Chinnadurai, G. (2002). CtBP, an unconventional transcriptional corepressor in development and oncogenesis. *Mol Cell* **9**, 213-24.

Choi, G. B., Dong, H. W., Murphy, A. J., Valenzuela, D. M., Yancopoulos, G. D., Swanson, L. W. and Anderson, D. J. (2005). Lhx6 delineates a pathway mediating innate reproductive behaviors from the amygdala to the hypothalamus. *Neuron* **46**, 647-60.

Choi, Y. S., Lin, S. L., Lee, B., Kurup, P., Cho, H. Y., Naegele, J. R., Lombroso, P. J. and Obrietan, K. (2007). Status epilepticus-induced somatostatinergic hilar interneuron degeneration is regulated by striatal enriched protein tyrosine phosphatase. *J Neurosci* **27**, 2999-3009.

Chow, A., Erisir, A., Farb, C., Nadal, M. S., Ozaita, A., Lau, D., Welker, E. and Rudy, B. (1999). K(+) channel expression distinguishes subpopulations of parvalbumin- and somatostatin-containing neocortical interneurons. *J Neurosci* **19**, 9332-45.

Chu, S. H., Ma, Y. B., Feng, D. F., Zhang, H., Zhu, Z. A., Li, Z. Q. and Jiang, P. C. (2012). Upregulation of SATB1 is associated with the development and progression of glioma. *J Transl Med* **10**, 149.

Close, J., Xu, H., De Marco Garcia, N., Batista-Brito, R., Rossignol, E., Rudy, B. and Fishell, G. (2012). Satb1 is an activity-modulated transcription factor required for the terminal differentiation and connectivity of medial ganglionic eminence-derived cortical interneurons. *J Neurosci* **32**, 17690-705.

Cobos, I., Calcagnotto, M. E., Vilaythong, A. J., Thwin, M. T., Noebels, J. L., Baraban, S. C. and Rubenstein, J. L. (2005). Mice lacking Dlx1 show subtype-specific loss of interneurons, reduced inhibition and epilepsy. *Nat Neurosci* **8**, 1059-68.

Colasante, G., Collombat, P., Raimondi, V., Bonanomi, D., Ferrai, C., Maira, M., Yoshikawa, K., Mansouri, A., Valtorta, F., Rubenstein, J. L. et al. (2008). Arx is a direct target of Dlx2 and thereby contributes to the tangential migration of GABAergic interneurons. *J Neurosci* **28**, 10674-86.

Colombo, E., Collombat, P., Colasante, G., Bianchi, M., Long, J., Mansouri, A., Rubenstein, J. L. and Broccoli, V. (2007). Inactivation of Arx, the murine ortholog of the X-linked lissencephaly with ambiguous genitalia gene, leads to severe disorganization of the ventral telencephalon with impaired neuronal migration and differentiation. *J Neurosci* **27**, 4786-98.

Corbin, J. G., Gaiano, N., Machold, R. P., Langston, A. and Fishell, G. (2000). The Gsh2 homeodomain gene controls multiple aspects of telencephalic development. *Development* **127**, 5007-20.

Corbin, J. G., Rutlin, M., Gaiano, N. and Fishell, G. (2003). Combinatorial function of the homeodomain proteins Nkx2.1 and Gsh2 in ventral telencephalic patterning. *Development* **130**, 4895-906.

Corlew, R., Bosma, M. M. and Moody, W. J. (2004). Spontaneous, synchronous electrical activity in neonatal mouse cortical neurones. *J Physiol* **560**, 377-90.

Cossart, R., Dinocourt, C., Hirsch, J. C., Merchan-Perez, A., De Felipe, J., Ben-Ari, Y., Esclapez, M. and Bernard, C. (2001). Dendritic but not somatic GABAergic inhibition is decreased in experimental epilepsy. *Nat Neurosci* **4**, 52-62.

D'Arcangelo, G. (2005). The reeler mouse: anatomy of a mutant. *Int Rev Neurobiol* **71**, 383-417.

Dawid, I. B., Breen, J. J. and Toyama, R. (1998). LIM domains: multiple roles as adapters and functional modifiers in protein interactions. *Trends Genet* **14**, 156-62.

de Belle, I., Cai, S. and Kohwi-Shigematsu, T. (1998). The genomic sequences bound to special AT-rich sequence-binding protein 1 (SATB1) in vivo in Jurkat T cells are tightly associated with the nuclear matrix at the bases of the chromatin loops. *J Cell Biol* **141**, 335-48.

de Carlos, J. A., Lopez-Mascaraque, L. and Valverde, F. (1996). Dynamics of cell migration from the lateral ganglionic eminence in the rat. *J Neurosci* **16**, 6146-56.

DeFelipe, J., López-Cruz, P. L., Benavides-Piccione, R., Bielza, C., Larrañaga, P., Anderson, S., Burkhalter, A., Cauli, B., Fairén, A., Feldmeyer, D. et al. (2013). New insights into the classification and nomenclature of cortical GABAergic interneurons. *Nat Rev Neurosci* **14**, 202-16.

de la Serna, I. L., Ohkawa, Y. and Imbalzano, A. N. (2006). Chromatin remodelling in mammalian differentiation: lessons from ATP-dependent remodellers. *Nat Rev Genet* **7**, 461-73.

De Marco Garcia, N. V., Karayannis, T. and Fishell, G. (2011). Neuronal activity is required for the development of specific cortical interneuron subtypes. *Nature* **472**, 351-5.

del Rio, J. A., de Lecea, L., Ferrer, I. and Soriano, E. (1994). The development of parvalbumin-immunoreactivity in the neocortex of the mouse. *Brain Res Dev Brain Res* **81**, 247-59.

Denaxa, M., Kalaitzidou, M., Garefalaki, A., Achimastou, A., Lasrado, R., Maes, T. and Pachnis, V. (2012). Maturation-promoting activity of SATB1 in MGE-derived cortical interneurons. *Cell Rep* **2**, 1351-62.

Denaxa, M., Sharpe, P. T. and Pachnis, V. (2009). The LIM homeodomain transcription factors Lhx6 and Lhx7 are key regulators of mammalian dentition. *Dev Biol* **333**, 324-36.

Dickinson, L. A., Dickinson, C. D. and Kohwi-Shigematsu, T. (1997). An atypical homeodomain in SATB1 promotes specific recognition of the key structural element in a matrix attachment region. *J Biol Chem* **272**, 11463-70.

Dickinson, L. A., Joh, T., Kohwi, Y. and Kohwi-Shigematsu, T. (1992). A tissue-specific MAR/SAR DNA-binding protein with unusual binding site recognition. *Cell* **70**, 631-45.

Dobreva, G., Chahrour, M., Dautzenberg, M., Chirivella, L., Kanzler, B., Farinas, I., Karsenty, G. and Grosschedl, R. (2006). SATB2 is a multifunctional determinant of craniofacial patterning and osteoblast differentiation. *Cell* **125**, 971-86.

Dobreva, G., Dambacher, J. and Grosschedl, R. (2003). SUMO modification of a novel MAR-binding protein, SATB2, modulates immunoglobulin mu gene expression. *Genes Dev* **17**, 3048-61.

Douglas, R. J. and Martin, K. A. (2007). Mapping the matrix: the ways of neocortex. *Neuron* **56**, 226-38.

Du, T., Xu, Q., Ocbina, P. J. and Anderson, S. A. (2008). NKX2.1 specifies cortical interneuron fate by activating Lhx6. *Development* **135**, 1559-67.

Ebert, D. H., Gabel, H. W., Robinson, N. D., Kastan, N. R., Hu, L. S., Cohen, S., Navarro, A. J., Lyst, M. J., Ekiert, R., Bird, A. P. et al. (2013). Activity-dependent phosphorylation of MeCP2 threonine 308 regulates interaction with NCoR. *Nature* **499**, 341-5.

Edlund, T. and Jessell, T. M. (1999). Progression from extrinsic to intrinsic signaling in cell fate specification: a view from the nervous system. *Cell* **96**, 211-24.

Elias, L. A., Turmaine, M., Parnavelas, J. G. and Kriegstein, A. R. (2010). Connexin 43 mediates the tangential to radial migratory switch in ventrally derived cortical interneurons. *J Neurosci* **30**, 7072-7.

Erisir, A., Lau, D., Rudy, B. and Leonard, C. S. (1999). Function of specific K(+) channels in sustained high-frequency firing of fast-spiking neocortical interneurons. *J Neurophysiol* **82**, 2476-89.

Erlander, M. G., Tillakaratne, N. J., Feldblum, S., Patel, N. and Tobin, A. J. (1991). Two genes encode distinct glutamate decarboxylases. *Neuron* **7**, 91-100.

Feil, R., Wagner, J., Metzger, D. and Chambon, P. (1997). Regulation of Cre recombinase activity by mutated estrogen receptor ligand-binding domains. *Biochem Biophys Res Commun* **237**, 752-7.

Fertuzinhos, S., Krsnik, Z., Kawasawa, Y. I., Rasin, M. R., Kwan, K. Y., Chen, J. G., Judas, M., Hayashi, M. and Sestan, N. (2009). Selective depletion of molecularly defined cortical interneurons in human holoprosencephaly with severe striatal hypoplasia. *Cereb Cortex* **19**, 2196-207.

Fessing, M. Y., Mardaryev, A. N., Gdula, M. R., Sharov, A. A., Sharova, T. Y., Rapisarda, V., Gordon, K. B., Smorodchenko, A. D., Poterlowicz, K., Ferone, G. et al. (2011). p63 regulates Satb1 to control tissue-specific chromatin remodeling during development of the epidermis. *J Cell Biol* **194**, 825-39.

Feuerstein, R., Wang, X., Song, D., Cooke, N. E. and Liebhaber, S. A. (1994). The LIM/double zinc-finger motif functions as a protein dimerization domain. *Proc Natl Acad Sci U S A* **91**, 10655-9.

Fishell, G. and Rudy, B. (2011). Mechanisms of inhibition within the telencephalon: "where the wild things are". *Annu Rev Neurosci* **34**, 535-67.

Fiumelli, H., Kiraly, M., Ambrus, A., Magistretti, P. J. and Martin, J. L. (2000). Opposite regulation of calbindin and calretinin expression by brain-derived neurotrophic factor in cortical neurons. *J Neurochem* **74**, 1870-7.

Fiumelli, H. and Woodin, M. A. (2007). Role of activity-dependent regulation of neuronal chloride homeostasis in development. *Curr Opin Neurobiol* **17**, 81-6.

Flames, N., Long, J. E., Garratt, A. N., Fischer, T. M., Gassmann, M., Birchmeier, C., Lai, C., Rubenstein, J. L. and Marin, O. (2004). Short- and long-range attraction of cortical GABAergic interneurons by neuregulin-1. *Neuron* **44**, 251-61.

Flames, N., Pla, R., Gelman, D. M., Rubenstein, J. L., Puelles, L. and Marin, O. (2007). Delineation of multiple subpallial progenitor domains by the combinatorial expression of transcriptional codes. *J Neurosci* **27**, 9682-95.

Flavell, S. W. and Greenberg, M. E. (2008). Signaling mechanisms linking neuronal activity to gene expression and plasticity of the nervous system. *Annu Rev Neurosci* **31**, 563-90.

Fogarty, M., Grist, M., Gelman, D., Marin, O., Pachnis, V. and Kessaris, N. (2007). Spatial genetic patterning of the embryonic neuroepithelium generates GABAergic interneuron diversity in the adult cortex. *J Neurosci* **27**, 10935-46.

Fragkouli, A., Hearn, C., Errington, M., Cooke, S., Grigoriou, M., Bliss, T., Stylianopoulou, F. and Pachnis, V. (2005). Loss of forebrain cholinergic neurons and

impairment in spatial learning and memory in LHX7-deficient mice. *Eur J Neurosci* **21**, 2923-38.

Fragkouli, A., Pachnis, V. and Stylianopoulou, F. (2009a). Sex differences in water maze performance and cortical neurotrophin levels of LHX7 null mutant mice. *Neuroscience* **158**, 1224-33.

Fragkouli, A., Stamatakis, A., Zographos, E., Pachnis, V. and Stylianopoulou, F. (2006). Sexually dimorphic effects of the Lhx7 null mutation on forebrain cholinergic function. *Neuroscience* **137**, 1153-64.

Fragkouli, A., van Wijk, N. V., Lopes, R., Kessaris, N. and Pachnis, V. (2009b). LIM homeodomain transcription factor-dependent specification of bipotential MGE progenitors into cholinergic and GABAergic striatal interneurons. *Development* **136**, 3841-51.

Freyd, G., Kim, S. K. and Horvitz, H. R. (1990). Novel cysteine-rich motif and homeodomain in the product of the Caenorhabditis elegans cell lineage gene lin-11. *Nature* **344**, 876-9.

Friocourt, G., Kanatani, S., Tabata, H., Yozu, M., Takahashi, T., Antypa, M., Raguenes, O., Chelly, J., Ferec, C., Nakajima, K. et al. (2008). Cell-autonomous roles of ARX in cell proliferation and neuronal migration during corticogenesis. *J Neurosci* **28**, 5794-805.

Gabay, L., Lowell, S., Rubin, L. L. and Anderson, D. J. (2003). Deregulation of dorsoventral patterning by FGF confers trilineage differentiation capacity on CNS stem cells in vitro. *Neuron* **40**, 485-99.

Galande, S., Dickinson, L. A., Mian, I. S., Sikorska, M. and Kohwi-Shigematsu, T. (2001). SATB1 cleavage by caspase 6 disrupts PDZ domain-mediated dimerization, causing detachment from chromatin early in T-cell apoptosis. *Mol Cell Biol* **21**, 5591-604.

Galande, S., Purbey, P. K., Notani, D. and Kumar, P. P. (2007). The third dimension of gene regulation: organization of dynamic chromatin loopscape by SATB1. *Curr Opin Genet Dev* **17**, 408-14.

Ganguly, K., Schinder, A. F., Wong, S. T. and Poo, M. (2001). GABA itself promotes the developmental switch of neuronal GABAergic responses from excitation to inhibition. *Cell* **105**, 521-32.

Gao, P., Sultan, K. T., Zhang, X. J. and Shi, S. H. (2013). Lineage-dependent circuit assembly in the neocortex. *Development* **140**, 2645-55.

Gaston-Massuet, C., Henderson, D. J., Greene, N. D. and Copp, A. J. (2005). Zic4, a zinc-finger transcription factor, is expressed in the developing mouse nervous system. *Dev Dyn* **233**, 1110-5.

Gauvain, G., Chamma, I., Chevy, Q., Cabezas, C., Irinopoulou, T., Bodrug, N., Carnaud, M., Levi, S. and Poncer, J. C. (2011). The neuronal K-Cl cotransporter KCC2 influences postsynaptic AMPA receptor content and lateral diffusion in dendritic spines. *Proc Natl Acad Sci U S A* **108**, 15474-9.

Gelman, D., Griveau, A., Dehorter, N., Teissier, A., Varela, C., Pla, R., Pierani, A. and Marin, O. (2011). A wide diversity of cortical GABAergic interneurons derives from the embryonic preoptic area. *J Neurosci* **31**, 16570-80.

Gelman, D. M., Marin and Rubenstein, J. L. R. (2012). The Generation of Cortical Interneurons. In: Noebels, J. L., Avoli, M., Rogawski, M. A., Olsen, R. W. and Delgado-Escueta, A.V. eds. Jasper's Basic Mechanisms of the Epilepsies. 4th Edition. Bethesda (MD): NCBI Bookshelf Online Book Version. Available from: http://www.ncbi.nlm.nih.gov/books/NBK98190/

Gelman, D. M. and Marin, O. (2010). Generation of interneuron diversity in the mouse cerebral cortex. *Eur J Neurosci* **31**, 2136-41.

Gelman, D. M., Martini, F. J., Nobrega-Pereira, S., Pierani, A., Kessaris, N. and Marin, O. (2009). The embryonic preoptic area is a novel source of cortical GABAergic interneurons. *J Neurosci* **29**, 9380-9.

Goebbels, S., Bormuth, I., Bode, U., Hermanson, O., Schwab, M. H. and Nave, K. A. (2006). Genetic targeting of principal neurons in neocortex and hippocampus of NEX-Cre mice. *Genesis* **44**, 611-21.

Gonchar, Y., Wang, Q. and Burkhalter, A. (2008). Multiple distinct subtypes of GABAergic neurons in mouse visual cortex identified by triple immunostaining. *Front Neuroanat* **1**, 3.

Gorski, J. A., Talley, T., Qiu, M., Puelles, L., Rubenstein, J. L. and Jones, K. R. (2002). Cortical excitatory neurons and glia, but not GABAergic neurons, are produced in the Emx1-expressing lineage. *J Neurosci* **22**, 6309-14.

Gotz, M., Williams, B. P., Bolz, J. and Price, J. (1995). The specification of neuronal fate: a common precursor for neurotransmitter subtypes in the rat cerebral cortex in vitro. *Eur J Neurosci* **7**, 889-98.

Greig, L. C., Woodworth, M. B., Galazo, M. J., Padmanabhan, H. and Macklis, J. D. (2013). Molecular logic of neocortical projection neuron specification, development and diversity. *Nat Rev Neurosci* **14**, 755-69.

Grigoriou, M., Tucker, A. S., Sharpe, P. T. and Pachnis, V. (1998). Expression and regulation of Lhx6 and Lhx7, a novel subfamily of LIM homeodomain encoding genes, suggests a role in mammalian head development. *Development* **125**, 2063-74.

Gulacsi, A. and Anderson, S. A. (2006). Shh maintains Nkx2.1 in the MGE by a Gli3-independent mechanism. *Cereb Cortex* **16 Suppl 1**, i89-95.

Gulyas, A. I., Sik, A., Payne, J. A., Kaila, K. and Freund, T. F. (2001). The KCl cotransporter, KCC2, is highly expressed in the vicinity of excitatory synapses in the rat hippocampus. *Eur J Neurosci* **13**, 2205-17.

Gupta, A., Wang, Y. and Markram, H. (2000). Organizing principles for a diversity of GABAergic interneurons and synapses in the neocortex. *Science* **287**, 273-8.

Gyorgy, A. B., Szemes, M., de Juan Romero, C., Tarabykin, V. and Agoston, D. V. (2008). SATB2 interacts with chromatin-remodeling molecules in differentiating cortical neurons. *Eur J Neurosci* **27**, 865-73.

Hallonet, M., Hollemann, T., Pieler, T. and Gruss, P. (1999). Vax1, a novel homeobox-containing gene, directs development of the basal forebrain and visual system. *Genes Dev* **13**, 3106-14.

Han, H. J., Russo, J., Kohwi, Y. and Kohwi-Shigematsu, T. (2008). SATB1 reprogrammes gene expression to promote breast tumour growth and metastasis. *Nature* **452**, 187-93.

Hansen, D. V., Lui, J. H., Flandin, P., Yoshikawa, K., Rubenstein, J. L., Alvarez-Buylla, A. and Kriegstein, A. R. (2013). Non-epithelial stem cells and cortical interneuron production in the human ganglionic eminences. *Nat Neurosci* **16**, 1576-87.

Hawkins, S. M., Kohwi-Shigematsu, T. and Skalnik, D. G. (2001). The matrix attachment region-binding protein SATB1 interacts with multiple elements within the gp91phox promoter and is down-regulated during myeloid differentiation. *J Biol Chem* **276**, 44472-80.

Hebert, J. M. and Fishell, G. (2008). The genetics of early telencephalon patterning: some assembly required. *Nat Rev Neurosci* **9**, 678-85.

Henshall, D. C. and Meldrum, B. S. (2012). Cell death and survival mechanisms after single and repeated brief seizures. In: Noebels, J. L., Avoli, M., Rogawski, M. A., Olsen, R. W. and Delgado-Escueta, A.V. eds. Jasper's Basic Mechanisms of the Epilepsies. 4th Edition. Bethesda (MD): NCBI Bookshelf Online Book Version. Available from: http://www.ncbi.nlm.nih.gov/books/NBK98209/

Hevner, R. F., Daza, R. A., Englund, C., Kohtz, J. and Fink, A. (2004). Postnatal shifts of interneuron position in the neocortex of normal and reeler mice: evidence for inward radial migration. *Neuroscience* **124**, 605-18.

Hevner, R. F., Daza, R. A., Rubenstein, J. L., Stunnenberg, H., Olavarria, J. F. and Englund, C. (2003). Beyond laminar fate: toward a molecular classification of cortical projection/pyramidal neurons. *Dev Neurosci* **25**, 139-51.

Hippenmeyer, S., Vrieseling, E., Sigrist, M., Portmann, T., Laengle, C., Ladle, D. R. and Arber, S. (2005). A developmental switch in the response of DRG neurons to ETS transcription factor signaling. *PLoS Biol* **3**, e159.

Hobert, O. and Westphal, H. (2000). Functions of LIM-homeobox genes. *Trends Genet* **16**, 75-83.

Huang, Y., Zhang, L., Song, N. N., Hu, Z. L., Chen, J. Y. and Ding, Y. Q. (2011). Distribution of Satb1 in the central nervous system of adult mice. *Neurosci Res* **71**, 12-21.

Huang, Z. J., Di Cristo, G. and Ango, F. (2007). Development of GABA innervation in the cerebral and cerebellar cortices. *Nat Rev Neurosci* **8**, 673-86.

Hubner, C. A., Stein, V., Hermans-Borgmeyer, I., Meyer, T., Ballanyi, K. and Jentsch, T. J. (2001). Disruption of KCC2 reveals an essential role of K-Cl cotransport already in early synaptic inhibition. *Neuron* **30**, 515-24.

Jaglin, X. H., Hjerling-Leffler, J., Fishell, G. and Batista-Brito, R. (2012). The origin of neocortical nitric oxide synthase-expressing inhibitory neurons. *Front Neural Circuits* **6**, 44.

Jessell, T. M. (2000). Neuronal specification in the spinal cord: inductive signals and transcriptional codes. *Nat Rev Genet* **1**, 20-9.

Jiang, Y. H., Yuen, R. K., Jin, X., Wang, M., Chen, N., Wu, X., Ju, J., Mei, J., Shi, Y., He, M. et al. (2013). Detection of clinically relevant genetic variants in autism spectrum disorder by whole-genome sequencing. *Am J Hum Genet* **93**, 249-63.

Jimenez, D., Lopez-Mascaraque, L. M., Valverde, F. and De Carlos, J. A. (2002). Tangential migration in neocortical development. *Dev Biol* **244**, 155-69.

Joyner, A. L. and Zervas, M. (2006). Genetic inducible fate mapping in mouse: establishing genetic lineages and defining genetic neuroanatomy in the nervous system. *Dev Dyn* **235**, 2376-85.

Kadrmas, J. L. and Beckerle, M. C. (2004). The LIM domain: from the cytoskeleton to the nucleus. *Nat Rev Mol Cell Biol* **5**, 920-31.

Kanatani, S., Yozu, M., Tabata, H. and Nakajima, K. (2008). COUP-TFII is preferentially expressed in the caudal ganglionic eminence and is involved in the caudal migratory stream. *J Neurosci* **28**, 13582-91.

Karagiannis, A., Gallopin, T., David, C., Battaglia, D., Geoffroy, H., Rossier, J., Hillman, E. M., Staiger, J. F. and Cauli, B. (2009). Classification of NPY-expressing neocortical interneurons. *J Neurosci* **29**, 3642-59.

Karlsson, O., Thor, S., Norberg, T., Ohlsson, H. and Edlund, T. (1990). Insulin gene enhancer binding protein Isl-1 is a member of a novel class of proteins containing both a homeo- and a Cys-His domain. *Nature* **344**, 879-82.

Karube, F., Kubota, Y. and Kawaguchi, Y. (2004). Axon branching and synaptic bouton phenotypes in GABAergic nonpyramidal cell subtypes. *J Neurosci* **24**, 2853-65.

Kawaguchi, Y. and Kondo, S. (2002). Parvalbumin, somatostatin and cholecystokinin as chemical markers for specific GABAergic interneuron types in the rat frontal cortex. *J Neurocytol* **31**, 277-87.

Kawaguchi, Y. and Kubota, Y. (1997). GABAergic cell subtypes and their synaptic connections in rat frontal cortex. *Cereb Cortex* **7**, 476-86.

Kawaguchi, Y., Wilson, C. J., Augood, S. J. and Emson, P. C. (1995). Striatal interneurones: chemical, physiological and morphological characterization. *Trends Neurosci* **18**, 527-35.

Kessaris, N., Fogarty, M., Iannarelli, P., Grist, M., Wegner, M. and Richardson, W. D. (2006). Competing waves of oligodendrocytes in the forebrain and postnatal elimination of an embryonic lineage. *Nat Neurosci* **9**, 173-9.

Khalilov, I., Chazal, G., Chudotvorova, I., Pellegrino, C., Corby, S., Ferrand, N., Gubkina, O., Nardou, R., Tyzio, R., Yamamoto, S. et al. (2011). Enhanced Synaptic Activity and Epileptiform Events in the Embryonic KCC2 Deficient Hippocampus. *Front Cell Neurosci* **5**, 23.

Kitamura, K., Yanazawa, M., Sugiyama, N., Miura, H., Iizuka-Kogo, A., Kusaka, M., Omichi, K., Suzuki, R., Kato-Fukui, Y., Kamiirisa, K. et al. (2002). Mutation of ARX causes abnormal development of forebrain and testes in mice and X-linked lissencephaly with abnormal genitalia in humans. *Nat Genet* **32**, 359-69.

Klausberger, T. and Somogyi, P. (2008). Neuronal diversity and temporal dynamics: the unity of hippocampal circuit operations. *Science* **321**, 53-7.

Kobayashi, M. and Buckmaster, P. S. (2003). Reduced inhibition of dentate granule cells in a model of temporal lobe epilepsy. *J Neurosci* **23**, 2440-52.

Kohwi-Shigematsu, T. and Kohwi Y. (1997). High unwinding capability of matrix attachment regions and ATC-sequence context-specific MAR-binding proteins. In: Bird, R. C., Stein, G. S., Lian, J. B. and Stein, J. L. eds. Nuclear Structure and Gene Expression. New York, USA: Academic Press, pp111-141.

Kohwi-Shigematsu, T., Kohwi, Y., Takahashi, K., Richards, H. W., Ayers, S. D., Han, H. J. and Cai, S. (2012). SATB1-mediated functional packaging of chromatin into loops. *Methods* **58**, 243-54.

Kohwi-Shigematsu, T., Maass, K. and Bode, J. (1997). A thymocyte factor SATB1 suppresses transcription of stably integrated matrix-attachment region-linked reporter genes. *Biochemistry* **36**, 12005-10.

Kohwi, M., Petryniak, M. A., Long, J. E., Ekker, M., Obata, K., Yanagawa, Y., Rubenstein, J. L. and Alvarez-Buylla, A. (2007). A subpopulation of olfactory bulb GABAergic interneurons is derived from Emx1- and Dlx5/6-expressing progenitors. *J Neurosci* **27**, 6878-91.

Konrat, R., Weiskirchen, R., Krautler, B. and Bister, K. (1997). Solution structure of the carboxyl-terminal LIM domain from quail cysteine-rich protein CRP2. *J Biol Chem* **272**, 12001-7.

Kubota, Y., Shigematsu, N., Karube, F., Sekigawa, A., Kato, S., Yamaguchi, N., Hirai, Y., Morishima, M. and Kawaguchi, Y. (2011). Selective coexpression of multiple chemical markers defines discrete populations of neocortical GABAergic neurons. *Cereb Cortex* **21**, 1803-17.

Kumar, P. P., Bischof, O., Purbey, P. K., Notani, D., Urlaub, H., Dejean, A. and Galande, S. (2007). Functional interaction between PML and SATB1 regulates chromatin-loop architecture and transcription of the MHC class I locus. *Nat Cell Biol* **9**, 45-56.

Kumar, P. P., Purbey, P. K., Ravi, D. S., Mitra, D. and Galande, S. (2005). Displacement of SATB1-bound histone deacetylase 1 corepressor by the human immunodeficiency virus type 1 transactivator induces expression of interleukin-2 and its receptor in T cells. *Mol Cell Biol* **25**, 1620-33.

Kuschel, S., Ruther, U. and Theil, T. (2003). A disrupted balance between Bmp/Wnt and Fgf signaling underlies the ventralization of the Gli3 mutant telencephalon. *Dev Biol* **260**, 484-95.

Kwan, K. Y., Sestan, N. and Anton, E. S. (2012). Transcriptional co-regulation of neuronal migration and laminar identity in the neocortex. *Development* **139**, 1535-46.

Lalonde, R. and Strazielle, C. (2011). Brain regions and genes affecting limb-clasping responses. *Brain Res Rev* **67**, 252-9.

Lavdas, A. A., Grigoriou, M., Pachnis, V. and Parnavelas, J. G. (1999). The medial ganglionic eminence gives rise to a population of early neurons in the developing cerebral cortex. *J Neurosci* **19**, 7881-8.

Le, T. N., Du, G., Fonseca, M., Zhou, Q. P., Wigle, J. T. and Eisenstat, D. D. (2007). Dlx homeobox genes promote cortical interneuron migration from the basal forebrain by direct repression of the semaphorin receptor neuropilin-2. *J Biol Chem* **282**, 19071-81.

Lee, S., Hjerling-Leffler, J., Zagha, E., Fishell, G. and Rudy, B. (2010). The largest group of superficial neocortical GABAergic interneurons expresses ionotropic serotonin receptors. *J Neurosci* **30**, 16796-808.

Leone, D. P., Genoud, S., Atanasoski, S., Grausenburger, R., Berger, P., Metzger, D., Macklin, W. B., Chambon, P. and Suter, U. (2003). Tamoxifen-inducible glia-specific Cre mice for somatic mutagenesis in oligodendrocytes and Schwann cells. *Mol Cell Neurosci* **22**, 430-40.

Letinic, K., Zoncu, R. and Rakic, P. (2002). Origin of GABAergic neurons in the human neocortex. *Nature* **417**, 645-9.

Li, H., Khirug, S., Cai, C., Ludwig, A., Blaesse, P., Kolikova, J., Afzalov, R., Coleman, S. K., Lauri, S., Airaksinen, M. S. et al. (2007). KCC2 interacts with the dendritic cytoskeleton to promote spine development. *Neuron* **56**, 1019-33.

Lin, Y., Bloodgood, B. L., Hauser, J. L., Lapan, A. D., Koon, A. C., Kim, T. K., Hu, L. S., Malik, A. N. and Greenberg, M. E. (2008). Activity-dependent regulation of inhibitory synapse development by Npas4. *Nature* **455**, 1198-204.

Liodis, P., Denaxa, M., Grigoriou, M., Akufo-Addo, C., Yanagawa, Y. and Pachnis, V. (2007). Lhx6 activity is required for the normal migration and specification of cortical interneuron subtypes. *J Neurosci* **27**, 3078-89.

Liu, J., Bramblett, D., Zhu, Q., Lozano, M., Kobayashi, R., Ross, S. R. and Dudley, J. P. (1997). The matrix attachment region-binding protein SATB1 participates in negative regulation of tissue-specific gene expression. *Mol Cell Biol* **17**, 5275-87.

Lopes, R., Verhey van Wijk, N., Neves, G. and Pachnis, V. (2012). Transcription factor LIM homeobox 7 (Lhx7) maintains subtype identity of cholinergic interneurons in the mammalian striatum. *Proc Natl Acad Sci U S A* **109**, 3119-24.

Lopez-Bendito, G., Sanchez-Alcaniz, J. A., Pla, R., Borrell, V., Pico, E., Valdeolmillos, M. and Marin, O. (2008). Chemokine signaling controls intracortical migration and final distribution of GABAergic interneurons. *J Neurosci* **28**, 1613-24.

Lopez-Bendito, G., Sturgess, K., Erdelyi, F., Szabo, G., Molnar, Z. and Paulsen, O. (2004). Preferential origin and layer destination of GAD65-GFP cortical interneurons. *Cereb Cortex* **14**, 1122-33.

Lupo, G., Harris, W. A. and Lewis, K. E. (2006). Mechanisms of ventral patterning in the vertebrate nervous system. *Nat Rev Neurosci* **7**, 103-14.

Ma, Y., Hu, H., Berrebi, A. S., Mathers, P. H. and Agmon, A. (2006). Distinct subtypes of somatostatin-containing neocortical interneurons revealed in transgenic mice. *J Neurosci* **26**, 5069-82.

Ma, T., Wang, C., Wang, L., Zhou, X., Tian, M., Zhang, Q., Zhang, Y., Li, J., Liu, Z., Cai, Y. et al. (2013). Subcortical origins of human and monkey neocortical interneurons. *Nat Neurosci* **16**, 1588-97.

Ma, T., Zhang, Q., Cai, Y., You, Y., Rubenstein, J. L. and Yang, Z. (2012). A subpopulation of dorsal lateral/caudal ganglionic eminence-derived neocortical interneurons expresses the transcription factor Sp8. *Cereb Cortex* **22**, 2120-30.

Magno, L., Oliveira, M. G., Mucha, M., Rubin, A. N. and Kessaris, N. (2012). Multiple embryonic origins of nitric oxide synthase-expressing GABAergic neurons of the neocortex. *Front Neural Circuits* **6**, 65.

Maharana, C., Sharma, K. P. and Sharma, S. K. (2013). Feedback mechanism in depolarization-induced sustained activation of extracellular signal-regulated kinase in the hippocampus. *Sci Rep* **3**, 1103.

Marin, O. (2012). Interneuron dysfunction in psychiatric disorders. *Nat Rev Neurosci* **13**, 107-20.

Marin, O., Anderson, S. A. and Rubenstein, J. L. (2000). Origin and molecular specification of striatal interneurons. *J Neurosci* **20**, 6063-76.

Marin, O., Plump, A. S., Flames, N., Sanchez-Camacho, C., Tessier-Lavigne, M. and Rubenstein, J. L. (2003). Directional guidance of interneuron migration to the cerebral cortex relies on subcortical Slit1/2-independent repulsion and cortical attraction. *Development* **130**, 1889-901.

Marin, O. and Rubenstein, J. L. (2001). A long, remarkable journey: tangential migration in the telencephalon. *Nat Rev Neurosci* **2**, 780-90.

Marin, O., Valiente, M., Ge, X. and Tsai, L. H. (2010). Guiding neuronal cell migrations. *Cold Spring Harb Perspect Biol* **2**, a001834.

Marin, O., Yaron, A., Bagri, A., Tessier-Lavigne, M. and Rubenstein, J. L. (2001). Sorting of striatal and cortical interneurons regulated by semaphorin-neuropilin interactions. *Science* **293**, 872-5.

Marklund, M., Sjodal, M., Beehler, B. C., Jessell, T. M., Edlund, T. and Gunhaga, L. (2004). Retinoic acid signalling specifies intermediate character in the developing telencephalon. *Development* **131**, 4323-32.

Markram, H., Toledo-Rodriguez, M., Wang, Y., Gupta, A., Silberberg, G. and Wu, C. (2004). Interneurons of the neocortical inhibitory system. *Nat Rev Neurosci* **5**, 793-807.

McInnes, N., Sadlon, T. J., Brown, C. Y., Pederson, S., Beyer, M., Schultze, J. L., McColl, S., Goodall, G. J. and Barry, S. C. (2012). FOXP3 and FOXP3-regulated microRNAs suppress SATB1 in breast cancer cells. *Oncogene* **31**, 1045-54.

Meng, W. J., Yan, H., Zhou, B., Zhang, W., Kong, X. H., Wang, R., Zhan, L., Li, Y., Zhou, Z. G. and Sun, X. F. (2012). Correlation of SATB1 overexpression with the progression of human rectal cancer. *Int J Colorectal Dis* **27**, 143-50.

Merot, Y., Retaux, S. and Heng, J. I. (2009). Molecular mechanisms of projection neuron production and maturation in the developing cerebral cortex. *Semin Cell Dev Biol* **20**, 726-34.

Metin, C., Baudoin, J. P., Rakic, S. and Parnavelas, J. G. (2006). Cell and molecular mechanisms involved in the migration of cortical interneurons. *Eur J Neurosci* **23**, 894-900.

Meyer, G., Soria, J. M., Martinez-Galan, J. R., Martin-Clemente, B. and Fairen, A. (1998). Different origins and developmental histories of transient neurons in the marginal zone of the fetal and neonatal rat cortex. *J Comp Neurol* **397**, 493-518.

Michelsen, J. W., Sewell, A. K., Louis, H. A., Olsen, J. I., Davis, D. R., Winge, D. R. and Beckerle, M. C. (1994). Mutational analysis of the metal sites in an LIM domain. *J Biol Chem* **269**, 11108-13.

Mione, M. C., Cavanagh, J. F., Harris, B. and Parnavelas, J. G. (1997). Cell fate specification and symmetrical/asymmetrical divisions in the developing cerebral cortex. *J Neurosci* **17**, 2018-29.

Misteli, T. (2007). Beyond the sequence: cellular organization of genome function. *Cell* **128**, 787-800.

Miyoshi, G., Butt, S. J., Takebayashi, H. and Fishell, G. (2007). Physiologically distinct temporal cohorts of cortical interneurons arise from telencephalic Olig2-expressing precursors. *J Neurosci* **27**, 7786-98.

Miyoshi, G. and Fishell, G. (2011). GABAergic interneuron lineages selectively sort into specific cortical layers during early postnatal development. *Cereb Cortex* **21**, 845-52.

Miyoshi, G., Hjerling-Leffler, J., Karayannis, T., Sousa, V. H., Butt, S. J., Battiste, J., Johnson, J. E., Machold, R. P. and Fishell, G. (2010). Genetic fate mapping

reveals that the caudal ganglionic eminence produces a large and diverse population of superficial cortical interneurons. *J Neurosci* **30**, 1582-94.

Mohler, H. (2012). The GABA system in anxiety and depression and its therapeutic potential. *Neuropharmacology* **62**, 42-53.

Molyneaux, B. J., Arlotta, P., Menezes, J. R. and Macklis, J. D. (2007). Neuronal subtype specification in the cerebral cortex. *Nat Rev Neurosci* **8**, 427-37.

Mori, T., Yuxing, Z., Takaki, H., Takeuchi, M., Iseki, K., Hagino, S., Kitanaka, J., Takemura, M., Misawa, H., Ikawa, M. et al. (2004). The LIM homeobox gene, L3/Lhx8, is necessary for proper development of basal forebrain cholinergic neurons. *Eur J Neurosci* **19**, 3129-41.

Nadarajah, B., Alifragis, P., Wong, R. O. and Parnavelas, J. G. (2002). Ventricle-directed migration in the developing cerebral cortex. *Nat Neurosci* **5**, 218-24.

Nakagomi, K., Kohwi, Y., Dickinson, L. A. and Kohwi-Shigematsu, T. (1994). A novel DNA-binding motif in the nuclear matrix attachment DNA-binding protein SATB1. *Mol Cell Biol* **14**, 1852-60.

Nepveu, A. (2001). Role of the multifunctional CDP/Cut/Cux homeodomain transcription factor in regulating differentiation, cell growth and development. *Gene* **270**, 1-15.

Nery, S., Fishell, G. and Corbin, J. G. (2002). The caudal ganglionic eminence is a source of distinct cortical and subcortical cell populations. *Nat Neurosci* **5**, 1279-87.

Neves, G., Shah, M. M., Liodis, P., Achimastou, A., Denaxa, M., Roalfe, G., Sesay, A., Walker, M. C. and Pachnis, V. (2012). The LIM Homeodomain Protein Lhx6 Regulates Maturation of Interneurons and Network Excitability in the Mammalian Cortex. *Cereb Cortex*.

Nickerson, J. (2001). Experimental observations of a nuclear matrix. *J Cell Sci* **114**, 463-74.

Nimchinsky, E. A., Sabatini, B. L. and Svoboda, K. (2002). Structure and function of dendritic spines. *Annu Rev Physiol* **64**, 313-53.

Niwa, H., Yamamura, K. and Miyazaki, J. (1991). Efficient selection for high-expression transfectants with a novel eukaryotic vector. *Gene* **108**, 193-9.

Nobrega-Pereira, S., Gelman, D., Bartolini, G., Pla, R., Pierani, A. and Marin, O. (2010). Origin and molecular specification of globus pallidus neurons. *J Neurosci* **30**, 2824-34.

Nobrega-Pereira, S., Kessaris, N., Du, T., Kimura, S., Anderson, S. A. and Marin, O. (2008). Postmitotic Nkx2-1 controls the migration of telencephalic interneurons by direct repression of guidance receptors. *Neuron* **59**, 733-45.

Nobrega-Pereira, S. and Marin, O. (2009). Transcriptional control of neuronal migration in the developing mouse brain. *Cereb Cortex* **19 Suppl 1**, i107-13.

Okaty, B. W., Miller, M. N., Sugino, K., Hempel, C. M. and Nelson, S. B. (2009). Transcriptional and electrophysiological maturation of neocortical fast-spiking GABAergic interneurons. *J Neurosci* **29**, 7040-52.

Papp, E., Rivera, C., Kaila, K. and Freund, T. F. (2008). Relationship between neuronal vulnerability and potassium-chloride cotransporter 2 immunoreactivity in hippocampus following transient forebrain ischemia. *Neuroscience* **154**, 677-89.

Parikshak, N. N., Luo, R., Zhang, A., Won, H., Lowe, J. K., Chandran, V., Horvath, S. and Geschwind, D. H. (2013). Integrative functional genomic analyses implicate specific molecular pathways and circuits in autism. *Cell* **155**, 1008-21.

Pathak, H. R., Weissinger, F., Terunuma, M., Carlson, G. C., Hsu, F. C., Moss, S. J. and Coulter, D. A. (2007). Disrupted dentate granule cell chloride regulation enhances synaptic excitability during development of temporal lobe epilepsy. *J Neurosci* **27**, 14012-22.

Pavan Kumar, P., Purbey, P. K., Sinha, C. K., Notani, D., Limaye, A., Jayani, R. S. and Galande, S. (2006). Phosphorylation of SATB1, a global gene regulator, acts as a molecular switch regulating its transcriptional activity in vivo. *Mol Cell* **22**, 231-43.

Payne, J. A., Stevenson, T. J. and Donaldson, L. F. (1996). Molecular characterization of a putative K-Cl cotransporter in rat brain. A neuronal-specific isoform. *J Biol Chem* **271**, 16245-52.

Pei, Z., Wang, B., Chen, G., Nagao, M., Nakafuku, M. and Campbell, K. (2011). Homeobox genes Gsx1 and Gsx2 differentially regulate telencephalic progenitor maturation. *Proc Natl Acad Sci U S A* **108**, 1675-80.

Penzes, P., Cahill, M. E., Jones, K. A., VanLeeuwen, J. E. and Woolfrey, K. M. (2011). Dendritic spine pathology in neuropsychiatric disorders. *Nat Neurosci* **14**, 285-93.

Perez-Alvarado, G. C., Kosa, J. L., Louis, H. A., Beckerle, M. C., Winge, D. R. and Summers, M. F. (1996). Structure of the cysteine-rich intestinal protein, CRIP. *J Mol Biol* **257**, 153-74.

Perez-Alvarado, G. C., Miles, C., Michelsen, J. W., Louis, H. A., Winge, D. R., Beckerle, M. C. and Summers, M. F. (1994). Structure of the carboxy-terminal LIM domain from the cysteine rich protein CRP. *Nat Struct Biol* **1**, 388-98.

Perrenoud, Q., Geoffroy, H., Gauthier, B., Rancillac, A., Alfonsi, F., Kessaris, N., Rossier, J., Vitalis, T. and Gallopin, T. (2012). Characterization of Type I and Type II nNOS-Expressing Interneurons in the Barrel Cortex of Mouse. *Front Neural Circuits* **6**, 36.

Petanjek, Z., Berger, B. and Esclapez, M. (2009). Origins of cortical GABAergic neurons in the cynomolgus monkey. *Cereb Cortex* **19**, 249-62.

Pleasure, S. J., Anderson, S., Hevner, R., Bagri, A., Marin, O., Lowenstein, D. H. and Rubenstein, J. L. (2000). Cell migration from the ganglionic eminences is

required for the development of hippocampal GABAergic interneurons. *Neuron* **28**, 727-40.

Pollard, S. M., Wallbank, R., Tomlinson, S., Grotewold, L. and Smith, A. (2008). Fibroblast growth factor induces a neural stem cell phenotype in foetal forebrain progenitors and during embryonic stem cell differentiation. *Mol Cell Neurosci* **38**, 393-403.

Polleux, F., Whitford, K. L., Dijkhuizen, P. A., Vitalis, T. and Ghosh, A. (2002). Control of cortical interneuron migration by neurotrophins and PI3-kinase signaling. *Development* **129**, 3147-60.

Powell, E. M., Mars, W. M. and Levitt, P. (2001). Hepatocyte growth factor/scatter factor is a motogen for interneurons migrating from the ventral to dorsal telencephalon. *Neuron* **30**, 79-89.

Pozas, E. and Ibanez, C. F. (2005). GDNF and GFRalpha1 promote differentiation and tangential migration of cortical GABAergic neurons. *Neuron* **45**, 701-13.

Puelles, L., Kuwana, E., Puelles, E., Bulfone, A., Shimamura, K., Keleher, J., Smiga, S. and Rubenstein, J. L. (2000). Pallial and subpallial derivatives in the embryonic chick and mouse telencephalon, traced by the expression of the genes Dlx-2, Emx-1, Nkx-2.1, Pax-6, and Tbr-1. *J Comp Neurol* **424**, 409-38.

Purbey, P. K., Singh, S., Kumar, P. P., Mehta, S., Ganesh, K. N., Mitra, D. and Galande, S. (2008). PDZ domain-mediated dimerization and homeodomain-directed specificity are required for high-affinity DNA binding by SATB1. *Nucleic Acids Res* **36**, 2107-22.

Purbey, P. K., Singh, S., Notani, D., Kumar, P. P., Limaye, A. S. and Galande, S. (2009). Acetylation-dependent interaction of SATB1 and CtBP1 mediates transcriptional repression by SATB1. *Mol Cell Biol* **29**, 1321-37.

Purves, D., Augustine, G. J., Fitzpatrick, D., Hall, W. C., LaMantia, A. S. and White, L. E. eds. (2012). Neuroscience. 5th ed. Sunderland, MA, USA: Sinauer Associates.

Rallu, M., Corbin, J. G. and Fishell, G. (2002). Parsing the prosencephalon. *Nat Rev Neurosci* **3**, 943-51.

Rash, B. G. and Grove, E. A. (2007). Patterning the dorsal telencephalon: a role for sonic hedgehog? *J Neurosci* **27**, 11595-603.

Rauch, A., Wieczorek, D., Graf, E., Wieland, T., Endele, S., Schwarzmayr, T., Albrecht, B., Bartholdi, D., Beygo, J., Di Donato, N. et al. (2012). Range of genetic mutations associated with severe non-syndromic sporadic intellectual disability: an exome sequencing study. *Lancet* **380**, 1674-82.

Rinehart, J., Maksimova, Y. D., Tanis, J. E., Stone, K. L., Hodson, C. A., Zhang, J., Risinger, M., Pan, W., Wu, D., Colangelo, C. M. et al. (2009). Sites of regulated phosphorylation that control K-Cl cotransporter activity. *Cell* **138**, 525-36.

Rivera, C., Voipio, J., Payne, J. A., Ruusuvuori, E., Lahtinen, H., Lamsa, K., Pirvola, U., Saarma, M. and Kaila, K. (1999). The K+/Cl- co-transporter KCC2 renders GABA hyperpolarizing during neuronal maturation. *Nature* **397**, 251-5.

Rivera, C., Voipio, J., Thomas-Crusells, J., Li, H., Emri, Z., Sipila, S., Payne, J. A., Minichiello, L., Saarma, M. and Kaila, K. (2004). Mechanism of activity-dependent downregulation of the neuron-specific K-Cl cotransporter KCC2. *J Neurosci* **24**, 4683-91.

Rodriguez, C. I., Buchholz, F., Galloway, J., Sequerra, R., Kasper, J., Ayala, R., Stewart, A. F. and Dymecki, S. M. (2000). High-efficiency deleter mice show that FLPe is an alternative to Cre-loxP. *Nat Genet* **25**, 139-40.

Rossignol, E. (2011). Genetics and function of neocortical GABAergic interneurons in neurodevelopmental disorders. *Neural Plast* **2011**, 649325.

Rubin, A. N., Alfonsi, F., Humphreys, M. P., Choi, C. K., Rocha, S. F. and Kessaris, N. (2010). The germinal zones of the basal ganglia but not the septum generate GABAergic interneurons for the cortex. *J Neurosci* **30**, 12050-62.

Rucker, E. B., 3rd, Dierisseau, P., Wagner, K. U., Garrett, L., Wynshaw-Boris, A., Flaws, J. A. and Hennighausen, L. (2000). Bcl-x and Bax regulate mouse primordial germ cell survival and apoptosis during embryogenesis. *Mol Endocrinol* **14**, 1038-52.

Rudy, B., Fishell, G., Lee, S. and Hjerling-Leffler, J. (2011). Three groups of interneurons account for nearly 100% of neocortical GABAergic neurons. *Dev Neurobiol* **71**, 45-61.

Runyan, C. A., Schummers, J., Van Wart, A., Kuhlman, S. J., Wilson, N. R., Huang, Z. J. and Sur, M. (2010). Response features of parvalbumin-expressing interneurons suggest precise roles for subtypes of inhibition in visual cortex. *Neuron* **67**, 847-57.

Rymar, V. V., Sasseville, R., Luk, K. C. and Sadikot, A. F. (2004). Neurogenesis and stereological morphometry of calretinin-immunoreactive GABAergic interneurons of the neostriatum. *J Comp Neurol* **469**, 325-39.

Sanchez-Alcaniz, J. A., Haege, S., Mueller, W., Pla, R., Mackay, F., Schulz, S., Lopez-Bendito, G., Stumm, R. and Marin, O. (2011). Cxcr7 controls neuronal migration by regulating chemokine responsiveness. *Neuron* **69**, 77-90.

Schmeichel, K. L. and Beckerle, M. C. (1994). The LIM domain is a modular protein-binding interface. *Cell* **79**, 211-9.

Schwaller, B., Meyer, M. and Schiffmann, S. (2002). 'New' functions for 'old' proteins: the role of the calcium-binding proteins calbindin D-28k, calretinin and parvalbumin, in cerebellar physiology. Studies with knockout mice. *Cerebellum* **1**, 241-58.

Selinger, C. I., Cooper, W. A., Al-Sohaily, S., Mladenova, D. N., Pangon, L., Kennedy, C. W., McCaughan, B. C., Stirzaker, C. and Kohonen-Corish, M. R. (2011). Loss of special AT-rich binding protein 1 expression is a marker of poor survival in lung cancer. *J Thorac Oncol* **6**, 1179-89.

Seo, J., Lozano, M. M. and Dudley, J. P. (2005). Nuclear matrix binding regulates SATB1-mediated transcriptional repression. *J Biol Chem* **280**, 24600-9.

Shimamura, K., Hartigan, D. J., Martinez, S., Puelles, L. and Rubenstein, J. L. (1995). Longitudinal organization of the anterior neural plate and neural tube. *Development* **121**, 3923-33.

Shimamura, K. and Rubenstein, J. L. (1997). Inductive interactions direct early regionalization of the mouse forebrain. *Development* **124**, 2709-18.

Simat, M., Ambrosetti, L., Lardi-Studler, B. and Fritschy, J. M. (2007). GABAergic synaptogenesis marks the onset of differentiation of basket and stellate cells in mouse cerebellum. *Eur J Neurosci* **26**, 2239-56.

Smart, I. H. (1976). A pilot study of cell production by the ganglionic eminences of the developing mouse brain. *J Anat* **121**, 71-84.

Smart, I. H. (1985). Differential growth of the cell production systems in the lateral wall of the developing mouse telencephalon. *J Anat* **141**, 219-29.

Sousa, V. H. and Fishell, G. (2010). Sonic hedgehog functions through dynamic changes in temporal competence in the developing forebrain. *Curr Opin Genet Dev* **20**, 391-9.

Sousa, V. H., Miyoshi, G., Hjerling-Leffler, J., Karayannis, T. and Fishell, G. (2009). Characterization of Nkx6-2-derived neocortical interneuron lineages. *Cereb Cortex* **19 Suppl 1**, i1-10.

Squire, L., Berg, D., Bloom, F., du Lac, S., Ghosh, A. and Spitzer, N. eds. (2008). Fundamental Neuroscience. 3rd ed. Burlington, MA, USA: Academic Press.

Srinivas, S., Watanabe, T., Lin, C. S., William, C. M., Tanabe, Y., Jessell, T. M. and Costantini, F. (2001). Cre reporter strains produced by targeted insertion of EYFP and ECFP into the ROSA26 locus. *BMC Dev Biol* **1**, 4.

Stenman, J., Toresson, H. and Campbell, K. (2003). Identification of two distinct progenitor populations in the lateral ganglionic eminence: implications for striatal and olfactory bulb neurogenesis. *J Neurosci* **23**, 167-74.

Strausfeld, N. J. and Hirth, F. (2013). Deep homology of arthropod central complex and vertebrate basal ganglia. *Science* **340**, 157-61.

Stuhmer, T., Anderson, S. A., Ekker, M. and Rubenstein, J. L. (2002). Ectopic expression of the Dlx genes induces glutamic acid decarboxylase and Dlx expression. *Development* **129**, 245-52.

Stumm, R. K., Zhou, C., Ara, T., Lazarini, F., Dubois-Dalcq, M., Nagasawa, T., Hollt, V. and Schulz, S. (2003). CXCR4 regulates interneuron migration in the developing neocortex. *J Neurosci* **23**, 5123-30.

Sussel, L., Marin, O., Kimura, S. and Rubenstein, J. L. (1999). Loss of Nkx2.1 homeobox gene function results in a ventral to dorsal molecular respecification within

the basal telencephalon: evidence for a transformation of the pallidum into the striatum. *Development* **126**, 3359-70.

Taglialatela, P., Soria, J. M., Caironi, V., Moiana, A. and Bertuzzi, S. (2004). Compromised generation of GABAergic interneurons in the brains of Vax1-/- mice. *Development* **131**, 4239-49.

Taira, M., Evrard, J. L., Steinmetz, A. and Dawid, I. B. (1995). Classification of LIM proteins. *Trends Genet* **11**, 431-2.

Talkowski, M. E., Rosenfeld, J. A., Blumenthal, I., Pillalamarri, V., Chiang, C., Heilbut, A., Ernst, C., Hanscom, C., Rossin, E., Lindgren, A. M. et al. (2012). Sequencing chromosomal abnormalities reveals neurodevelopmental loci that confer risk across diagnostic boundaries. *Cell* **149**, 525-37.

Tamamaki, N., Fujimori, K. E. and Takauji, R. (1997). Origin and route of tangentially migrating neurons in the developing neocortical intermediate zone. *J Neurosci* **17**, 8313-23.

Tamamaki, N. and Tomioka, R. (2010). Long-Range GABAergic Connections Distributed throughout the Neocortex and their Possible Function. *Front Neurosci* **4**, 202.

Tamamaki, N., Yanagawa, Y., Tomioka, R., Miyazaki, J., Obata, K. and Kaneko, T. (2003). Green fluorescent protein expression and colocalization with calretinin, parvalbumin, and somatostatin in the GAD67-GFP knock-in mouse. *J Comp Neurol* **467**, 60-79.

Tan, S. S., Kalloniatis, M., Sturm, K., Tam, P. P., Reese, B. E. and Faulkner-Jones, B. (1998). Separate progenitors for radial and tangential cell dispersion during development of the cerebral neocortex. *Neuron* **21**, 295-304.

Tanahira, C., Higo, S., Watanabe, K., Tomioka, R., Ebihara, S., Kaneko, T. and Tamamaki, N. (2009). Parvalbumin neurons in the forebrain as revealed by parvalbumin-Cre transgenic mice. *Neurosci Res* **63**, 213-23.

Tanaka, D., Nakaya, Y., Yanagawa, Y., Obata, K. and Murakami, F. (2003). Multimodal tangential migration of neocortical GABAergic neurons independent of GPI-anchored proteins. *Development* **130**, 5803-13.

Tanaka, D. H., Maekawa, K., Yanagawa, Y., Obata, K. and Murakami, F. (2006). Multidirectional and multizonal tangential migration of GABAergic interneurons in the developing cerebral cortex. *Development* **133**, 2167-76.

Tanaka, D. H., Yanagida, M., Zhu, Y., Mikami, S., Nagasawa, T., Miyazaki, J., Yanagawa, Y., Obata, K. and Murakami, F. (2009). Random walk behavior of migrating cortical interneurons in the marginal zone: time-lapse analysis in flat-mount cortex. *J Neurosci* **29**, 1300-11.

Tang, K., Rubenstein, J. L., Tsai, S. Y. and Tsai, M. J. (2012). COUP-TFII controls amygdala patterning by regulating neuropilin expression. *Development* **139**, 1630-9.

Taniguchi, H., He, M., Wu, P., Kim, S., Paik, R., Sugino, K., Kvitsiani, D., Fu, Y., Lu, J., Lin, Y. et al. (2011). A resource of Cre driver lines for genetic targeting of GABAergic neurons in cerebral cortex. *Neuron* **71**, 995-1013.

Tepper, J. M. and Bolam, J. P. (2004). Functional diversity and specificity of neostriatal interneurons. *Curr Opin Neurobiol* **14**, 685-92.

Theil, T., Alvarez-Bolado, G., Walter, A. and Ruther, U. (1999). Gli3 is required for Emx gene expression during dorsal telencephalon development. *Development* **126**, 3561-71.

Tiveron, M. C., Boutin, C., Daou, P., Moepps, B. and Cremer, H. (2010). Expression and function of CXCR7 in the mouse forebrain. *J Neuroimmunol*.

Tiveron, M. C., Rossel, M., Moepps, B., Zhang, Y. L., Seidenfaden, R., Favor, J., Konig, N. and Cremer, H. (2006). Molecular interaction between projection neuron precursors and invading interneurons via stromal-derived factor 1 (CXCL12)/CXCR4 signaling in the cortical subventricular zone/intermediate zone. *J Neurosci* **26**, 13273-8.

Tole, S., Ragsdale, C. W. and Grove, E. A. (2000). Dorsoventral patterning of the telencephalon is disrupted in the mouse mutant extra-toes(J). *Dev Biol* **217**, 254-65.

Toledo-Rodriguez, M., Blumenfeld, B., Wu, C., Luo, J., Attali, B., Goodman, P. and Markram, H. (2004). Correlation maps allow neuronal electrical properties to be predicted from single-cell gene expression profiles in rat neocortex. *Cereb Cortex* **14**, 1310-27.

Tomioka, R., Okamoto, K., Furuta, T., Fujiyama, F., Iwasato, T., Yanagawa, Y., Obata, K., Kaneko, T. and Tamamaki, N. (2005). Demonstration of long-range GABAergic connections distributed throughout the mouse neocortex. *Eur J Neurosci* **21**, 1587-600.

Toresson, H. and Campbell, K. (2001). A role for Gsh1 in the developing striatum and olfactory bulb of Gsh2 mutant mice. *Development* **128**, 4769-80.

Toresson, H., Potter, S. S. and Campbell, K. (2000). Genetic control of dorsal-ventral identity in the telencephalon: opposing roles for Pax6 and Gsh2. *Development* **127**, 4361-71.

Tricoire, L., Pelkey, K. A., Daw, M. I., Sousa, V. H., Miyoshi, G., Jeffries, B., Cauli, B., Fishell, G. and McBain, C. J. (2010). Common origins of hippocampal Ivy and nitric oxide synthase expressing neurogliaform cells. *J Neurosci* **30**, 2165-76.

Tricoire, L., Pelkey, K. A., Erkkila, B. E., Jeffries, B. W., Yuan, X. and McBain, C. J. (2011). A blueprint for the spatiotemporal origins of mouse hippocampal interneuron diversity. *J Neurosci* **31**, 10948-70.

Valcanis, H. and Tan, S. S. (2003). Layer specification of transplanted interneurons in developing mouse neocortex. *J Neurosci* **23**, 5113-22.

van den Pol, A. N. (2012). Neuropeptide transmission in brain circuits. *Neuron* **76**, 98-115.

van Vliet, E. A., Aronica, E., Tolner, E. A., Lopes da Silva, F. H. and Gorter, J. A. (2004). Progression of temporal lobe epilepsy in the rat is associated with immunocytochemical changes in inhibitory interneurons in specific regions of the hippocampal formation. *Exp Neurol* **187**, 367-79.

Wang, Y., Dye, C. A., Sohal, V., Long, J. E., Estrada, R. C., Roztocil, T., Lufkin, T., Deisseroth, K., Baraban, S. C. and Rubenstein, J. L. (2010). Dlx5 and Dlx6 regulate the development of parvalbumin-expressing cortical interneurons. *J Neurosci* **30**, 5334-45.

Wang, D. D. and Kriegstein, A. R. (2009). Defining the role of GABA in cortical development. *J Physiol* **587**, 1873-9.

Wang, Y., Li, G., Stanco, A., Long, J. E., Crawford, D., Potter, G. B., Pleasure, S. J., Behrens, T. and Rubenstein, J. L. (2011). CXCR4 and CXCR7 have distinct functions in regulating interneuron migration. *Neuron* **69**, 61-76.

Wang, Y., Spatz, M. K., Kannan, K., Hayk, H., Avivi, A., Gorivodsky, M., Pines, M., Yayon, A., Lonai, P. and Givol, D. (1999). A mouse model for achondroplasia produced by targeting fibroblast growth factor receptor 3. *Proc Natl Acad Sci U S A* **96**, 4455-60.

Wang, Z., Yang, X., Chu, X., Zhang, J., Zhou, H., Shen, Y. and Long, J. (2012). The structural basis for the oligomerization of the N-terminal domain of SATB1. *Nucleic Acids Res* **40**, 4193-202.

Watson, C., Paxinos, G. and Puelles, L. eds. (2012). The Mouse Nervous System. London, UK: Academic Press.

Way, J. C. and Chalfie, M. (1988). mec-3, a homeobox-containing gene that specifies differentiation of the touch receptor neurons in C. elegans. *Cell* **54**, 5-16.

Weiser, M., Bueno, E., Sekirnjak, C., Martone, M. E., Baker, H., Hillman, D., Chen, S., Thornhill, W., Ellisman, M. and Rudy, B. (1995). The potassium channel subunit KV3.1b is localized to somatic and axonal membranes of specific populations of CNS neurons. *J Neurosci* **15**, 4298-314.

Wichterle, H., Garcia-Verdugo, J. M., Herrera, D. G. and Alvarez-Buylla, A. (1999). Young neurons from medial ganglionic eminence disperse in adult and embryonic brain. *Nat Neurosci* **2**, 461-6.

Wichterle, H., Turnbull, D. H., Nery, S., Fishell, G. and Alvarez-Buylla, A. (2001). In utero fate mapping reveals distinct migratory pathways and fates of neurons born in the mammalian basal forebrain. *Development* **128**, 3759-71.

Willi-Monnerat, S., Migliavacca, E., Surdez, D., Delorenzi, M., Luthi-Carter, R. and Terskikh, A. V. (2008). Comprehensive spatiotemporal transcriptomic analyses of the ganglionic eminences demonstrate the uniqueness of its caudal subdivision. *Mol Cell Neurosci* **37**, 845-56.

Wonders, C. P., Taylor, L., Welagen, J., Mbata, I. C., Xiang, J. Z. and Anderson, S. A. (2008). A spatial bias for the origins of interneuron subgroups within the medial ganglionic eminence. *Dev Biol* **314**, 127-36.

Woo, N. S., Lu, J., England, R., McClellan, R., Dufour, S., Mount, D. B., Deutch, A. Y., Lovinger, D. M. and Delpire, E. (2002). Hyperexcitability and epilepsy associated with disruption of the mouse neuronal-specific K-Cl cotransporter gene. *Hippocampus* **12**, 258-68.

Xu, Q., Cobos, I., De La Cruz, E., Rubenstein, J. L. and Anderson, S. A. (2004). Origins of cortical interneuron subtypes. *J Neurosci* **24**, 2612-22.

Xu, Q., Guo, L., Moore, H., Waclaw, R. R., Campbell, K. and Anderson, S. A. (2010b). Sonic hedgehog signaling confers ventral telencephalic progenitors with distinct cortical interneuron fates. *Neuron* **65**, 328-40.

Xu, Q., Tam, M. and Anderson, S. A. (2008). Fate mapping Nkx2.1-lineage cells in the mouse telencephalon. *J Comp Neurol* **506**, 16-29.

Xu, Q., Wonders, C. P. and Anderson, S. A. (2005). Sonic hedgehog maintains the identity of cortical interneuron progenitors in the ventral telencephalon. *Development* **132**, 4987-98.

Xu, X., Roby, K. D. and Callaway, E. M. (2006). Mouse cortical inhibitory neuron type that coexpresses somatostatin and calretinin. *J Comp Neurol* **499**, 144-60.

Xu, X., Roby, K. D. and Callaway, E. M. (2010a). Immunochemical characterization of inhibitory mouse cortical neurons: three chemically distinct classes of inhibitory cells. *J Comp Neurol* **518**, 389-404.

Yamaguchi, H., Tateno, M. and Yamasaki, K. (2006). Solution structure and DNA-binding mode of the matrix attachment region-binding domain of the transcription factor SATB1 that regulates the T-cell maturation. *J Biol Chem* **281**, 5319-27.

Yasui, D., Miyano, M., Cai, S., Varga-Weisz, P. and Kohwi-Shigematsu, T. (2002). SATB1 targets chromatin remodelling to regulate genes over long distances. *Nature* **419**, 641-5.

Yozu, M., Tabata, H. and Nakajima, K. (2005). The caudal migratory stream: a novel migratory stream of interneurons derived from the caudal ganglionic eminence in the developing mouse forebrain. *J Neurosci* **25**, 7268-77.

Yu, C. R., Power, J., Barnea, G., O'Donnell, S., Brown, H. E., Osborne, J., Axel, R. and Gogos, J. A. (2004). Spontaneous neural activity is required for the establishment and maintenance of the olfactory sensory map. *Neuron* **42**, 553-66.

Yuan, W., Zhou, L., Chen, J. H., Wu, J. Y., Rao, Y. and Ornitz, D. M. (1999). The mouse SLIT family: secreted ligands for ROBO expressed in patterns that suggest a role in morphogenesis and axon guidance. *Dev Biol* **212**, 290-306.

Yun, K., Potter, S. and Rubenstein, J. L. (2001). Gsh2 and Pax6 play complementary roles in dorsoventral patterning of the mammalian telencephalon. *Development* **128**, 193-205.

Zhao, Y., Flandin, P., Long, J. E., Cuesta, M. D., Westphal, H. and Rubenstein, J. L. (2008). Distinct molecular pathways for development of telencephalic interneuron subtypes revealed through analysis of Lhx6 mutants. *J Comp Neurol* **510**, 79-99.

Zhao, Y., Guo, Y. J., Tomac, A. C., Taylor, N. R., Grinberg, A., Lee, E. J., Huang, S. and Westphal, H. (1999). Isolated cleft palate in mice with a targeted mutation of the LIM homeobox gene lhx8. *Proc Natl Acad Sci U S A* **96**, 15002-6.

Zhao, Y., Marin, O., Hermesz, E., Powell, A., Flames, N., Palkovits, M., Rubenstein, J. L. and Westphal, H. (2003). The LIM-homeobox gene Lhx8 is required for the development of many cholinergic neurons in the mouse forebrain. *Proc Natl Acad Sci U S A* **100**, 9005-10.

Zheng, Q. and Zhao, Y. (2007). The diverse biofunctions of LIM domain proteins: determined by subcellular localization and protein-protein interaction. *Biol Cell* **99**, 489-502.

Zimmer, C., Tiveron, M. C., Bodmer, R. and Cremer, H. (2004). Dynamics of Cux2 expression suggests that an early pool of SVZ precursors is fated to become upper cortical layer neurons. *Cereb Cortex* **14**, 1408-20.